Investigation of long-range transport and chemical fate of organophosphate esters (OPEs) in the marine environment

Dissertation with the aim of achieving a doctoral degree

at the Faculty of Mathematics, Informatics and Natural Sciences

Department of Earth Sciences

of Universität Hamburg

submitted by

Jing Li

Hamburg

2019

Accepted as Dissertation at the Department of Earth Sciences

Day of oral defense: 16.12.2019 (date of defense)

Reviewers: Prof. Dr. Kay-Christian Emeis
Prof. Dr. Ralf Ebinghaus

Chair of the Subject Doctoral Committee: Prof. Dr. Dirk Gajewski

Dean of Faculty of MIN: Prof. Dr. Heinrich Graener

Abstract

Organophosphate esters (OPEs) are a group of man-made industrial chemicals that have been widely applied in many industrial processes and household products. The use of OPEs throughout the world has drastically increased partly because these chemicals have been proposed as alternatives for brominated flame retardants (BFRs). Most OPEs are applied as additive materials on the surface of products, which allows these chemicals to easily spread into the environment by volatilization, leaching, and abrasion. To identify and evaluate the OPE fingerprints in the marine environment and the long-range transport (LRT) potential, occurrences of OPEs in the North Atlantic Ocean, the Arctic Ocean as well as the Bohai and Yellow Seas (China) have been investigated in this study. For a more holistic view of OPEs in the environment, different models have been used in combination with experimental data, including air-seawater exchange, gas-particle partitioning and LRT models. This study has been designed to improve our understanding of the OPE interactions between land, atmosphere, and oceans, the source-to-concentration relationships and the contributions of OPE source regions to polar areas.

Due to political regulations, the produced substance amounts and compound patterns change over time in a given region. At the same time, production capacities are relocated to less regulated regions. As a result, different OPE occurrence patterns are observed in Europe and East Asia. This study also highlighted that OPEs are subject to LRT via both air and seawater from the European continent and seas to the North Atlantic and Arctic regions. A net deposition occurs over the North Atlantic and Arctic oceans based on the air-sea exchange fluxes calculated by the two-film resistance model. The gas-particle partitioning analysis based on the samples collected from the Bohai and Yellow Seas suggests that OPEs have a low potential to achieve equilibrium or are sensitive to the artificial sampling method.

This study also seeks to characterize and constrain the uncertainties in global source-to-concentration relationships for tris-(1-chloro-2-propyl) phosphate (TCPP), which is one of the most widely used OPE congeners. The global gridded emission rate of TCPP to air and water has been developed in this study with the total release ranges from 12.0 to 157 kt/y (1 kt/y=1 Gg/y). Europe (38%), North America (24%) and East Asia (13%) release the most TCPP into the global environment. In a scenario with global emission rates to air and water of 78.6 kt/y 39.8 kt/y, respectively, an amount of 114 t TCPP is found in Arctic (after spin-up for eight years) which is three orders of magnitude higher than that found in Antarctic (0.36 t). More than 95% of TCPP in polar regions are distributed in seawater. Oceanic transport is the major pathway that conveys TCPP to Arctic seawater (89%). Whereas, for Antarctic, oceanic and atmospheric transport are both important. Europe, Asia and North America are identified as the major source areas for Arctic TCPP contamination, due to not only the high emission rates in these regions but also their relative proximity to the Arctic. For the Antarctic, TCPP mainly originates from South America and the Indonesia to Australia region, which reflects that it is not efficiently transported across the equator from regions of higher emission in the northern hemisphere. A seasonal trend is shown for TCPP transport in air with higher concentrations in winter than in summer in polar regions, mainly due to the variation in hydroxyl radical concentrations and temperatures.

Zusammenfassung

Organophosphorsäureester (OPEs) sind eine Gruppe anthropogener Industriechemikalien, die vielfältig in Industrieprozessen und Konsumgütern eingesetzt werden. Die weltweite Verwendung von OPEs ist stark gestiegen, unter anderen weil die Chemikalien als Alternativstoffe für bromierte Flammschutzmittel (BFRs) vorgeschlagen wurden. Da die meisten OPEs als Hilfsstoffe auf der Oberfläche von Produkten eingesetzt werden, können sie durch Verflüchtigung, Auswaschung und Abrieb leicht in die Umwelt eingetragen werden.

In der vorliegenden Arbeit wurde das Vorkommen von OPEs im Nordatlantik, dem Arktischen Ozean sowie im Golf von Bohai und dem Gelben Meer (China) untersucht, um Verteilungsmuster in der marinen Umwelt zu identifizieren und zu beurteilen und das mögliche Potential für Langstreckentransports (LRT) zu bewerten. Für eine ganzheitlichere Betrachtung von OPEs in der Umwelt wurden verschiedene Modelle in Kombination mit experimentellen Daten eingesetzt, darunter Modelle für den Luft-Meerwasser-Austausch, die Gas-Partikel-Verteilung und den Langstreckentransport. Ziel der Arbeit war es, das Verständnis der OPE-Wechselwirkungen zwischen Land, Atmosphäre und Ozeanen, des Zusammenhangs zwischen Quellen und Umweltkonzentrationen sowie des Einflusses verschiedener OPE-Quellregionen auf polare Gebiete zu verbessern.

Infolge von politischen Vorschriften ändern sich Produktionsvolumina und Substanzmuster in einer bestimmten Region im Laufe der Zeit. Damit einhergehend werden Produktionskapazitäten in weniger regulierte Regionen ausgelagert. Aufgrund dessen wurden in Europa und China unterschiedliche Verteilungsmuster beobachtet. Darüber hinaus zeigt die Arbeit, dass OPEs sowohl über die Atmosphäre als auch über Meerwasser vom europäischen Kontinent und den europäischen Meeren aus über weite Strecken bis in den Nordatlantik und in arktische Regionen transportiert werden. Über dem Nordatlantik und dem Arktischen Ozean findet basierend auf den Luft-Meerwasser-Austauschflüssen, die mithilfe des *two-film*

resistance-Modells berechnet wurden, eine Nettodeposition statt. Die Analyse der Gas-Partikel-Verteilung auf Grundlage der Proben aus dem Golf von Bohai und dem Gelben Meer deutet darauf hin, dass OPEs ein geringes Potential besitzen, den Gleichgewichtszustand zu erreichen, oder empfindlich in Bezug auf die künstliche Probenahme sind.

Ziel der Arbeit war es auch, die Unsicherheiten in globalen „Quelle-zu-Konzentration“-Zusammenhängen für Tris(2-chlorisopropyl)phosphat (TCPP), eines der am meisten verwendeten OPE-Kongenere, zu charakterisieren und auf Ursachen zurückzuführen. Die globale gitterbasierte Emissionsrate von TCCP in Luft und Wasser wurde mit einer Gesamtfreisetzung von 12 bis 157 kt/y (1 kt/y = 1 Gg/y) berechnet. Dabei setzten Europa (38%), Nordamerika (24%) und Ostasien (13%) am meisten TCPP in die globale Umwelt frei. Ein Szenario mit globalen Emissionsraten von 78.6 kt/y bzw. 39.8 kt/y in Luft und Wasser ergibt eine Menge von 114 t TCPP in der Arktis (nach einer achtjährigen Einschwingphase), was um drei Größenordnungen über der Menge in der Antarktis liegt (0.4 t). Über 95% des TCPPs in Polarregionen liegen im Meerwasser vor. Ozeanischer Transport ist der Haupteintragsweg von TCPP in arktisches Meerwasser (89%), wohingegen für die Antarktis sowohl ozeanischer als auch atmosphärischer Transport von Relevanz sind. Europa und Asien werden als bedeutende Quelle für TCPP in der Arktis identifiziert, was nicht nur in den hohen Emissionsraten dieser Regionen begründet ist, sondern auch in ihrer Nähe zur Arktis. Das TCPP in der Antarktis stammt hauptsächlich aus Südamerika und der Region Indonesien/Australien. Dies spiegelt wider, dass die Substanz von Regionen mit höherer Emission in der nördlichen Hemisphäre aus nicht effizient über den Äquator hinaus transportiert wird. Für den TCPP-Transport in der Luft wird in den Polarregionen ein saisonaler Trend mit höheren Konzentrationen im Winter als im Sommer aufgezeigt, was hauptsächlich auf die Unterschiede der Hydroxylradikalkonzentrationen zurückzuführen ist.

Acknowledgements

I sincerely wish to acknowledge my principal supervisors Prof. Dr. Kay-Christian Emeis, for his invaluable support and trust on my PhD work. Thanks him for organizing panel meetings and providing me with open and free discussion atmosphere. I also greatly appreciate his patient guidance, constructive comments and great efforts to improve my scientific writing.

I would like to thank to my co-supervisor Prof. Dr. Ralf Ebinghaus, for giving me the opportunity to pursue PhD studies and encouraging my research. Thank him for providing me many chances to present this work at meetings and conferences. I also participated many training courses under his suggestion, which help me accumulate lots of important knowledge on environmental research.

I am very grateful to my co-supervisor Dr. Zhiyong Xie, for his precious guidance and countless help on my research proposal and PhD studies. He is enthusiasm and has deep insight into chemical and environmental research. I have learnt a lot from him on exploration of persistent organic pollutants (POPs). Thank him for encouraging my studies and promoting my independent thinking.

I want to express my gratitude to my Advisory Panel Chair Prof. Dr. Matthew MacLeod. He is also my supervisor on chemical fate modeling. He is always available to help me in solving my questions and problems on modeling. His pleasant personality and high passion on science make our talks/discussions very enjoyable and inspirable. I had good times when I was in Sweden and achieved assistance from his group.

I wish to express my thankfulness to Dr. Chongguo Tian for his guidance on long-range atmospheric modeling and the Canadian Model for Environmental Transport of Organochlorine Pesticides (CanMETOP). I also thank him for the valuale discussion on the polar pollution modeling research. I am indebted to Dr. Jianhui Tang for his supporting on the research of POPs in Bohai and Yellow Seas, as well as his help on English polishing. I also

very thankful for Wenying Mi who have provided me constant support both in academic and spirit during my PhD.

I appreciate Hanna Jörss for translating my thesis abstract to “Zusammenfassung”. I would like to thank Dr. Pu Wang for his insightful discussion on the gas-particle partitioning methods. Many thanks also to Dr. Celia Bento for her guidance on statistical analysis. I would also like to thank Dr. Fangyuan Zhao for helping me with Berkeley-Trent Global (BETR-Global) Contaminant Fate Model and fruitful discussions on chemical emission adjustion methods. I would like to thank Dr. Senchao Lai for enhancing my learning experiences and attending my first panel meeting.

I also thank the School of Integrated Climate System Sciences (SICSS) for accepting me as a member and providing useful courses and retreats. Many thanks to Chinese Scholarship Council (CSC) for their financial support.

My sincere appreciation goes to my colleagues Franzika, Christina, Ina, Celia, Hanna, Danilo, Rui, Danijela, Jürgen, Andreas, Hendrik and Volker, for their kindness and providing support and help in daily work, and for the happy Christmas parties and team activities, and for making my time at HZG rich and unforgettable. Thanks Franzika, Christina and Hanna for sharing your culture, traditions and beautiful places with me.

I am very thankful for all my friends for their favor and support, and for all memorable moments we share together.

Special thanks to my family for their constant love, support and encouragement in all aspects of my life.

Contents

Acronym list

Acronym	Definition
BETR-Global	Berkeley-Trent Global Contaminant Fate Model
BFRs	brominated flame retardants
CanMETOP	Canadian Model for Environmental Transport of Organochlorine Pesticides
DCM	dichloromethane
EU	European Union
GC-MS/MS	gas chromatograph coupled to a triple quadrupole mass spectrometer
GFF	glass fiber filter
TF-HTAP	Task Force on Hemispheric Transport of Air Pollution
LRT	long-range transport
NHI	North Huangcheng Island
OPEs	Organophosphate esters
PBDEs	polybrominated diphenyl ethers
PCBs	polychlorinated biphenyls
PTV	programmed temperature vaporizer
PUR	polyurethane
REACH	Registration, Evaluation and Authorization of Chemicals
SSCTC	Shanghai Shuoxun Chemical Technology Company
TBEP	tris (2-butoxyethyl) phosphate
TCEP	tris-(2-chloroethyl) phosphate
TCP	Tricresyl phosphate
TCPP	tris-(1-chloro-2-propyl) phosphate
TDCP	tris-[2-chloro-1-(chloromethyl)ethyl] phosphate
TEHP	tris (2-ethylhexyl) phosphate
TiBP	tri-*iso*-butylphosphate
TnBP	tri-*n*-butylphosphate
TPhP	triphenyl phosphate

1. Introduction

1.1. Sources of organophosphate esters (OPEs) as environmental pollutions

1.1.1. Production and usage

Organophosphate esters (OPEs) are a group of man-made industrial chemicals that have been widely applied in many industrial processes and household products, such as flame retardants, plasticizers, antifoaming agents, and additives in hydraulic fluids, lacquers, and floor polishes.[1, 2] Chlorinated OPEs are predominantly utilized as flame retardants, while non-chlorinated OPEs are mainly used as plasticizers and in other applications.[1] Recently, the production and usage of OPEs has continually increased as OPEs can be used as substitutes for brominated flame retardants (BFRs) in many cases.[1, 2] In 2013, the consumption of OPEs accounted for approximately 19% (370 kt) of the global flame retardant usage, comparable to that of globally used BFRs (21%).[3] In Western Europe, the consumption of OPEs increased from 58 kt in 1998 to 91 kt in 2006 and to 110 kt in 2013 (Figure 1-1, Table 1-1).[3-5] The consumed OPEs in Europe are dominated by tris-(1-chloro-2-propyl) phosphate (TCPP), which accounts for a proportion of ~50% in 2000 and is thought to have been stable or increased since then.[6] This phenomenon reflects the replacement of tris-(2-chloroethyl) phosphate (TCEP) by TCPP in Europe.[2] TCEP has been banned in the European Union (EU) under the Registration, Evaluation and Authorization of Chemicals (REACH) legislation due to the human health concerns associated with TCEP.[7] In Germany, the annual production volumes of the summed production volume of tri-*iso*-butylphosphate (TiBP) and tri-*n*-butylphosphate (TnBP) in 1991 were estimated at approximately 0.50 kt/y, respectively.[8] From 2000 to 2015, the accumulated consumption of TCPP was 24 kt in European Nordic countries, including Sweden (1.9 kt), Norway (1.1 kt), Denmark (4.0 kt) and Finland (18 kt), as indicated by statistics from the online database of substances in preparations in Nordic countries (SPIN).[9] The usage of OPEs in North America was 70 kt in 2013.[3] In China, the price of the brominated intermediates has risen continuously since 2005 due to limitations in the supply of bromate.[3] As a result, the market-prices for brominated flame retardants (BFRs) are higher than those of flame retardants from OPEs.[3] Consequently, the consumption of OPEs increased from 11 kt in 1995 to 70 kt in 2007 and to 180 kt in 2012.[3] The annual consumption of OPEs in Japan was 9.3 kt in 1992 and increased to 29 kt in 2008 (Figure 1-1, Table 1-1).[10]

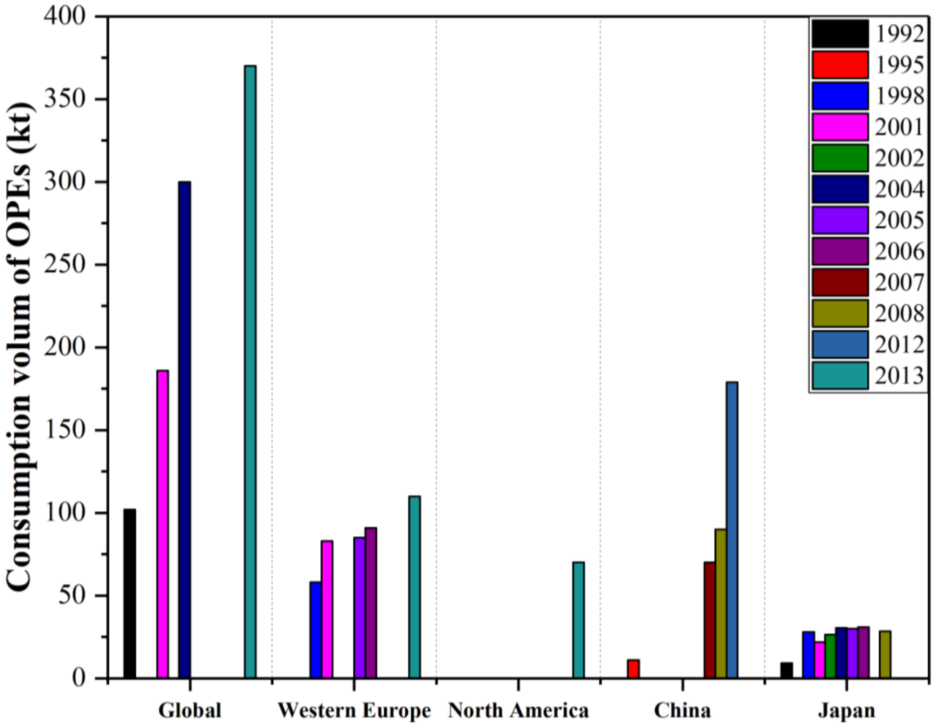

Figure 1-1: Consumption of OPEs in different regions

Table 1-1: Consumption of OPEs in different regions (unit: kt)

Year	Global	Western Europe	North America	Japan	China
1992	102[11]			9.3[10]	
1995					11[12]
1998		58[5]		28[10]	
2001	190[5]	83[5]		22[13]	
2002				27[11]	
2004	300[14]			31[10]	
2005		85[4]		30[15]	
2006		91[4]		31[10]	
2007					70[16]
2008				29[10]	90[17]
2012					180[17]
2013	370[3]	110[3]	70[3]		

EU risk assessment reports show that more than 98% of consumed TCPP (~40 kt) was used as a flame retardant in the production of polyurethane (PUR) for use in construction and furniture in year 2000.[6] TCPP tends not to be applied in flexible PUR for automotive uses due to its volatility and fogging potential.[6] Most consumed tris-[2-chloro-1-(chloromethyl)ethyl] phosphate (TDCP) is used in the production of flexible PUR foam, and the formed foam is mainly used in the automotive industry, with some use in furniture.[18] In Finland, Sweden and Norway, TCPP is mainly used in the construction and manufacture of rubber and plastic products according to SPIN data.[9] In Denmark, in addition to the aforementioned two applications, TCPP is also consumed in the manufacture of chemicals and chemical products.[9] In China, OPEs are mainly consumed in the plastic, textile, paint and other industries, as stated by a market report of the Shanghai Shuoxun Chemical Technology Company (SSCTC).[19]

1.1.2. Environmental release

The broad application of OPEs and the fact that these chemicals are applied as additives may allow them to easily spread into the environment through volatilization, leaching, and abrasion.[1, 2] In addition, in step with the rapid rise in OPE production and consumption, their emissions into the environment are expected to have increased. The continental release levels of TCPP into air, wastewater, surface water and industrial soil are estimated at 33, 8.8, 2.2, and 2.8 t/y, respectively, in the EU based on production and usage data in 2000.[6] The release of TDCP in the EU was assessed to be approximately one order of magnitude lower than that of TCPP.[6, 18] The modeled air emission of six OPE congeners in the city of Toronto ranged from 0.19~190 t/y (mean: 3.3 t/y), which was 10~100 times higher than the emissions of polychlorinated biphenyls (PCBs) and polybrominated diphenyl ethers (PBDEs).[20] The rising usage and higher release of OPEs compared to the other POPs highlight the need and importance of tracking OPE emissions, transport, and pools. To our knowledge, there are no scientific studies reporting on the OPE emissions in other regions or at the global scale. Since

OPEs are relatively new flame retardants that are globally used, the specific lack of production and usage information limits the emission estimates.

1.2. Occurrence in the global marine environment

OPEs have been detected in the atmosphere and seawater of the open oceans and the remote regions (Figure 1-2 and 1-3). The occurrences of OPEs have been reported in air over the North Sea (eight OPEs; mean: 500 pg/m^3)[21], Mediterranean (14 OPEs; mean: 2,300 pg/m^3) and black Seas (14 OPEs; mean: 2,800 pg/m^3)[22], Great Lakes (six OPEs; mean: 600 pg/m^3)[23],South China Sea (nine OPEs; median: 91 pg/m^3)[24], the East China Sea (four OPEs in one sample; 1,100 pg/m^3)[25], and the Japan Sea (eight OPEs in two samples; 450 and 2,900 pg/m^3)[15] and so on. Several studies analyzed OPEs in the Arctic region: nine OPEs were found in the air of Ny-Ålesund, Svalbard, by Green et al. in 2008;[2] Möller et al. reported eight OPEs in the air over the northern Pacific Ocean (mean: 400 pg/m^3) to the Arctic Ocean (mean: 600 pg/m^3) in 2012;[15] Salamova et al. detected eight OPEs in Longyearbyen, Svalbard (mean: 550 pg/m^3), in 2014;[26] Sühring et al. detected fourteen OPEs in Canadian Arctic (ship based: 300 pg/m^3; land-based: 400 pg/m^3) air in 2016[27]. Rauert et al. also reported OPEs globally based on the Global Atmospheric Passive Sampling Network (GAPS).[28] The concentrations of OPEs that detected in air were generally one to two orders of magnitude higher than those of BFRs.[15, 26] A few of studies also detected OPEs in seawater. For example, Bollmann et al. reported OPEs in the North Sea seawater with a range of 5.0~50 ng/L.[29] In the waters off the Fildes Peninsula, Antarctica, the OPE levels ranged from non-detectable to 20 ng/L, with an easier detection of OPEs in lake waters compared to marine waters.[30] In Canada Arctic surface water, eleven OPEs were measured ranging from not detected to 47 ng/L.[31] Lower OPE levels were present in the deep-water moorings of the Fram Strait (0.0~2.3 ng/L).[31] Seawater samples were also collected in New York State with OPE levels of 0.0~36 ng/L.[32]

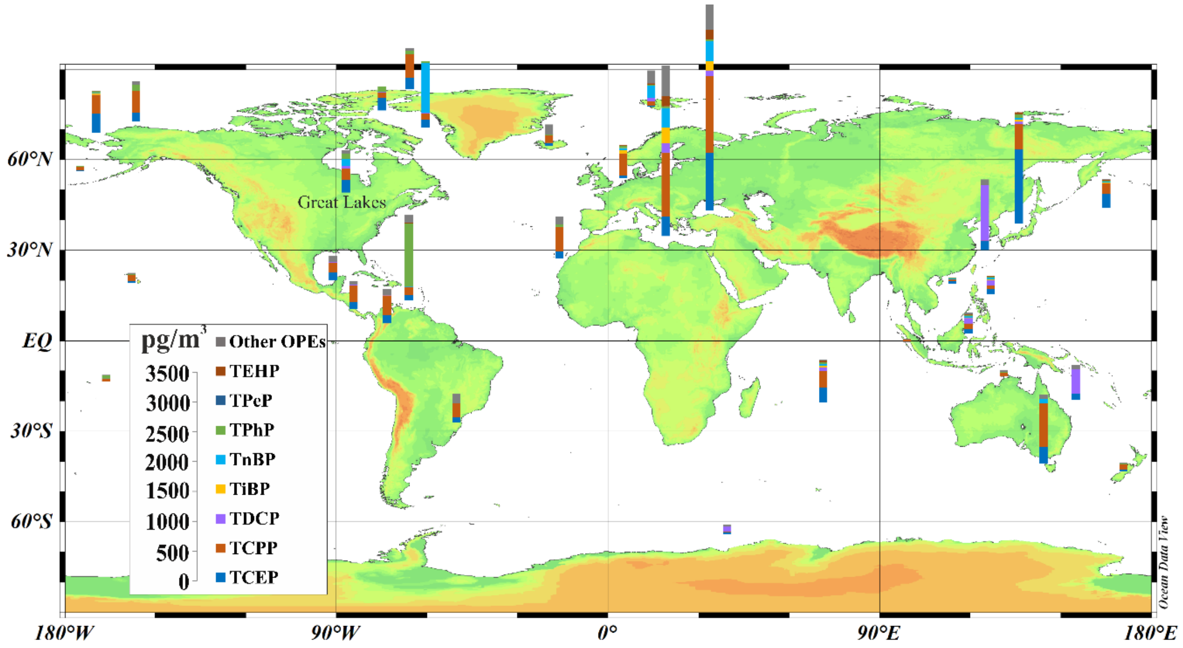

Figure 1-2: Occurrence of OPEs in global marine air (average value showed for each region).

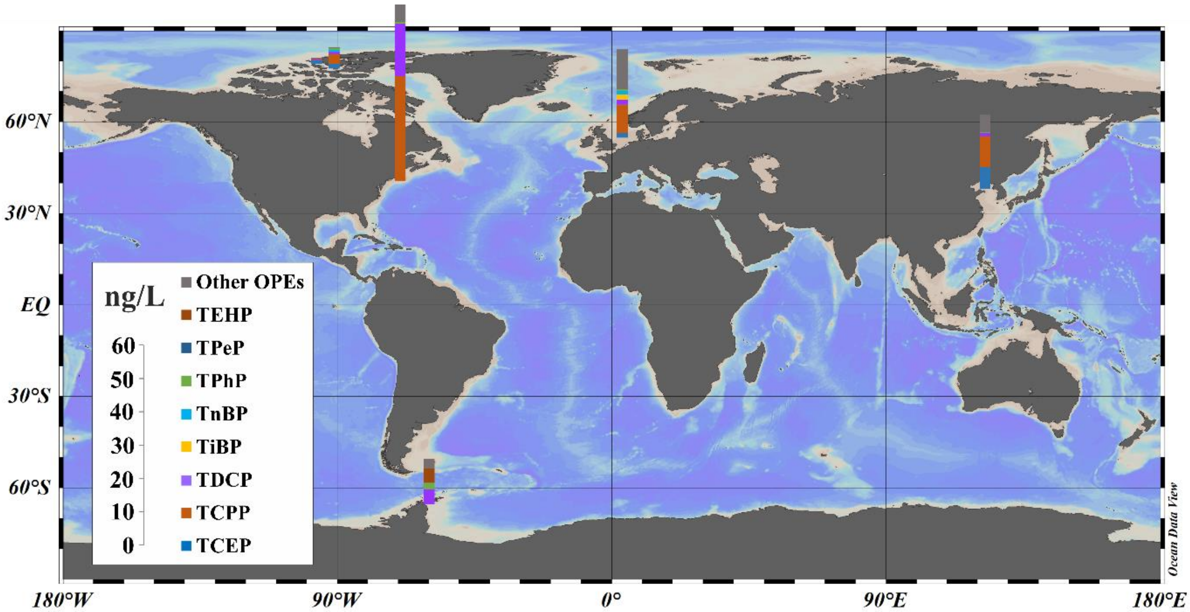

Figure 1-3: Occurrence of OPEs in global oceans (average value showed for each region).

1.3. Environmental impact of the OPEs

OPEs have various toxic effects.[33, 34] For example, TCPP is considered potentially carcinogenic and could accumulate in human livers and kidneys.[1] TCEP is toxic to aquatic organisms and carcinogenic in animals, and it has adverse effects on the human health, such as hemolytic and reproductive effects.[1] TDCP is harmful when inhaled and can easily enter the blood stream.[1] The potential of OPEs to bioaccumulate and magnify might be limited, owing to their relatively low octanol/water partition ratio ($\log K_{\mathrm{ow}} < 5$ for most OPEs).[4] However, Sundkvist et al. detected OPEs in human breast milk as well as in fish and mussels from Swedish lakes and coastal areas.[35] Kim et al. also found OPEs in fish collected from Manila Bay, the Philippines.[36] Because of the human health concerns associated with TCEP, the substance has already been restricted in the EU.[7]

1.4. Environmental fate and persistence

OPEs have been measured in remote areas, which show strong evidence that these chemicals have the potential to undergo LRT in the atmosphere.[26, 27, 37, 38] However, the environmental fate of OPEs is ambiguous and little is known about their LRT pathways. For example, the atmospheric half-lifetimes ($t_{1/2,\mathrm{Air}}$) of OPEs are highly uncertain, e.g., the $t_{1/2,\mathrm{Air}}$ estimates of TCPP range from 0.5~20 days.[39] In addition, it has been found that the atmospheric lifetime of particle-bound OPEs are range from 2.6 days of tris (2-butoxyethyl) phosphate (TBEP) to 13 days of TDCP. [40, 41] Previous studies focused mainly on OPEs in the particulate phase, and only a few papers reported the occurrence of OPEs in the gaseous phase. Wolschke et al. reported that, on average, 45% of the OPEs could be detected in the gaseous phase based on samples collected from the German Coast.[42] These studies highlighted the requirements of research on OPE gas/particle partitioning and their persistence in the atmosphere. Rodgers et al. reported that chlorinated OPEs fit the profile of persistent and mobile organic compounds due to their mobility and persistence in surface waters.[20] As OPEs can be transported over long distances via air and water, it is interesting to know how they are conveyed to the remote environment especially in polar regions. It is published that atmospheric deposition, streams, and wastewater treatment plants accounts for 13%, 18% and 70% for the loadings of OPEs into Lake Ontario.[20] However, to our knowledge, there is no research for the polar areas on OPE transport pathways and their relatively distribution in the media.

2. Thesis aim and objective

Although many studies have been performed on the occurrence and properties of OPEs, their sources, behaviors and chemical fate are still not clear. Furthermore, in step with the rapid rise in OPE consumption, their emission rates into the environment are expected to have increased. This situation creates the need for OPE emission estimates as well as OPE LRT modeling, which are essential for risk assessment and the effectiveness of possible future regulation of OPEs.[43, 44]

The main aim of this thesis is to research OPEs in marine environments and their behaviors, sources and LRT potential, which can help us better understand OPE pollution. In **Paper I**, samples in air, seawater and snow from the North Atlantic and Arctic regions were collected to determine the occurrence of OPEs in remote oceanic areas. Based on these measurements, their spatial distribution, atmospheric deposition and air-seawater exchange processes are studied. Due to the restriction of OPEs (TCEP) in Europe, production capacities are expected to have been relocated to less regulated regions like East Aisa. In **Paper II**, the abundance, spatial distribution and seasonal trend of OPEs have been examined. This paper also focuses on the gas-particle partitioning behavior of OPEs. As mentioned above, the quantification of OPE emissions is very important. However, at present, OPE emission estimates are sparse. In **Paper III**, gridded global release rates into air and water have been estimated for TCPP. Based on the estimated global emissions, source-receptor relationships have been studied using the LRT models in **Paper IV**, which focuses on the impact of OPE pollutions on polar regions.

3. Methods

3.1. Sampling methods

In **Paper I**, samples were collected in the northeast Atlantic and Arctic Oceans (50°N-80°N) during expedition cruise ARK-XXVIII/2 onboard research vessel *Polarstern*. Nine air samples were collected with a high-volume air sampler from 8th to 24th of June 2014. Six snow samples were collected from 15th to 25th of June 2014. Twenty-five seawater samples were collected from 8th to 26th of June 2014. Atmospheric particle samples were collected with a glass fiber filter (GFF) with a diameter of 150 mm and a pore size of 0.7 µm, and a PUF/XAD-2 resin column was used to collect the gaseous phase.

In **Paper II**, fifteen air samples were obtained over the Bohai and Yellow Seas during a research cruise between 28th June and 13th July 2016 on research vessel *Dongfanghong-2*. Eighty-one air samples were collected from North Huangcheng Island (NHI) between 16th May 2015 and 21st March 2016. A high-volume air sampler was used to collect the air samples. Atmospheric particle and gaseous samples were collected with GFFs and PUF/XAD-2 resin columns, respectively.

3.2. Analysis methods

Air sample pretreatment and analysis followed the approach given by Möller et al.[21] Briefly, the PUF/XAD-2 resin columns and GFFs were spiked with 20 ng of d_{27}-TnBP, d_{12}-TCEP and d_{15}-TPhP as surrogates and extracted with an MX-Soxhlet using dichloromethane (DCM) for 16 h. Eight-hundred milliliters (800 mL) of melting snow water and seawater from each sample were subjected to liquid-liquid extraction using 50 ml DCM three times. All samples were concentrated down to 150 µl and then spiked with 500 pg $^{13}C_6$-PCB 208 as the injection standard. The samples were then analyzed using a gas chromatograph coupled to a triple quadrupole mass spectrometer (GC-MS/MS) equipped with a programmed temperature vaporizer (PTV) injector (Agilent, USA). More details are provided in **Papers I** and **II**.

In **Paper I**, eight OPEs were analyzed including TCPP (including three isomers), TCEP, TDCP, TnBP, TiBP, TPhP (triphenyl phosphate), TPeP (tripentyl phosphate), TEHP (tris(2-ethylhexyl) phosphate). Besides the above eight OPEs, **Paper II** also detected TCP (tricresyl phosphate, including four isomers).

3.3. Air-seawater gas exchange fluxes

In **Paper I**, the equilibrium status (or direction) of air-seawater gas exchange has been calculated, which is estimated based on[45]:

$$f_A / f_W = C_A R T_A / (C_w H) \tag{1}$$

where f_A / f_W is the fugacity ratio, C_A and C_w are the gaseous and dissolved concentrations in air and seawater, respectively (pg/m^3), and H is the Henry's law constant (Pa·m^3/mol) corrected by the given water temperature and salinity according to Schwarzenbach et al.[46] R is gas constant (8.31 Pa·m^3/K/mol), T_A is temperature in air (K).

The net air-water gas exchange fluxes are estimated using the modified Whitman two-film resistance model[47, 48]:

$$F_{AW} = K_{OL}\left(C_W - \frac{C_A}{H'_{salt,T}}\right) \tag{2}$$

where F_{AW} is the flux (pg/m^2/day). F_{AW} <0 represents OPE deposition from air into seawater, and F_{AW} >0 represents the volatilization from seawater into air. K_{OL} (m/day) is the gas phase overall mass transfer coefficient. $H'_{salt,T}$ is the dimensionless Henry's Law constant defined as $H'_{salt,T} = H/RT$.

3.4. Gas/particle partitioning methods

In **Paper II**, two prediction models are adopted: the Junge-Pankow (J-P) adsorption model and the octanol/air partition coefficient (K_{oa}-based) absorption model. The J-P model, proposed by Pankow in 1987, is based on subcooled vapor pressure (P_L°).[49] The particle-bound fraction φ_{J-P} of a target compound is estimated by[49]:

$$\varphi_{J-P} = \frac{c\theta}{p_L^{\circ} + c\theta} \tag{3}$$

where c is a constant that depends on the properties of the substance and θ is the surface area of the particle per unit volume of air (cm^2/cm^3). This study assumes c to be 17.2 Pa cm for OPEs[50] and θ to be 1.0 ×10^{-6} for rural air[51].

The predicted gas/particle partitioning coefficient $K_{p,koa}$ through the K_{oa}-based model is[52]:

$$logK_{p,koa} = logK_{oa} + logf_{OM} - 11.9 \tag{4}$$

where f_{OM} is the fraction of the organic matter (OM) phase in the aerosols. The temperature-dependent $logK_{oa}$ values were obtained from the report of Wang et al.[53]

The field-predicted particle-bound fraction based on the K_{oa}-based model (φ_{koa}) can be calculated from the following equation[49]:

$$\varphi_{koa} = \frac{K_{p,koa}C_{TSP}}{K_{p,koa}C_{TSP} + 1} \tag{5}$$

Where C_{TSP} is the total suspended particle concentration (µg/m^3).

3.5. Long-range transport modeling

LRT models have been applied in **Papers III** and **IV**, which are the Berkeley-Trent Global Contaminant Fate Model (BETR-Global)[54, 55] and the Canadian Model for Environmental Transport of Organochlorine Pesticides (CanMETOP)[56], respectively. BETR-Global is a multimedia fate and transport model at the global scale.[54, 55] The model divides the globe into grid cells, and the chemical fate in each grid cell is described using a multimedia model, with adjacent cells linked by air and water flows. CanMETOP is a three-dimensional dispersion model coupled with two-film models for air-water and air-snow/ice exchange and a fugacity-based mass balance model for soil-air exchange.[56]

3.6. Top-down estimate method for emissions

In **Paper III**, the top-down approach method is used for the TCPP emission estimates, which combines field measurements of atmospheric concentrations and inverse chemical fate modeling to calculate the emissions. We present gridded global emission estimates into air and water that are initially based on the assumption that the emissions are directly proportional to the intensity of nighttime artificial light emitted to space from Earth. Then, we update the initial emission rate by comparing the measured concentrations of TCPP with the predictions from a global chemical fate and transport model. Our updated global gridded emission rate thus combines information from measurements in air and water with global atmospheric transport modeling. The emission rate is updated based on the atmospheric and oceanic transport simulated using BETR-Global. A separate and independent model, CanMETOP, is used to cross-validate selected scenarios for TCPP properties and emission factors.

3.7. Source-receptor relationships

Seven continental areas are studied as TCPP source regions in this study, including four northern hemisphere areas defined by the Task Force on Hemispheric Transport of Air Pollution (TF-HTAP)[57] (North America, Europe, East Asia, South Asia, Figure 3-1) and three southern hemisphere areas (South America, Africa and the Indonesia to Australia region, Figure 3-1). The polar regions (Arctic and Antarctic) are defined as the principal receptor regions of interest (Figure 3-1). The source-receptor relationships are simulated by running the model with global emissions first and then with emissions only occurring in one source region at a time (eight scenarios). The rest of the world, excluding the target source regions, is also set as an emission region in a ninth scenario to validate the results. In each scenario, the model is run for eight years (spin-up) to achieve stable environmental TCPP levels, considering the accumulations from the various media. The statistics in this study for source-receptor relationships are conducted using the results of 8th years. More details on scenarios and calculations are shown in **Paper IV**.

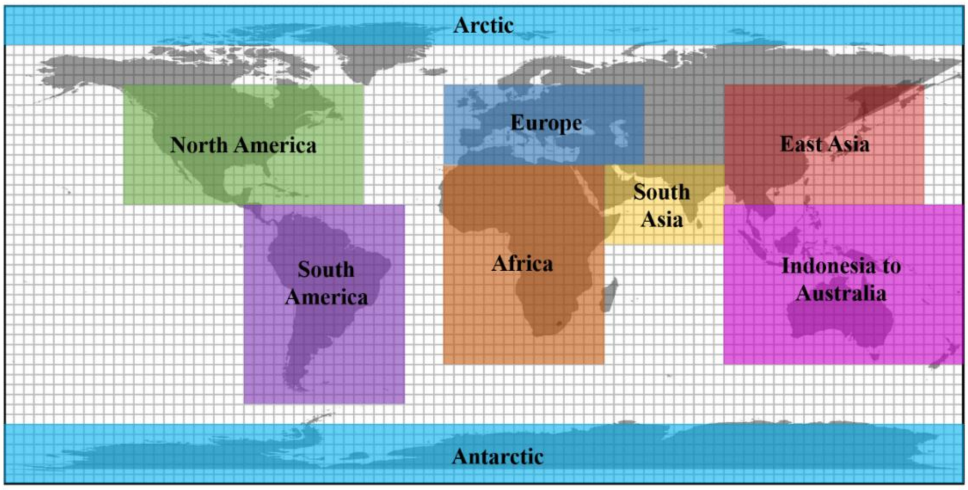

Figure 3-1: Source and receptor regions investigated in this study

4. Results and discussion

4.1. Occurrence and behaviors of OPEs in air

4.1.1. Occurrence of OPEs in air

OPEs in the air over the northeast Atlantic and Arctic regions have been reported in **Paper I**. The sum of gaseous and particle concentrations (∑OPE) ranged from 35 to 340 pg/m^3. Three chlorinated OPEs accounted for 88 ± 5.0% of the ∑OPE. The most abundant OPE is TCEP, with concentrations ranging from 30 to 230 pg/m^3, followed by three major OPEs, TCPP (0.80 to 82 pg/m^3), TnBP (2.0 to 19 pg/m^3) and TiBP (0.30 to 14 pg/m^3).

In **Paper II**, atmospheric OPEs were determined for the Bohai and Yellow Seas. The total concentration of nine OPEs ranged from 100 to 750 pg/m^3 (median: 280 pg/m^3). Three chlorinated OPEs account for 66 ± 15% of the total OPEs, and the remainder is composed of six nonchlorinated OPEs (34 ± 15%). TCPP is the most abundant OPE (range: 43-530 pg/m^3), followed by TCEP (range: 27-150 pg/m^3), TiBP (range: 19-210 pg/m^3), and TnBP (range: 3.0-37 pg/m^3).

Compared to the detected OPEs over the North Sea[21], decreasing trends are observed from the North Sea towards the Atlantic and Arctic Oceans (Figure 4-1). Due to decades-long regulation of TCEP in Europe, TCPP is the dominant OPE congener as excepted, which has been used as a TCEP substitute and accounts for >50% of the total OPE consumption.[2, 6] However, TCEP predominated in the atmosphere of European Arctic region. This finding demonstrates that TCEP has a higher persistence potential in air compared to TCPP. Due to the regulations, OPE production capacities are relocated to less regulated regions such as East Asia. As a result, different OPE occurrence patterns are observed over the Bohai and Yellow Seas, with TCEP being the major component together with TCPP and TiBP. However, similar ∑OPE concentrations were observed over the North Sea (390 ± 120 pg/m^3)[21] and the Bohai and Yellow Seas (320 ± 160 pg/m^3, Figure 4-1).

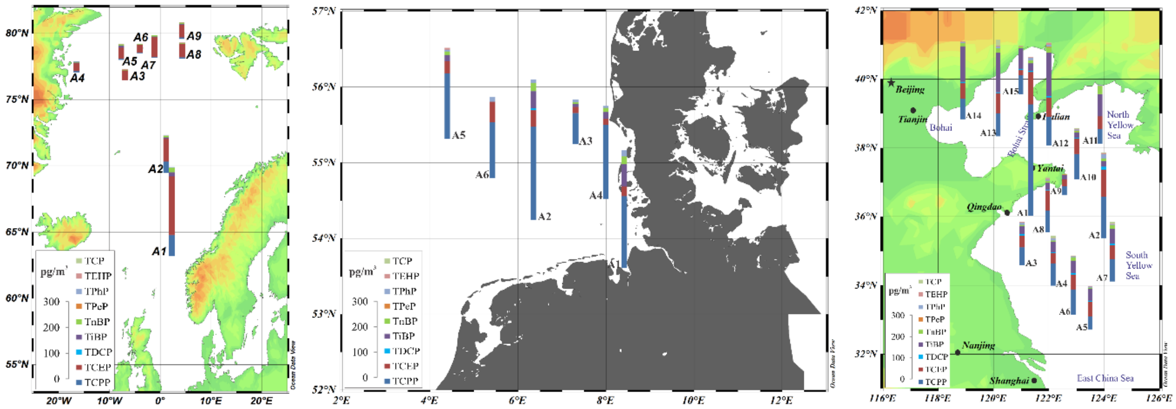

a b c

Figure 4-1: a. spatial distribution of OPEs in air of the North Atlantic and Arctic (this study); b. spatial distribution of OPEs in air of the North Sea (Möller et al.)[21]; c. spatial distribution of OPEs in air of the Bohai and Yellow Seas, China (this study).

4.1.2. Seasonal trend of OPEs

The seasonal trend of OPEs has been analyzed in **Paper II**, based on the 81 air samples that were collected on the NHI between May 16th, 2015, and March 21st, 2016. There is no significant difference between the ∑OPE concentrations in air among the different seasons. In only the gaseous phase, significantly higher concentrations of ∑OPEs and individual OPEs ($p < 0.05$) are found in summer than in winter due to higher temperature and higher relative humidity (RH) in summer. For the particulate phase, higher TCPP and TiBP concentrations are observed in summer than in winter, which is opposite to the TPhP and TEHP concentrations ($p<0.05$). The seasonal variation patterns of particle-bound OPEs are more indicative of the varying air mass origins than the ambient environmental conditions, which is contrary to the gaseous OPEs.

4.1.3. Measured particle-bound fractions of OPEs

Over the northeast Atlantic and Arctic regions, the particle phase OPEs contribute 67 ± 17% of the total OPEs on average (in **Paper I**). The particle-bound fractions of the four major OPEs are found in the sequence of TCEP (74 ± 15%) > TnBP (72 ± 28%) > TiBP (30 ± 26%) > TCPP (27 ± 30%). Over the Bohai and Yellow Seas (in **Paper II**), on average, the particle-bound OPEs account for 51 ± 21% of the total OPEs. The mean particle-bound fractions of the four major OPEs are in the order of TCPP (63 ± 19%) > TCEP (51 ± 19%) > TnBP (47± 23%) > TiBP (30 ± 25%). The particle-bound fractions in these two regions are lower than that over the North Sea reported by Möller et al. (mean, 86 ± 25%)[21] and comparable to that along the German coast (an average of 55%).[42]

4.1.4. Gas-particle partitioning prediction

OPEs can be detected in both the particulate and gaseous phases, and it is important to know how OPEs partition between the two phases in the atmosphere, which can affect the fate and LRT of OPEs in the environment. In **Paper II**, the partitioning behavior of OPEs between the gaseous and particulate phases is investigated based on the 81 samples obtained from NHI, with the temperature, RH and C_{TSP} ranges are -4.0 to 27 °C, 30% to 94% and 16 to 240 μg/m^3, respectively. Among the investigated samples, significant correlations between the measured OPE gas/particle partitioning coefficients ($K_{p,m}$) and P_L° ($p<0.05$) are found for only 14 samples, suggesting that OPEs have a low potential to achieve equilibrium or are sensitive to the artificial sampling method.

4.1.5. Dry deposition of OPEs in air

The dry particle deposition fluxes are determined by multiplying the particle OPE concentration by the dry deposition velocity.[22, 58] As no measured OPE velocities are available for the target area, a value of 0.10 cm/s (86 m/day)[58] has been chosen for the Atlantic and Arctic regions (in **Paper I**) and 0.55 cm/s (475 m/day)[59] for the Bohai and Yellow Seas (**Paper II**) based on the literature.

The particle phase dry depositions into the Atlantic and Arctic regions of ∑OPE vary from 2.0 to 16 ng/m^2/day. The ΣOPE dry depositions into the Bohai and Yellow Seas range from 21 to 250 ng/m^2/day. The deposition fluxes of ∑OPE in the Atlantic and Arctic regions are comparable to the levels estimated in the South China Sea (mean 16 ± 6.7 ng/m^2/day),[24] and are 1-2 orders of magnitude lower than those estimated in the North Sea (46-240 ng/m^2/day)[21] and the Bohai and Yellow Seas (21–250 ng/m^2/day), the Mediterranean Sea (70–880 ng/m^2/day)[22] and the Black Sea (~300–1,100 ng/m^2/day)[22] (Figure 4-2).

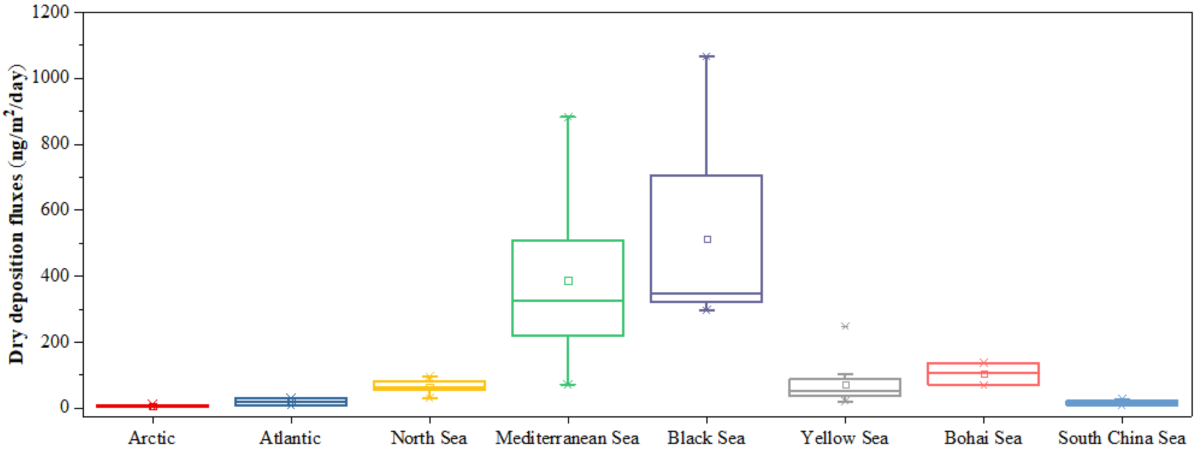

Figure 4-2: Dry depositions of OPEs in different marine environment.

4.2. Occurrence of OPEs in snow

The concentrations of ∑OPE range from 4,400 to 10,600 pg/L with a mean of 7,800 ± 2,700 pg/L. Chlorinated OPEs account for 66 ± 14% and non-chlorinated OPEs account for 34 ± 14% of the total OPEs. TCPP is the most abundant OPE in snow, followed by TiBP, TCEP and TnBP. There is a decreasing ΣOPE concentration trend from the coast to the open ocean (more details in **Paper I**). The mean concentration of dominated OPE (TCPP: ~3.9 ng/L) in this study is one to three orders of magnitude lower than those in urban areas, such as in central Germany (range of 46-2,700 ng/L, rainwater)[60], Italy (range of 630-740 ng/L, rainwater)[61], and northern Sweden (range of 100-220 ng/kg, snow) [62].

4.3. Occurrence of OPEs in seawater

The ∑OPE concentrations in Atlantic and Arctic seawater (**Paper I**) ranged from 350 to 8,400 pg/L. The highest concentrations of ∑OPE are found at sites near continents. When the ship is heading to the open ocean, much lower ∑OPE concentrations are shown. Near the European continent, a fresh discharge of OPEs might have originated from the North Sea, with reported OPE concentrations in the North Sea being 5-10 times higher than those in samples collected towards the Atlantic Ocean. Along the Greenland and Svalbard coasts, glacier and snow melting contributed to the OPEs in seawater to a certain degree, considering the high OPE concentrations in snow detected in this study. Furthermore, closer to Greenland and Svalbard, higher ∑OPE concentrations were detected in snow. The discharge of melting snow and ice in the Arctic summer can be a secondary source of organic contaminates and may cause elevated concentrations in the Arctic Ocean.

4.4. Air-seawater exchanges

The result of **Paper I** shows that there was volatilization of OPEs from seawater into the atmosphere in the Atlantic and Arctic Oceans based on the H values from the SPARC On-Line Calculator.[63] However, the calculated H values based on the measured solubility (SL) and vapor pressure (P_L°) ($H = MW \times P_L^{\circ}/SL$, MW: molecular weight; Table 4-1) have a large discrepancy with the estimated H values from SPARC. Considering the reliability, we recalculated the air-seawater exchange fluxes based on H values derived from measured solubility and vapor pressure here. Generally, $f_A / f_W = 1$ means a system at equilibrium, whereas $f_A / f_W < 1$ and $f_A / f_W > 1$ indicate volatilization and deposition, respectively.

The uncertainty of H has been calculated according to the method proposed by MacLeod et al.[64] In MacLeod et al.'s paper, the uncertainty of a variable is described using its confidence factor (*Cf*). A confidence factor of, e.g., 3 indicates that 95% of all values in the distribution lie between 1/3 and 3 times the median.[64] The uncertainty of H lies in the variance of SL and P_L°. Then Cf of H is described as:

$$Cf_H = \exp[S_{SL}^2(\ln Cf_{SL})^2 + S_P^2(\ln Cf_P)^2]^{1/2} \tag{6}$$

S_{SL} and S_P is the sentivity (S) of H to changes in SL and P_L°, respectively. By modifiy the vaules of SL and P_L° separately by 0.1% (ΔI, I: input), and mornitoring the corresponding change in H (ΔO, O: output), then S can be achieved ($S = (\frac{\Delta O}{O})/(\frac{\Delta I}{I})$). Cf of P_L° (Cf_P) for TCEP and TCPP can be devised from Brommer et al. which are 1.6 (Table 4-1).[65] Cf_P of TiBP and TnBP are assumed as same as TCEP and TCPP, since there measured uncertainties are not available. The Cf of SL for the four OPEs are not obtainable either, then a avule of 1.5 is adopted here as referred the assumption of MacLeod et al.[64] Then the calculated Cf of H is 1.8, which means the standard deviation (σ) is 0.30 ($\sigma = 0.5 lnCf$)[64].

Table 4-1: Paramaters used for the calculation of henrry's law constant.

OPEs	P_L° (Pa)	SL (mg/L)	Cf of P_L°	Cf of SL
TCEP	0.048[65]	8,380[66]	1.6	1.5
TCPP	0.035[65]	1,160[67]	1.6	1.5
TiBP	0.200[a]	260[a]	1.6	1.5
TnBP	0.151[68]	280[69]	1.6	1.5

[a]: Use the estimate value from EPI suite 4.1.

The uncertainty of H for OPEs is samilar with that of PCBs estimated by Bruhn et al. (0.31).[70] Considering the uncertainties of H and concentrations in air and seawater, a range of 0.30 to 3.0 is adopted for f_A / f_W (*Cf*=3.0), which shows a system at dynamic equilibrium (more details in paper of Bruhn et al.).[70]

The recalculated results show that the f_A / f_W values of TCEP ranged from 46 to 4,900 (Figure 4-3), indicating that deposition from air into seawater dominated in all samples. The fluxes of TCEP range from -72 to -1.1 ng/m^2/day (Figure 4-3). There is a net deposition for TCPP, with all f_A / f_W values >3.0 except for sample W19 (f_A / f_W = 1.5), which dues to relatively low concentration in air and relatively high level in seawater. The fluxes of TCPP range from -36 to -0.16 ng/m^2/day. For TiBP, most f_A / f_W values are in a range of 0.30 to 30, which indicates the equilibrium state achieved with fluxes in a range of -2.0 to 9.6 ng/m^2/day. TnBP in more than half amount of stations shows net deposition with a median f_A / f_W values is 3.2 and the fluxes are from -3.2 to 0.60 ng/m^2/day.

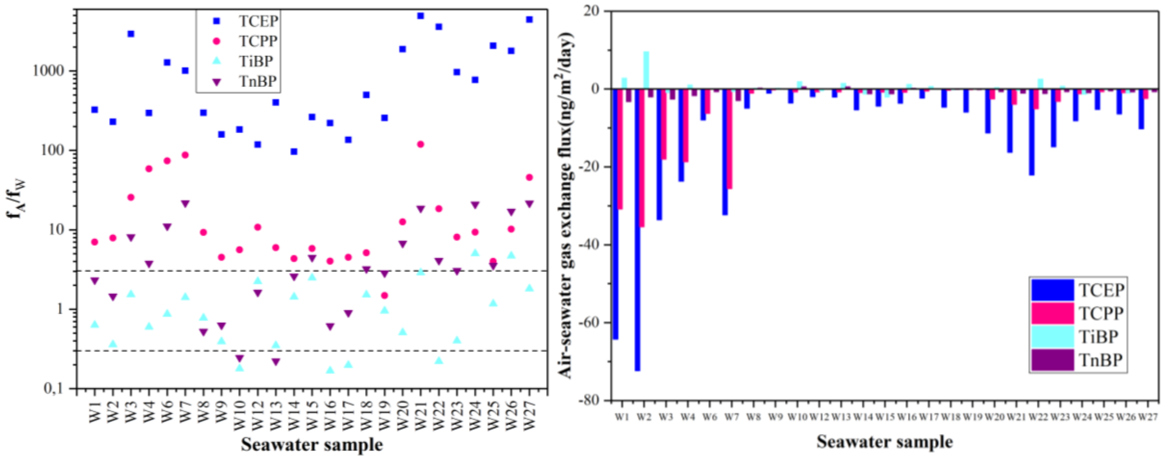

Figure 4-3: Air-seawater exchange ratios (left) and fluxes (right) of four major OPEs in seawater of the North Atlantic and the Arctic.

4.5. Gridded global emission of TCPP

In **Paper III**, thirty-six scenarios that represent combinations of different degradation half-lifetime values of TCPP in air ($t_{1/2,\ \mathrm{Air}}$: 12, 60, and 300 h) and in water ($t_{1/2,\ \mathrm{Water}}$: 1440, 3600, 7200, and 36000 h), as well as a range of direct-to-water emission factors (E_W: 0, 0.5 and 1 times the emission into air (E_A)), are tested. The modeled TCPP concentrations in the global environment are compared to a database of 129 measurements in air and 22 measurements in ocean water that we assembled from the literature. The correlation coefficients (r^2) between the modeled and measured concentrations range between 0.45 and 0.50 in the different scenarios, indicating that the model scenarios account for up to 50% of the variability in the measured TCPP concentrations. Our updated global TCPP emission scenarios result in total emissions into air and water between 12.0 and 157 kt/y (1 kt/y=1 Gg/y). Among the emission source regions, Europe (38%), North America (24%) and East Asia (13%) release the most

TCPP into the global environment in the updated emission scenarios. The model scenario with values of $t_{1/2,\text{ Air}}$ and $t_{1/2,\text{ Water}}$ of 12 h and 3,600 h, respectively, using updated global emissions into air and water of 78.6 kt/y (Figure 4-4) and 39.3 kt/y, respectively, is in good agreement with the measurements (r^2 = 0.48 and 0.46 and RMSE = 0.94 and 0.81 for the model-measurement comparisons of the atmospheric and oceanic data, respectively) and is suggested as a useful base case reference scenario.

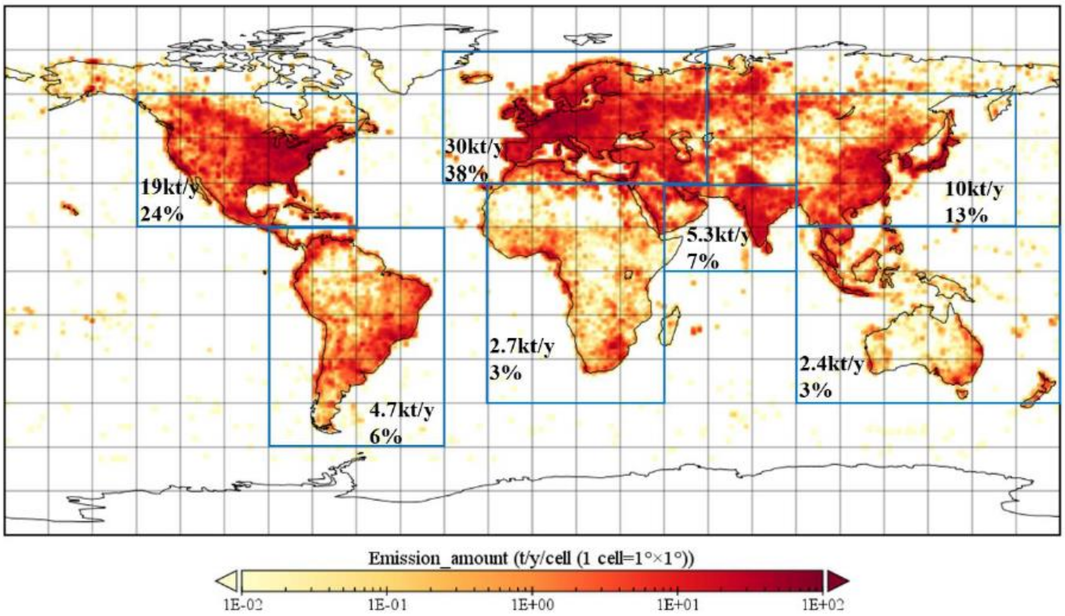

Figure 4-4: Gridded global emissions of TCPP and contributions of source regions as well as corresponding emission rate (globe: 78.6 kt/y).

4.6. Loading to the polar regions

4.6.1. TCPP pollution in the polar regions

The research of **Paper IV** shows that The annual average TCPP concentrations are 16.2 pg/m^3, 38.1 pg/m^3 and 136 pg/L in the Arctic lower air, upper air and seawater compartments, respectively. In total, 114 t of TCPP is found in the Arctic, with 98.4% distributed in seawater (113 t) and 1.6% in air (1.85 t). The major contributor of TCPP in the Arctic is Europe (23.0%, 26.4 t), followed by East Asia (7.8%, 8.9 t) and North America (0.86%, 0.98 t) (Figure 4-5).

The other major contributors are northern Europe and northern Asia (north of Russia), which are not included in target source regions in this study.

For the Antarctic, the annual mean concentrations of TCPP are 0.10 pg/m^3, 0.13 pg/m^3 and 0.10 pg/L in lower air, upper air and seawater, receptively. An amount of 0.36 t TCPP is found in the Antarctic, with 95.7% in seawater and 4.3% in air, which are similar to the results of the Arctic. South America (57.0%), the Indonesia to Australia region (18.4%) and Africa (2.3%) are the main sources of TCPP in the Antarctic (Figure 4-5).

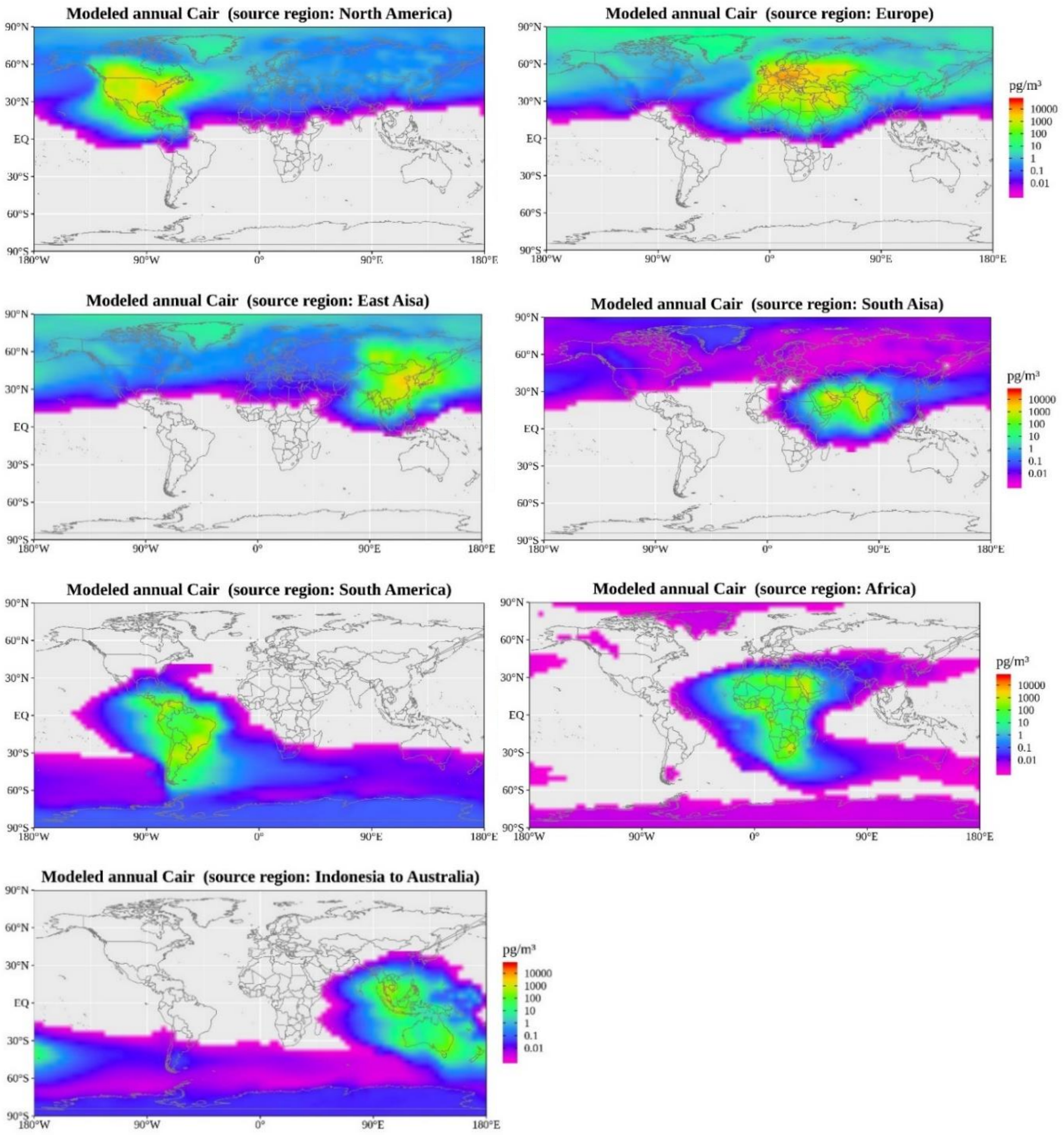
Modeled annual Cair (source region: North America)

Modeled annual Cair (source region: Europe)

Modeled annual Cair (source region: East Aisa)

Modeled annual Cair (source region: South Aisa)

Modeled annual Cair (source region: South America)

Modeled annual Cair (source region: Africa)

Modeled annual Cair (source region: Indonesia to Australia)

Figure 4-5: Global distribution of TCPP concentrations in lower air with different source regions

4.6.2. Loading pathways to polar regions

Most of the inventory of TCPP in polar regions is distributed in seawater (Arctic: 98.4%, Antarctic: 95.7%). Then it is important to know the transport pathways of TCPP to popar seawater which is investigated in **Paper IV**. Oceanic transport accounts for 89.1% of TCPP in Arctic seawater, followed by wet deposition (9.7%). Whereas, dry deposition and air-seawater exchange processes have little impact. For the Antarctic, the dominant input pathway is also oceanic transport (46.3%), although its role is less important than that in the Arctic. Atmospheric deposition contributes more than 40.0% of TCPP in Antarctic seawater (wet deposition: 24.9%, dry deposition: 9.7%, air-seawater exchange: 8.1%).

4.6.3. Seasonal variation in TCPP LRT

A seasonal trend is observed for modeled TCPP levels in the air in the polar receptor regions, with higher concentrations in winter than in summer. In February, a total of 5,070 kg TCPP is found in Arctic air, which is two orders of magnitude higher than in August (35.4 kg) (scenario: Ew+Ea). For the Antarctic, there is 45.6 kg of TCPP in August (winter in the southern hemisphere), which is two orders of magnitude higher than that of February (0.47 kg). The analysis of **Paper IV** indicates that the variable hydroxyl radical (·OH) concentration is the major contributor to this phenomenon, followed by temperature (Table S15). However, wind pattern and precipitation have little effect on the seasonal variance of TCPP levels in polar regions. The ·OH radical is the major oxidant that destroys chemicals in the atmosphere. It is produced by a photochemical reaction, so it occurs at higher levels in the summer (when there is more direct sunlight) than in the winter. Especially in the polar regions when it is dark for up to 24 hours in the winter, the ·OH radical concentrations are basically zero in the winter.

5. Conclusions and future perspectives

The overall focus of this thesis is on the occurrence and behavior of OPEs in marine environments as well as their LRT from source regions to remote areas. **Paper I** presents a decreasing trend for the ∑OPE concentrations in the atmosphere and seawater from the North Atlantic to the Arctic Ocean, indicating the current ongoing atmospheric and water releases of these compounds from Europe. Although TCEP was replaced by TCPP in Europe, TCEP is still detected as the dominant OPE in the atmosphere, and the TCEP concentration is approximately nine times higher than the TCPP concentration. On the other hand, in snow and seawater, the dominant OPE is TCPP. This finding suggests that TCEP is more stable than TCPP in the atmosphere. The mean ∑OPE concentration in snow is 7,800 pg/L, which is approximately two times as high as that in seawater (2,900 pg/L), suggesting that snow is an important intermediate for OPE accumulation in the Arctic region.

In Paper II, the spatial and seasonal variances of OPEs have been investigated. Significantly seasonal trend of OPE levels are found in the gaseous phase. The gas-particle partitioning process has been studied, and OPEs show a low potential to achieve equilibrium or are sensitive to artificial sampling. The dry deposition levels of OPEs from air into seawater in the Bohai and Yellow Seas and North Sea are comparable, which are two to four times higher than that into the northeast Atlantic Ocean and one order of magnitude higher than that into the Arctic Ocean.

For the first time, gridded global TCPP emissions have been evaluated in **Paper III**. The negligible effect of volatilization from seawater to the atmosphere confirms that the TCPP in remote regions mainly originates from atmospheric transport from source regions and seawater appears to be a TCPP sink. The suggested half-lifetimes in air (12 h) and seawater (3,600 h) contribute to a more accurate characterization of the fate of TCPP in the global environment. Due to the uncertainties inherent in our method, the paucity of the measurement data in the global atmosphere and oceans, and the poor agreement between our emission estimates and those for the city of Toronto and the EU, the global emission range (12.0 ~ 157 kt/y) should at best be treated as a preliminary estimate with high uncertainties. On the other hand, the established spatial patterns of TCPP release in this study are an important step for a better clarification of its environmental fate for further research on risk management and policymaking. Based on the estimated gridded emissions, **Paper IV** evaluated the contributions of TCPP source regions to polar environments. Results show that water transport is the major pathways for TCPP pollution in seawater of the polar regions. The high emissions in North hemisphere are the dominated source of TCPP in the Arctic, while it is not efficiently conveyed across the equator to the Antarctic.

In the future, it will be meaningful to investigate the environmental behavior, emission levels and LRT potential of other OPE congeners as well as other POPs, which will help improve the knowledge of these pollutants and increase the understanding of environmental contamination. In addition, it is necessary to conduct further research on human exposure risk assessment of these compounds to obtain useful information for pollutant regulation and policymaking.

6. References

1. Van der Veen, I.; de Boer, J., Phosphorus flame retardants: Properties, production, environmental occurrence, toxicity and analysis. *Chemosphere* **2012,** *88*, (10), 1119-1153.
2. Green, N.; Schlabach, M.; Bakke, T.; Brevik, E.; Dye, C.; Herzke, D.; Huber, S.; Plosz, B.; Remberger, M.; Schøyen, M., Screening of selected metals and new organic contaminants 2007. Phosphorus flame retardents, polyfluorinated organic compounds, nitro-PAHs, silver, platinum and sucralose in air, wastewater treatment falcilities, and freshwater and marine recipients. **2008**.
3. Zhang, Y., Global market analysis of flame retardant (in Chinese with English abstract). *Fine Specialty Chem.* **2014,** *22*, (8), 20-24.
4. Reemtsma, T.; Quintana, J. B.; Rodil, R.; Garcia-Lopez, M.; Rodriguez, I., Organophosphorus flame retardants and plasticizers in water and air I. Occurrence and fate. *Trac.-Trend Anal. Chem.* **2008,** *27*, (9), 727-737.
5. Marklund, A.; Andersson, B.; Haglund, P., Organophosphorus flame retardants and plasticizers in air from various indoor environments. *J. Environ. Monit.* **2005,** *7*, (8), 814-819.
6. EU Risk Assessment Report, Tris(2-chloro-1-methylethyl) phosphate (TCPP). CAS No.: 13674-84-5. EINECS No.: 237-158-7. **2008**.
7. Annex XIV of REACH. Authorisation List. https://echa.europa.eu/authorisation-list.
8. Fries, E.; Mihajlovic, I., Pollution of soils with organophosphorus flame retardants and plasticizers. *J. Environ. Monitor.* **2011,** *13*, (10), 2692-2694.
9. Substance in preparations in Nordic countries (SPIN) online database. http://www.spin2000.net/spinmyphp/. Accessed in 01.2018.
10. Watanabe, I., Historical Developments of BFR Research. Fifth international symposium on brominated flame retardants. Kyoto, Japan. 2010.
11. OECD, Risk Reduction Monograph No. 3: Selected Brominated Flame Retardants Background and National Experience with Reducing Risk. *Organisation for Economic Co-operation and Development, Paris* **1995**.
12. Ao, C.; Lin, J., Present situation and development prospect of organophosphorus flame retardants (in Chinese). *Sichuan Chem. Ind.* **1999,** *2*, (5), 30-34.
13. Wei, G. L.; Li, D. Q.; Zhuo, M. N.; Liao, Y. S.; Xie, Z. Y.; Guo, T. L.; Li, J. J.; Zhang, S. Y.; Liang, Z. Q., Organophosphorus flame retardants and plasticizers: Sources, occurrence, toxicity and human exposure. *Environ. Pollut.* **2015,** *196*, 29-46.
14. Makinen, M. S. E.; Makinen, M. R. A.; Koistinen, J. T. B.; Pasanen, A. L.; Pasanen, P. O.; Kalliokoski, P. I.; Korpi, A. M., Respiratory and Dermal Exposure to Organophosphorus Flame Retardants and Tetrabromobisphenol A at Five Work Environments. *Environ. Sci. Technol.* **2009,** *43*, (3), 941-947.
15. Möller, A.; Sturm, R.; Xie, Z. Y.; Cai, M. H.; He, J. F.; Ebinghaus, R., Organophosphorus Flame Retardants and Plasticizers in Airborne Particles over the Northern Pacific and Indian Ocean toward the Polar Regions: Evidence for Global Occurrence. *Environ. Sci. Technol.* **2012,** *46*, (6), 3127-3134.
16. Ou, Y., Developments of organic phosphorus flame retardant industry in China (in Chinese with English abstract). *Chem. Ind. Eng. Prog.* **2011,** *30*, (1), 210-215.
17. China's flame retardant industry in 2015 will be steady development. http://www.chinairn.com/news/20150114/164023439.shtml *ChinaIRN.com* **2015.1.14**.
18. EU Risk Assessment Report, Tris(2-chloro-1-(chloromethyl)ethyl) phosphate (TDCP). CAS No.: 13674-87-8. EINECS No.: 237-159-2. **2008**.
19. Shanghai Shuoxun Chemical Technology Company (SSCTC). The Market Research Report of PFRs. http://www.shuoxun-report.com/. **2017**.

20. Rodgers, T. F. M.; Truong, J. W.; Jantunen, L. M.; Helm, P. A.; Diamond, M. L., Organophosphate Ester Transport, Fate, and Emissions in Toronto, Canada, Estimated Using an Updated Multimedia Urban Model. *Environ. Sci. Technol.* **2018,** *52*, (21), 12465-12474.
21. Möller, A.; Xie, Z. Y.; Caba, A.; Sturm, R.; Ebinghaus, R., Organophosphorus flame retardants and plasticizers in the atmosphere of the North Sea. *Environ. Pollut.* **2011,** *159*, (12), 3660-3665.
22. Castro-Jimenez, J.; Berrojalbiz, N.; Pizarro, M.; Dachs, J., Organophosphate Ester (OPE) Flame Retardants and Plasticizers in the Open Mediterranean and Black Seas Atmosphere. *Environ. Sci. Technol.* **2014,** *48*, (6), 3203-3209.
23. Salamova, A.; Peverly, A. A.; Venier, M.; Hites, R. A., Spatial and Temporal Trends of Particle Phase Organophosphate Ester Concentrations in the Atmosphere of the Great Lakes. *Environ. Sci. Technol.* **2016,** *50*, (24), 13249-13255.
24. Lai, S.; Xie, Z.; Song, T.; Tang, J.; Zhang, Y.; Mi, W.; Peng, J.; Zhao, Y.; Zou, S.; Ebinghaus, R., Occurrence and dry deposition of organophosphate esters in atmospheric particles over the northern South China Sea. *Chemosphere* **2015,** *127*, 195-200.
25. Cheng, W. H.; Xie, Z. Q.; Blais, J. M.; Zhang, P. F.; Li, M.; Yang, C. Y.; Huang, W.; Ding, R.; Sun, L. G., Organophosphorus esters in the oceans and possible relation with ocean gyres. *Environ. Pollut.* **2013,** *180*, 159-164.
26. Salamova, A.; Hermanson, M. H.; Hites, R. A., Organophosphate and Halogenated Flame Retardants in Atmospheric Particles from a European Arctic Site. *Environ. Sci. Technol.* **2014,** *48*, (11), 6133-6140.
27. Sühring, R.; Diamond, M. L.; Scheringer, M.; Wong, F.; Pucko, M.; Stern, G.; Burt, A.; Hung, H.; Fellin, P.; Li, H.; Jantunen, L. M., Organophosphate Esters in Canadian Arctic Air: Occurrence, Levels and Trends. *Environ. Sci. Technol.* **2016,** *50*, (14), 7409-7415.
28. Rauert, C.; Schuster, J. K.; Eng, A.; Harner, T., Global Atmospheric Concentrations of Brominated and Chlorinated Flame Retardants and Organophosphate Esters. *Environ. Sci. Technol.* **2018,** *52*, (5), 2777-2789.
29. Bollmann, U. E.; Möller, A.; Xie, Z. Y.; Ebinghaus, R.; Einax, J. W., Occurrence and fate of organophosphorus flame retardants and plasticizers in coastal and marine surface waters. *Water Res.* **2012,** *46*, (2), 531-538.
30. Gao, X. Z.; Huang, C.; Rao, K. F.; Xu, Y. P.; Huang, Q. H.; Wang, F.; Ma, M.; Wang, Z. J., Occurrences, sources, and transport of hydrophobic organic contaminants in the waters of Fildes Peninsula, Antarctica. *Environ. Pollut.* **2018,** *241*, 950-958.
31. McDonough, C. A.; De Silva, A. O.; Sun, C. X.; Cabrerizo, A.; Adelman, D.; Soltwedel, T.; Bauerfeind, E.; Muir, D. C. G.; Lohmann, R., Dissolved Organophosphate Esters and Polybrominated Diphenyl Ethers in Remote Marine Environments: Arctic Surface Water Distributions and Net Transport through Fram Strait. *Environ. Sci. Technol.* **2018,** *52*, (11), 6208-6216.
32. Kim, U. J.; Kannan, K., Occurrence and Distribution of Organophosphate Flame Retardants/Plasticizers in Surface Waters, Tap Water, and Rainwater: Implications for Human Exposure. *Environ. Sci. Technol.* **2018,** *52*, (10), 5625-5633.
33. Camarasa, J. G.; Serra-Baldrich, E., Allergic contact dermatitis from triphenyl phosphate. *Contact Dermatitis* **1992,** *26*, (4), 264-5.
34. Matthews, H. B.; Eustis, S. L.; Haseman, J., Toxicity and carcinogenicity of chronic exposure to tris(2-chloroethyl)phosphate. *Fundam. Appl. Toxicol.* **1993,** *20*, (4), 477-85.
35. Sundkvist, A. M.; Olofsson, U.; Haglund, P., Organophosphorus flame retardants and plasticizers in marine and fresh water biota and in human milk. *J. Environ. Monit.* **2010,** *12*, (4), 943-51.

36. Kim, J. W.; Isobe, T.; Chang, K. H.; Amano, A.; Maneja, R. H.; Zamora, P. B.; Siringan, F. P.; Tanabe, S., Levels and distribution of organophosphorus flame retardants and plasticizers in fishes from Manila Bay, the Philippines. *Environ. Pollut.* **2011,** *159*, (12), 3653-3659.
37. Li, J.; Xie, Z.; Mi, W.; Lai, S.; Tian, C.; Emeis, K.-C.; Ebinghaus, R., Organophosphate Esters in Air, Snow and Seawater in the North Atlantic and the Arctic. *Environ. Sci. Technol.* **2017,** *51*, 6887−6896.
38. Castro-Jimenez, J.; Gonzalez-Gaya, B.; Pizarro, M.; Casal, P.; Pizarro-Alvarez, C.; Dachs, J., Organophosphate Ester Flame Retardants and Plasticizers in the Global Oceanic Atmosphere. *Environ. Sci. Technol.* **2016,** *50*, (23), 12831-12839.
39. Li, C.; Chen, J. W.; Xie, H. B.; Zhao, Y. H.; Xia, D. M.; Xu, T.; Li, X. H.; Qiao, X. L., Effects of Atmospheric Water on ·OH-initiated Oxidation of Organophosphate Flame Retardants: A DFT Investigation on TCPP. *Environ. Sci. Technol.* **2017,** *51*, (9), 5043-5051.
40. Liu, Y.; Liggio, J.; Harner, T.; Jantunen, L.; Shoeib, M.; Li, S. M., Heterogeneous OH Initiated Oxidation: A Possible Explanation for the Persistence of Organophosphate Flame Retardants in Air. *Environ. Sci. Technol.* **2014,** *48*, (2), 1041-1048.
41. Liu, Y.; Huang, L.; Li, S. M.; Harner, T.; Liggio, J., OH-initiated heterogeneous oxidation of tris-2-butoxyethyl phosphate: implications for its fate in the atmosphere. *Atmos. Chem. Phys.* **2014,** *14*, (22), 12195-12207.
42. Wolschke, H.; Sühring, R.; Mi, W. Y.; Moller, A.; Xie, Z. Y.; Ebinghaus, R., Atmospheric occurrence and fate of organophosphorus flame retardants and plasticizer at the German coast. *Atmos. Environ.* **2016,** *137*, 1-5.
43. Breivik, K.; Sweetman, A.; Pacyna, J. M.; Jones, K. C., Towards a global historical emission inventory for selected PCB congeners - a mass balance approach 2. Emissions. *Sci. Total Environ.* **2002,** *290*, (1-3), 199-224.
44. Breivik, K.; Sweetman, A.; Pacyna, J. M.; Jones, K. C., Towards a global historical emission inventory for selected PCB congeners - A mass balance approach-3. An update. *Sci. Total Environ.* **2007,** *377*, (2-3), 296-307.
45. Xie, Z.; Koch, B. P.; Moller, A.; Sturm, R.; Ebinghaus, R., Transport and fate of hexachlorocyclohexanes in the oceanic air and surface seawater. *Biogeosciences* **2011,** *8*, (9), 2621-2633.
46. Schwarzenbach, R. P.; Gschwend, P. M. I., D. M., *Environmental organic chemistry* Second Edition ed.; New Jersey: A John Wiley & Sons, Inc: 2003.
47. Liss, P. S.; Slater, P. G., Flux of Gases across Air-Sea Interface. *Nature* **1974,** *247*, (5438), 181-184.
48. Bidleman, T. F.; Mcconnell, L. L., A Review of Field Experiments to Determine Air-Water Gas-Exchange of Persistent Organic Pollutants. *Sci. Total. Environ.* **1995,** *159*, (2-3), 101-117.
49. Pankow, J. F., Review and Comparative-Analysis of the Theories on Partitioning between the Gas and Aerosol Particulate Phases in the Atmosphere. *Atmos. Environ.* **1987,** *21*, (11), 2275-2283.
50. Wang, Z.; Na, G. S.; Ma, X. D.; Fang, X. D.; Ge, L. K.; Gao, H.; Yao, Z. W., Occurrence and gas/particle partitioning of PAHs in the atmosphere from the North Pacific to the Arctic Ocean. *Atmos. Environ.* **2013,** *77*, 640-646.
51. Lohmann, R.; Lammel, G., Adsorptive and absorptive contributions to the gas-particle partitioning of polycyclic aromatic hydrocarbons: State of knowledge and recommended parametrization for modeling. *Environ. Sci. Technol.* **2004,** *38*, (14), 3793-3803.
52. Harner, T.; Bidleman, T. F., Octanol-air partition coefficient for describing particle/gas partitioning of aromatic compounds in urban air. *Environ. Sci. Technol.* **1998,** *32*, (10), 1494-1502.

53. Wang, Q.; Zhao, H.; Wang, Y.; Xie, Q.; Chen, J.; Quan, X., Determination and prediction of octanol-air partition coefficients for organophosphate flame retardants. *Ecotoxicol. Environ. Saf.* **2017,** *145*, 283-288.

54. MacLeod, M.; von Waldow, H.; Tay, P.; Armitage, J. M.; Wöhrnschimmel, H.; Riley, W. J.; McKone, T. E.; Hungerbuhler, K., BETR global–A geographically-explicit global-scale multimedia contaminant fate model. *Environ. Pollut.* **2011,** *159*, (5), 1442-1445.

55. McLachlan, M. S.; Undeman, E.; Zhao, F. Y.; MacLeod, M., Predicting global scale exposure of humans to PCB 153 from historical emissions. *Environ. Sci.: Proc. Imp.* **2018,** *20*, (5), 747-756.

56. Zhang, L. S.; Ma, J. M.; Venkatesh, S.; Li, Y. F.; Cheung, P., Modeling Evidence of Episodic Intercontinental Long-Range Transport of Lindane. *Environ. Sci. Technol.* **2008,** *42*, (23), 8791-8797.

57. The Task Force on Hemispheric Transport of Air Pollution (TF HTAP). http://www.htap.org/.

58. Jurado, E.; Jaward, F. M.; Lohmann, R.; Jones, K. C.; Simo, R.; Dachs, J., Atmospheric dry deposition of persistent organic pollutants to the Atlantic and inferences for the global oceans. *Environ. Sci. Technol.* **2004,** *38*, (21), 5505-5513.

59. Gao, Y.; Arimoto, R.; Duce, R. A.; Lee, D. S.; Zhou, M. Y., Input of Atmospheric Trace-Elements and Mineral Matter to the Yellow Sea during the Spring of a Low-Dust Year. *J. Geophys. Res.-Atmos.* **1992,** *97*, (D4), 3767-3777.

60. Regnery, J.; Puttmann, W., Organophosphorus Flame Retardants and Plasticizers in Rain and Snow from Middle Germany. *Clean-Soil Air Water* **2009,** *37*, (4-5), 334-342.

61. Bacaloni, A.; Cucci, F.; Guarino, C.; Nazzari, M.; Samperi, R.; Lagana, A., Occurrence of organophosphorus flame retardant and plasticizers in three volcanic lakes of Central Italy. *Environ. Sci. Technol.* **2008,** *42*, (6), 1898-1903.

62. Marklund, A.; Andersson, B.; Haglund, P., Traffic as a source of organophosphorus flame retardants and plasticizers in snow. *Environ. Sci. Technol.* **2005,** *39*, (10), 3555-3562.

63. Hilal, S.; Karickhoff, S. W.; Carreira, L. A., SPARC− Performs Automated Reasoning in Chemistry. Athens, USA. 2005.

64. MacLeod, M.; Fraser, A. J.; Mackay, D., Evaluating and expressing the propagation of uncertainty in chemical fate and bioaccumulation models. *Environ. Toxicol. Chem.* **2002,** *21*, (4), 700-709.

65. Brommer, S.; Jantunen, L. M.; Bidleman, T. F.; Harrad, S.; Diamond, M. L., Determination of Vapor Pressures for Organophosphate Esters. *J. Chem. Eng. Data* **2014,** *59*, (5), 1441-1447.

66. EU Risk Assessment Report, Tris(2-chloroethyl) phosphate (TCEP) CAS-No.: 115-96-8. EINECS-No.: 204-118-5. **2009**.

67. Cuthbert, J. M., DM., TCPP: Determination of general physicochemical properties, Report 1613/002. *SafePharm Laboratories, PO Box 45, Derby, UK.* **2002**.

68. Skene, W. G.; Krzymien, M. E., Vapor-Pressure of Tri-N-Butyl Phosphate. *J. Chem. Eng. Data* **1995,** *40*, (2), 394-397.

69. Saeger, V. W.; Hicks, O.; Kaley, R. G.; Michael, P. R.; Mieure, J. P.; Tucker, E. S., Environmental fate of selected phosphate esters. *Environ. Sci. Technol.* **1979,** *13*, (7), 840-844.

70. Bruhn, R.; Lakaschus, S.; McLachlan, M. S., Air/sea gas exchange of PCBs in the southern Baltic Sea. *Atmos. Environ.* **2003,** *37*, (24), 3445-3454.

7. List of Publications

The thesis is based on four publications:

Li, J., Xie, Z., Mi, W., Lai, S., Tian, C., Emeis, K. C., & Ebinghaus, R. (2017). Organophosphate esters in air, snow, and seawater in the North Atlantic and the Arctic. *Environmental Science & Technology*, *51*(12), 6887-6896.

Li, J., Tang, J., Mi, W., Tian, C., Emeis, K. C., Ebinghaus, R., & Xie, Z. (2018). Spatial distribution and seasonal variation of organophosphate esters in air above the Bohai and Yellow Seas, China. *Environmental Science & Technology*, *52*(1), 89-97.

Li, J., Zhao, F., Xie, Z., Emeis, K. C., Ebinghaus, R., Tian, C., & MacLeod, M. (2019). Global gridded emissions and atmospheric transport of tris-(1-chloro-2-propyl) phosphate (TCPP). Submitted to *Environmental Science & Technology*, *52*(1), 89-97.

Li, J., Zhao, F., Xie, Z., Emeis, K. C., Ebinghaus, R., Tian, C., & MacLeod, M. (2019). Global multimedia source-receptor relationships for tris-(1-chloro-2-propyl) phosphate (TCPP). Manuscript.

Appendix A: Individual contribution to the publications

A.1 Li et al. (2017)

Li, J., Xie, Z., Mi, W., Lai, S., Tian, C., Emeis, K. C., & Ebinghaus, R. (2017). Organophosphate esters in air, snow, and seawater in the North Atlantic and the Arctic. Environmental Science & Technology, 51(12), 6887-6896.

J.L. and Z.X. conducted data management and wrote the manuscript; Z.X. designed the research and carried out the field work; W.M. and Z.X. performed sample preparation and instrumental analysis; C.T. guided the calculation method; S.L., K.E., and R.E. provided important comments and polished the manuscript.

A.2 Li et al. (2018)

Li, J., Tang, J., Mi, W., Tian, C., Emeis, K. C., Ebinghaus, R., & Xie, Z. (2018). Spatial distribution and seasonal variation of organophosphate esters in air above the Bohai and Yellow Seas, China. Environmental Science & Technology, 52(1), 89-97.

J.L. and Z.X. conducted data management and wrote the manuscript; Z.X. and T.J. designed the research; T.J. carried out the field work; W.M. and Z.X. performed sample preparation and instrumental analysis; C.T. guided the calculation method; T.J., K.E., and R.E. provided important comments and polished the manuscript.

A.3 Li et al. (Submitted)

Li, J., Zhao, F., Xie, Z., Emeis, K. C., Ebinghaus, R., Tian, C., & MacLeod, M. (2019). Global gridded emissions and atmospheric transport of Tris-(1-chloro-2-propyl) phosphate (TCPP). Submitted to Environmental Science & Technology, 52(1), 89-97.

Z.X. and M.M. designed the research; M.M., J.L. and F.Z. conducted data analysis and method optimization; J.L. and F.Z. carried out modeling; C.T. guided the CanMETOP model; K.E., and R.E. provided important comments and polished the manuscript.

A.4 Li et al. (Manuscript)

Li, J., Zhao, F., Xie, Z., Emeis, K. C., Ebinghaus, R., Tian, C., & MacLeod, M. (2019). Global multimedia source-receptor relationships for tris-(1-chloro-2-propyl) phosphate (TCPP). Manuscript.

Z.X. and M.M. designed the research; M.M., J.L. and F.Z. conducted data analysis and method optimization; J.L. and F.Z. carried out modeling; C.T. guided the CanMETOP model; K.E., and R.E. provided important comments and polished the manuscript.

Paper I

Organophosphate esters in air, snow and seawater in the North Atlantic and the Arctic

Environmental Science & Technology

Article

pubs.acs.org/est

Organophosphate Esters in Air, Snow, and Seawater in the North Atlantic and the Arctic

Jing Li,[†,‡] Zhiyong Xie,[*,†] Wenying Mi,[§] Senchao Lai,[∥] Chongguo Tian,[⊥] Kay-Christian Emeis,[†,‡] and Ralf Ebinghaus[†]

[†]Helmholtz-Zentrum Geesthacht, Centre for Materials and Coastal Research, Institute of Coastal Research, Geesthacht, 21502, Germany

[‡]University of Hamburg, School of Integrated Climate System Sciences, Hamburg, 20144, Germany

[§]MINJIE Analytical Laboratory, Geesthacht, 21502, Germany

[∥]Guangdong Provincial Engineering and Technology Research Center for Environmental Risk Prevention and Emergency Disposal, School of Environment and Energy, South China University of Technology, Guangzhou, 510006, China

[⊥]Key Laboratory of Coastal Environmental Processes and Ecological Remediation, Yantai Institute of Coastal Zone Research, CAS, Yantai, 264003, China

Ⓢ *Supporting Information*

ABSTRACT: The concentrations of eight organophosphate esters (OPEs) have been investigated in air, snow and seawater samples collected during the cruise of ARK-XXVIII/2 from sixth June to third July 2014 across the North Atlantic and the Arctic. The sum of gaseous and particle concentrations (ΣOPE) ranged from 35 to 343 pg/m^3. The three chlorinated OPEs accounted for 88 ± 5% of the ΣOPE. The most abundant OPE was tris(2-chloroethyl) phosphate (TCEP), with concentrations ranging from 30 to 227 pg/m^3, followed by three major OPEs, such as tris(1-chloro-2-propyl) phosphate (TCPP, 0.8 to 82 pg/m^3), tri-*n*-butyl phosphate (TnBP, 2 to 19 pg/m^3), and tri-iso-butyl phosphate (TiBP, 0.3 to 14 pg/m^3). The ΣOPE concentrations in snow and seawater ranged from 4356 to 10561 pg/L and from 348 to 8396 pg/L, respectively. The atmospheric particle-bound dry depositions of TCEP ranged from 2 to 12 ng/m^2/day. The air−seawater gas exchange fluxes were dominated by net volatilization from seawater to air for TCEP (mean, 146 ± 239 ng/m^2/day), TCPP (mean, 1670 ± 3031 ng/m^2/day), TiBP (mean, 537 ± 581 ng/m^2/day) and TnBP (mean, 230 ± 254 ng/m^2/day). This study highlighted that OPEs are subject to long-range transport via both air and seawater from the European continent and seas to the North Atlantic and the Arctic.

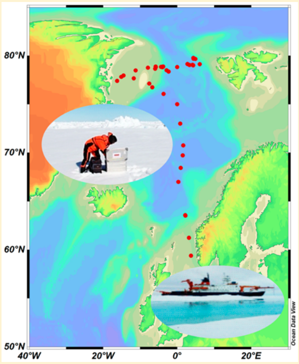

INTRODUCTION

Organophosphate esters (OPEs) are a group of man-made industrial chemicals, which have been widely applied in many industrial processes and household products, such as flame-retardants, plasticizers, antifoaming agents, and additives in hydraulic fluids, lacquers, and floor polishes.[1,2] Chlorinated OPEs are predominantly utilized as flame retardants, while nonchlorinated OPEs are mainly used as plasticizers and in other applications. Recently, the production and usage of OPEs has increased continually as OPEs can be used in many cases as substitutes for polybrominated diphenyl ether (PBDEs).[2,3] The global consumption of OPEs was 186 000 tons in 2001, which rose to 370 000 tons in 2004.[4,5] In western Europe, the consumption of OPEs increased from 58 000 tons in 1998 to 91 000 tons in 2006 and to 110 000 tons in 2013.[2,4,6] In Germany, the annual production volumes of tris(2-chloroethyl) phosphate (TCEP) and the sum of tri-*iso*-butylphosphate (TiBP) and tri-*n*-butylphosphate (TnBP) in 1991 were estimated at approximately 4000−5000 and 500 tons/year, respectively.[7] In Sweden, the annual import quantities of several OPEs ranged from 30 to 200 tons in 2000.[4]

The broad application of OPEs and the fact that they are applied as additives may allow them to easily spread into the environment by volatilization, leaching, and abrasion.[1] Several chlorinated OPEs have various toxic effects.[8,9] For example, tris(1-chloro-2-propyl) phosphate (TCPP) is considered potentially carcinogenic and could accumulate in human livers and kidneys.[10] TCEP is toxic to aquatic organisms, carcinogenic for animals, and has adverse effects on human health, such as hemolytic and reproductive effects.[10] Tris(1,3-dichloro-2-propyl) phosphate (TDCP) is harmful when inhaled and can easily enter the bloodstream.[10] The potential of OPEs to bioaccumulate and magnify might be limited, owing to their relatively low log k_{ow} value (<5 for most OPEs).[2] However, Sundkvist et al. detected OPEs in human breast milk as well as in fish and mussels from Swedish lakes and coastal areas.[11] Kim et al. also found OPEs in fish collected from Manila Bay, the Philippines.[12]

Received: March 10, 2017
Revised: May 23, 2017
Accepted: May 24, 2017
Published: May 24, 2017

ACS Publications © 2017 American Chemical Society

DOI: 10.1021/acs.est.7b01289

The occurrence of OPEs in remote areas was reported in a few studies. Liu et al. found that particle-bound OPEs are highly persistent in the air (TPhP, 5.6 days; TEHP, 13 days), indicating that OPEs can undergo medium or long-range transport in the atmosphere.[13−15] The concentrations of OPEs that detected in the air were generally 1−2 orders of magnitude higher than those of brominated flame retardants, highlighting the importance of research on the global occurrence and environmental fate of OPEs.[13,16]

Polar regions have been used as monitoring sites to represent global background levels of persistent organic pollutants (POPs), and research on POPs in polar regions such as the Arctic provides important knowledge about the fate of these compounds.[16] Several studies that analyzed OPEs in the Arctic, such as nine OPEs were found in Ny-Ålesund, Svalbard air by Green et al. in 2008;[17] Möller et al. reported eight OPEs in air from the northern Pacific Ocean to the Arctic Ocean in 2012;[13] Salamova et al. analyzed eight OPEs in Longyearbyen, Svalbard in 2014;[16] Sühring et al. detected 14 OPEs in Canadian Arctic air in 2016.[18] There is, however, no report on OPEs in the North Atlantic, and there is a lack of data on OPEs in seawater and snow in the Arctic. More research is necessary to understand the occurrence, transport, and interaction between different environmental phases for OPEs in the remote Arctic.

In this work, the occurrence and spatial distribution of eight OPEs was investigated in air, snow, and seawater samples collected during an expedition cruise in the North Atlantic and the Arctic, and atmospheric particle-bound dry deposition and the air−seawater gas exchange fluxes of OPEs were estimated. This work will improve understanding of long-range transport and the fate of OPEs in the Arctic ecosystem.

■ MATERIALS AND METHODS

Sampling Campaign. The samples were collected in the northeast Atlantic and the Arctic Ocean (50°N−80°N) during the expedition cruise ARK-XXVIII/2 on board R/V *Polarstern*. Nine air samples were collected with a high volume air sampler from eighth to 24th June 2014. Six snow samples were collected from 15th to 25th June 2014. Twenty-five seawater samples were collected from eighth to 26th June 2014. Atmospheric particle samples were collected with a glass fiber filter (GFF diameter, 150 mm; pore size, 0.7 μm) and a PUF/XAD-2 resin column was used to collect the gaseous phase, respectively. Each set of air samples was collected using a high-volume air pump operating at ~15 m^3/h for 24−48 h. Field blanks were prepared by shortly exposing the columns and filters to the sampling site. PUF/XAD-2 and GFF samples were stored at 4 and −20 °C in a cooling room, respectively. Snow samples were collected on the Arctic sea ice via helicopter and boat using 10-L stainless steel barrels and then stored at −20 °C in a cooling room. 1 L seawater samples were collected in glass bottles from the ship's intake system located in the keel (depth: 11 m), and stored at 4 °C in a cooling room. Details on the air, snow, and seawater sampling information are summarized in Tables S1−S3.

Analysis. Air sample pretreatment and analysis followed the approach given by Möller et al.[14] Briefly, PUF/XAD-2 and GFFs were spiked with 20 ng of d_{27}-TnBP, d_{12}-TCEP, and d_{15}-TPhP as surrogates, and extracted with MX-Soxhlet using dichloromethane (DCM) for 16 h. Eight hundred milliliters (800 mL) of melting snow water and seawater from each sample were performed with liquid−liquid extraction using 50 mL DCM three times. All samples were concentrated down to 150 μL and then spiked with 500 pg $^{13}C_6$-PCB 208 as the injection standard. The samples were then analyzed using a gas chromatograph couple to a triple quadrupole mass spectrometer (GC-MS/MS) equipped with a programmed temperature vaporizer (PTV) injector (Agilent, USA). The parameter details for GC-MS/MS are given in Text S1.

Eight OPEs have been analyzed in this work, which include tris(2-chloroethyl) phosphate (TCEP), tris(1-chloro-2-propyl) phosphate (TCPP, including three isomers), tris(1,3-dichloro-2-propyl) phosphate (TDCP), tri-iso-butyl phosphate (TiBP), tri-*n*-butyl phosphate (TnBP), triphenyl phosphate (TPhP), tripentyl phosphate (TPeP), and tris(2-ethylhexyl) phosphate (TEHP). More details about these OPEs are shown in Table S4.

Quality Assurance/Quality Control (QA/QC). The method detection limits (MDLs) were derived from the mean field blank concentrations plus three times the standard deviation (3σ) of the field blanks,[19] which were within 0.0003−1.5 pg/m^3 for the gaseous phase, 0.0002−6.5 pg/m^3 for the particle phase, 7−210 pg/L for snow and seawater. The OPE concentrations are corrected with the recoveries of internal standards.[19] The mean recovery rates of spiked experiments were from 88 ± 13% (TiBP) to 145 ± 9% (TCEP) for PUF/XAD-2 columns (n = 5), from 107 ± 4% (TCCP) to 139 ± 12% (TEHP) for the filters (n = 3), and from 78 ± 3% (TiBP) to 95 ± 8% (TCEP) for LLE extraction (n = 5), respectively. Detailed information for recovery rates, field blanks and MDLs is summarized in Table S6.

To monitor the background levels of OPEs in the air of the working places during the cruise, XAD-2-based passive air samplers were deployed on the upper deck next to the high-volume air sampler and in the chemical lab. The result shows that total OPE masses in the chemical lab (235 ng) were about eight times higher than those of the upper deck (28.4 ng, see Table S7). During this cruise, the air columns and filters were placed on the upper deck directly, which could eliminate certain contamination from the indoor lab air.

Breakthrough of target compounds for the vapor phase was evaluated using tandem columns for samples A2 and A9 aboard R/V *Polarstern*. In the lower columns, no TnBP, TPhP, or TEHP was detected above MDLs; TDCP was only observed at sample A2, which accounted for 28% to total TDCP (sum concentration of upper and lower columns); TiBP contributed to 15% of total TiBP and TCEP contributed to 28%; TCPP accounted for 46%, which was a little higher than other OPEs. Since the breakthrough of compounds is a complicated process, it is difficult to find an appropriate method to correct the concentrations. Therefore, only the concentrations on the first column were reported in this study, which was inevitable to underestimate the OPE concentrations.

OPEs are subject to air sampling artifacts, as sorption to the filter could occur when the vapor phase OPEs pass through, and fine aerosol particles may pass the filter and end up trapped on the column during sampling. The diameter of the filters used in this work is <0.7 mm, which might allow the fine particles to pass through. Pankow et al. described the possible impact that could increase the uncertainties, such as temperature change, adsorption and desorption during sampling.[20] Those factors discussed above will lead to over or underestimation of OPEs in the gaseous and particle phases, and as a consequence lead to uncertainties when estimating the air-particle partitioning, the dry deposition fluxes and the air−seawater gas exchange fluxes.

Air Mass Back Trajectories. Air mass back trajectories (BTs) were calculated for the air stations using NOAA's HYSPLIT model.[21] BTs were calculated for every sample in 6 h steps during the sampling cruises, and were tracked for 120 h at 10 m above sea level (see Figure S1).

■ RESULTS AND DISCUSSION

Atmospheric Concentrations of OPEs. The concentrations of eight OPEs have been investigated in both particle and gaseous phases. The minimum, maximum, mean, and median concentrations of individual OPEs in the air are presented in Table 1. Among the chlorinated OPEs, TCPP (sum of three isomers) and TCEP were detected in all air samples, while TDCP was detected in 33%. Among the nonchlorinated OPEs, TiBP, TnBP, TPhP, and TEHP were present in all air samples, while TPeP was detected in 56%. The sum concentrations of the eight OPEs (ΣOPE) ranged from 35 to 343 pg/m^3, with a mean of 98 ± 98 pg/m^3. The three chlorinated OPEs accounted for 88 ± 5% of the total ΣOPE, and the five nonchlorinated OPEs accounted for 12 ± 5%. The most abundant OPE was TCEP, with concentrations ranging from 30 to 227 pg/m^3 (mean = 71 ± 62 pg/m^3), which was followed by three major OPEs, such as TCPP ranging from 0.8 to 82 pg/m^3 (mean = 17 ± 28 pg/m^3), TnBP ranging from 2 to 19 pg/m^3 (mean = 5.7 ± 5 pg/m^3), and TiBP ranging from 0.3 to 14.5 pg/m^3 (mean = 4.5 ± 4.5 pg/m^3).

To compare with previous reports, OPE concentrations measured in the air of different remote areas are summarized in Table 2. Chlorinated OPEs (TCPP, TCEP, and TDCP) have been reported as the dominant OPE congeners in different geographic regions, except from an Arctic site.[16] The mean total OPE concentrations varied from 100 pg/m^3 in this study to 2800 pg/m^3 over the Black Sea.[3] The OPE levels in this work are similar to those detected over the South China Sea,[19] 2−6 times lower than those of the Canadian Arctic,[18] Longyearbyen,[16] the North Sea,[14] the Great Lakes,[22] the Latin America,[23] and the Pacific and Indian Oceans.[13] High concentrations (≥1000 pg/m^3) were detected in three areas, that is, in East Asia, such as in the East China Sea and Japan Sea;[13,15] in Europe, such as in the Mediterranean Sea and Black Sea;[3] in North America, such as in the Great Lakes.[24] Western Europe, North America and East Asia are the highest consumption regions for flame retardants.[25] In 2013, the usage of OPEs in Western Europe (110 000 tons) and North America (70 000 tons) accounted for approximately 30% and 20% of worldwide usage, respectively.[6] The production of OPEs in China was 179 000 tons in 2012.[26] Relatively low concentrations, however, were also detected in those areas, such as 100 pg/m^3 over the South China Sea and 400 pg/m^3 over the North Sea.[14,19] In this study, the most abundant OPE was TCEP (mean, 71 pg/m^3), which was lower than in other remote areas, with the exception of Longyearbyen (mean, 19 pg/m^3) and near the Antarctic Peninsula (mean, 41 pg/m^3).[15,16] In addition to TCEP, the other seven OPEs (i.e., TCPP, TDCP, TiBP, TnBP, TPeP, TPhP, and TEHP) were all lower than those measured in the atmosphere of other oceans.

The ratio of mean concentration of TCEP to TCPP was ~4 in this study, which was ten times as high as that of a German coast site (0.4).[27] This might result from the slower photochemical degradation of TCEP than TCPP in the atmosphere.[27] The half-life of TCEP (17.5 h) is two times as long as TCPP (8.6 h) in the gaseous phase.[28,29] The TiBP/TnBP ratios were ~1 in this work and the German coast site, with the two

Table 1. Minimum, Maximum, Mean, and Median of Individual OPE Concentrations in Air (pg/m^3), Snow (pg/L), and Seawater (pg/L)

	gaseous phase (pg/m^3)				particle phase (pg/m^3)				snow (pg/L)				seawater (pg/L)			
OPE	min	max	mean	median	min	max	mean	median	min	max	mean	median	min	max	mean	median
TCEP	4	92	23	10	26	136	48	35	554	2440	1293	1147	n.d.	2401	695	605
TCPP	0.8	55	12	1.9	n.d.	27	5	2.3	1522	6256	3890	3451	279	5773	1843	1626
TDCP	n.d.	0.06	0.01	n.d.	n.d.	n.d.	n.d.	n.d.	n.d.	2.8	0.8	n.d.	n.d.	43	7	4
TiBP	0.3	7.5	2.7	1.7	n.d.	7	1.8	2	1121	5129	2004	1319	39	638	258	230
TnBP	n.d.	8.8	2.2	1.4	1.6	10	3.5	3	390	1044	630	596	n.d.	412	122	105
TPeP	n.d.	0.02	0.01	0.001	n.d.	n.d.	n.d.	n.d.	n.d.	0.7	0.3	0.14	n.d.	35	5	n.d.
TPhP	0.01	1.5	0.2	0.017	n.d.	0.09	0.01	0.03	2.5	38	11	4	n.d.	n.d.	n.d.	n.d.
TEHP	n.d.	0.6	0.1	n.d.	n.d.	0.06	0.02	0.02	1.3	13	5.5	4	n.d.	69	6	n.d.
ΣOPE	7	163	40	17	29	180	58	48	4356	10561	7834	7922	348	8396	2935	2635

Table 2. Comparison of Atmospheric Concentrations (pg/m^3) of OPEs (Range and Mean Value) in This Study and Those Measured in Open Seas and Remote Areas[a]

location	TCEP	TCPP	TDCP	TiBP	TnBP	TPhP	TPeP	TEHP	other OPEs	ΣOPE (mean value)[g]	refs
North Sea[b]	6–160 (43)	38–1200 (331)	n.d.–78 (6)	n.d.–150 (45)	n.d.–150 (29)	4–290 (35)	n.a.	n.d.–31 (6)		500	14
Sea of Japan[c]	237/1960	130/620	16/52	11/63	10/33	25/97	n.a.	5/38	15/81	1700	13
Northern Pacific Ocean[c]	160–280 (204)	98–270 (160)	5–8 (5)	14–21 (17)	6–14 (11)	9–24 (19)	n.a.	1–12 (2)	n.d.–16	400	13
Philippine Sea[c]	20–156 (77)	22–411 (74)	50–780 (80)	10–23 (16)	10–100 (14)	n.d.–155 (17)	n.a.	6–92 (12)	n.d.–77	500	13
Indian Ocean[c]	46–570 (223)	37–550 (251)	n.d.–220 (52)	7–96 (31)	7–75 (27)	n.d.–74 (26)	n.a.	4–51 (20)	n.d.–44	650	13
East China Sea	134	9	828	n.a.	n.a.	n.a.	n.a.	n.a.	95	1000	15
Coral Sea	88	7	370	n.a.	n.a.	n.a.	n.a.	n.a.	66	500	15
Southern Ocean	74	55	80	16	14	19	n.a.	7		300	13
Near Antarctic Peninsula	41	4	76	n.a.	n.a.	n.a.	n.a.	n.a.	20	140	15
Arctic Ocean[c]	126–585 (289)	85–529 (281)	n.d.–5 (–)	16–35 (25)	n.d.–36 (11)	10–60 (19)	n.a.	n.d.–6 (1)	n.d.–11	600	13
Mediterranean Sea[d]	70–854 (300)	126–2340 (963)	n.d.–460 (135)	4–650 (237)	56–600 (295)	n.d.–80 (28)	n.a.	56–307 (149)	~500	2500	3
Black Sea	300–2417 (869)	540–2722 (1159)	n.d.–97 (80)	66–190 (139)	202–370 (298)	3–40 (28)	n.a.	36–190 (144)	~380	2800	3
Great Lakes(2014)[e]	5.5 ± 0.9–180 ± 25 (93)	25 ± 7–850 ± 300 (345)	n.d.–520 ± 220 (154)	n.a.	34 ± 7–250 ± 53 (148)	42 ± 9–200 ± 27 (103)	n.a.	4.7 ± 0.7–66 ± 9 (28)	~200	1000	24
Great Lakes(2016)[f]	193	173	36	n.a.	110	82	n.a.	n.a.	38	600	22
Longyearbyen	4.0–63 (19)	10–186 (62)	2.3–294 (59)	n.a.	5.6–1000 (174)	1.1–52 (20)	n.a.	1.0–42 (12)	~200	550	16
Ny-Ålesund	<200–270	<200–330	87–250	<10–140	n.a.	<50	n.a.	n.a.	<500	<1300	17
South China Sea	14–107 (46)	15–38 (25)	1.3–4.5 (2.6)	1.1–3.8 (2.3)	1.4–4.8 (2.7)	3.4–15 (8.1)	n.a.	2.3–16 (5.1)	2	100	19
Canadian Arctic (ship-based)	187 ± 181	85 ± 105	2.7 ± 2.9	n.a.	2.3 ± 15	84 ± 264	n.a.	0.56 ± 1.4	1.6	400	18
Canadian Arctic (land-based)	118 ± 120	92 ± 88	10 ± 12	n.a.	747 ± 876	22 ± 26	n.a.	n.a.	12	300	18
North Atlantic and Arctic (g.)	4–92 (23)	0.8–55 (12)	n.d.–0.06 (0.01)	0.3–7.5 (2.7)	n.d.–8.8 (2.2)	0.01–1.5 (0.2)	n.d.–0.02 (0.01)	n.d.–0.6 (0.1)		40	this study
North Atlantic and Arctic (p.)	26–136 (48)	n.d.–27 (5)	n.d.	n.d.–7 (1.8)	2–10 (3.5)	n.d.–0.09 (0.01)	n.d.	n.d.–0.06 (0.02)		60	this study
North Atlantic and Arctic (sum)	30–227 (71)	0.8–82 (17)	n.d.–0.06 (0.01)	0.3–14.5 (4.5)	2–19 (5.7)	0.02–1.5 (0.2)	n.d.–0.02 (0.01)	n.d.–0.7 (0.1)		100	this study

[a] n.d. = not detected; n.a. = not analyzed; g. = gaseous phase; p. = particle phase; sum = sum of gaseous and particle phase. [b] Mean values and the range of TDCP were from the source document (Table S5 of ref 14). [c] Median concentrations are given in brackets. [d] Calculated mean values from the source document (Table S4 of ref 3). [e] Calculated mean values from the source document (Table 1 of ref 24). [f] Calculated mean values from the source document with the median values of 50% percentiles (Table 1 of ref 22). [g] The mean values of total OPEs were estimated according to the source document of the references.

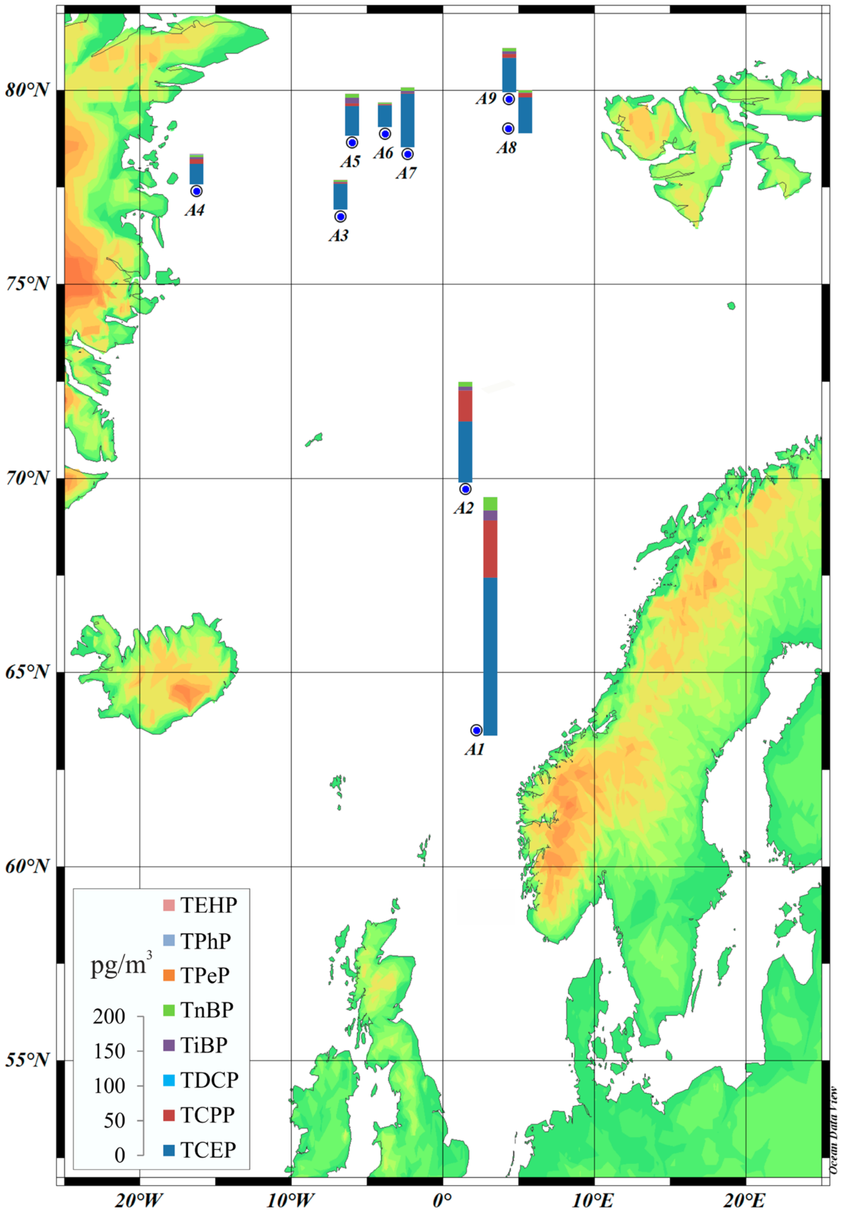

Figure 1. Spatial distribution of OPEs in air of the North Atlantic and the Arctic.

OPEs both present relatively low half-life (<5 h) in the gaseous phase.[27,28]

Brominated flame retardants, that is, decabromdiphenylether (BDE-209, <0.1 pg/m^3), hexabromobenzene (HBB, <1 pg/m^3) and dechlorane plus isomers (DPs, 0.01−4.1 pg/m^3) have been determined in the European Arctic. In comparison to the results of this study, OPE concentrations were 1−2 orders of magnitude higher than those of BFRs.[30,31]

Spatial Distribution in the Atmosphere. The spatial distribution of OPEs in the atmosphere is shown in Figure 1. The air mass back trajectories are shown in Figure S1. The highest two ∑OPE concentrations in the air were observed at samples A1 and A2, with their mean concentration was ~3 times higher than that of others (samples A3−A9), which mainly resulted from the varying air masses. Sample A1 was influenced by air masses passing the Ireland, the United Kingdom and the eastern coastline of the North Sea. At sample A2, the air masses were influenced by North Sea air. However, the other Samples were dominated by high Arctic oceanic air masses.

At samples A1 and A2, TCEP was still detected as the dominant OPE, although TCEP has already been replaced by TCPP in Europe, demonstrating that the emission of TCEP still exists on the European continent.[17]

Gas/Particle Partitioning. The concentrations of ΣOPE ranged from 7 to 163 pg/m^3 (mean, 40 ± 53 pg/m^3) in the gaseous phase and from 29 to 180 pg/m^3 (mean, 58 ± 48 pg/m^3) in the particle phase. TCEP was the dominant OPE in both the gaseous and particle phases. The composition profile of OPEs in the air is shown in Figure S2. Particle phase OPEs contributed to 67 ± 17% of the total OPEs on average, which was lower than in the North Sea reported by Möller et al. (mean, 86 ± 25%)[14] and an indoor environment analyzed by Carlsson et al. (>99%).[32] The particle-bound fractions of four major OPEs were found in the sequence of TCEP (74%) > TnBP (72%) > TiBP (30%) > TCPP (27%). As the breakthrough of the OPEs occurred during sampling, the particle fraction might be overestimated.

The ambient temperature, relative humidity (RH), the type and concentration of particles could impact the gas/particle

DOI: 10.1021/acs.est.7b01289
Environ. Sci. Technol. 2017, 51, 6887−6896

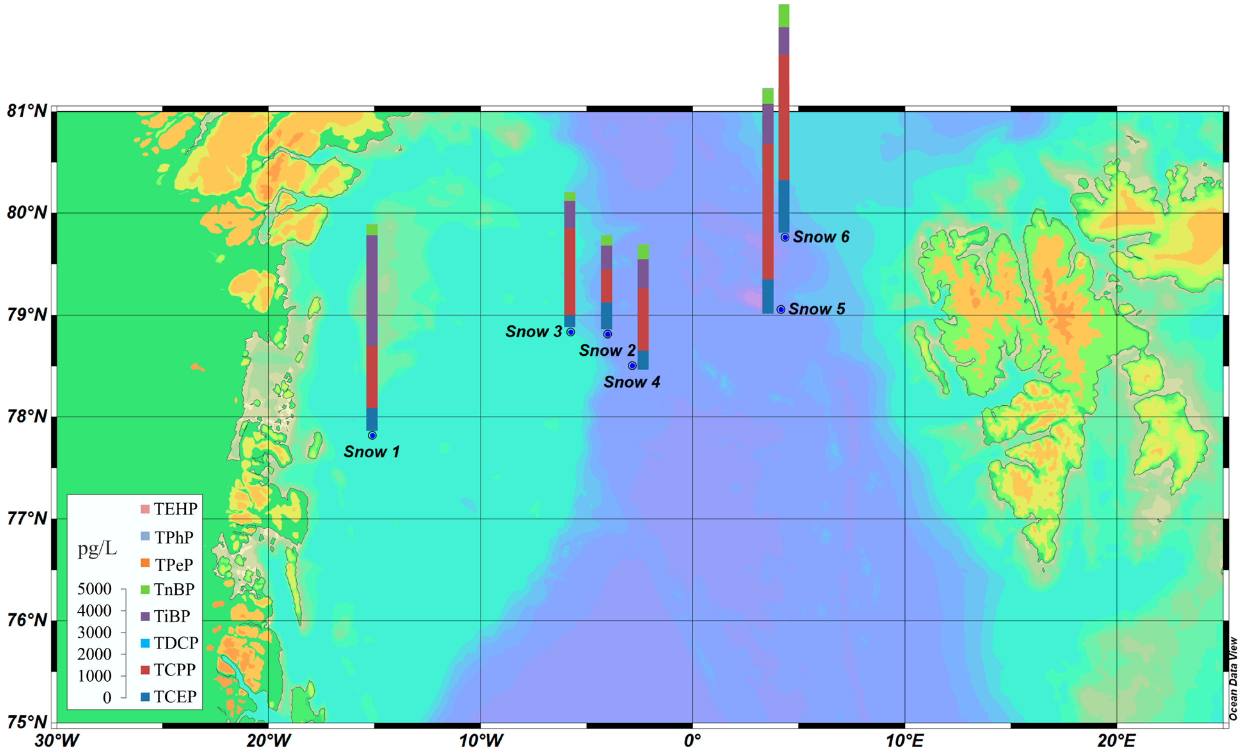

Figure 2. Spatial distribution of OPEs in snow of the North Atlantic and the Arctic.

partitioning. Strong reverse correlations between partitioning coefficients and temperatures were confirmed for volatile organic compounds by Goss et al.[33] Storey et al. reported that the partitioning coefficients will decrease by more than a log unit, with the increase of RH by 10% to over 70%.[34] Pankow et al. stated that the coefficients were unlikely to be exactly the same from one type of particle to another, even under the same atmospheric conditions.[20] In this study, the particle fractions at samples A1 (52%) and A2 (38%) were lower than others. At those two samples, the temperatures (7−12 °C) were higher than others (−4−4 °C), while the RHs were similar (75−98%), and the C_{TSP} lay in between.

OPEs in Snow. The concentrations and spatial distribution of OPEs in snow are shown in Figure 2. The details of individual OPE concentrations are shown in Table 1. TCEP, TCPP, TiBP, TnBP, TPhP, and TEHP were detected in all snow samples, while TPeP and TDCP were detected in 60% and 40% of samples, respectively. The concentrations of ΣOPE ranged from 4356 to 10560 pg/L with a mean of 7834 ± 2684 pg/L. Chlorinated OPEs accounted for 66 ± 14% and nonchlorinated OPEs accounted for 34 ± 14% of total OPEs, respectively. TCPP was the most abundant OPE in snow with concentrations ranging from 1522 to 6256 pg/L, with a mean of 3890 ± 1838 pg/L, followed by TiBP (1121−5129 pg/L, mean 2004 ± 1552 pg/L), TCEP (554−2440 pg/L, mean 1293 ± 661 pg/L) and TnBP (390−1044 pg/L, mean 630 ± 234 pg/L). There was a decreasing trend for ΣOPE concentrations from coast to open ocean, with the mean concentration of costal snow samples (snows 1, 5, and 6) was ~2 times as high as the open ocean samples (snows 2−4).

The dominant OPE (TCPP) is compared to concentrations from urban precipitation, as reports on OPEs in polar region snow are rare. The mean concentration of TCPP (~3.9 ng/L) in this study was 1−3 orders of magnitude lower than in the urban areas, such as in central Germany (range 46−2659 ng/L, rainwater),[35] Italy (range 633−739 ng/L, rainwater),[36] and northern Sweden (range 100−220 ng/kg, snow).[1]

OPEs in Seawater. The concentrations and spatial distribution of OPEs in seawater are shown in Figure 3. Among the measured eight OPEs, TCPP, and TiBP were detected in all seawater samples, while TPhP was not detected in any seawater sample. Other OPEs, TnBP, TCEP, TDCP, TPeP, and TEHP were detected in 92%, 88%, 56%, 32%, and 16% of the seawater samples, respectively. The total OPE concentrations ranged from 348 to 8396 pg/L, with a mean of 2935 ± 1890 pg/L. The three chlorinated OPEs accounted for 87 ± 8% of the total ΣOPE in seawater, and the five nonchlorinated OPEs accounted for 13 ± 8%. The concentrations of OPEs were found in sequence of TCPP (279−5773 pg/L, mean 1843 ± 1323pg/L) > TCEP (MDL−2401 pg/L, mean 695 ± 589 pg/L) > TiBP(39−638 pg/L, mean, 258 ± 191 pg/L) > TnBP (MDL−412 pg/L, mean 122 ± 116 pg/L). The details of individual OPE concentrations are summarized in Table 1.

Literature data on OPEs in seawater from the oceans is rare. Bollmann et al. have reported OPEs in coastal surface waters of the River Elbe and marine surface waters of the German Bight (North Sea), with total OPE concentrations ranging from 85 to 500 ng/L and from 5 to 50 ng/L, respectively.[37] Harino et al. measured OPEs in water samples from Maizuru Bay, with total concentrations ranging from 3.0 to 62 ng/L.[38] Regnery et al. detected OPEs in urban and remote lentic surface waters in Germany, with a mean of 200 and 25 ng/L, respectively.[39] The concentrations of ΣOPE (0.2−8 ng/L) determined in this study are 1−2 orders of magnitude lower than those detected in rural regions and 2−3 orders of magnitude lower than in urban areas.

Latitudinal Trends in Seawater. The four highest concentrations of ΣOPE were measured at sites near continents,

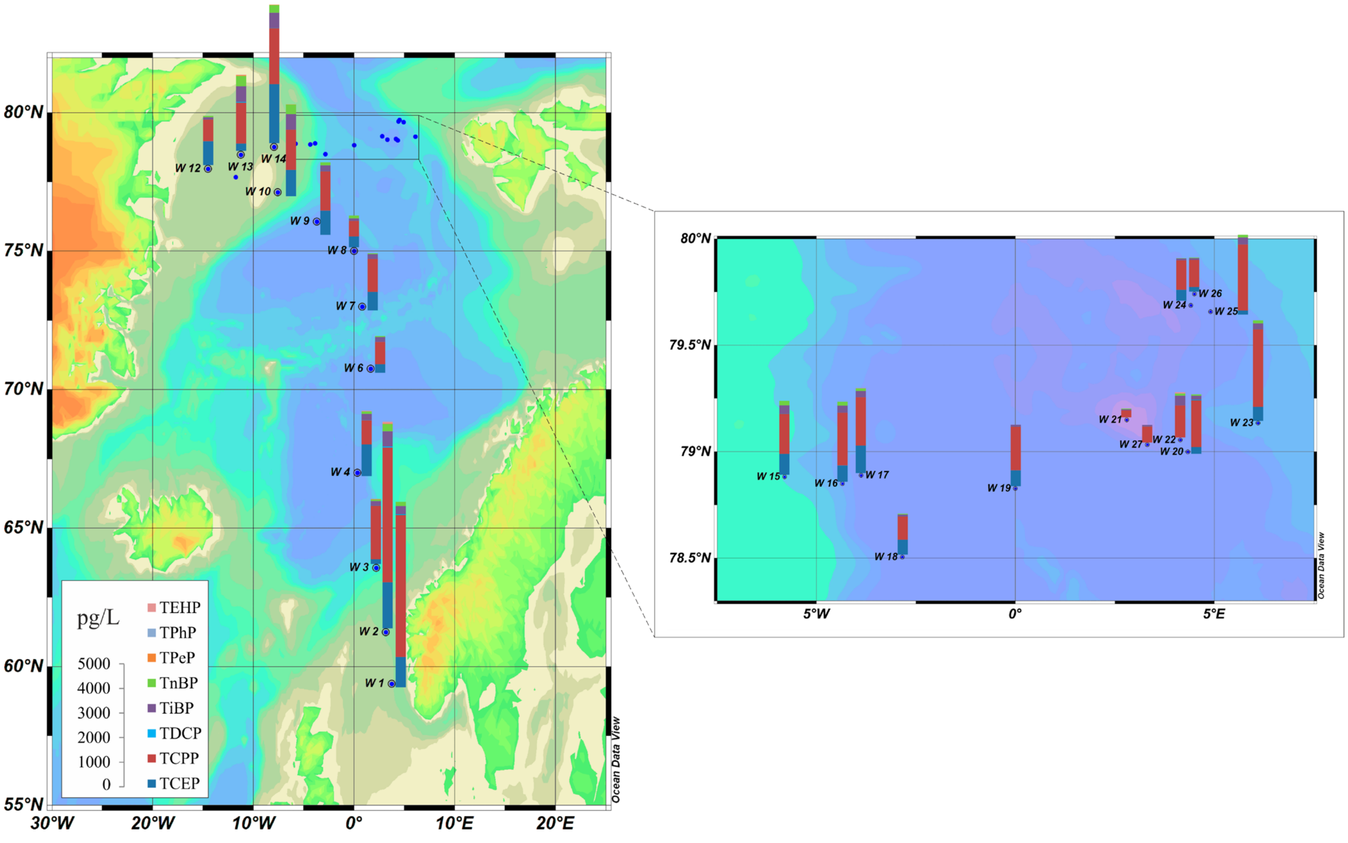

Figure 3. Spatial distribution of OPEs in seawater of the North Atlantic and the Arctic.

including samples W2 (8396 pg/L), W1 (7541 pg/L) (close to the European continent), W14 (5636 pg/L, near Greenland), and W23 (4086 pg/L, near Svalbard). When the ship was heading to the open ocean, much lower ΣOPE concentrations were measured. Near the European continent, fresh discharge of OPEs might have originated from the North Sea. Bollmann et al.[37] reported OPE concentrations in the German Bight (North Sea), ranging from 5 to 50 ng/L, which are 5−10 times higher than at samples W1−W6 in this study (range 1.5−8 ng/L), suggesting that there was a decreasing trend of ΣOPE concentrations from the North Sea to the Arctic. At the Greenland and Svalbard coasts, the glacier and snow melting contributed to OPEs in seawater to some degree, considering the high OPE concentrations in snow detected in this study (mean 7834 pg/L). Furthermore, closer to Greenland and Svalbard, higher ΣOPE concentrations were detected in snow. The discharge of melting snow and ice in the Arctic summer can be a secondary source of the organic contaminates and may cause elevated concentrations in the Arctic.

Particle Dry Deposition Fluxes. The dry particle deposition flux was determined by multiplying the concentration of particle OPEs by a dry deposition velocity (details see Text S2).[3,40] As no measured velocities for OPEs are available in the target area, a value of 0.1 cm/s (86.4 m/day) has been chosen, which was proposed by Möller et al. for calculating the dry deposition of PBDEs in the European Arctic.[30]

The dry deposition fluxes of four major OPEs in the individual air samples are shown in Figure 4a. The particle phase dry depositions of ΣOPE ranged from 2 to 16 ng/m^2/day, with a mean of 5 ± 4 ng/m^2/day. The atmospheric dry deposition was dominated by TCEP, ranging from 2 to 12 ng/m^2/day, and followed by TCPP from 0 to 2 ng/m^2/day, TnBP from 0.1 to 0.9 ng/m^2/day and TiBP from 0 to 0.6 ng/m^2/day, respectively. Possible uncertainties in the OPE dry deposition calculation are related to the estimated deposition velocity and to gas-particle interactions during sampling and have been explained in more detail in the QA/QC section.

The dry deposition fluxes of ΣOPE in this study were comparable to the levels estimated in the South China Sea (mean 16.3 ± 6.7 ng/m^2/day),[19] and were 1−2 orders of magnitude lower than those estimated in the North Sea (46−237 ng/m^2/day),[14] the Mediterranean Sea (70−880 ng/m^2/day),[3] and the Black Sea (∼300−1060 ng/m^2/day).[3]

Air−Seawater Gas Exchange Fluxes. The equilibrium status (f_A/f_W) and fluxes (F_{AW}) of air−seawater gas exchange for four major OPEs (TCEP, TCPP, TiBP, TnBP) were estimated in this study. The results of f_A/f_W and F_{AW} are shown in Figures S3 and Figure 4b, respectively. The details of the calculation method are presented in Text S3. Generally, $f_A/f_W = 1$ indicates equilibrium status of a system, whereas $f_A/f_W < 1$ and $f_A/f_W > 1$ indicate volatilization and deposition, respectively.[41] The Henry's law constants (HLCs) of OPEs were estimated by SPARC as suggested by Zhang et al., and corrected by the given temperature and salinity.[42] Considering the uncertainties existing with H values, a range of 0.3 to 3 is adopted for f_A/f_W, which shows a system at dynamic equilibrium.[41,43,44]

The f_A/f_W values of TCEP ranged from 0.01 to 0.7, indicating that volatilization from seawater to air dominated in all samples. The fluxes of TCEP ranged from 5 to 1075 ng/m^2/day. Equilibrium was reached at sample W3 and five samples near Svalbard (samples W20−W22, W25, and W27), which were caused by relatively low TCEP concentrations in seawater. There was a net volatilization for TCPP, with all f_A/f_W values lower

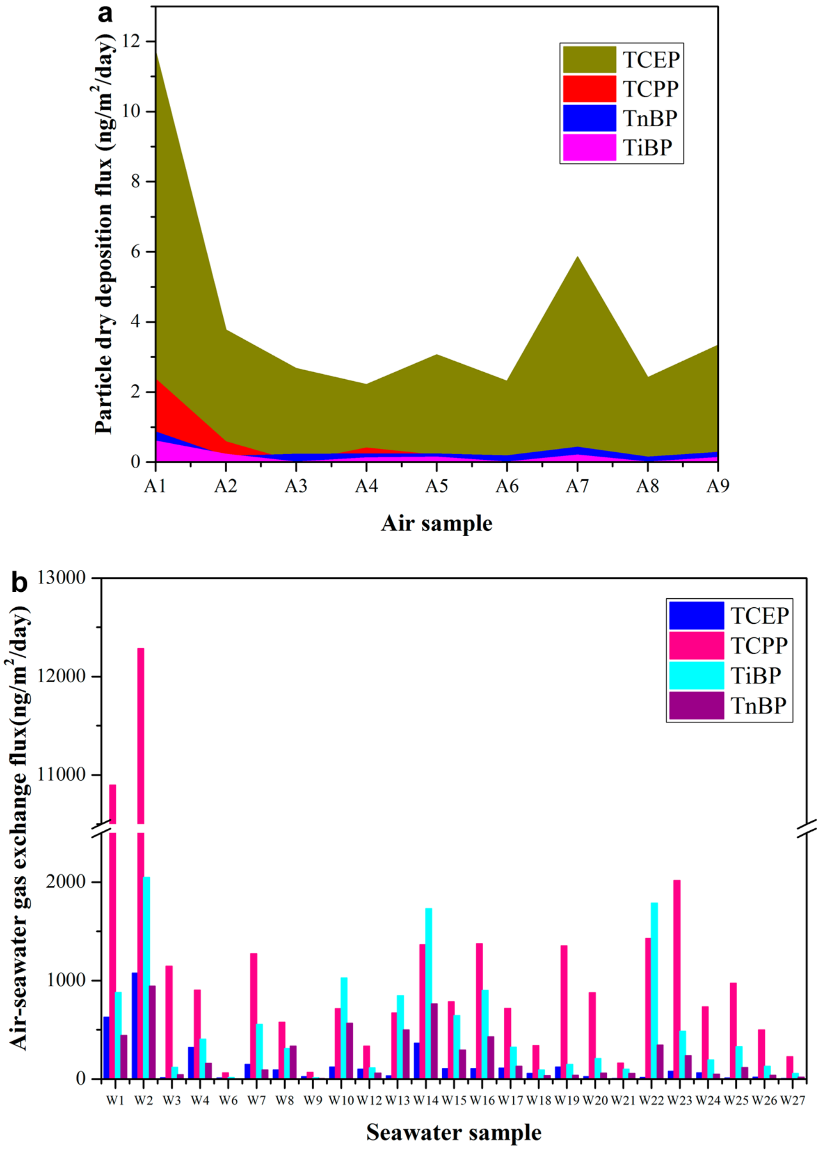

Figure 4. (a) Particle dry deposition fluxes of four major OPEs over the sea in the North Atlantic and the Arctic. (b) Air−seawater exchange fluxes of four major OPEs over the sea in the North Atlantic and the Arctic.

than 0.3, and the fluxes ranged from 61 to 12283 ng/m^2/day, with a mean of 1670 ± 3031 ng/m^2/day. The highest volatilization flux was observed at sample W2 as a result of relatively high TCPP concentration in seawater and high surface water temperature, as well as the strong wind speed (9 m/s). As for TiBP and TnBP, the f_A/f_W values were all lower than 0.3, with the fluxes ranging from 12 to 2049 ng/m^2/day for TiBP and from 3 to 943 ng/m^2/day for TnBP. These results indicated that air−seawater gas exchange processes may interfere with long-range transport potential for OPEs and drive their remobilization in the Arctic summer (or ice free period).

Because of the low concentrations of the other four OPEs (i.e., TDCP, TPhP, TPeP, and TEHP), their fluxes were not estimated considering the high uncertainty. Nevertheless, to our knowledge, this is the first report for air-seawater gas exchange fluxes of OPEs. The deviation of the measured OPE concentrations and HLCs can increase the uncertainty of the estimated fluxes. Further investigations on more accurate HLCs for OPEs are required to improve the understanding of their air-seawater gas exchange processes.

Implications. This work presents a decreasing trend for ΣOPE concentrations in the atmosphere and seawater from the North Atlantic to the Arctic, indicating the current ongoing atmospheric and water releases of these compounds from Europe. Although TCEP was replaced by TCPP in Europe, TCEP was still detected as the dominant OPE in the atmosphere and was about nine times higher than the mean TCPP concentration. On the other hand, in snow and seawater, the dominant OPE was TCPP. This suggests that TCEP is more stable than TCPP in the atmosphere. More research is necessary for understanding OPE properties and their fate in the environment. The mean ΣOPE concentration in snow was 7834 pg/L, which was about two times as high as that in seawater (2935 pg/L), suggesting that snow is an important intermediate for OPE accumulation in the Arctic. From the Greenland and Svalbard coasts to the open ocean, there was a slightly decreasing trend for ΣOPE concentrations in seawater, which was due to the glacier and snow melting to some degree. In terms of the effect of global warming on the Arctic, OPEs deposited in sinks such as snow and ice in the polar region are expected to remobilize into the atmosphere and water. Consequently, it is suggested that more studies are required to elucidate the influences of climate change on the occurrence, transport and fate of persistent or semipersistent compounds such as OPEs in the Arctic.

■ ASSOCIATED CONTENT

Ⓢ Supporting Information

The Supporting Information is available free of charge on the ACS Publications website at DOI: 10.1021/acs.est.7b01289.

> Detailed information on air sampling, snow sampling, and seawater sampling, full Names, acronyms, formulas, Chemical Abstract System numbers and physicochemical parameters of the selected organophosphate esters, parameters for the determination of organophosphate esters using GC-MS/MS, recovery rate, field blanks and method detection limits of organophosphate esters, mass of organophosphate esters measured for passive air samples, 120 h air mass back trajectories, composition profile and air−seawater gas exchange fugacity ratio of selected organophosphate esters, instrumental analysis method, particle dry deposition fluxes calculate method, and calculation of the air−seawater gas exchange calculate method (PDF)

■ AUTHOR INFORMATION

Corresponding Author

*Phone: +49-4152-872330. E-mail: zhiyong.xie@hzg.de.

ORCID

Zhiyong Xie: 0000-0001-8997-3930
Senchao Lai: 0000-0002-4990-3679
Chongguo Tian: 0000-0001-6058-9353

Author Contributions

J.L. and Z.X. conducted data management and wrote the manuscript; Z.X. designed the research and carried out the field work; W.M. and Z.X. performed sample preparation and instrumental analysis; C.T. guided the calculation method; S.L., K.E., and R.E. provided important comments and polished the manuscript.

Notes

The authors declare no competing financial interest.

■ ACKNOWLEDGMENTS

We acknowledge the Alfred Wegener Institute, Helmholtz-Centre for Polar and Marine Research (AWI), Bremerhaven, Germany, for the opportunity to take part in the expedition cruise. We are grateful to the captain and the crew of R/V Polarstern, the chief scientist Ingo Schewe (AWI) and the research team of ARK-XXVIII/2 for their support and assistance on sample collection during the cruise. J.L. gratefully acknowledges the China Scholarship Council.

■ REFERENCES

(1) Marklund, A.; Andersson, B.; Haglund, P. Traffic as a source of organophosphorus flame retardants and plasticizers in snow. *Environ. Sci. Technol.* **2005**, *39* (10), 3555−3562.

(2) Reemtsma, T.; Quintana, J. B.; Rodil, R.; Garcia-Lopez, M.; Rodriguez, I. Organophosphorus flame retardants and plasticizers in water and air I. Occurrence and fate. *TrAC, Trends Anal. Chem.* **2008**, *27* (9), 727−737.

(3) Castro-Jimenez, J.; Berrojalbiz, N.; Pizarro, M.; Dachs, J. Organophosphate Ester (OPE) Flame Retardants and Plasticizers in the Open Mediterranean and Black Seas Atmosphere. *Environ. Sci. Technol.* **2014**, *48* (6), 3203−3209.

(4) Marklund, A.; Andersson, B.; Haglund, P. Organophosphorus flame retardants and plasticizers in air from various indoor environments. *J. Environ. Monit.* **2005**, *7* (8), 814−819.

(5) Makinen, M. S. E.; Makinen, M. R. A.; Koistinen, J. T. B.; Pasanen, A. L.; Pasanen, P. O.; Kalliokoski, P. I.; Korpi, A. M. Respiratory and Dermal Exposure to Organophosphorus Flame Retardants and Tetrabromobisphenol A at Five Work Environments. *Environ. Sci. Technol.* **2009**, *43* (3), 941−947.

(6) Zhang, Y. Global market analysis of flame retardant (in Chinese). *Fine and Specialty Chem.* **2014**, *22* (8), 20−24.

(7) Fries, E.; Puttmann, W. Occurrence of organophosphate esters in surface water and ground water in Germany. *J. Environ. Monit.* **2001**, *3* (6), 621−626.

(8) Camarasa, J. G.; Serra-Baldrich, E. Allergic contact dermatitis from triphenyl phosphate. *Contact Dermatitis* **1992**, *26* (4), 264−265.

(9) Matthews, H. B.; Eustis, S. L.; Haseman, J. Toxicity and carcinogenicity of chronic exposure to tris(2-chloroethyl)phosphate. *Toxicol. Sci.* **1993**, *20* (4), 477−485.

(10) Van der Veen, I.; de Boer, J. Phosphorus flame retardants: Properties, production, environmental occurrence, toxicity and analysis. *Chemosphere* **2012**, *88* (10), 1119−1153.

(11) Sundkvist, A. M.; Olofsson, U.; Haglund, P. Organophosphorus flame retardants and plasticizers in marine and fresh water biota and in human milk. *J. Environ. Monit.* **2010**, *12* (4), 943−951.

(12) Kim, J. W.; Isobe, T.; Chang, K. H.; Amano, A.; Maneja, R. H.; Zamora, P. B.; Siringan, F. P.; Tanabe, S. Levels and distribution of organophosphorus flame retardants and plasticizers in fishes from Manila Bay, the Philippines. *Environ. Pollut.* **2011**, *159* (12), 3653−3659.

(13) Möller, A.; Sturm, R.; Xie, Z.; Cai, M. H.; He, J. F.; Ebinghaus, R. Organophosphorus Flame Retardants and Plasticizers in Airborne Particles over the Northern Pacific and Indian Ocean toward the Polar Regions: Evidence for Global Occurrence. *Environ. Sci. Technol.* **2012**, *46* (6), 3127−3134.

(14) Möller, A.; Xie, Z.; Caba, A.; Sturm, R.; Ebinghaus, R. Organophosphorus flame retardants and plasticizers in the atmosphere of the North Sea. *Environ. Pollut.* **2011**, *159* (12), 3660−3665.

(15) Cheng, W. H.; Xie, Z. Q.; Blais, J. M.; Zhang, P. F.; Li, M.; Yang, C. Y.; Huang, W.; Ding, R.; Sun, L. G. Organophosphorus esters in the oceans and possible relation with ocean gyres. *Environ. Pollut.* **2013**, *180*, 159−164.

(16) Salamova, A.; Hermanson, M. H.; Hites, R. A. Organophosphate and Halogenated Flame Retardants in Atmospheric Particles from a European Arctic Site. *Environ. Sci. Technol.* **2014**, *48* (11), 6133−6140.

(17) Green, N.; Schlabach, M.; Bakke, T.; Brevik, E.; Dye, C.; Herzke, D.; Huber, S.; Plosz, B.; Remberger, M.; Schøyen, M. *Screening of Selected Metals and New Organic Contaminants 2007. Phosphorous Flame Retardents, Polyfluorinated Organic Compounds, Nitro-PAHs, Silver, Platinum and Sucralose in Air, Wastewater, Treatment Facilities, and Freshwater and Marine Recipients*, Report TA2367; Norwegian Pollution Control Authority, 2008.

(18) Sühring, R.; Diamond, M. L.; Scheringer, M.; Wong, F.; Pucko, M.; Stern, G.; Burt, A.; Hung, H.; Fellin, P.; Li, H.; Jantunen, L. M. Organophosphate Esters in Canadian Arctic Air: Occurrence, Levels and Trends. *Environ. Sci. Technol.* **2016**, *50* (14), 7409−7415.

(19) Lai, S.; Xie, Z.; Song, T.; Tang, J.; Zhang, Y.; Mi, W.; Peng, J.; Zhao, Y.; Zou, S.; Ebinghaus, R. Occurrence and dry deposition of organophosphate esters in atmospheric particles over the northern South China Sea. *Chemosphere* **2015**, *127*, 195−200.

(20) Pankow, J. F.; Bidleman, T. F. Interdependence of the Slopes and Intercepts from Log Log Correlations of Measured Gas Particle Partitioning and Vapor-Pressure 0.1. Theory and Analysis of Available Data. *Atmos. Environ., Part A* **1992**, *26* (6), 1071−1080.

(21) Draxler, R. R.; Hess, G. *Description of the HYSPLIT4 Modeling System*, NOAA Technical Memorandum ERL ARL-224; Air Resources Laboratory: Silver Spring, Maryland, 1997.

(22) Salamova, A.; Peverly, A. A.; Venier, M.; Hites, R. A. Spatial and Temporal Trends of Particle Phase Organophosphate Ester Concentrations in the Atmosphere of the Great Lakes. *Environ. Sci. Technol.* **2016**, *50* (24), 13249−13255.

(23) Rauert, C.; Harner, T.; Schuster, J. K.; Quinto, K.; Fillmann, G.; Castillo, L. E.; Fentanes, O.; Ibarra, M. V.; Miglioranza, K. S. B.; Rivadeneira, I. M.; Pozo, K.; Puerta, A. P.; Zuluaga, B. H. A. Towards a regional passive air sampling network and strategy for new POPs in the GRULAC region: Perspectives from the GAPS Network and first results for organophosphorus flame retardants. *Sci. Total Environ.* **2016**, *573*, 1294−1302.

(24) Salamova, A.; Ma, Y. N.; Venier, M.; Hites, R. A. High Levels of Organophosphate Flame Retardants in the Great Lakes Atmosphere. *Environ. Sci. Technol. Lett.* **2014**, *1* (1), 8−14.

(25) Gao, L. H.; Shi, Y. L.; Li, W. H.; Liu, J. M.; Cai, Y. Q. Occurrence and distribution of organophosphate triesters and diesters in sludge from sewage treatment plants of Beijing, China. *Sci. Total Environ.* **2016**, *544*, 143−149.

(26) China's flame retardant industry in 2015 will be steady development. ChinaIRN.com 2015.1.14. http://www.chinairn.com/news/20150114/164023439.shtml.

(27) Wolschke, H.; Sühring, R.; Mi, W. Y.; Möller, A.; Xie, Z.; Ebinghaus, R. Atmospheric occurrence and fate of organophosphorus flame retardants and plasticizer at the German coast. *Atmos. Environ.* **2016**, *137*, 1−5.

(28) Wei, G. L.; Li, D. Q.; Zhuo, M. N.; Liao, Y. S.; Xie, Z. Y.; Guo, T. L.; Li, J. J.; Zhang, S. Y.; Liang, Z. Q. Organophosphorus flame retardants and plasticizers: Sources, occurrence, toxicity and human exposure. *Environ. Pollut.* **2015**, *196*, 29−46.

(29) Liu, Y. C.; Liggio, J.; Harner, T.; Jantunen, L.; Shoeib, M.; Li, S. M. Heterogeneous OH Initiated Oxidation: A Possible Explanation for the Persistence of Organophosphate Flame Retardants in Air. *Environ. Sci. Technol.* **2014**, *48* (2), 1041−1048.

(30) Möller, A.; Xie, Z.; Sturm, R.; Ebinghaus, R. Polybrominated diphenyl ethers (PBDEs) and alternative brominated flame retardants in air and seawater of the European Arctic. *Environ. Pollut.* **2011**, *159* (6), 1577−1583.

(31) Möller, A.; Xie, Z.; Sturm, R.; Ebinghaus, R. Large-Scale Distribution of Dechlorane Plus in Air and Seawater from the Arctic to Antarctica. *Environ. Sci. Technol.* **2010**, *44* (23), 8977−8982.

(32) Carlsson, H.; Nilsson, U.; Becker, G.; Ostman, C. Organophosphate ester flame retardants and plasticizers in the indoor environment: Analytical methodology and occurrence. *Environ. Sci. Technol.* **1997**, *31* (10), 2931−2936.

(33) Goss, K. U.; Eisenreich, S. J. Sorption of volatile organic compounds to particles from a combustion source at different temperatures and relative humidities. *Atmos. Environ.* **1997**, *31* (17), 2827−2834.

(34) Storey, J. M. E.; Luo, W.; Isabelle, L. M.; Pankow, J. F. Gas-Solid Partitioning of Semivolatile Organic-Compounds to Model Atmospheric Solid-Surfaces as a Function of Relative-Humidity 0.1. Clean Quartz. *Environ. Sci. Technol.* **1995**, *29* (9), 2420−2428.

(35) Regnery, J.; Puttmann, W. Organophosphorus Flame Retardants and Plasticizers in Rain and Snow from Middle Germany. *Clean: Soil, Air, Water* **2009**, *37* (4−5), 334−342.

(36) Bacaloni, A.; Cucci, F.; Guarino, C.; Nazzari, M.; Samperi, R.; Lagana, A. Occurrence of organophosphorus flame retardant and plasticizers in three volcanic lakes of Central Italy. *Environ. Sci. Technol.* **2008**, *42* (6), 1898−1903.

(37) Bollmann, U. E.; Möller, A.; Xie, Z.; Ebinghaus, R.; Einax, J. W. Occurrence and fate of organophosphorus flame retardants and plasticizers in coastal and marine surface waters. *Water Res.* **2012**, *46* (2), 531−538.

(38) Harino, H.; Yatsuzuka, E.; Yamao, C.; Ueno, M.; Ohji, M. Current status of organophosphorus compounds contamination in Maizuru Bay, Japan. *J. Mar. Biol. Assoc. U. K.* **2014**, *94* (1), 43−49.

(39) Regnery, J.; Puttmann, W. Occurrence and fate of organophosphorus flame retardants and plasticizers in urban and remote surface waters in Germany. *Water Res.* **2010**, *44* (14), 4097−4104.

(40) Jurado, E.; Jaward, F. M.; Lohmann, R.; Jones, K. C.; Simo, R.; Dachs, J. Atmospheric dry deposition of persistent organic pollutants to the Atlantic and inferences for the global oceans. *Environ. Sci. Technol.* **2004**, *38* (21), 5505−5513.

(41) Xie, Z.; Koch, B. P.; Möller, A.; Sturm, R.; Ebinghaus, R. Transport and fate of hexachlorocyclohexanes in the oceanic air and surface seawater. *Biogeosciences* **2011**, *8* (9), 2621−2633.

(42) Zhang, X. M.; Suhring, R.; Serodio, D.; Bonnell, M.; Sundin, N.; Diamond, M. L. Novel flame retardants: Estimating the physical-chemical properties and environmental fate of 94 halogenated and organophosphate PBDE replacements. *Chemosphere* **2016**, *144*, 2401−2407.

(43) Bruhn, R.; Lakaschus, S.; McLachlan, M. S. Air/sea gas exchange of PCBs in the southern Baltic Sea. *Atmos. Environ.* **2003**, *37* (24), 3445−3454.

(44) Lohmann, R.; Gioia, R.; Jones, K. C.; Nizzetto, L.; Temme, C.; Xie, Z.; Schulz-Bull, D.; Hand, I.; Morgan, E.; Jantunen, L. Organochlorine Pesticides and PAHs in the Surface Water and Atmosphere of the North Atlantic and Arctic Ocean. *Environ. Sci. Technol.* **2009**, *43* (15), 5633−5639.

DOI: 10.1021/acs.est.7b01289
Environ. Sci. Technol. 2017, 51, 6887−6896

Supporting information of

Organophosphate esters in air, snow and seawater in the North Atlantic and the Arctic

Jing Li[†,‡], Zhiyong Xie[†*], Wenying Mi[§], Senchao Lai[ǀ], Chongguo Tian[⊥], Kay-Christian Emeis[†,‡], Ralf Ebinghaus[†]

[†]Helmholtz-Zentrum Geesthacht, Centre for Materials and Coastal Research, Institute of Coastal Research, Geesthacht, 21502, Germany

[‡]University of Hamburg, School of Integrated Climate System Sciences, Hamburg, 20144, Germany

[§]MINJIE Analytical Laboratory, Geesthacht, 21502, Germany

[ǀ]Guangdong Provincial Engineering and Technology Research Center for Environmental Risk Prevention and Emergency Disposal, School of Environment and Energy, South China University of Technology, Guangzhou, 510006, China

[⊥]Key Laboratory of Coastal Environmental Processes and Ecological Remediation, Yantai Institute of Coastal Zone Research, CAS, Yantai, 264003, China

*Corresponding author.

Phone: +49-4152-872330; Fax: +49-4152-872332;

E-mail address: zhiyong.xie@hzg.de

Pages: 17

Tables: 7

Figures: 3

Content list:

Table S1. Detailed information on air sampling. T_a represents the mean air temperature values during the sampling period

Air sample	**Date**	**Time**	**Date**	**Time**	**Latitude**	**Longitude**	**Latitude**	**Longitude**	**Volume (m^3)**	**T_a (°C)**	**Humidity (%)**	**C_{TSP} (ug/m^3)**
A1	08.06.14	20:00:00	09.06.14	22:00:00	61.338	3.137	65.671	0.312	337	11.6	78	15
A2	10.06.14	5:40:00	11.06.14	20:00:00	66.470	0.123	73.058	0.803	434	6.9	95	-
A3	11.06.14	20:57:00	14.06.14	7:10:00	73.214	0.741	77.999	-14.316	931	-4.2	89	5
A4	14.06.14	7:30:00	16.06.14	7:30:00	77.981	-14.040	78.500	-11.517	775	3.8	78	7
A5	16.06.14	7:30:00	18.06.14	9:00:00	78.537	-10.596	78.828	-4.272	692	-0.3	85	5
A6	18.06.14	9:25:00	20.06.14	10:20:00	78.820	-4.301	78.600	-2.838	693	-2.2	75	6
A7	20.06.14	10:40:00	22.06.14	11:00:00	78.582	-2.786	79.061	4.026	729	-2.1	98	10
A8	22.06.14	11:50:00	24.06.14	11:20:00	79.059	4.034	79.018	4.069	606	0.8	92	40
A9	24.06.14	11:47:00	26.06.14	17:30:00	79.017	4.098	61.333	3.138	568	0.7	98	18

Table S2. Detailed information on snow sampling. T_w represents seawater temperature, T_a represents air temperature

Snow sample	**Date**	**Time**	**Latitude**	**Longitude**	**Volume (m^3)**	**T_w(°C)**	**T_a (°C)**
S1	15.06.14	13:50:00	77.819	-15.105	10	-1.35	3.2
S2	18.06.14	17:00:00	78.811	-4.019	10	-1.43	-2.6
S3	17.06.14	11:46:00	78.832	-5.752	10	-1.27	0.5
S4	20.06.14	19:30:00	78.504	-2.840	10	-1.6	-0.7
S5	22.06.14	9:40:00	79.053	4.150	10	1.39	0.7
S6	25.06.14	13:40:00	79.764	4.361	10	-1.35	0.9

Table S3. Detailed information on seawater sampling

Seawater sample	Date	Time	Latitude	Longitude	T_w (°C)	T_a (°C)	Salinity(‰)	Wind speed (m/s)
W 1	08.06.14	8:14:00	59.38	3.73	14.55	14.9	29.48	7.9
W 2	08.06.14	19:30:00	61.24	3.17	13.95	12.7	32.5	9.1
W 3	09.06.14	9:06:00	63.56	2.20	11.88	11.6	33.92	3.4
W 4	10.06.14	8:45:00	67.00	0.34	8.74	9	35.13	5.7
W 6	11.06.14	6:48:00	70.76	1.65	7.41	4	35.15	0.9
W 7	11.06.14	19:30:00	73.00	0.83	3.08	1.2	34.73	8.3
W 8	12.06.14	7:24:00	75.00	0.00	2.04	0.4	34.84	8.6
W 9	12.06.14	15:35:00	76.06	-3.69	0.54	-1.5	33.51	0.7
W 10	13.06.14	6:35:00	77.13	-7.56	-1.29	-4.8	31.9	5.9
W 12	14.06.14	7:58:00	77.96	-14.51	-0.55	0.6	31.41	4.8
W 13	16.06.14	7:10:00	78.48	-11.23	-0.77	2.6	31.65	5.2
W 14	16.06.14	21:30:00	78.76	-7.92	-1.41	0.6	31.23	8.2
W 15	17.06.14	12:17:00	78.88	-5.80	-1.12	0.7	31.04	6.4
W 16	18.06.14	7:45:00	78.85	-4.34	-1.45	-0.6	30.81	8.8
W 17	19.06.14	7:12:00	78.89	-3.87	-1.59	2.2	31.86	5.1
W 18	20.06.14	20:07:00	78.50	-2.84	-1.57	-0.5	33.89	5
W 19	21.06.14	17:30:00	78.83	0.00	2.98	-0.4	34.79	6.8
W 20	22.06.14	7:10:00	79.00	4.33	1.32	0.4	33.8	4.9
W 21	23.06.14	21:47:00	79.15	2.80	-1.05	0.8	33.21	7.7
W 22	24.06.14	7:40:00	79.06	4.14	1.36	1.7	33.7	11
W 23	24.06.14	22:50:00	79.13	6.10	0.85	1.4	33.35	6.9
W 24	25.06.14	6:58:00	79.69	4.41	-1.36	0.5	33.2	8.3
W 25	25.06.14	22:12:00	79.66	4.90	-1.08	0.1	33.03	4.8
W 26	26.06.14	7:25:00	79.74	4.50	-1.35	-0.8	33.35	6.2
W 27	26.06.14	21:46:00	79.03	3.32	-0.24	0.5	33.2	4.3

Table S4. Full Names, acronyms, formulas, Chemical Abstract System (CAS) numbers and physicochemical parameters of the selected organophosphate esters

Acronym	Full Name	CAS No.	Chemical form	MW	H from SPRAC ($Pa \cdot m^3/mol$)
TCEP	Tris-(2-chloroethyl) phosphate	115-96-8	$C_6H_{12}Cl_3O_4P$	285.5	5.06
TCPP	Tris-(1-chloro-2-propyl) phosphate	13674-84-5	$C_9H_{18}Cl_3O_4P$	327.6	72.77
TDCP	Tris-(1,3-dichloro-2-propyl) phosphate	13674-87-8	$C_9H_{15}Cl_6O_4P$	430.9	0.13
TiBP	Tri-iso-butyl phosphate	126-71-6	$C_{12}H_{27}O_4P$	266.3	9210
TnBP	Tri-n-butyl phosphate	126-73-8	$C_{12}H_{27}O_4P$	266.3	962.9
TPhP	Triphenyl phosphate	115-86-6	$C_{18}H_{15}O_4P$	326.3	3.12
TPeP	Tripentyl phosphate	2528-38-3	$C_{15}H_{33}O_4P$	308.4	643.6
TEHP	Tris-(2-ethylhexyl) phosphate	78-42-2	$C_{24}H_{51}O_4P$	434.6	280.7

Table S5. Parameters for determining organophosphate esters using GC-MS/MS

Acronym	**Name**	**Retention time (min)**	**Quantifier***	**Qualifier***
TCEP	Tris-(2-chloroethyl)phosphate	22.21	249.0/99.0	249.0/187.0
TCPP1	Tris-(1-chloro-2-propyl)phosphate	22.95	157.0/117.0	277.0/125.0
TCPP2	Tris-(1-chloro-2-propyl)phosphate	23.24	157.0/117.0	277.0/125.0
TCPP3	Tris-(1-chloro-2-propyl)phosphate	23.48	157.0/117.0	277.0/125.0
TDCP	Tri-(dichlorisopropyl)phosphate	32.66	381.0/159.0	191.0/75.0
T*i*BP	Tri-*iso*-butylphosphate	16.79	99.0/81.0	155.0/99.0
TnBP	Tri-*n*-butylphosphate	19.76	99.0/81.0	155.0/99.0
TPhP	Triphenylphosphate	33.68	326.0/215.0	326.0/170.0
TPeP	Tripentylphosphate	25.52	99.0/81.0	239.0/99.0
TEHP	Tris-(2-ethylhexyl)phosphate	34.96	99.0/81.0	113.0/99.0
d_{27}-TnBP	d_{27}-Tri-*n*-butylphosphate	19.38	103.0/83.0	167.0/103.0
d_{12}-TCEP	d_{12}-Tris-(2-chloroethyl)phosphate	22.00	261.0/103.0	261.0/196.0
d_{15}-TPhP	d_{15}-Triphenylphosphate	33.55	341.0/223.0	341.0/178.0
$^{13}C_6$-PCB 208	$^{13}C_6$-2,2',3,3',4,5,5',6,6'-Nonachlorobiphenyl	37.73	476.0/406.0	-

* Precursor ion/product ion

Table S6. Recovery rate, field blanks and method detection limits (MDLs) of OPEs. MDLs were derived from mean blank values plus three times the standard deviation. A mean volume of 300 m^3 was estimated for air samples, 800ml for snow and seawater

OPE	**Recovery Rate (%)**				**Gaseous phase (pg/m^3)**		**Particle phase (pg/m^3)**		**Dissolved phase Snow & Seawater (pg/L)**	
	Clean-up	LLE	PUF/XAD-2 (Gaseous phase)	GFF (particle phase)	Blank	MDL	Blank	MDL	Blank	MDL
TCEP	59	95 ± 8	145 ± 9	137 ± 13	0.6	1.2	1.2	3.8	86	210
TCPP	85	82 ± 4	92 ± 6	107 ± 4	0.5	0.8	5	6.5	110	190
TDCP	68	84 ± 3	110 ± 6	122 ± 4	0.001	0.002	0.005	0.01	4	8
TiBP	87	78 ± 3	88 ± 13	112 ± 4	0.1	0.2	1	1.8	27	47
TnBP	85	80 ± 3	95 ± 11	116 ± 4	1	1.5	0.5	0.6	13	30
TPhP	74	82 ± 2	97 ± 5	109 ± 2	0.0001	0.01	0.0001	0.007	2	88
TPeP	85	81 ± 3	102 ± 11	122 ± 5	0.01	0.0003	0.003	0.0002	30	7
TEHP	67	81 ± 5	118± 14	139 ± 12	0.01	0.02	0.003	0.008	9	23

Table S7. Mass of OPEs (ng) measured for passive air samples (PAS) deployed in the chemical lab and on the top deck next to the high-volume air sampler

OPE	In chemical lab			Next to the air sampler		
	PAS01	**PAS02**	**Mean**	**PAS03**	**PAS04**	**Mean**
TCEP	78	103	90	23	22	22.6
TCPP	65	95	80	6	4	5
TDCP	0.006	0.013	0.01	0.003	0.005	0.004
TiBP	31	31	31	0.09	0.13	0.1
TnBP	24	27	26	0.1	0.1	0.1
TPhP	3	11	7	0.1	0.09	0.1
TPeP	0.005	0.008	0.007	0.004	0.016	0.01
TEHP	0.03	0.08	0.05	0.02	0.06	0.04
ΣOPEs	201	267	235	29	27	28.4

Figure S1. 120 h air mass back trajectories (6 h steps)

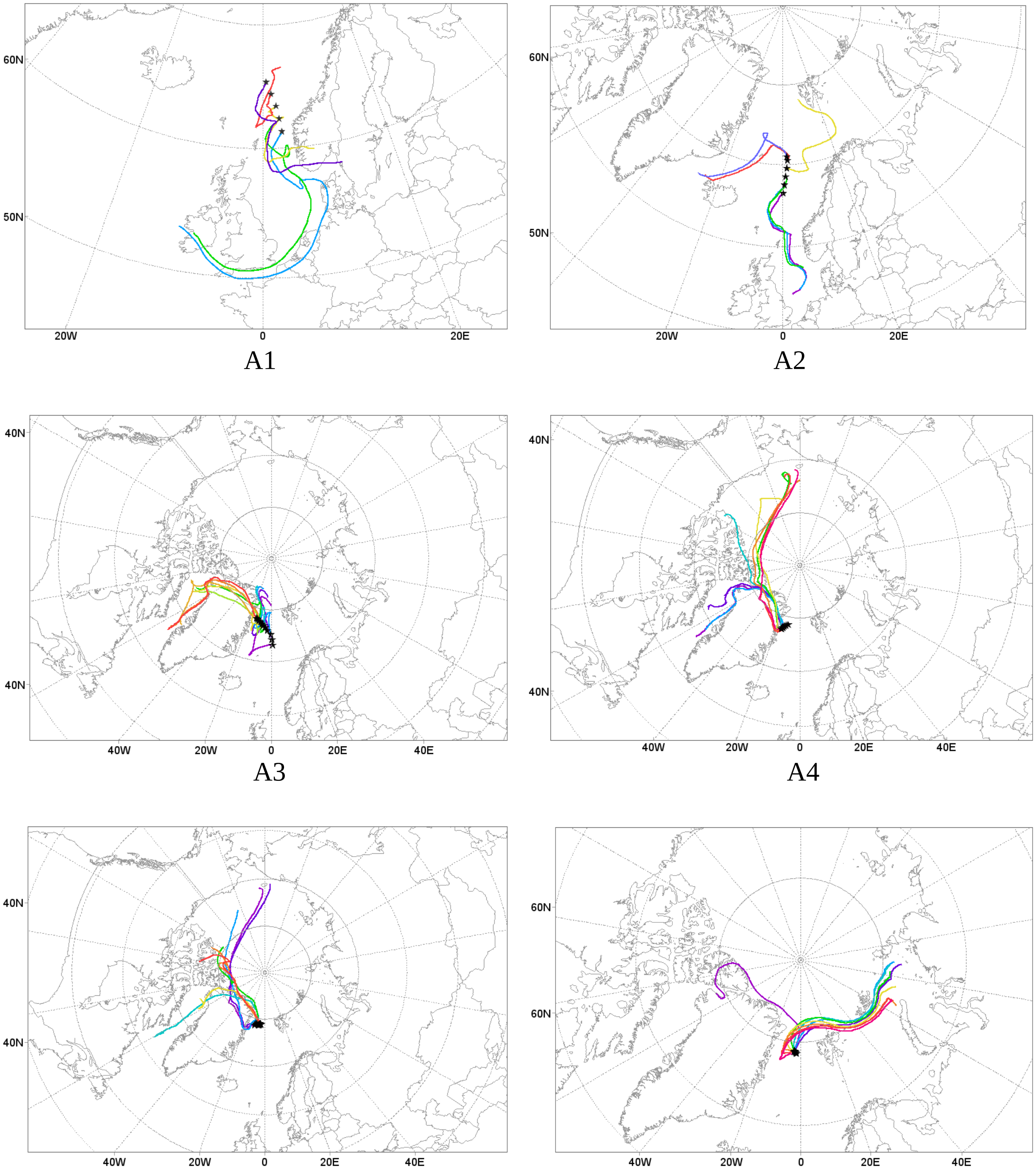

A1 A2

A3 A4

A5 A6

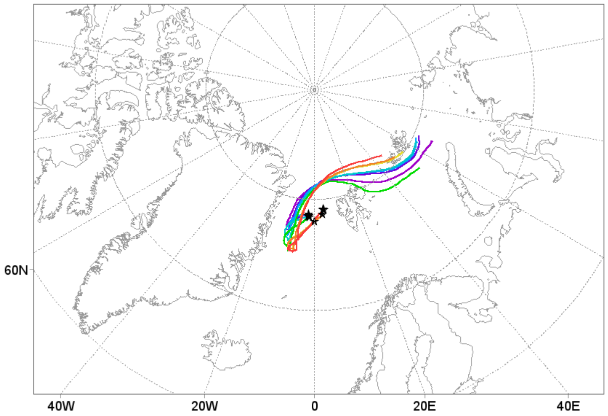

A7

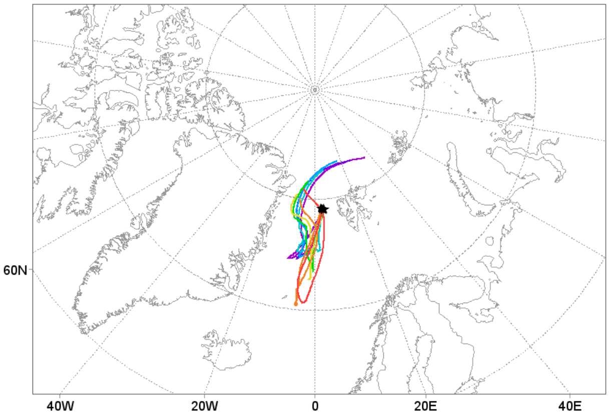

A8

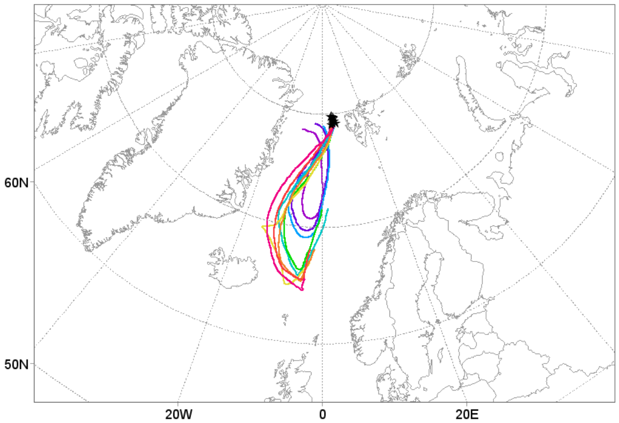

A9

Figure S2. Composition profile of selected OPEs in gaseous and particle phases

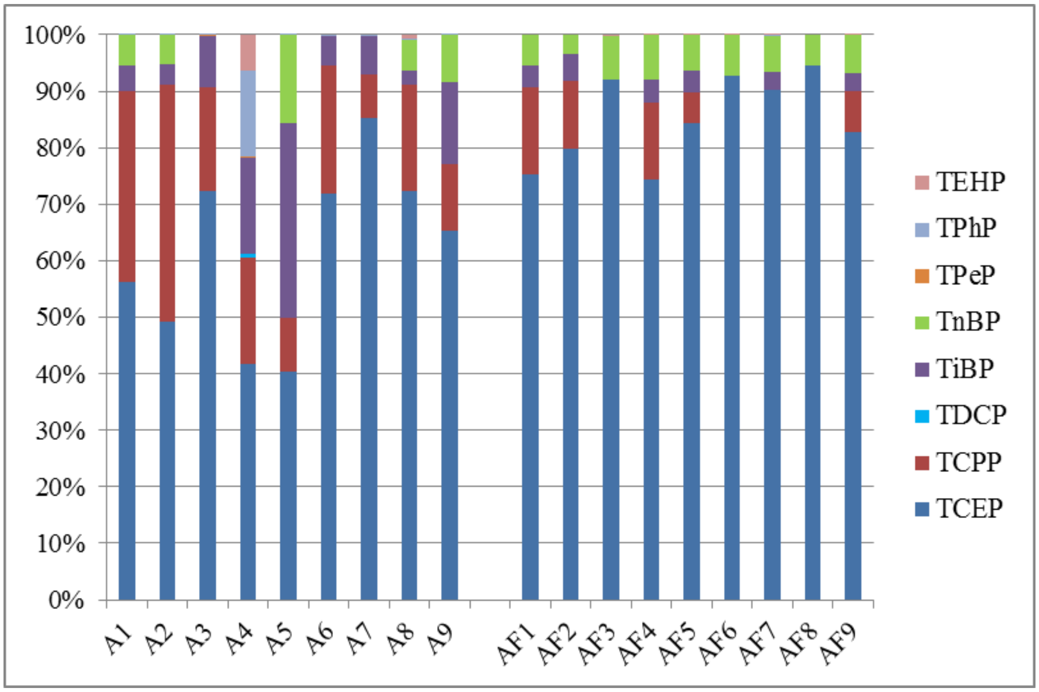

Figure S3. Air-water gas exchange fugacity ratio of four major OPEs, the dash line represents f_A / f_W = 0.3

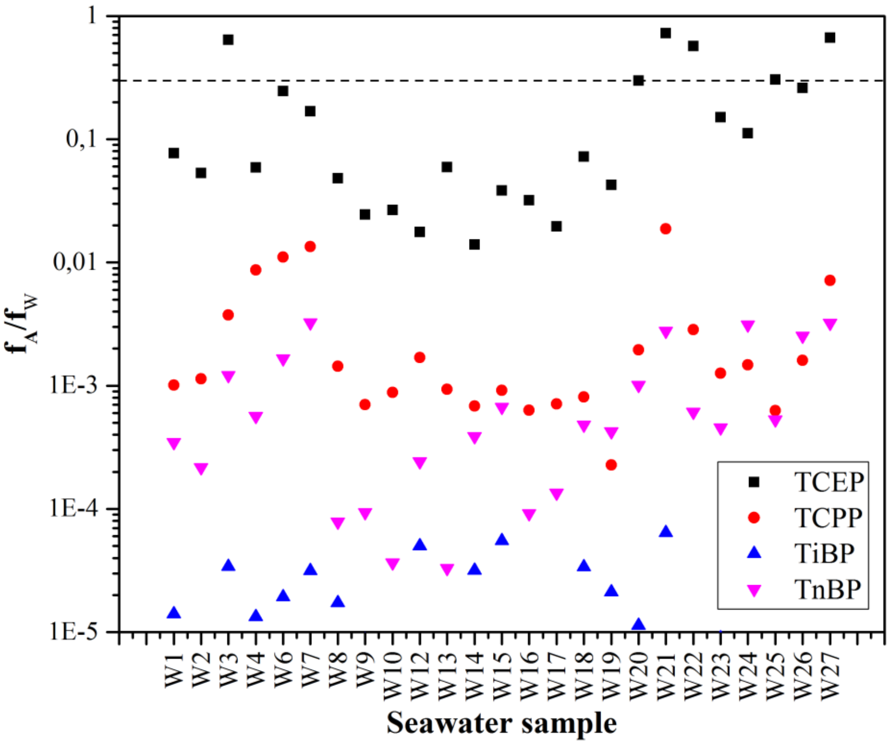

Text S1. Instrumental analysis method

The samples were analyzed using a gas chromatograph (GC, Agilent 7890A) couple to a triple quadrupole mass spectrometer (MS, Agilent 7010) equipped with a programmed temperature vaporizer (PTV) injector (Agilent, USA). The MS transfer line and the high sensitivity electron impact ionization source (HSEI) were held at 280 °C and 230 °C, respectively. The MS/MS was operated in Multiple Reaction Monitoring (MRM) mode. The collision cell gases were nitrogen (1.5 mL/min) and helium (2.25 mL/min). Analyses were separated on a HP-5MS Ultra Inert capillary column (30 m × 0.25 mm i.d. × 0.25 μm film thickness, J&W Scientific and Agilent Technologies, CA). One microliter of the sample was injected in the pulsed splitless mode with an inlet temperature program held at 50 °C for 0.2 min, increased to 300 °C at 300°C/min and then held for 20 min. High purity helium (99.999%) was used as the carrier gas. The GC oven temperature was held at 50 °C for 2 min, increased to 80 °C at 20 °C /min, then increased to 250 °C at 5 °C/min, finally increased to 300 °C at 15 °C/min, and held for 10 min. Selected ions for quantification and quantitation are listed in Table S5. MassHunter quantitative analysis software (version B06.00, Agilent Technologies, USA) was used for data processing.

Text S2. Particle dry deposition fluxes calculation method

The dry particle-bound deposition flux F_d (F_d, ng/m^2/day) was determined by multiplying the concentration of particle-bound OPEs (C_p, ng/m^3) by a dry deposition velocity (V_d, m/day) [1, 2]:

$$F_d = V_d C_p \tag{1}$$

The deposition velocity highly depends on both physicochemical parameters, size and meteorological parameters of the airborne particle and of the pollutant itself.[3] Since no measured velocities for OPEs are available, a value of 0.1cm/s (86.4 m/day) has been chosen, which was proposed by Möller et al. for the dry deposition of polybrominated diphenyl ethers (PBDEs) into the European Arctic.[4] However, an uncertainty factor of three is assumed, which is caused by lack of measurement of V_d in the sampling area. [4]

Text S3. The calculation of the air–seawater gas exchange calculation method

The equilibrium status (or direction) of the air-seawater gas exchange was estimated based on Eq. (2):

$$f_A / f_W = C_A R T_A / (C_w H) \tag{2}$$

where f_A / f_W is the fugacity ratio, C_A and C_w are the gaseous and dissolved concentrations in air and seawater (pg/m^3), H is the Henry's law constant (Pa/m^3/mol) estimated from SPARC for OPEs (see Table S4), and corrected by the given water temperature and the salinity according to Schwarzenbach et al.[5, 6] Generally, $f_A / f_W = 1$ means a system at equilibrium, whereas $f_A / f_W < 1$ and $f_A / f_W > 1$ indicate volatilization and deposition, respectively. Considering that large uncertainties exist for H values of OPEs, we assume that values of f_A / f_W from 0.3 to 3 represent a system at dynamic equilibrium.[7]

Air-water gas exchange fluxes were estimated using the modified Whitman two-film resistance model[8, 9]:

$$F_{AW} = K_{OL}(C_W - \frac{C_A}{H'_{salt,T}}) \tag{3}$$

where F_{AW} is the flux (pg/m^2/day). F_{AW}<0 represents OPE deposition from air into seawater, and F_{AW}>0 represents the volatilization from seawater into air. C_A and C_W are the gaseous and dissolved concentrations in air and water (pg/m^3), respectively. K_{OL} (m/day) is the gas phase overall mass transfer coefficient. $H'_{salt,T}$ is the dimensionless Henry's Law constant defined as $H' = H / RT$ (R = gas constant, T = temperature). The dimensionless Henry's Law constant was corrected for salinity using Eq:[5]

$$H'_{salt,T} = H' \times 10^{K_S C_S}$$

where C_S is the averaged salt concentrations (0.5 mol/L is used in this study) and K_S is the Setschenow constant (L/mol) which was calculated following Eq:[10]

$$K_S = 0.04 \log K_{OW} + 0.114$$

When C_A or C_W were not available, 2/3 of the MDL was used. Because fewer air than water samples were available, the nearby air sample surrounding the water sample station is adopted (see the table below).

Seawater sample	**Air sample**
W 1	A1

W 2	A1
W 3	A1
W 4	A2
W 6	A2
W 7	A2
W 8	A3
W 9	A3
W 10	A3
W 12	A4
W 13	A4
W 14	A5
W 15	A5
W 16	A6
W 17	A6
W 18	A7
W 19	A7
W 20	A8
W 21	A8
W 22	A8
W 23	A8
W 24	A9
W 25	A9
W 26	A9
W 27	A8

K_{OL} (m/day) is the gaseous phase overall mass transfer coefficient compromising the resistances to mass transfer in both water (K_W, m/day) and air (K_A, m/day), and is defined by:

$$\frac{1}{K_{OL}} = \frac{1}{K_W} + \frac{1}{K_A H'}$$

where [11]

$$K_A = (0.2U_{10} + 0.3) \times \left(\frac{D_{i,air}}{D_{H_2O,air}} \right)^{0.61} \times 864$$

$$K_W = (0.45U_{10}{}^{1.64}) \times \left(\frac{Sc_i}{Sc_{CO_2}} \right)^{-0.5} \times 0.24$$

U_{10} is the wind speed at 10 m height above sea level (m/s) (See Table S3 for the wind speed values used in this study). $D_{i,air}$ and $D_{H_2O,air}$ are the diffusivities of OPEs and water in air, respectively. The values of $D_{i,air}$ can be calculated as the following equation introduced by Schwarzenbach et al.[12]

$$D_{i,air} = 10^{-3} \frac{T^{1.75}\left[(1/M_{air}) + (1/M_i)\right]^{1/2}}{p\left[\overline{V_{air}^{1/3}} + \overline{V_i^{1/3}}\right]^2} \ (\mathrm{cm^2/s})$$

The molar volume (V) was calculated following the method provided by Fuller et al.[13] Sc is the water phase Schmidt number, namely the ratio of kinematic viscosity v ($\mathrm{cm^2/s}$) and diffusivity $D_{i,water}$ ($\mathrm{cm^2/s}$) given by $Sc_{CO_2} = v / D_{i,water}$. Sc_{CO_2} was taken from Schwarzenbach et al. ($S_{CO_2} = 600$).[14] The value of the kinematic viscosity of seawater is adopted from Patterson et al. (v =1.04×10^{-2} $\mathrm{cm^2/s}$) .[15] The values for $D_{i,water}$ were calculated using the method described by Hayduk et al.[16]

References

1. Castro-Jimenez, J.; Berrojalbiz, N.; Pizarro, M.; Dachs, J., Organophosphate Ester (OPE) Flame Retardants and Plasticizers in the Open Mediterranean and Black Seas Atmosphere. *Environ Sci Technol* **2014,** *48*, (6), 3203-3209.
2. Jurado, E.; Jaward, F. M.; Lohmann, R.; Jones, K. C.; Simo, R.; Dachs, J., Atmospheric dry deposition of persistent organic pollutants to the Atlantic and inferences for the global oceans. *Environ Sci Technol* **2004,** *38*, (21), 5505-5513.
3. Franz, T. P.; Eisenreich, S. J.; Holsen, T. M., Dry deposition of particulate polychlorinated biphenyls and polycyclic aromatic hydrocarbons to Lake Michigan. *Environ Sci Technol* **1998,** *32*, (23), 3681-3688.
4. Möller, A.; Xie, Z. Y.; Sturm, R.; Ebinghaus, R., Polybrominated diphenyl ethers (PBDEs) and alternative brominated flame retardants in air and seawater of the European Arctic. *Environ Pollut* **2011,** *159*, (6), 1577-1583.
5. Schwarzenbach, R. P.; Gschwend, P. M. I., D. M., *Environmental organic chemistry* Second Edition ed.; New Jersey: A John Wiley & Sons, Inc: 2003.
6. Zhang, X. M.; Suhring, R.; Serodio, D.; Bonnell, M.; Sundin, N.; Diamond, M. L., Novel flame retardants: Estimating the physical-chemical properties and environmental fate of 94 halogenated and organophosphate PBDE replacements. *Chemosphere* **2016,** *144*, 2401-2407.
7. Xie, Z.; Koch, B. P.; Moller, A.; Sturm, R.; Ebinghaus, R., Transport and fate of hexachlorocyclohexanes in the oceanic air and surface seawater. *Biogeosciences* **2011,** *8*, (9), 2621-2633.
8. Liss, P. S.; Slater, P. G., Flux of Gases across Air-Sea Interface. *Nature* **1974,** *247*, (5438), 181-184.
9. Bidleman, T. F.; Mcconnell, L. L., A Review of Field Experiments to Determine Air-Water Gas-Exchange of Persistent Organic Pollutants. *Sci Total Environ* **1995,** *159*, (2-3), 101-117.
10. Ni, N.; Yalkowsky, S. H., Prediction of Setschenow constants. *Int J Pharm* **2003,** *254*, (2), 167-172.

11. Hornbuckle, K. C.; Jeremiason, J. D.; Sweet, C. W.; Eisenreich, S. J., Seasonal-Variations in Air-Water Exchange of Polychlorinated-Biphenyls in Lake-Superior. *Environ Sci Technol* **1994,** *28*, (8), 1491-1501.

12. Schwarzenbach, R. P.; Gschwend, P. M. I., D. M., *Environmental organic chemistry* Second Edition ed.; New Jersey: A John Wiley & Sons, Inc: 2003; Fig. 18.9.

13. Fuller, E. N.; Schettle.Pd; Giddings, J. C., A New Method for Prediction of Binary Gas-Phase Diffusion Coeffecients. *Ind Eng Chem* **1966,** *58*, (5), 18-27.

14. Schwarzenbach, R. P.; Gschwend, P. M. I., D. M., *Environmental organic chemistry* Second Edition ed.; New Jersey: A John Wiley & Sons, Inc: 2003; Eq. 20-16.

15. Patterson, M. R.; Sebens, K. P., Forced convection modulates gas exchange in cnidarians. *Proceedings of the National Academy of Sciences of the United States of America* **1989,** *86*, 8833-8836.

16. Hayduk, W.; Laudie, H., Prediction of Diffusion-Coefficients for Nonelectrolytes in Dilute Aqueous-Solutions. *Aiche J* **1974,** *20*, (3), 611-615.

Paper II

Spatial distribution and seasonal variation of organophosphate esters in air above the Bohai and Yellow Seas, China

Downloaded via HELMHOLTZ-ZENTRUM GEESTHACHT on October 7, 2019 at 13:30:44 (UTC).
See https://pubs.acs.org/sharingguidelines for options on how to legitimately share published articles.

Environmental Science & Technology

Article

Cite This: Environ. Sci. Technol. 2018, 52, 89−97

pubs.acs.org/est

Spatial Distribution and Seasonal Variation of Organophosphate Esters in Air above the Bohai and Yellow Seas, China

Jing Li,[†,⊥] Jianhui Tang,*[,‡] Wenying Mi,[§] Chongguo Tian,[‡] Kay-Christian Emeis,[†,⊥] Ralf Ebinghaus,[†] and Zhiyong Xie*[,†]

[†]Centre for Materials and Coastal Research, Institute of Coastal Research, Helmholtz-Zentrum Geesthacht, Geesthacht 21502, Germany

[‡]Key Laboratory of Coastal Environmental Processes and Ecological Remediation, Yantai Institute of Coastal Zone Research, CAS, Yantai 264003, China

[§]MINJIE Analytical Laboratory, Geesthacht 21502, Germany

[⊥]School of Integrated Climate System Sciences, University of Hamburg, Hamburg 20144, Germany

Supporting Information

ABSTRACT: Nine organophosphate esters (OPEs) were investigated in air samples collected over the Bohai and Yellow Seas (East Asia) during a research cruise between June 28 and July 13, 2016. These same OPEs were quantified at a research site (North Huangcheng Island, NHI) in the middle of the Bohai Strait from May 16, 2015, to March 21, 2016. The median total OPE (ΣOPE) concentration over the Bohai and Yellow Seas was 280 pg/m^3. Tris(1-chloro-2-propyl) (TCPP) was the most abundant OPE, followed by tris(2-chloroethyl) phosphate (TCEP), tri-iso-butyl phosphate (TiBP), and tri-*n*-butyl phosphate (TnBP). Particle-bound OPEs accounted for 51 ± 21% of the total OPEs. On NHI, the median ΣOPE concentration was 210 pg/m^3, and the average particle-bound fraction was 82 ± 17%. For samples collected on NHI, significant negative linear correlations were found between the gaseous OPEs and $1/T$ (T: temperature (K)) (except TDCP, TPeP, and TCP). Among the 79 investigated samples, significant correlations between the measured OPE gas/particle partitioning coefficients ($K_{p,m}$) and subcooled liquid pressure (P_L°) ($p < 0.05$) were found for only 14 samples, suggesting that OPEs have low potential to achieve equilibrium or ascribe to the artificial sampling. The annual dry deposition input of OPEs into the Bohai and Yellow Seas is estimated to be 12 tons/year.

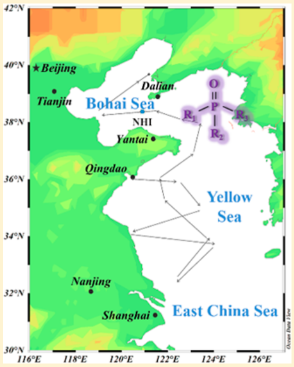

INTRODUCTION

Organophosphate esters (OPEs) are commonly used as flame retardants and plasticizers.[1,2] In recent years, global production and usage of OPEs has increased sharply, and from 1992 to 2013, the volume of worldwide OPE consumption increased from 102,000 to 370,000 tons.[3,4] In China, the price of the brominated intermediates has risen continuously since 2005 due to limitations in the supply of bromate.[4] As a result, the market prices for brominated flame retardants (BFRs) are higher than those of flame retardants (FRs) from OPEs.[4] Consequently, the consumption of OPEs increased from 11,000 tons in 1995 to 70,000 tons in 2007 and to 179,000 tons in 2012. Aside from the high OPE consumption, China is also the largest global e-waste importer and recycler.[5] If such recycling is performed improperly (i.e., direct burning), it contributes to the release of chemicals, including OPEs.[6]

The occurrence of atmospheric OPEs has been reported above the European seas,[7,8] the open oceans,[9−11] and the polar regions.[9,12] In East Asia, OPEs have been detected over the South China Sea (nine OPEs; median of total OPEs: 91 pg/m^3),[13] over the East China Sea (four OPEs in one sample; 1066 pg/m^3 in total),[12] and over the Japan Sea (eight OPEs in two samples; 450 and 2900 pg/m^3 in total, respectively).[11] However, no data are available over the Bohai and Yellow Seas, which are influenced by East Asian continental air masses, especially from the east coast of China.

Previous studies focused mainly on OPE in the particulate phase, and only a few papers reported OPE in the gaseous phase. Recently, Wolschke et al. reported that on average 55% of OPEs could be detected in the gaseous phase.[14] Li et al. detected gaseous OPEs in air over the North Atlantic and Arctic (mean fraction of gaseous OPEs: 33 ± 17%).[9] These studies highlighted the importance of the research on OPE gas/particle partitioning, which determines the environmental fate and long-range transport mechanisms of OPEs.

The Bohai Sea is a nearly enclosed interior sea with an area of approximately 78,000 km^2, length of coastline of 3,784 km, and average depth of 18 m.[15] The Yellow Sea, which is nearly surrounded by mainland China and the Korean Peninsula, is at the margin of the western Pacific Ocean and is connected with the Bohai Sea via the Bohai Strait (Figure 1).[16] The Bohai and

Received: August 16, 2017
Revised: November 28, 2017
Accepted: November 29, 2017
Published: November 29, 2017

ACS Publications © 2017 American Chemical Society

DOI: 10.1021/acs.est.7b03807

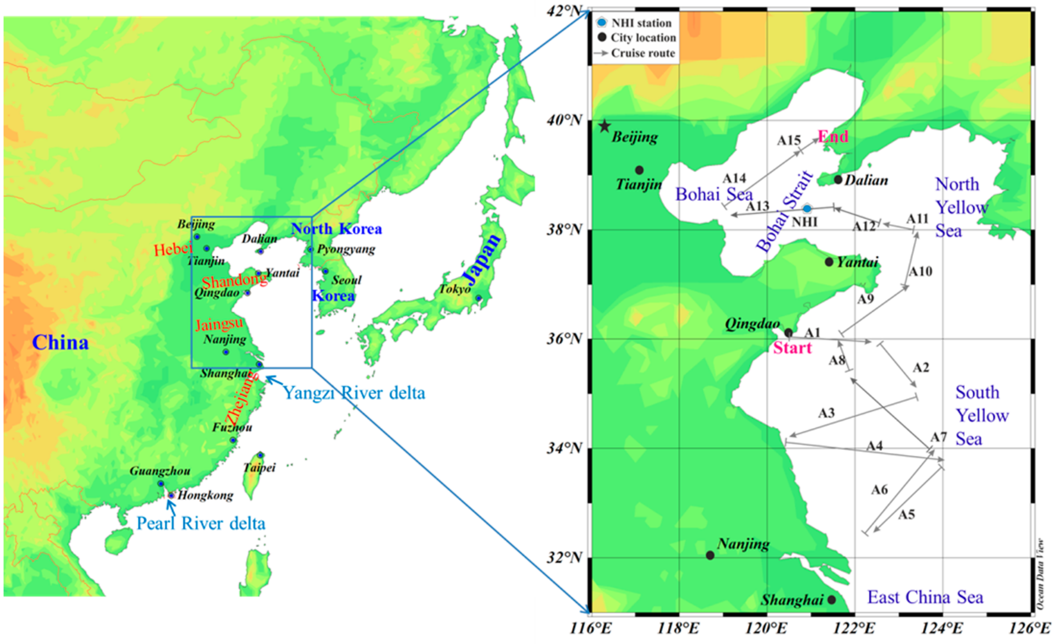

Figure 1. Map of the research area showing the sampling cruise route (gray arrows) and the location of the long-term sampling station at North Huangcheng Island (NHI).

Yellow Seas have a combined total area about 458,000 km^2.[15,17] North Huangcheng Island (NHI) is situated in the center of the Bohai Strait, where the Bohai Sea and Yellow Sea meet (Figure 1).[18] Because NHI has a low population density and high vegetation coverage and is separated from the mainland by 65 km, it is suitable for monitoring baseline pollution and the seasonal variability of OPEs in the region.[18]

This study investigated the annual variability of OPEs in air over NHI and the spatial distribution of OPEs over the Bohai and Yellow Seas. The data are examined to estimate the gas/particle partitioning of OPEs employing the Junge−Pankow adsorption model (J−P model) and the absorption model based on the octanol/air partition coefficient (K_{oa}-based model). Further, atmospheric particle-bound dry deposition of OPEs was calculated with the data measured at the Bohai and Yellow Seas. This work improves understanding of the occurrence and fate of OPEs in the marine environment.

■ MATERIALS AND METHODS

Sampling Campaign. Fifteen air samples were taken over the Bohai and Yellow Seas during a research cruise between June 28 and July 13, 2016, on the research vessel *Dongfanghong* 2 (Figure 1). Eighty-one air samples were collected from NHI between May 16, 2015, and March 21, 2016 (Figure 1). A high-volume air sampler was used to collect the air samples. The details of the sampling procedures were published previously.[9] Briefly, atmospheric particle samples were collected using a glass fiber filter (GFF; pore size: 0.7 μm; diameter: 150 mm), and gaseous phase samples were collected by follow-up PUF/XAD-2 resin column. Prior to deployment, the PUF/XAD-2 columns were cleaned with dichloromethane (DCM), hexane/acetone (1:1$_{V:V}$), and methanol for 16 h each. Prior to deployment, the GFF filters were baked at 450 °C for 12 h to remove organic residue. All solvents were residue grade. Ten field blanks were collected by briefly exposing the columns and filters to the atmosphere at the sampling sites (five for the cruise and five for NHI). Detailed sampling information is presented in Tables S1 and S2.

Sample Analysis. The air sample pretreatment and analysis followed the method published by Xie et al.[19] Briefly, GFFs and PUF/XAD-2 were spiked with 20 ng of d_{12}-TCEP, d_{15}-TPhP, and d_{27}-TnBP as surrogates and extracted with MX-Soxhlet for 16 h using 200 mL of DCM. The GFFs and PUF/XAD-2 were extracted separately. Ten mL of hexane was added to all extracts, followed by a preconcentration to 1 mL by rotary evaporation, and further volume reduction down to 150 μL with a nitrogen evaporator (Barkey GmbH, Germany). $^{13}C_6$-PCB 208 was used as the injection standard.

An Agilent 7890A gas chromatograph coupled to an Agilent 7010A Triple Quadrupole mass spectrometer (GC-MS/MS) and equipped with a programmed temperature vaporizer (PTV) injector (Agilent, USA) was used for analysis. The MS transfer line and the high sensitivity electron impact ionization source (HSEI) were held at 280 and 230 °C, respectively. The MS/MS was operated in Multiple Reaction Monitoring (MRM) mode. Detailed information regarding the GC-MS/MS setup was published previously and is presented in Text S1.[9]

Nine OPEs were analyzed in this work (Table S3): TCPP (tris(1-chloro-2-propyl) phosphate, including three isomers), TCEP (tris(2-chloroethyl) phosphate), TDCP (tris(1,3-dichloro-2-propyl) phosphate), TnBP (tri-*n*-butyl phosphate), TiBP (tri-iso-butyl phosphate), TPhP (triphenyl phosphate), TPeP (tripentyl phosphate), TEHP (tris(2-ethylhexyl) phosphate), and TCP (tricresyl phosphate, including four isomers).

Quality Assurance/Quality Control (QA/QC). Five blanks were collected for the cruise and NHI station, respectively. For the gaseous phase, the lowest absolute blank was detected for TPeP (cruise: 1.4 ± 1.4 pg; NHI: 1.7 ± 1.0 pg), whereas the highest was found for TCPP (cruise: 110 ± 27 pg; NHI: 260 ± 130 pg). For the particulate phase, the absolute blank ranged from 1.2 ± 0.22 pg for TPeP to 380 ± 48 pg for TCP on NHI (cruise: 2.8 ± 1.1 pg for TPeP; 530 ± 88 pg for

TCP; Table S4). The concentrations of field blanks were obtained through absolute blank divided by the sample volume (300 m^3 for the gaseous phase and 150 m^3 for the particulate phase, as only half of each filter was analyzed; Table S5). The OPE concentrations in samples are blank corrected.

The method detection limits (MDLs) were calculated based on field blank concentrations plus three times their standard deviation (3σ). For the Bohai and Yellow Seas, the MDLs were 0.02−0.79 pg/m^3 in the gaseous phase and 0.04−5.3 pg/m^3 in the particulate phase (Table S5). On NHI, the MDLs were 0.02−2.2 pg/m^3 for the gaseous phase and 0.01−5.0 pg/m^3 for the particulate phase (Table S5).

For the gaseous phase, mean recovery rates of the spiked experiments varied between 82 ± 22% (TEHP) and 140 ± 15% (TDCP) (n = 5; Table S6). The analytical method for the particle phase was validated with reference material NIST SRM 2585, which has been suggested by several laboratories, although it is not certified for OPEs. NIST SRM 2585 dust was wrapped in the GFF filters and extracted in the same way as particle samples (results in Table S8). The OPE levels in SRM 2585 were compared with those reported in the literature (Table S9), and similar concentrations were determined for all OPEs except TCEP.[10,20−27] The mean TCEP concentration in this study (1.9 ± 0.15 μg/g) was approximately double that of other reports (0.68−0.88 μg/g, Table S9). The TiBP concentrations (mean: 0.013 ± 0.005 μg/g) were comparable to those reported by Brandsma et al. (on average: 0.017 μg/g)[25] and lower than those reported by Ali et al. (1.6 ± 0.39 μg/g).[22] TPeP was detected in NIST SRM 2585, with a mean concentration of 0.003 ± 0.0001 μg/g. The extraction efficiency was tested by extracting NIST SRM 2585 dust samples twice. The recoveries in the first extraction ranged from 79 ± 4.1% (TEHP) to 99.5 ± 0.15% (TCP; Table S10).

Air Mass Back Trajectories. Air mass back trajectories for the sampling stations were obtained using the NOAA HYSPLIT model.[28] During the Bohai and Yellow Seas sampling cruises, back trajectories were calculated at 10 m above sea level in 6 h increments for each sample for a total of 120 h (Figure S2). For NHI, the cluster-mean trajectories of the four seasons during the sampling period (height: 100 m) are given in Figure S1.

Gas/Particle Partitioning Methods. The particle-bound fractions measured in this study (φ_m) were calculated from the following equation based on C_p (OPE concentration in the particulate phase, pg/m^3) and C_g (OPE concentration in the gaseous phase, pg/m^3):

$$\varphi_m = \frac{C_p}{C_p + C_g} \tag{1}$$

The measured partitioning coefficient $K_{p,m}$ can be calculated by[29]

$$K_{p,m} = \frac{C_p/C_{TSP}}{C_g} \tag{2}$$

where C_{TSP} is the total suspended particle concentration (μg/m^3).

The subcooled vapor pressure P_L° is an important factor for the gas/particle partitioning of organic compounds. Generally, a highly correlated linear regression can be obtained between log $K_{p,m}$ and log P_L° for given samples for a group of compounds[29]

$$\log K_{p,m} = m \log p_L^\circ + b \tag{3}$$

where the slope m and intercept b are fitting constants. At the ideal equilibrium, the slope m should be close to −1. In this study, the linear relation between log $K_{p,m}$ and log P_L° was investigated for each sample on NHI. Temperature-dependent P_L° values for TCEP, TCPP, TDCP, TPhP, and TEHP were estimated according to the equations reported by Brommer et al.[30] For the other four OPEs, the vapor pressures were obtained from EPI Suite 4.1.

Two prediction models were adopted in this study, the J−P model and the K_{oa}-based model. The J−P model, proposed by Pankow in 1987, is based on P_L°.[31] The particle-bound fraction φ_{J-P} of a target compound is estimated by[31]

$$\varphi_{J-P} = \frac{c\theta}{p_L^\circ + c\theta} \tag{4}$$

where c is a constant that depends on the properties of the substance, and θ is the surface area of particle per unit volume of air (cm^2/cm^3). This study assumes c to be 17.2 Pa cm for OPEs[32] and θ to be 1.0×10^{-6} for rural air.[33]

The predicted gas/particle partitioning coefficient $K_{p,koa}$ through the K_{oa}-based model is (details in Text S2)[34]

$$K_{p,koa} = \log K_{oa} + \log f_{OM} - 11.9 \tag{5}$$

where f_{OM} is the fraction of organic matter (OM) phase in the aerosol (f_{OM} was assumed as 0.1). The temperature-dependent log K_{oa} values were obtained from the report of Wang et al.[35]

The field predicted particle-bound fraction based on the K_{oa}-based model (φ_{koa}) can be calculated from the following equation:[31]

$$\varphi_{koa} = \frac{K_{p,koa}C_{TSP}}{K_{p,koa}C_{TSP} + 1} \tag{6}$$

Statistical Analysis. The Spearman's correlation coefficient was used to evaluate the correlations (by SPSS 20), because the data set was not normally distributed. Linear regression was performed with Excel 2016. The nonparametric ANOVA test (Kruskal−Wallis Test) coupled with the Dunn posthoc test (by GraphPad InStat 3.10) were adopted to analyze significant differences of OPE levels between the four seasons. The value of 0.05 was used as the p-value to determine statistical significance. Concentrations below the MDLs were replaced by 2/3 of the MDL for the statistical analysis. As a nonparametric test was conducted in this study, outliers were included. The outliers that were excluded for the regression are explained in the corresponding text.

■ RESULTS AND DISCUSSION

OPE Concentrations over the Bohai and Yellow Seas. All targeted OPEs except TEHP (93%) and TCP (73%) were detected in all air samples (gaseous and particulate phases). The sum of the nine OPE concentrations (ΣOPE) ranged from 100 to 750 pg/m^3 (median: 280 pg/m^3). The three chlorinated OPEs accounted for 66 ± 15% of the total OPEs, and the remainder was composed of the six nonchlorinated OPEs (34 ± 15%). TCPP was the most abundant OPE (range: 43−530 pg/m^3; median: 100 pg/m^3), followed by TCEP (range: 27−150 pg/m^3; median: 71 pg/m^3), TiBP (range: 19−210 pg/m^3; median: 57 pg/m^3), and TnBP (range: 3.0−37 pg/m^3; median: 13 pg/m^3). The details of the individual OPE concentrations are summarized in Table 1. The composition profiles of the OPEs are shown in Figure S3.

In the gaseous phase, the ΣOPE concentrations ranged from 2.3 to 270 pg/m^3 (median: 170 pg/m^3), and these were dominated by three OPEs, TiBP, TCPP, and TCEP, which contributed 32 ± 18%, 27 ± 15%, and 25 ± 11% to ΣOPEs, respectively. In the particulate phase, the ΣOPE concentrations ranged from 44 to 520 pg/m^3 (median: 150 pg/m^3), with a predominance of TCPP (50 ± 11% of ΣOPEs), followed by TCEP (25 ± 7%) and TiBP (14 ± 12%).

OPE Concentrations on NHI. Most of the nine OPEs were detected in all samples, but TDCP and TCP were detected in 98% and 75% of the total samples, respectively. The ΣOPE concentrations ranged from 36 to 1600 pg/m^3 (median: 210 pg/m^3) which is comparable to the values measured in marine air above the Bohai and Yellow Seas detected during the ship expedition. The mean concentrations of the major OPEs detected on NHI were (in decreasing order): TCEP (median: 77 pg/m^3) > TCPP (29 pg/m^3) ≈ TiBP (28 pg/m^3) > TPhP (18 pg/m^3) > TnBP (12 pg/m^3; Table 1). The chlorinated OPEs accounted for 55 ± 16% of the total OPEs.

In the gaseous phase, the ΣOPE concentrations ranged from 1.2 to 360 pg/m^3 (median: 31 pg/m^3), which is lower than ΣOPE levels in the particulate phase (range: 5.0 to 1500 pg/m^3, median: 170 pg/m^3). Similar patterns were found for OPEs between the gaseous and the particle phases, with TCEP being the most abundant OPE (gaseous phase: 31%; particulate phase: 38%), followed by TiBP, TCPP, TPhP, and TnBP.

Most previous studies analyzed particle-bound OPEs. Therefore, the OPE levels in the particulate and gaseous phases were compared separately with those reported in the literature. The total and individual OPE concentrations in the particulate phase were generally in the low range of OPE levels reported for most oceanic atmosphere and remote sites (Table S11). Concentration of total OPE reported for one sample collected over the East China Sea in October 2009 was 1100 pg/m^3 (four OPEs)[12] and thus approximately six times higher than in this study (nine OPEs; median: 150 pg/m^3). The higher OPE levels in the East China Sea likely reflect the influence of the Yangzi River Delta region (Figure 1), a major production region for OPEs.[4] Two samples taken over the Sea of Japan had total OPE levels (eight OPEs) of 450 pg/m^3 and 2900 pg/m^3, respectively.[11] The author argued that the high concentration (2900 pg/m^3) signals continental air from Asia. In the South China Sea, lower concentrations (eight OPEs; median: 91 pg/m^3)[13] were found than in this work. Furthermore, the median of the ΣOPE levels in this study (150 pg/m^3) was two times higher than that reported from the North Atlantic and Arctic (eight OPEs; median: 48 pg/m^3)[9] but similar to that measured near the Antarctic Peninsula (four OPEs; median: 141 pg/m^3; Table S11).[12] It was lower than that reported from the North Sea (eight OPEs; median: 281 pg/m^3)[7], the Canadian Arctic (median ship-based: 237 pg/m^3);[36] and in Longyearbyen (334 pg/m^3).[37] Compared to the Mediterranean Sea (14 OPEs; median: ~1,455 pg/m^3; Table S11),[8] the Black Sea (14 OPEs; median: 2,006 pg/m^3),[8] and concentrations reported from open oceans as reported by Castro-Jimenez et al. (nine OPEs; median range: 1,500−2,200 pg/m^3),[10] the median found in Bohai and Yellow Sea is 1 order of magnitude lower (Table S11).

Several papers have reported OPE levels in the gaseous phase, such as OPEs in the North Sea (eight OPEs; median: 54 pg/m^3) and the North Atlantic and Arctic (eight OPEs;

Table 1. Range, Mean ± Standard Deviation, and Median of Individual OPE Concentrations in Air (pg/m^3) above the Bohai and Yellow Seas and North Huangcheng Island (NHI)

	Bohai and Yellow Seas (n = 15)						North Huangcheng Island (n = 81)					
	gaseous phase			particulate phase			gaseous phase			particulate phase		
OPE (pg/m^3)	range	mean	median	range	mean	median	range	mean	median	range	mean	median
TCPP	n.d.−130	45 ± 35	42	19−390	86 ± 88	66	0.2−26	5.6 ± 5.6	3.2	n.d.−160	34 ± 33	26
TCEP	n.d.−73	38 ± 18	38	14−94	38 ± 23	28	0.69−120	14 ± 17	10	0.40−1000	100 ± 170	63
TDCP	n.d.−4.3	0.81 ± 1.0	0.57	0.75−13	4.5 ± 3.1	4.6	n.d.−2.6	0.35 ± 0.61	n.d.	n.d.−80	7.1 ± 11	3.8
TiBP	0.30−170	54 ± 50	30	2.3−95	24 ± 29	12	n.d.−82	8.1 ± 12	4.8	1.0−164	33 ± 29	24
TnBP	0.46−36	8.9 ± 8.7	8.0	1.2−14	4.8 ± 3.6	4.6	n.d.−190	11 ± 28	2.7	n.d.−1100	61 ± 180	8.2
TPeP	0.03−1.2	0.43 ± 0.38	0.27	0.04−0.30	0.13 ± 0.08	0.10	n.d.−0.41	0. 05 ± 0.07	0.03	0.01−2.4	0.24 ± 0.31	0.16
TPhP	0.19−4.7	2.0 ± 1.2	1.7	1.4−15	5.0 ± 4.0	2.8	0.17−22	4.4 ± 4.3	2.7	n.d.−110	22 ± 25	11
TEHP	n.d.−5.3	1.6 ± 1.4	1.0	n.d.−8.5	1.8 ± 2.5	1.8	n.d.−30	2.3 ± 4.4	1.1	n.d.−180	10 ± 30	1.5
TCP	n.d.−5.2	1.7 ± 1.7	1.6	n.d.−26	2.6 ± 7.0	n.d.	n.d.−7.1	0.60 ± 1.4	n.d.	n.d.−18	1.7 ± 3.1	0.35
ΣOPEs	2.3−270	150 ± 77	170	44−520	170 ± 120	150	1.2−360	47 ± 54	31	5.0−1500	270 ± 300	170

median: 17 pg/m^3; Table S12), which are both lower than those of the Bohai and Yellow Seas (eight OPEs; median: 170 pg/m^3). However, the concentrations found at NHI (median: 31 pg/m^3) are similar to those from the literature. The difference of OPE levels between samples from the NHI and the Bohai and Yellow Seas is caused by the variance of distribution in the gaseous and particulate phases, as discussed in the section *Measured Particle-Bound Fractions* below.

To provide an overall perspective of particle-bound OPE levels in global oceanic and remote regions, seven widely measured OPEs, including three chlorinated OPEs (TCEP, TCPP, TDCP) and four nonchlorinated OPEs (TiBP, TnBP, TEHP, TPhP), were chosen for a statistical evaluation (data sourced from the literature and this study). From the 27 regions listed in Table S11, 21 regions, in which at least five of the seven OPEs were detected, were selected for the analysis. Data for the Canadian Arctic (land-based) were not included, because TnBP was only analyzed at Resolute Bay and showed quite high concentrations (median: 416 pg/m^3) compared with other OPEs. According to the statistical results, the chlorinated OPEs accounted for 50% to 96% of the total seven OPEs (median: 76%, Table S13), and the four nonchlorinated OPEs contributed 3.7% to 50% of the total OPEs (median: 24%, Table S13). Among the chlorinated OPEs, the fractions of TCPP (median: 39%, Table S13) and TCEP (median: 24%, Table S13) were higher than the fraction of TDCP (median: 4.2%, Table S13); however, the contributions of the four nonchlorinated OPEs were similar (median: TnBP: 7.6%, TiBP: 4.7%, TEHP: 3.7%, TPhP: 3.0%; Table S13).

Spatial Distribution of OPEs. The highest $\sum$OPE concentration was observed in Sample A1, which was influenced by air masses that originated from the southern Yellow Sea and passed through the coast of Jiangsu before being collected (Figures 2 and S2). The lowest $\sum$OPE concentration was found in Sample A9, and the source of the air masses was tracked to the Pacific Ocean (Figures 2 and S2). FRs production in China is generally distributed in the Yangtze River and Pearl River Deltas (Figure 1), where the Jiangsu and Zhejiang regions mainly produce OPE-based FRs.[4] Therefore, it is likely that Jiangsu was the primary source of the OPEs measured in Sample A1.

For Samples A1 to A10, transported by air masses that came mainly from the Pacific Ocean and passed partly though the coastal region of China (Yangzi River Delta and Jiangsu Provinces), the dominant OPE was TCPP (mean: 45 ± 10% of total OPEs). For Samples A11 to A14, for which the air masses passed through the west coast of South Korea and the continent (Samples A12−14) or coast (Sample A11) of Shandong Province (Figure S2) before collection, TiBP was the most abundant OPE (mean: 42 ± 3% of total OPEs). For Sample A15, the dominant OPEs were TiBP and TCPP, which accounted for 42% and 39% of the total OPEs, respectively. All air masses of Sample A15 had finally passed over the northern Bohai Sea region, although they were of different origin (Russia, Mongolia, and China), indicating that this area may be a source region of OPEs.

Seasonal Variation of OPEs. There was no significant difference of $\sum$OPE concentrations (gaseous and particulate phases) between the different seasons. The median levels were approximately 200 pg/m^3 (summer: 220 pg/m^3; winter: 190 pg/m^3; autumn: 210 pg/m^3; spring: 200 pg/m^3; Figure 3). This phenomenon is a result of the similar particle-bound $\sum$OPE levels in the four seasons, because the particle-bound OPEs accounted for 82 ± 17% of the total OPEs in air (gaseous and particulate phases). In only the gaseous phase, significantly higher concentrations of $\sum$OPEs and individual OPEs ($p < 0.05$) were measured in summer than in winter (TDCP and TCP were not included because these have low detectability in the gaseous phase, ~30%). A significantly negative correlation ($p < 0.02$) exists between C_g and $1/T$ of most OPEs except TDCP, TPeP, and TCP (Table S14, Figure S4). Relative humidity (RH) had a positive influence on the gaseous OPEs ($p < 0.05$, Table S15), which is consistent with the finding that water hinders degradation of OPEs in air.[38] For the particulate phase, higher concentrations of TCPP and TiBP were observed in summer than in winter, opposite to TPhP and TEHP ($p < 0.05$). C_{TSP}, RH, and temperature had little effect on the

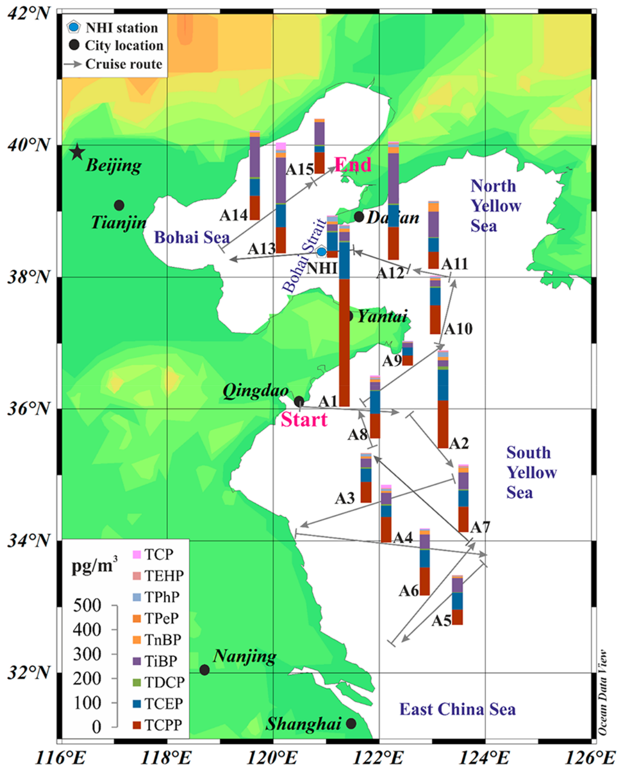

Figure 2. Spatial distribution of OPEs over the Bohai and Yellow Seas and median OPE concentrations at North Huangcheng Island (NHI).

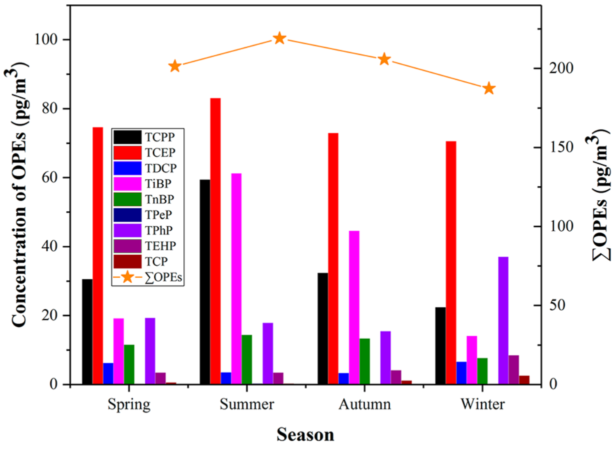

Figure 3. Seasonal variation of individual OPE and $\sum$OPE concentrations in air at North Huangcheng Island (NHI). The figure shows median values.

seasonal variance of particle-bound OPEs according to the correlation analysis (Table S16). This result suggests that the seasonal variation patterns of particle-bound OPEs are more indicative of varying air mass origin than the ambient environmental conditions. In winter, the air masses originated mainly from northern China (65% from Mongolia and Russia, 35% from the Hebei and Shandong Provinces), but in summer, oceanic air masses were the dominant source (64% from the Yellow Sea, 19% from the Hebei and Tianjin Provinces; Figure S1). As for spring and autumn, no clear distinction between air mass origins was evident, and both continental and oceanic air masses were main sources. The air masses that originated from the ocean may have passed by the industrial region of the Yangzi River Delta region (Figure 1), which accounts for the high levels of particle-bound TiBP and TCPP as well as the gaseous OPEs in summer.

Measured Particle-Bound Fractions of OPEs. Over the Bohai and Yellow Seas, particle-bound OPEs composed on average 51 ± 21% of the total OPEs. The mean particle-bound fractions of the four major OPEs were in the order of TCPP (63 ± 19%) > TCEP (51 ± 19%) > TnBP (47 ± 23%) > TiBP (30 ± 25%; Figure S4).

On NHI, particle-bound OPEs composed an average 82 ± 17% of the total OPEs, with four major OPEs in the order of TCPP (83 ± 17%) ≈ TCEP (83 ± 16%) > TiBP (82 ± 16%) > TnBP (72 ± 24%; Figure S5).

The particle-bound fractions of ship samples and NHI station samples differed. Over the Bohai and Yellow Seas, OPEs distributed evenly in both gaseous and particulate phases, whereas on NHI OPEs were mainly in the particulate phase. Several factors may be responsible for this different behavior. First, RH is an important factor. Li et al. found that water inhibits the ·OH-initiated degradation of TCPP, which increases the lifetime of gaseous TCPP from the calculated 1.7 h to 0.5−20.2 days.[38] The RH during the ship cruise ranged from 81% to 97% (median: 88%), which was in the upper part of the range at NHI (range: 30−94%; median: 67%). Second, the sampling height on the ship was ∼10 m, which was lower than that on NHI (∼100 m). OPEs have the potential to volatilize from seawater into the air, as demonstrated for the North Atlantic and Arctic.[9] Thus, more gaseous OPEs are expected closer to the surface of the sea. In addition, different air masses also account for the variation of the fractions, as was discussed in sections *Spatial Distribution of OPEs* and *Seasonal Variation of OPEs* above.

On NHI, significantly higher particle-bound fractions of ∑OPEs and individual OPEs were found in winter than in summer. This is likely to reflect low temperature and RH in winter, because significant negative correlations were found between the fractions and temperature ($p < 0.02$; Table S17), as well as with RH ($p < 0.02$; Table S17). In addition, significant positive correlations were observed for OPE fractions and C_{TSP} ($p < 0.002$; Table S17) except for TPeP ($p = 0.94$), indicating that C_{TSP} also contributed the variance of distribution between gaseous and particulate phases.

Previous studies have reported OPE particle-bound fractions in air. Möller et al. detected a mean fraction of 86 ± 25% for the North Sea in 2011.[7] Lower levels were found at the German coast in 2016 (45% on average), which was ascribed mainly to the improved method, as described in the report.[9] Over the North Atlantic and Arctic (2017), the mean fraction was 67 ± 17%.[9] In our study, particle-bound OPEs contributed to 51 ± 21% of total OPEs in ship samples and 82 ± 17% in NHI samples. According to the data reported in the literature and this study, the gas/particle partitioning of OPEs showed a large variation in air samples. Many factors might be responsible for this result, such as C_{TSP}, temperature, RH, and air mass sources as mentioned above, as well as the analytical methodology as reported by Wolschke et al.[9]

Gas/Particle Partitioning Prediction. OPEs can be detected in both the particulate and gaseous phases, and it is important to know how they partition between the two phases in the atmosphere, which can affect the fate and long-range transport of OPEs in the environment. The 81 samples obtained on NHI were used for gas/particle partitioning prediction, with the ranges of temperature, RH, and C_{TSP} being −4 to 27 °C, 30% to 94%, and 16 to 240 $\mu g/m^3$, respectively. Only the OPEs that were detectable in both the gaseous and particulate phases in a given sample were included.

Significant correlations between $\log K_{p,m}$ and $1/T$ (K^{-1}) were found for TCEP, TiBP, TnBP, TPhP, and TEHP ($p < 0.05$; Table S18, Figure S6). The r^2 values for TCEP, TPhP, and TEHP were >0.40, but the values for TiBP (0.08) and TnBP (0.05) were very low. The regression slopes were positive, showing that $K_{p,m}$ decreased with increasing temperature.

Among the 79 samples investigated (two samples were excluded because of a lack of C_{TSP} data), significant correlations between $\log K_{p,m}$ and $\log P_L^\circ$ of OPE congeners were found for only 14 samples ($p < 0.05$; Table S19). This result suggests that OPEs have low potential to achieve equilibrium or ascribe to the artificial sampling, and the gas/particle partitioning of polar compounds such as OPEs is more complex than the partitioning of nonpolar chemicals.

As $\log K_{p,m}$ was correlated with $1/T$ (K^{-1}) for TCEP, TPhP, and TEHP ($p < 0.05$; $r^2 > 0.40$), prediction of their gas/particle partitioning was conducted using the J−P and the K_{oa}-based models. Significant regressed correlations were found between the predicted and measured particle-bound fractions for these three OPEs ($p < 0.01$; r^2 range: 0.23−0.61, Table S20). However, TCEP was predicted to be mainly in the gaseous phase (>95%), which was contrary with the measured data. This discrepancy might result from TCEP strongly absorbed to particles and/or glass fiber filter used for air sampling, which was suggested by Brommer et al.[30] For TEHP and TPhP, the predictions were closer to the measurements than for TCEP (Figure 4), with the ratios of measured to predicted fractions being close to 1 (Table S20). Both the J−P and K_{oa}-based models performed well for TEHP when $\log K_{oa} > 12$ (Figure 4b), while they were overestimating the particle-bound fractions when $\log K_{oa} < 12$ (Figure 4b). TEHP tends to be in the particulate phase when $\log K_{oa} > 13$, while it was in the gaseous phase when $\log K_{oa} < 12$. For TPhP, both models underestimate the particle-bound fractions (Figure 4a). The measured data show that approximately 100% of TPhP partitions into the particulate phase when $\log K_{oa} > 12$, while the variance increased at $\log K_{oa} < 12$ (range: 30% to 99%). The varying partitioning behaviors under similar $\log K_{oa}$ values for TPhP may reflect the different environmental conditions, such as the variation of RH, C_{TSP}, and degradation rate of gaseous OPEs. In addition, the nonexchangeability might also contribute to this result, due to the polarity and low volatility of OPEs.

Dry Deposition Flux into the Bohai and Yellow Seas. The deposition flux F_d (ng/m^2/day) is the product of C_p (ng/m^3, OPE concentration in particulate phase) and V_d (m/day, deposition velocity). As there is no field measured V_d for OPEs

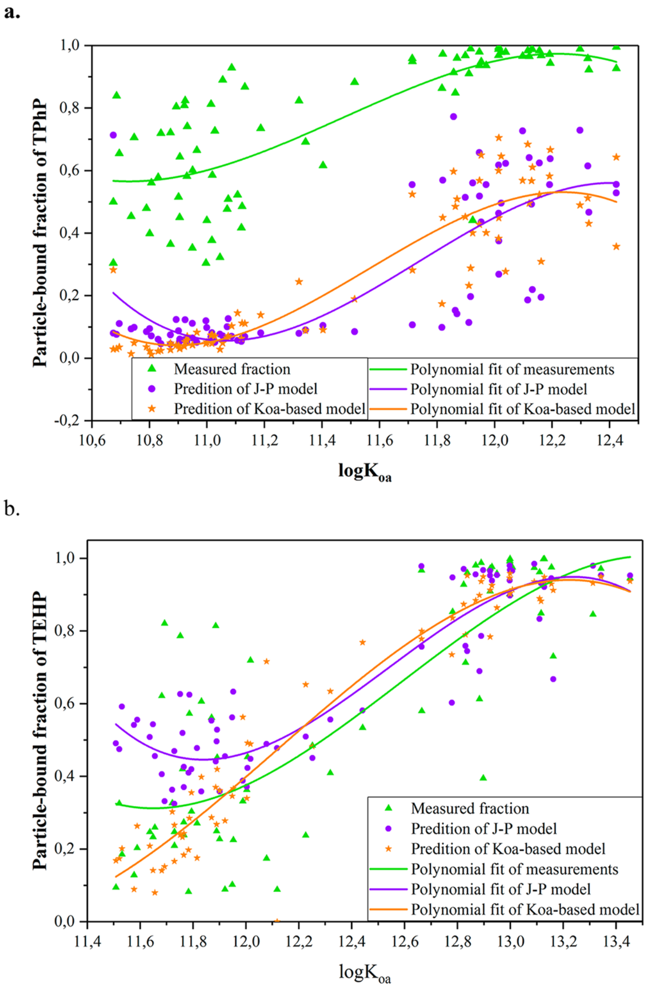

Figure 4. a. Comparison of predicted and measured particle-bound fractions of TPhP (for each sample). b. Comparison of predicted and measured particle-bound fractions of TEHP (for each sample).

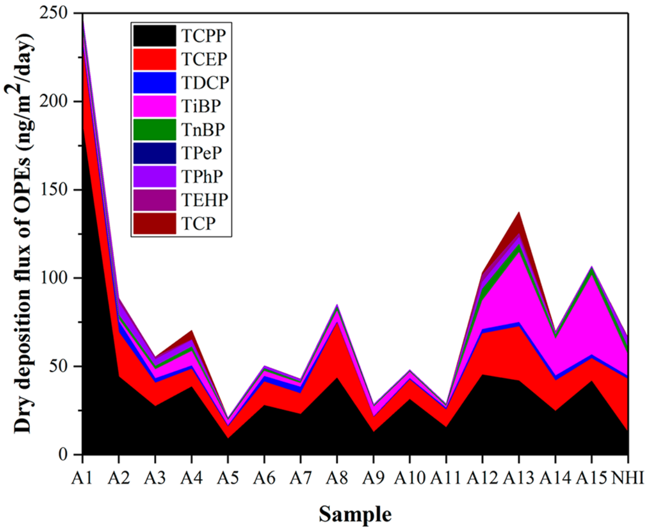

Figure 5. Dry deposition fluxes of OPEs into the Bohai and Yellow Seas at each sample and median fluxes onto North Huangcheng Island (NHI).

or other families of compounds in the Bohai and Yellow Seas, a value of 0.55 cm/s (475.2 m/day) was used for V_d in the present work, which was suggested previously for pollutants over the Yellow Sea.[39] The lack of measured OPE dry deposition velocities results in uncertainties in the estimation of deposition fluxes. The adsorption, desorption, and temperature change during the sampling introduces uncertainties. In addition, breakthrough of target compounds to the vapor phase would affect the concentrations of gaseous OPEs.[9] All of these factors may lead to an over- or underestimation of the dry deposition fluxes.

The ΣOPE dry deposition into the Bohai and Yellow Seas ranged from 21 to 250 ng/m^2/day (median: 70 ng/m^2/day) and was dominated by TCPP (median: 31 ng/m^2/day), followed by TCEP (13 ng/m^2/day), TiBP (5.6 ng/m^2/day), and TnBP (2.2 ng/m^2/day; Figure 5).

On NHI, the median deposition flux was estimated as 79 ng/m^2/day. The individual fluxes were in the order of TCEP (30 ng/m^2/day) > TCPP (13 ng/m^2/day) ≈ TiBP (12 ng/m^2/day) > TnBP (4.0 ng/m^2/day; Figure 5).

The ΣOPE deposition fluxes into the Bohai and Yellow Seas (median: 70 ng/m^2/day) were higher than those published for the South China Sea (16.3 ± 6.7 ng/m^2/day)[13] and the North Atlantic and Arctic Oceans (5 ± 4 ng/m^2/day).[9] They were similar to those estimated for deposition over in the North Sea (9–240 ng/m^2/day),[7] much lower than those over the Mediterranean Sea (70–880 ng/m^2/day),[8] and the Black Sea (300–1060 ng/m^2/day).[8]

Considering the combined surface area of 458,000 km^2 of the Bohai and Yellow Seas, the annual OPE input from dry deposition is estimated to be 12 tons/year (median flux: 70 ng/m^2/day; Samples A1–A15 and NHI).[15,17] This annual OPE input is 1 order of magnitude lower than that into the Black Sea (~50–170 tons/year), which has a similar surface area (440,000 km^2). For only the Bohai Sea, the estimated atmospheric flux was 2.2 tons/year (area: 78,000 km^2, median flux: 79 ng/m^2/day; Samples A14, A15, and NHI), which is higher than that of the German North Sea (area: 42,000 km^2; mean flux: 0.71 ± 0.58 tons/year).[7] The annual atmospheric OPE input into the Bohai Sea was ~6 times lower than the riverine input (16 ± 3.2 tons/year; 40 major rivers involved).[40] However, atmospheric transport can lead to faster and larger spatial distribution of OPEs and transports OPEs to the remote ocean.

■ ASSOCIATED CONTENT

Ⓢ Supporting Information

The Supporting Information is available free of charge on the ACS Publications website at DOI: 10.1021/acs.est.7b03807.

> Tables S1–S20, Figures S1–S6, Text S1 (instrumental analysis method), and Text S2 (calculation methods of the gas/particle partitioning of OPEs) (PDF)

■ AUTHOR INFORMATION

Corresponding Authors

*Phone: +86-535-2109151. Fax: +86-535-2109000. E-mail: jhtang@yic.ac.cn.
*Phone: +49-4152-872330. Fax: +49-4152-872332. E-mail: zhiyong.xie@hzg.de.

ORCID

Jing Li: 0000-0003-0187-9179
Jianhui Tang: 0000-0002-9006-263X
Chongguo Tian: 0000-0001-6058-9353
Zhiyong Xie: 0000-0001-8997-3930

Notes

The authors declare no competing financial interest.

■ ACKNOWLEDGMENTS

This study was supported by the Chinese Academy of Sciences (2013T2Z0032, KZZD-EW-14, 13337KYSB20130013, 4177338, and XDA11020401), and Bundesministerium für Bildung und Forschung (03F0786C). We are grateful for the field assistant from the crew of Research Vessel *Dongfanghong 2* of the Ocean University of China. J.L. gratefully acknowledges the China Scholarship Council.

■ REFERENCES

(1) Marklund, A.; Andersson, B.; Haglund, P. Traffic as a source of organophosphorus flame retardants and plasticizers in snow. *Environ. Sci. Technol.* **2005**, *39* (10), 3555−3562.

(2) Reemtsma, T.; Quintana, J. B.; Rodil, R.; Garcia-Lopez, M.; Rodriguez, I. Organophosphorus flame retardants and plasticizers in water and air I. Occurrence and fate. *TrAC, Trends Anal. Chem.* **2008**, *27* (9), 727−737.

(3) Hartmann, P. C.; Burgi, D.; Giger, W. Organophosphate flame retardants and plasticizers in indoor air. *Chemosphere* **2004**, *57* (8), 781−787.

(4) Zhang, Y. Global market analysis of flame retardant (in Chinese with English abstract). *Fine and Specialty Chem.* **2014**, *22* (8), 20−24.

(5) Zhang, K.; Schnoor, J. L.; Zeng, E. Y. E-Waste recycling: Where does it go from here? *Environ. Sci. Technol.* **2012**, *46*, 10861−10867.

(6) Matsukami, H.; Tue, N. M.; Suzuki, G.; Someya, M.; Tuyen, L. H.; Viet, P. H.; Takahashi, S.; Tanabe, S.; Takigami, H. Flame retardant emission from e-waste recycling operation in northern Vietnam: Environmental occurrence of emerging organophosphorus esters used as alternatives for PBDEs. *Sci. Total Environ.* **2015**, *514*, 492−499.

(7) Möller, A.; Xie, Z. Y.; Caba, A.; Sturm, R.; Ebinghaus, R. Organophosphorus flame retardants and plasticizers in the atmosphere of the North Sea. *Environ. Pollut.* **2011**, *159* (12), 3660−3665.

(8) Castro-Jimenez, J.; Berrojalbiz, N.; Pizarro, M.; Dachs, J. Organophosphate Ester (OPE) Flame Retardants and Plasticizers in the Open Mediterranean and Black Seas Atmosphere. *Environ. Sci. Technol.* **2014**, *48* (6), 3203−3209.

(9) Li, J.; Xie, Z.; Mi, W.; Lai, S.; Tian, C.; Emeis, K.-C.; Ebinghaus, R. Organophosphate Esters in Air, Snow and Seawater in the North Atlantic and the Arctic. *Environ. Sci. Technol.* **2017**, *51*, 6887−6896.

(10) Castro-Jimenez, J.; Gonzalez-Gaya, B.; Pizarro, M.; Casal, P.; Pizarro-Alvarez, C.; Dachs, J. Organophosphate Ester Flame Retardants and Plasticizers in the Global Oceanic Atmosphere. *Environ. Sci. Technol.* **2016**, *50* (23), 12831−12839.

(11) Möller, A.; Sturm, R.; Xie, Z. Y.; Cai, M. H.; He, J. F.; Ebinghaus, R. Organophosphorus Flame Retardants and Plasticizers in Airborne Particles over the Northern Pacific and Indian Ocean toward the Polar Regions: Evidence for Global Occurrence. *Environ. Sci. Technol.* **2012**, *46* (6), 3127−3134.

(12) Cheng, W. H.; Xie, Z. Q.; Blais, J. M.; Zhang, P. F.; Li, M.; Yang, C. Y.; Huang, W.; Ding, R.; Sun, L. G. Organophosphorus esters in the oceans and possible relation with ocean gyres. *Environ. Pollut.* **2013**, *180*, 159−164.

(13) Lai, S.; Xie, Z.; Song, T.; Tang, J.; Zhang, Y.; Mi, W.; Peng, J.; Zhao, Y.; Zou, S.; Ebinghaus, R. Occurrence and dry deposition of organophosphate esters in atmospheric particles over the northern South China Sea. *Chemosphere* **2015**, *127*, 195−200.

(14) Wolschke, H.; Sühring, R.; Mi, W. Y.; Möller, A.; Xie, Z. Y.; Ebinghaus, R. Atmospheric occurrence and fate of organophosphorus flame retardants and plasticizer at the German coast. *Atmos. Environ.* **2016**, *137*, 1−5.

(15) Zhang, Z. H.; Zhu, M. Y.; Wang, Z. L.; Wang, J. Monitoring and managing pollution load in Bohai Sea, PR China. *Ocean Coast. Manage.* **2006**, *49* (9−10), 706−716.

(16) Hwang, J. H.; Van, S. P.; Choi, B. J.; Chang, Y. S.; Kim, Y. H. The physical processes in the Yellow Sea. *Ocean Coast. Manage.* **2014**, *102*, 449−457.

(17) Jiang, X.; Teng, A. K.; Xu, W. Z.; Liu, X. S. Distribution and pollution assessment of heavy metals in surface sediments in the Yellow Sea. *Mar. Pollut. Bull.* **2014**, *83* (1), 366−375.

(18) Liu, Y.; Li, Y.; Chen, J. Research on Modes of Cargo Ro-Ro, Drop and Pull Transport in Land-Sea Transportation Channel between Shandong and Liaoning. *J. Service Sci. Manage.* **2015**, *8* (02), 229.

(19) Xie, Z. Y.; Ebinghaus, R. Analytical methods for the determination of emerging organic contaminants in the atmosphere. *Anal. Chim. Acta* **2008**, *610* (2), 156−178.

(20) Fan, X.; Kubwabo, C.; Rasmussen, P. E.; Wu, F. Simultaneous determination of thirteen organophosphate esters in settled indoor house dust and a comparison between two sampling techniques. *Sci. Total Environ.* **2014**, *491−492*, 80−6.

(21) van den Eede, N.; Dirtu, A. C.; Neels, H.; Covaci, A. Analytical developments and preliminary assessment of human exposure to organophosphate flame retardants from indoor dust. *Environ. Int.* **2011**, *37* (2), 454−461.

(22) Ali, N.; Dirtu, A. C.; Van den Eede, N.; Goosey, E.; Harrad, S.; Neels, H.; t Mannetje, A.; Coakley, J.; Douwes, J.; Covaci, A. Occurrence of alternative flame retardants in indoor dust from New Zealand: indoor sources and human exposure assessment. *Chemosphere* **2012**, *88* (11), 1276−82.

(23) Bergh, C.; Luongo, G.; Wise, S.; Ostman, C. Organophosphate and phthalate esters in standard reference material 2585 organic contaminants in house dust. *Anal. Bioanal. Chem.* **2012**, *402* (1), 51−59.

(24) Van den Eede, N.; Dirtu, A. C.; Ali, N.; Neels, H.; Covaci, A. Multi-residue method for the determination of brominated and organophosphate flame retardants in indoor dust. *Talanta* **2012**, *89* (Supplement C), 292−300.

(25) Brandsma, S. H.; de Boer, J.; Cofino, W. P.; Covaci, A.; Leonards, P. E. G. Organophosphorus flame-retardant and plasticizer analysis, including recommendations from the first worldwide interlaboratory study. *TrAC, Trends Anal. Chem.* **2013**, *43*, 217−228.

(26) Cristale, J.; Lacorte, S. Development and validation of a multiresidue method for the analysis of polybrominated diphenyl ethers, new brominated and organophosphorus flame retardants in sediment, sludge and dust. *J. Chromatogr. A* **2013**, *1305*, 267−75.

(27) Ionas, A. C.; Covaci, A. Simplifying multi-residue analysis of flame retardants in indoor dust. *Int. J. Environ. Anal. Chem.* **2013**, *93* (10), 1074−1083.

(28) Draxler, R. R.; Hess, G. *Description of the HYSPLIT4 modeling system*; NOAA Technical Memorandum ERL ARL-224; NOAA Air Resources Laboratory: Silver Spring, MD, 1997; pp 1−24.

(29) Pankow, J. F.; Bidleman, T. F. Interdependence of the Slopes and Intercepts from Log Log Correlations of Measured Gas Particle Partitioning and Vapor-Pressure 0.1. Theory and Analysis of Available Data. *Atmos. Environ., Part A* **1992**, *26* (6), 1071−1080.

(30) Brommer, S.; Jantunen, L. M.; Bidleman, T. F.; Harrad, S.; Diamond, M. L. Determination of Vapor Pressures for Organophosphate Esters. *J. Chem. Eng. Data* **2014**, *59* (5), 1441−1447.

(31) Pankow, J. F. Review and Comparative-Analysis of the Theories on Partitioning between the Gas and Aerosol Particulate Phases in the Atmosphere. *Atmos. Environ.* **1987**, *21* (11), 2275−2283.

(32) Wang, Z.; Na, G. S.; Ma, X. D.; Fang, X. D.; Ge, L. K.; Gao, H.; Yao, Z. W. Occurrence and gas/particle partitioning of PAHs in the atmosphere from the North Pacific to the Arctic Ocean. *Atmos. Environ.* **2013**, *77*, 640−646.

(33) Lohmann, R.; Lammel, G. Adsorptive and absorptive contributions to the gas-particle partitioning of polycyclic aromatic hydrocarbons: State of knowledge and recommended parametrization for modeling. *Environ. Sci. Technol.* **2004**, *38* (14), 3793−3803.

(34) Harner, T.; Bidleman, T. F. Octanol-air partition coefficient for describing particle/gas partitioning of aromatic compounds in urban air. *Environ. Sci. Technol.* **1998**, *32* (10), 1494−1502.

(35) Wang, Q.; Zhao, H.; Wang, Y.; Xie, Q.; Chen, J.; Quan, X. Determination and prediction of octanol-air partition coefficients for organophosphate flame retardants. *Ecotoxicol. Environ. Saf.* **2017**, *145*, 283−288.

(36) Sühring, R.; Diamond, M. L.; Scheringer, M.; Wong, F.; Pucko, M.; Stern, G.; Burt, A.; Hung, H.; Fellin, P.; Li, H.; Jantunen, L. M. Organophosphate Esters in Canadian Arctic Air: Occurrence, Levels and Trends. *Environ. Sci. Technol.* **2016**, *50* (14), 7409−7415.

(37) Salamova, A.; Hermanson, M. H.; Hites, R. A. Organophosphate and Halogenated Flame Retardants in Atmospheric Particles from a European Arctic Site. *Environ. Sci. Technol.* **2014**, *48* (11), 6133−6140.

(38) Li, C.; Chen, J.; Xie, H. B.; Zhao, Y.; Xia, D.; Xu, T.; Li, X.; Qiao, X. Effects of Atmospheric Water on.OH-initiated Oxidation of Organophosphate Flame Retardants: A DFT Investigation on TCPP. *Environ. Sci. Technol.* **2017**, *51* (9), 5043−5051.

(39) Gao, Y.; Arimoto, R.; Duce, R. A.; Lee, D. S.; Zhou, M. Y. Input of Atmospheric Trace-Elements and Mineral Matter to the Yellow Sea during the Spring of a Low-Dust Year. *J. Geophys. Res.* **1992**, *97* (D4), 3767−3777.

(40) Wang, R. M.; Tang, J. H.; Xie, Z. Y.; Mi, W. Y.; Chen, Y. J.; Wolschke, H.; Tian, C. G.; Pan, X. H.; Luo, Y. M.; Ebinghaus, R. Occurrence and spatial distribution of organophosphate ester flame retardants and plasticizers in 40 rivers draining into the Bohai Sea, north China. *Environ. Pollut.* **2015**, *198*, 172−178.

Supporting Information of

Spatial distribution and seasonal variation of organophosphate esters in air above the Bohai and Yellow Seas, China

Jing Li[†,⊥], Jianhui Tang[‡*], Wenying Mi[§], Chongguo Tian[‡], Kay-Christian Emeis[†,⊥], Ralf Ebinghaus[†], Zhiyong Xie[†*]

[†]Helmholtz-Zentrum Geesthacht, Centre for Materials and Coastal Research, Institute of Coastal Research, Geesthacht, 21502, Germany

[‡]Key Laboratory of Coastal Environmental Processes and Ecological Remediation, Yantai Institute of Coastal Zone Research, CAS, Yantai, 264003, China

[§]MINJIE Analytical Laboratory, Geesthacht, 21502, Germany

[⊥]University of Hamburg, School of Integrated Climate System Sciences, Hamburg, 20144, Germany

Corresponding Author

*Phone: +86-535-2109151; Fax: +86-535-2109000; E-mail address: jhtang@yic.ac.cn

*Phone: +49-4152-872330; Fax: +49-4152-872332; E-mail address: zhiyong.xie@hzg.de

Pages: 22

Tables: 20

Figures: 6

Contents

Table S1. Detailed information of air sampling during cruise in Bohai and Yellow Seas

Air sample	Date	Latitude	Longitude	Volume (m^3)	Ta (°C)	C_{TSP}(μg/m^3)	Relative Humidity (%)
A1	28.06.2016	120.057	36.094	343	21.2	-	95
A2	29.06.2016	122.523	35.999	463	23.7	56	87
A3	30.06.2016	123.485	35.002	355	24.3	52	94
A4	01.07.2016	120.340	34.153	317	22.5	20	91
A5	02.07.2016	123.999	33.775	379	23.7	53	88
A6	03.07.2016	122.293	32.382	412	23.8	242	97
A7	04.07.2016	123.729	33.922	352	24.4	61	97
A8	05.07.2016	121.576	35.541	294	23.1	22	87
A9	07.07.2016	121.526	36.076	375	23.8	5	93
A10	08.07.2016	123.290	36.999	289	23.3	10	88
A11	09.07.2016	123.244	38.135	395	23.9	-	86
A12	10.07.2016	122.703	38.140	403	25.3	44	85
A13	11.07.2016	121.437	38.468	408	25.7	50	81
A14	12.07.2016	119.042	38.310	349	25.7	55	91
A15	13.07.2016	120.906	39.479	387	24.8	44	82

Ta represents the mean air temperature during the sampling period. C_{TSP} is the total suspended particle concentrations.

Table S2. Detailed information on air sampling on North Huangcheng Island

Sample	Start Time	End Time	Volume (m^3)	Ta (°C)	C_{TSP}($\mu g/m^3$)	Relative Humidity (%)
SA1	16.05.2015 8:42	17.05.2015 8:26	317	18.0	75	30
SA2	19.05.2015 8:36	20.05.2015 8:27	283	18.2	77	44
SA3	22.05.2015 8:24	23.05.2015 8:23	303	20.2	62	46
SA4	25.05.2015 8:29	26.05.2015 8:29	266	21.8	72	38
SA5	28.05.2015 8:30	29.05.2015 8:30	302	18.2	41	60
SA6	31.05.2015 8:31	01.06.2015 8:31	308	21.1	79	54
SA7	03.06.2015 8:50	04.06.2015 8:47	309	20.0	58	59
SA8	06.06.2015 8:29	07.06.2015 8:29	322	18.5	110	78
SA9	09.06.2015 8:33	10.06.2015 8:33	321	19.1	52	72
SA10	12.06.2015 8:34	23.06.2015 8:34	302	22.5	45	56
SA11	15.06.2015 8:30	16.06.2015 8:30	316	20.5	44	74
SA12	18.06.2015 8:26	19.06.2015 8:26	300	20.2	38	82
SA13	24.06.2015 8:33	25.06.2015 8:32	331	21.9	53	82
SA14	27.06.2015 8:58	28.06.2015 8:58	282	22.4	43	80
SA15	30.06.2015 7:38	01.07.2015 7:38	246	19.2	48	88
SA16	03.07.2015 8:38	04.07.2015 8:38	282	20.5	40	69
SA17	06.07.2015 8:28	07.07.2015 8:38	295	21.4	40	86
SA18	09.07.2015 7:42	10.07.2015 7:42	337	22.9	30	87
SA19	22.07.2015 8:40	23.07.2015 8:37	307	24.3	30	86
SA20	25.07.2015 8:20	26.07.2015 8:20	348	25.3	75	83
SA21	12.08.2015 08:38	13.08.2015 08:39	267	26.8	51	81
SA22	15.08.2015 08:31	16.08.2015 08:30	313	26.5	52	72
SA23	18.08.2015 08:34	19.08.2015 08:35	296	26.4	60	77
SA24	21.08.2015 08:37	22.08.2015 08:37	300	25.5	21	74
SA25	24.08.2015 08:32	25.08.2015 08:32	256	24.5	49	85
SA26	27.08.2015 08:34	28.08.2015 08:34	250	24.2	16	76
SA27	30.08.2015 08:30	31.08.2015 08:30	291	23.7	28	79
SA28	02.09.2015 08:48	03.09.2015 08:48	274	22.3	31	87
SA29	05.09.2015 08:37	06.09.2015 08:37	299	22.9	55	75
SA30	08.09.2015 08:47	09.09.2015 08:47	299	23.5	30	70
SA31	11.09.2015 08:30	12.09.2015 08:30	274	20.9	-	58
SA32	14.09.2015 08:27	15.09.2015 08:27	282	23.0	67	67
SA33	17.09.2015 08:54	18.09.2015 08:54	266	21.8	38	77
SA34	20.09.2015 09:00	21.09.2015 09:00	273	22.0	33	71
SA35	23.09.2015 08:55	24.09.2015 08:55	292	22.3	45	77
SA36	26.09.2015 08:26	27.09.2015 08:26	290	21.4	26	73
SA37	30.09.2015 07:38	01.10.2015 07:38	292	19.6	37	67
SA38	04.10.2015 08:14	05.10.2015 08:14	263	19.5	58	74
SA39	07.10.2015 08:35	07.10.2015 08:35	244	20.1	75	83
SA40	10.10.2015 08:55	11.10.2015 08:55	329	14.1	42	46
SA41	14.10.2015 08:28	15.10.2015 08:28	304	18.9	107	67
SA42	16.10.2015 08:39	17.10.2015 08:39	281	17.0	171	94
SA43	22.10.2015 08:36	23.10.2015 08:29	261	16.3	-	72
SA44	26.10.2015 08:35	27.10.2015 08:35	258	14.6	91	62

SA45	29.10.2015 08:31	30.10.2015 08:31	308	14.1	36	60
SA46	10.11.2015 08:28	11.11.2015 08:28	262	11.1	98	48
SA47	19.11.2015 08:35	20.11.2015 08:35	257	13.1	68	49
SA48	27.11.2015 08:51	28.11.2015 08:51	260	7.6	70	67
SA49	30.11.2015 08:41	01.12.2015 08:45	243	5.8	37	76
SA50	07.12.2015 08:31	08.12.2015 08:31	270	0.1	58	59
SA51	10.12.2015 08:37	11.12.2015 08:53	311	4.2	94	62
SA52	13.12.2015 08:30	14.12.2015 08:31	244	4.9	238	62
SA53	16.12.2015 08:57	17.12.2015 08:57	318	5.0	45	77
SA54	19.12.2015 08:27	20.12.2015 08:25	289	0.8	51	54
SA55	22.12.2015 08:37	23.12.2015 08:37	275	4.1	154	50
SA56	25.12.2015 08:30	26.12.2015 08:30	278	2.5	187	61
SA57	28.12.2015 08:32	29.12.2015 08:30	234	0.6	111	63
SA58	31.12.2015 08:33	01.01.2016 08:33	285	2.5	77	64
SA59	03.01.2016 08:28	04.01.2016 08:28	238	3.5	119	87
SA60	06.01.2016 08:36	07.01.2016 08:36	268	0.7	47	54
SA61	09.01.2016 08:35	10.01.2016 08:35	279	0.6	90	54
SA62	12.01.2016 08:27	13.01.2016 08:27	230	-2.6	40	51
SA63	15.01.2016 08:35	16.01.2016 08:35	284	2.5	143	44
SA64	25.01.2016 08:51	26.01.2016 08:51	272	-2.6	69	54
SA65	28.01.2016 08:58	29.01.2016 08:58	263	2.4	85	67
SA66	31.01.2016 09:08	01.02.2016 09:08	271	-4.1	43	55
SA67	03.02.2016 08:34	04.02.2016 08:34	245	0.2	75	55
SA68	06.02.2016 08:37	07.02.2016 08:37	295	-0.4	32	49
SA69	09.02.2016 08:34	10.02.2016 08:34	234	3.6	35	55
SA70	17.02.2016 08:31	18.02.2016 08:31	249	2.5	75	63
SA71	20.02.2016 08:33	21.02.2016 08:33	277	2.1	50	62
SA72	24.02.2016 08:29	25.02.2016 08:29	288	-2.1	54	53
SA73	27.02.2016 08:27	28.02.2016 08:27	229	3.2	58	54
SA74	01.03.2016 08:32	02.03.2016 08:32	230	1.1	96	45
SA75	04.03.2016 08:38	05.03.2016 08:38	175	4.0	194	94
SA76	07.03.2016 08:49	08.03.2016 08:49	300	5.1	84	69
SA77	09.03.2016 08:51	10.03.2016 08:51	232	-0.5	43	43
SA78	12.03.2016 08:25	13.03.2016 08:25	244	3.6	101	69
SA79	14.03.2016 08:43	15.03.2016 08:43	298	4.4	84	50
SA80	17.03.2016 08:40	18.03.2016 08:40	298	7.6	62	75
SA81	20.03.2016 08:45	21.03.2016 08:45	281	5.8	68	52

Table S3. Full Names, acronyms, formulas, Chemical Abstract System (CAS) Numbers and physicochemical parameters of the selected OPEs

Acronym	Full Name	CAS No.	Chemical form	P_L° (Pa)	Solubility (mg/L)	HLC (Pa/m^3/mol)	$logK_{oa}$
TCEP	Tris-(2-chloroethyl) phosphate	115-96-8	$C_6H_{12}Cl_3O_4P$	4.8e-2*	878	5.06	7.98
TCPP	Tris-(1-chloro-2-propyl) phosphate	13674-84-5	$C_9H_{18}Cl_3O_4P$	3.5e-2*	51.9	72.77	9.68
TDCP	Tris-(1,3-dichloro-2-propyl) phosphate	13674-87-8	$C_9H_{15}Cl_6O_4P$	4.1e-4*	1.50	0.13	10.6
TiBP	Tri-iso-butyl phosphate	126-71-6	$C_{12}H_{27}O_4P$	1.72	16.2	9210	-
TnBP	Tri-n-butyl phosphate	126-73-8	$C_{12}H_{27}O_4P$	1.5e-1	7.36	962.9	7.55
TPhP	Triphenyl phosphate	115-86-6	$C_{18}H_{15}O_4P$	2.7e-4*	1.03	3.12	10.9
TPeP	Tripentyl phosphate	2528-38-3	$C_{15}H_{33}O_4P$	8.7e-3	0.33	643.6	9.31
TEHP	Tris-(2-ethylhexyl) phosphate	78-42-2	$C_{24}H_{51}O_4P$	2.1e-5*	1.5e-5	280.7	11.9
TCP	Tricresyl phosphate	1330-78-5	$C_{21}H_{21}O_4P$	8e-5	0.2	-	12.3

P_L°: Sub-cooled vapor pressure; HLC: Henry's low constant, sourced from SPARC software; $logK_{oa}$values of sourced from Wang et al.[1]; $^*P_L^\circ$ sourced from Brommer et al.[2]; the remain data sourced from EPI Suite 4.1 (at 25°C)

Table S4. Mean absolute field blank values of OPEs in pg

OPE	**Bohai and Yellow Seas (n=15)**				**North Huangcheng Island (n=81)**			
	Gaseous phase		**Particulate phase**		**Gaseous phase**		**Particulate phase**	
	Mean	SD	Mean	SD	Mean	SD	Mean	SD
TCEP	59	40	88	55	100	59	61	15
TCPP1	87	19	200	52	200	120	230	53
TCPP2	20	6.9	46	13	33	13	45	25
TCPP3	3.8	2.0	75	32	21	10	23	6.8
Total TCPP	110	27	320	80	260	130	340	140
TDCP	19	3.8	140	34	52	32	35	3.8
TiBP	34	16	60	14	61	20	98	16
TnBP	22	11	28	8.7	68	45	41	11
TPeP	1.4	1.4	2.8	1.1	1.7	1.0	1.2	0.22
TPhP	46	18	43	18	57	17	73	38
TEHP	79	52	46	12	21	7.8	26	11
TCP1	12	5.9	91	43	45	17	36	10
TCP2	11	6.0	150	42	38	15	26	8.0
TCP3	27	23	160	85	66	24	38	12
TCP4	22	21	190	50	53	25	280	30
Total TCP	72	52	530	88	200	81	380	48

SD: standard deviation

Table S5. Field blanks (mean, SD) and method detection limits (MDLs) of OPEs

OPE	Bohai and Yellow Seas (n=15)						North Huangcheng Island (n=81)					
	Gaseous phase			Particulate phase			Gaseous phase			Particulate phase		
	Mean	SD	MDL	Mean	SD	MDL	Mean	SD	MDL	Mean	SD	MDL
TCEP	0.20	0.13	0.59	0.59	0.37	1.7	0.34	0.20	0.92	0.40	0.10	0.70
TCPP1	0.29	0.06	0.48	1.4	0.35	2.4	0.67	0.39	1.8	1.5	0.35	2.6
TCPP2	0.07	0.02	0.14	0.31	0.09	0.57	0.11	0.04	0.24	0.30	0.17	0.81
TCPP3	0.01	0.01	0.03	0.50	0.22	1.2	0.07	0.03	0.17	0.15	0.04	0.29
Toal TCPP	0.37	0.09	0.64	2.2	0.53	3.8	0.85	0.43	2.2	2.3	0.92	5.0
TiBP	0.11	0.05	0.27	0.40	0.09	0.69	0.20	0.07	0.40	0.65	0.11	0.98
TnBP	0.07	0.04	0.19	0.19	0.06	0.36	0.23	0.15	0.68	0.27	0.08	0.50
TPeP	0.01	0.01	0.02	0.02	0.01	0.04	0.01	0.003	0.02	0.01	0.001	0.01
TDCP	0.06	0.01	0.10	0.93	0.23	1.6	0.17	0.11	0.49	0.24	0.03	0.31
TPhP	0.15	0.06	0.34	0.29	0.12	0.65	0.19	0.06	0.36	0.49	0.25	1.3
TEHP	0.26	0.17	0.79	0.31	0.08	0.54	0.07	0.03	0.15	0.17	0.07	0.38
TCP1	0.04	0.02	0.10	0.61	0.29	1.5	0.15	0.06	0.32	0.24	0.07	0.44
TCP2	0.04	0.02	0.10	0.98	0.28	1.8	0.13	0.05	0.27	0.17	0.05	0.34
TCP3	0.09	0.08	0.32	1.1	0.57	2.8	0.22	0.08	0.46	0.25	0.08	0.50
TCP4	0.07	0.07	0.28	1.3	0.33	2.3	0.18	0.08	0.43	1.9	0.20	2.5
Total TCP	0.24	0.17	0.76	3.5	0.58	5.3	0.67	0.27	1.5	2.5	0.32	3.5

MDLs were derived from mean blank values plus three times the standard deviation. A mean volume of 300 m^3 was estimated for air sample.

Table S6. Recovery rate (%) of OPEs in gaseous phase (n=5)

OPEs	Mean	SD
TCEP	130	12
TCPP-1	83	5.4
TCPP-2	17	0.84
TCPP-3	1.8	0.33
Total TCPP	100	5.9
TDCP	140	15
TiBP	110	9.0
TnBP	130	12
TPeP	160	25
TPhP	110	12
TEHP	82	22
TCP-1	38	6.6
TCP-2	39	6.0
TCP-3	27	3.8
TCP-4	31	5.8
Total TCP	140	20

Table S7. Parameters for determining OPEs using GC-MS/MS

Acronym	**Name**	**Quantifier***	**Qualifier***
TCEP	Tris-(2-chloroethyl)phosphate	249.0/99.0	249.0/187.0
TCPP1	Tris-(1-chloro-2-propyl)phosphate	157.0/117.0	277.0/125.0
TCPP2	Tris-(1-chloro-2-propyl)phosphate	157.0/117.0	277.0/125.0
TCPP3	Tris-(1-chloro-2-propyl)phosphate	157.0/117.0	277.0/125.0
TDCP	Tri-(dichlorisopropyl)phosphate	381.0/159.0	191.0/75.0
T*i*BP	Tri-*iso*-butylphosphate	99.0/81.0	155.0/99.0
TnBP	Tri-*n*-butylphosphate	99.0/81.0	155.0/99.0
TPhP	Triphenylphosphate	326.0/215.0	326.0/170.0
TPeP	Tripentylphosphate	99.0/81.0	239.0/99.0
TEHP	Tris-(2-ethylhexyl)phosphate	99.0/81.0	113.0/99.0
TCP	Tri-cresyl phosphate (4 isomers)	368.0/165.0	368.0/198.0
d_{27}-TnBP	d_{27}-Tri-*n*-butylphosphate	103.0/83.0	167.0/103.0
d_{12}-TCEP	d_{12}-Tris-(2-chloroethyl)phosphate	261.0/103.0	261.0/196.0
d_{15}-TPhP	d_{15}-Triphenylphosphate	341.0/223.0	341.0/178.0
$^{13}C_6$-PCB 208	$^{13}C_6$-2,2',3,3',4,5,5',6,6'-Nonachlorobiphenyl	476.0/406.0	-

* Precursor ion/product ion

Table S8. Field blanks and concentrations of OPEs in SRM 2585

OPEs	Blank (pg)		SRM 2585 (μg/g)						
	Mean	SD	Sample 01	Sample 02	Sample 03	Sample 04	Sample 05	Mean	SD
TCEP	74	130	1.8	1.9	1.7	2.0	2.1	1.9	0.15
TCPP-1	140	100	1.1	0.9	1.0	1.0	1.0	1.0	0.05
TCPP-2	37	34	0.33	0.29	0.31	0.29	0.31	0.31	0.02
TCPP-3	7.0	3.0	0.04	0.03	0.04	0.03	0.03	0.03	0.002
TCPP (total)	180	140	1.4	1.3	1.3	1.3	1.4	1.3	0.07
TDCP	65	30	3.9	4.1	3.4	3.2	3.3	3.6	0.41
TiBP	76	39	0.02	0.02	0.01	0.01	0.01	0.01	0.005
TnBP	27	21	0.39	0.35	0.35	0.37	0.39	0.37	0.02
TPeP	3.0	4.0	0.003	0.003	0.003	0.003	0.003	0.003	0.0001
TPhP	100	78	1.7	2.0	1.6	1.9	2.0	1.9	0.17
TEHP	39	14	1.3	1.2	1.2	1.1	1.1	1.2	0.06
TCP-1	26	6	0.39	0.54	0.45	0.42	0.45	0.45	0.06
TCP-2	29	14	0.42	0.55	0.44	0.43	0.44	0.45	0.05
TCP-3	44	16	0.27	0.35	0.31	0.27	0.29	0.30	0.03
TCP-4	180	58	0.24	0.26	0.26	0.24	0.30	0.26	0.02
TCP (total)	280	74	1.3	1.7	1.5	1.4	1.5	1.5	0.15
Weight (g)	-	-	0.106	0.10	0.10	0.10	0.101	0.10	0.002

Table S9. Comparison of the average concentrations (μg/g) of selected OPEs in SRM 2585 with those reported in the literature

Ref	n	Weight (g)	Method	TCEP	TCPP	TDCP	TiBP	TnBP	TPeP	TPhP	TEHP	TCP
Ref[3]	11	0.075	GC-MS-EI	0.7(0.17)	0.8(0.1)	2.0(0.26)	n.a.	0.18(0.02)	n.a.	0.99(0.07)	n.a.	1.07(0.11)
Ref[4]	6	0.075	GC-MS-EI	0.79(0.02)	0.8(0.02)	1.9(0.1)	1.6(0.39)	0.17(0.02)	n.a.	1.06(0.09)	n.a.	0.92(0.05)
Ref[5]	6	0.075	GC-MS-EI	0.68(0.06)	0.9(0.07)	3.2(0.07)	n.a.	0.19(0.01)	n.a.	1.2(0.14)	n.a.	1.14(0.03)
Ref[6]	7	0.1	GC-MS/MS-PCI	0.84(0.06)	0.9(0.14)	2.3(0.28)	n.d.	0.19(0.02)	n.d.	1.0(0.1)	0.37(0.04)	n.a.
Ref[7]	8-11	0.02-0.1	GC-MS or LC-MS	0.79	0.9	1.6	0.017	0.27	n.a.	1.10	0.96	0.84
Ref[8]	3	0.1	GC-MS	0.82(0.03)	1.2(0.08)	1.8(0.08)	n.a.	0.18(0.02)	n.a.	0.92(0.04)	0.37(0.19)	1.2(0.40)
Ref[9]	3	0.1	GC-MS/MS-EI	0.76(0.03)	0.9(0.07)	1.7(0.02)	n.a.	0.26(0.003)	n.a.	1.1(0.046)	0.30(0.006)	n.a.
Ref[10]	7	0.06	GC-MS/MS-PCI	0.88(0.12)	1.0(0.15)	2.3(0.16)	n.d.	0.24(0.04)	n.d.	0.92(0.13)	n.a.	n.a.
Ref[11]	-	-	GC-MS-EI	0.88	1.4	1.8	n.a.	0.25	n.a.	0.8	n.a.	n.a.
This study	5	0.1	GC-MS/MS-EI	1.9(0.15)	1.3(0.007)	3.6(0.41)	0.013(0.005)	0.37(0.002)	0.003(0.0001)	1.9(0.17)	1.2(0.006)	1.5(0.15)

n. number of analyzed samples; n.d.: not detected; n.a.: not analyzed. -: not available

Table S10. Extraction efficiency of OPEs in SRM 2585

OPEs	Extraction efficiency of OPEs in SRM 2585						
	Sample 01	Sample 02	Sample 03	Sample 04	Sample 05	Mean	SD
TCEP	81%	89%	86%	85%	92%	87%	4.2%
TCPP-1	93%	95%	94%	93%	96%	94%	1.4%
TCPP-2	93%	95%	94%	93%	96%	94%	1.3%
TCPP-3	93%	95%	94%	93%	96%	94%	1.3%
total TCPP	93%	95%	94%	93%	96%	94%	1.4%
TDCP	96%	99%	96%	95%	97%	97%	1.3%
TiBP	95%	95%	90%	89%	90%	92%	3.0%
TnBP	97%	98%	97%	97%	98%	97%	0.53%
TPeP	96%	98%	97%	97%	97%	97%	0.79%
TPhP	97%	99%	98%	98%	99%	98%	0.59%
TEHP	75%	79%	78%	75%	85%	79%	4.1%
TCP-1	99%	99.7%	99%	99%	99.6%	99%	0.17%
TCP-2	99%	99.6%	99.6%	99%	99.8%	99.6%	0.18%
TCP-3	99%	99.6%	99.5%	99%	99.9%	99.6%	0.19%
TCP-4	99%	99%	99%	99%	99%	99%	0.11%
total TCP	99%	99.6%	99%	99%	99.7%	99.5%	0.15%

The extraction efficiency was calculated with equation CE1/(CE1+CE2)×100 %, where CE1 is the concentration of OPEs in the first extraction, and CE2 is the concentration of OPEs in the second extraction.

Table S11. Comparison of particle-bound OPE concentrations (pg/m^3) in different open seas and remote areas[*]

Location	n	TCEP	TCPP	TDCP	TiBP	TnBP	TPhP	TPeP	TEHP	TCP	Other OPEs	∑OPE Range (median)	Ref
North Sea[a]	8	6-100 (26)	30-1200 (185)	n.d.-78 (n.d.)	n.d.-150 (32)	n.d.-150 (22)	4-150 (17)	n.a.	n.d.-31 (7)	n.a.	n.d.-53	69-1417 (281)	ref[12]
Sea of Japan	8	237/1960	130/620	16/52	11/63	10/33	25/97	n.a.	5/38	n.a.	15/81	450/2900	ref[13]
Northern Pacific Ocean	8	160-280 (204)	98-270 (160)	5-8 (5)	14-21 (17)	6-14 (11)	9-24 (19)	n.a.	1-12 (2)	n.a.	n.d.-16		ref[13]
Northern Pacific Ocean	9	n.d.-310 (80)	100-1460 (640)	n.d.-500 (90)	3-100 (30)	20-2500 (170)	n.d.-34 (10)	n.a.	60-380 (110)	n.a.	325	500-4430 (1860)	ref[11]
South Pacific Ocean	9	34-370 (140)	50-800 (530)	n.d.-1000 (60)	15-160 (50)	50-2170 (200)	n.d.-40 (4)	n.a.	40-350 (160)	n.a.	~400	1110-3160 (1640)	ref[11]
Philippine Sea	8	20-156 (77)	22-411 (74)	50-780 (80)	10-23 (16)	10-100 (14)	n.d.-155 (17)	n.a.	6-92 (12)	n.a.	n.d.-77		ref[13]
Indian Ocean	8	46-570 (223)	37-550 (251)	n.d.-220 (52)	7-96 (31)	7-75 (27)	n.d.-74 (26)	n.a.	4-51 (20)	n.a.	n.d.-44		ref[13]
Indian Ocean	9	50-620 (100)	30-1250 (370)	n.d.-1000 (20)	n.d.-110 (40)	70-940 (230)	n.d.-12 (8)	n.a.	n.d.-630 (180)	n.a.	~370	360-3220 (1520)	ref[11]
East China Sea	4	134	9	828	n.a.	n.a.	n.a.	n.a.	n.a.	n.a.	95	1066	ref[14]
Coral Sea	4	88	7	370	n.a.	n.a.	n.a.	n.a.	n.a.	n.a.	66	531	ref[14]
Southern Ocean	8	74	55	80	16	14	19	n.a.	7	n.a.		265	ref[13]
Near Antarctic Peninsula	4	41	4	76	n.a.	n.a.	n.a.	n.a.	n.a.	n.a.	20	141	ref[14]
Arctic Ocean	8	126-585 (289)	85-529 (281)	n.d.-5 (n.d.)	16-35 (25)	n.d.-36 (11)	10-60 (19)	n.a.	n.d.-6 (1)	n.a.	n.d.-11		ref[13]
Mediterranean Sea[b]	14	70-854 (138)	126-2340 (700)	n.d.-460 (58)	4-650 (109)	56-600 (238)	n.d.-80 (14)	n.a.	56-307 (136)	n.a.	~300	413-5107 (1455)	ref[15]
Black Sea	14	300-2417 (492)	540-2722 (820)	n.d.-97 (86)	66-190 (150)	202-370 (310)	3-40 (35)	n.a.	36-190 (175)	n.a.	~250	1717-6165 (2006)	ref[15]
Great Lakes(2013)[c]	12	5.5±0.9-180±25 (93)	25±7-850±300 (345)	n.d.-520±220 (154)	n.a.	34±7-250±53 (148)	42±9-200±27 (103)	n.a.	4.7±0.7-66±9 (28)	n.a.	~200	100-1390	ref[16]
Great Lakes(2016)[d]	6	193	173	36	n.a.	110	82	n.a.	n.a.	n.a.	38	93-1046 (509)	ref[17]
Longyearbyen	13	4.0-63 (15)	10-186 (57)	2.3-294 (10)	n.a.	5.6-1000 (56)	1.1-52 (17)	n.a.	1.0-42 (9)	n.a.	~200	33-1450 (334)	ref[18]
Ny-Ålesund	9	<200-270	<200-330	87-250	<10-140	n.a.	<50	n.a.	n.a.	n.a.	<500	<1300	ref[19]
South China Sea[e]	9	14-107 (43)	15-38 (25)	1.3-4.5 (2.2)	1.1-3.8 (2.1)	1.4-4.8 (2.5)	3.4-15 (6.2)	n.a.	2.3-16 (3.6)	0.8-4.1 (1.3)	1.6-6.4 (2.3)	47-160 (91)	ref[20]
Canadian Arctic (ship-based)	14	n.d.-856 (128)	n.d.-660 (55)	n.d.-13 (1.7)	n.a.	n.d.-97 (n.d.)	n.d.-1930 (4.7)	n.a.	n.d.-7.5 (n.d.)	n.a.		n.d.-2445 (237)	ref[21]

Canadian Arctic (land-based)	14	n.d.-433 (72)	n.d.-276 (54)	n.d.-46 (4.8)	n.a.	n.d.-2340 (416)	1.2-96 (12)	n.a.	n.a.	n.a.	3.7	2.7-2588 (50)	ref[21]
North Atlantic and Arctic	8	26-136 (35)	n.d.-27 (2.3)	n.d.	n.d.-7 (2)	2-10 (3)	n.d.-0.09 (0.03)	n.d.	n.d.-0.06 (0.02)	n.a.		29-180 (48)	ref[22]
North Atlantic Ocean	9	n.d.-1230 (50)	n.d.-1310 (770)	n.d.-425 (80)	5-380 (40)	10-1700 (90)	n.d.-50 (10)	n.a.	60-490 (140)	n.a.	~800	700-3930 (2200)	ref[11]
South Atlantic	9	10-540 (150)	20-980 (570)	n.d.-540 (130)	30-280 (100)	120-1180 (330)	n.d.-25 (10)	n.a.	50-890 (160)	n.a.	~500	870-4310 (1820)	ref[11]
Bohai and Yellow Seas	9	14-94 (28)	19-390 (66)	0.75-13 (4.6)	2.3-95 (12)	1.2-14 (4.6)	1.4-15 (2.8)	0.04-0.3 (0.1)	n.d.-8.5 (1.8)	n.d.-26		45-520 (150)	This study
North Huangcheng Island	9	0.4-1000 (63)	0.1-160 (26)	n.d.-80 (3.8)	1-164 (24)	n.d.-1100 (8.2)	n.d.-110 (11)	0.01-2.4 (0.16)	1-180 (1.5)	n.d.-18 (0.35)		5-1500 (170)	This study

[*] Median values are given in brackets; n = number of analyzed OPEs; n.d. = not detected; n.a. = not analyzed; [a] The ranges and median values were from the source document (Table S5 of ref [12]); [b] Calculated arithmetic mean of median values in different areas of Mediterranean Sea (Table S4 of ref [15]); [c] Arithmetic mean values calculated from source document (Table 1 of ref [16]); [d] Calculated mean of the 50% percentiles of different areas of Great Lakes (Table 1 of ref[17]); [e] The values were from the source document (Table A2 of ref[20])

Table S12. Comparison of gaseous OPE concentrations (pg/m^3) in different open seas and remote areas[*]

Location	**n**	**TCEP**	**TCPP**	**TDCP**	**TiBP**	**TnBP**	**TPhP**	**TPeP**	**TEHP**	**TCP**	**Other OPEs**	**∑OPE**	**Ref**
North Sea[a]	8	n.d.-76 (n.d.)	n.d.-180 (12)	n.d.	n.d.-20	n.d.	n.d.-140	n.a.	n.d.-9	n.a.	n.d.-50	n.d.-225 (54)	ref[12]
North Atlantic and Arctic	8	4-92 (10)	0.8-55 (1.9)	n.d.-0.06 (n.d.)	0.3-7.5 (1.7)	n.d.-8.8 (1.4)	0.01-1.5 (0.017)	n.d.-0.02 (0.001)	n.d.-0.6 (n.d.)	n.a.		7-163 (17)	ref[22]
Bohai and Yellow Seas	9	n.d.-73 (38)	n.d.-130 (42)	n.d.-4.3 (0.57)	0.3-170 (30)	0.46-36 (8.0)	0.19-4.7 (1.7)	0.03-1.2 (0.27)	n.d.-5.3 (1.0)	n.d.-5.2 (1.6)		2.3-270 (170)	This study
North Huangcheng Island	9	0.69-120 (10)	0.2-26 (3.2)	n.d.-2.6 (n.d.)	n.d.-82 (4.8)	n.d.-190 (2.7)	0.17-22 (2.7)	n.d.-0.41 (0.03)	n.d.-30 (1.1)	n.d.-7.1 (n.d.)		1.2-360 (31)	This study

[*] Median values are given in brackets; n = number of analyzed OPEs; [a] The ranges and median values were from the source document (Table S5 of ref [12])

Table S13. Abundance patterns of OPEs in different open seas and remote areas

	Concentration (pg/m^3)								Percentrage of total seven OPEs								
	Cl-OPEs			Non-Cl-OPEs				Total	Cl-OPEs			Non-Cl-OPEs				Total	
Areas	**TCEP**	**TCPP**	**TDCP**	**TiBP**	**TnBP**	**TEHP**	**TPhP**	**∑OPEs**	**TCEP**	**TCPP**	**TDCP**	**TiBP**	**TnBP**	**TEHP**	**TPhP**	**∑Cl-OPEs**	**∑non-Cl-OPEs**
North Sea	26	185	n.d.	32	22	7	17	289	9.0%	64%	0.0%	11%	7.6%	2.4%	5.9%	73%	27%
Sea of Japan	1120	375	34	37	22	22	61	1671	67%	22%	2.0%	2.2%	1.3%	1.3%	3.7%	92%	8.5%
Northern Pacific Ocean (2012)	204	160	5	17	11	2	19	418	49%	38%	1.2%	4.1%	2.6%	0.5%	4.5%	88%	12%
Northern Pacific Ocean (2016)	80	640	90	30	170	110	10	1130	7.1%	57%	8.0%	2.7%	15%	10%	0.9%	72%	28%
Philippine Sea	77	74	80	16	14	12	17	290	27%	26%	28%	5.5%	4.8%	4.1%	5.9%	80%	20%
Arctic Ocean	289	281	n.d.	25	11	1	19	626	46%	45%	0.0%	4.0%	1.8%	0.2%	3.0%	91%	8.9%
Mediterranean Sea	138	700	58	109	238	136	14	1393	10%	50%	4.2%	7.8%	17%	10%	1.0%	64%	36%
Black Sea	492	820	86	150	310	175	35	2068	24%	40%	4.2%	7.3%	15%	8.5%	1.7%	68%	32%
Great Lakes 2014	93	345	154	n.a.	148	28	103	871	11%	40%	18%	-	17%	3.2%	12%	68%	32%
Great Lakes 2016	193	173	36	n.a.	110	n.a.	76	588	33%	29%	6.1%	-	19%	-	13%	68%	32%
Longyearbyen	15	57	10	n.a.	56	9	17	164	9%	35%	6.1%	-	34%	5.5%	10%	50%	50%
South China Sea	43	25	2.2	2.1	2.5	3.6	6.2	85	51%	30%	2.6%	2.5%	3.0%	4.3%	7.3%	83%	17%
Canadian Arctic (ship-based)	128	55	1.7	n.a.	2.3	n.d.	4.7	192	67%	29%	0.9%	-	1.2%	0.0%	2.5%	96%	3.7%
North Atlantic and Arctic	35	2.3	n.d.	2	3	0.03	0.02	42	83%	5.4%	0.0%	4.7%	7.1%	0.07%	0.05%	88%	11.9%
North Atlantic Ocean	50	770	80	40	90	140	10	1180	4.2%	65%	6.8%	3.4%	7.6%	12%	0.8%	76%	24%
Bohai & Yellow Seas	28	66	4.6	12	4.6	1.8	2.8	120	23%	55%	3.8%	10%	3.8%	1.5%	2.3%	82%	18%
Indian Ocean (2012)	223	251	52	31	27	20	26	630	35%	40%	8.3%	4.9%	4.3%	3.2%	4.1%	83%	17%
Indian Ocean (2016)	100	370	20	40	230	180	8	948	11%	39%	2.1%	4.2%	24%	19%	0.8%	52%	48%
Southern Ocean	74	55	80	16	14	7	19	265	28%	21%	30%	6.0%	5%	3%	7.2%	79%	21%
South Atlantic	150	570	130	100	330	160	10	1450	10%	39%	9.0%	6.9%	23%	11%	0.7%	59%	41%
South Pacific	140	530	60	50	200	160	4	1144	12%	46%	5.2%	4.4%	17%	14%	0.3%	64%	36%
min	15	2.3	n.d.	2.0	2.3	n.d.	0.02	42	4.2%	5.4%	0.0%	2.2%	1.2%	0.0%	0.05%	50%	3.7%
max	1120	820	154	150	330	180	103	2068	83%	65%	30%	11%	34%	19%	13%	96%	50%
mean	176	310	55	42	96	62	23	741	29%	39%	6.9%	5.4%	11%	5.6%	4.2%	75%	25%
median	100	251	55	31	27	20	17	626	24%	39%	4.2%	4.7%	7.6%	3.7%	3.0%	76%	24%
SD	243	265	45	41	109	72	26	585	23%	15%	8.4%	2.5%	9.1%	5.4%	3.9%	13%	13%

Table S14. Regression parameters for gaseous OPE concentrations (C_g) and 1/T (K^{-1})[a]

OPEs	n	r	r^2	p value	B	A	Outlier (1/T, C_g)[b]
TCPP	78	-0.62	0.39	<0.001	81.85	-21999.17	A31 (0.0034. 25.45) A45 (0.00348. 26.12) A75 (0.00361. 21.72)
TCEP	80	-0.64	0.41	<0.001	232.94	-62917.55	A75 (0.00361. 121.39)
TDCP	28	0.29	0.09	0.13	-7.39	2453.86	
TiBP	79	-0.53	0.28	<0.001	131.24	-35449.68	A43 (0.00345. 81.23)
TnBP	71	-0.28	0.08	0.02	124.79	-33479.68	A43 (0.00345. 193.94) A9 (0.00342. 129.86)
TPeP	58	-0.04	0.001	0.79	0.11	-16.26	A44 (0.00347. 0.41) A42 (0.00344. 0.30)
TPhP	80	-0.67	0.45	<0.001	77.70	-21019.46	A31 (0.0034. 22.49)
TEHP	75	-0.50	0.25	<0.001	31.69	-8569.27	A31 (0.0034. 30.43) A48 (0.00356. 23.25)
TCP	27	0.12	0.01	0.55	-8.37	2954.89	
∑OPEs	79	-0.63	0.40	<0.001	752.70	-203425.69	A43 (0.00345. 355) A75 (0.00361. 180)

n: number of samples that included. B: intercept values of the regression. A: slope values of the regression. [a]Only gaseous OPE detectable samples were included. [b]The samples that had quite high C_g values (first three highest levles) and had influence for the regressions, were excluded.

Table S15. Spearman's correlation between C_g and C_{TSP} and RH

OPEs	C_{TSP} (µg/m^3)			RH (%)		
	r	r^2	p	r	r^2	p
TCPP	-0,18	0,03	0,12	0,30	0,09	0,01
TCEP	-0,14	0,02	0,23	0,32	0,10	0,004
TiBP	-0,28	0,08	0,01	0,35	0,12	0,001
TnBP	-0,14	0,02	0,22	0,25	0,06	0,03
TPeP	-0,11	0,01	0,35	0,12	0,01	0,30
TPhP	-0,10	0,01	0,38	0,32	0,10	0,004
TEHP	-0,21	0,04	0,06	0,42	0,18	<0.001
∑OPEs	-0,20	0,04	0,08	0,34	0,12	0,002

Table S16. Spearman's correlation between particle-bound OPE concentration (C_p) and C_{TSP}, T and RH

OPEs	C_{TSP} (µg/m^3)			T (°C)			RH (%)		
	r	r^2	p	r	r^2	p	r	r^2	p
TCPP	-0.17	0.03	0.14	0.22	0.05	0.05	0.17	0.03	0.12
TCEP	0.03	0.009	0.79	0.02	<0.001	0.89	0.13	0.02	0.27
TiBP	-0.19	0.04	0.09	0.34	0.11	0.002	0.25	0.06	0.03
TnBP	0.003	<0.001	0.98	<0.001	<0.001	1.00	0.04	0.001	0.75
TPeP	-0.44	0.19	0.70	0.01	<0.001	0.94	0.03	0.001	0.80
TPhP	0.16	0.03	0.16	-0.39	0.15	<0.001	-0.16	0.02	0.16
TEHP	0.21	0.05	0.06	-0.49	0.24	<0.001	-0.26	0.07	0.02
∑OPEs	0.02	0.00	0.88	0.02	<0.001	0.88	0.11	0.01	0.34

Table S17. Spearman's correlation between particle-bound OPE fractions and C_{TSP}, T and RH

OPEs	**C_{TSP}** (μg/m^3)			**T (°C)**			**RH (%)**		
	r	**r^2**	**p**	**r**	**r^2**	**p**	**r**	**r^2**	**p**
TCPP	0.34	0.12	0.002	-0.26	0.07	0.02	-0.26	0.07	0.02
TCEP	0.41	0.17	<0.001	-0.64	0.41	<0.001	-0.53	0.28	<0.001
TiBP	0.34	0.11	0.002	-0.59	0.34	<0.001	-0.48	0.23	<0.001
TnBP	0.40	0.16	<0.001	-0.49	0.28	<0.001	-0.30	0.09	0.008
TPeP	0.009	<0.001	0.94	-0.39	0.15	<0.001	-0.28	0.08	0.02
TPhP	0.49	0.24	<0.001	-0.76	0.58	<0.001	-0.55	0.30	<0.001
TEHP	0.37	0.14	0.001	-0.77	0.59	<0.001	-0.57	0.32	<0.001
∑OPEs	0.45	0.20	<0.001	-0.62	0.38	<0.001	-0.52	0.27	<0.001

Table S18. Regression of $logK_p$ and 1/T (K^{-1})[a]

OPEs	n	r	r^2	p	B	A	Outliers (1/T, $logK_p$)[b]
TCPP	79	0.12	0.01	0.29	-2.45	445.66	
TCEP	78	0.63	0.40	<0.001	-9.14	2365.75	A75 (0.003607, -2.27)
TDCP	26	-0.07	0.004	0.75	0.30	-392.41	
TiBP	78	0.29	0.08	0.01	-4.05	872.96	
TnBP	71	0.23	0.05	0.049	-4.88	1033.12	
TPeP	59	-0.21	0.04	0.11	2.44	-1035.89	
TPhP	78	0.83	0.69	<0.001	-16.02	4295.42	A75 (0.003607, -2.39)
TEHP	72	0.74	0.55	<0.001	-21.25	5664.71	
TCP	11	0.05	0.002	0.89	-3.01	313.56	

[a]Only samples that OPE detectable in both gaseous and particulate phases were included. [b]The samples that had quite high $logK_p$ values, and had influence for the regressions were excluded.

Table S19. Samples that were found significant regression correlations between corresponding $logK_p$ and $logP_L^{\circ}$[a]

Sample	**r**	**r^2**	**p**	**B**	**A**	**n**	**Excluded OPEs[a]**
A5	0.76	0.57	0.03	-0.68	0.20	8	TCP
A9	0.85	0.72	0.02	-0.75	0.26	7	TDCP, TCP
A13	0.76	0.58	0.046	-0.73	0.14	7	TDCP, TCP
A17	0.84	0.70	0.005	-0.60	0.30	9	
A19	0.82	0.67	0.02	-0.80	0.22	8	TDCP, TCP
A24	0.80	0.64	0.03	-0.38	0.31	7	TDCP, TCP
A33	0.88	0.78	0.004	-0.54	0.24	8	TCP
A49	0.80	0.64	0.03	-0.04	0.32	7	TDCP, TCP
A56	0.91	0.82	0.005	-1.34	-0.29	7	TDCP, TCP
A58	0.94	0.89	0.005	-1.43	-0.27	6	TPeP, TDCP, TCP
A59	0.87	0.76	0.01	-1.68	-0.18	7	TDCP, TCP
A69	0.87	0.76	0.03	-1.64	-0.21	6	TPeP, TDCP, TCP
A71	0.96	0.92	0.04	-0.79	-0.16	4	TnBP, TPeP, TEHP, TDCP, TCP
A80	0.91	0.83	0.004	-1.00	-0.13	7	TDCP, TCP

B: intercept values of the regression. A: slope values of the regression. n: The number of OPEs that used for the regression.
[a]Only OPEs that OPE detectable in both gaseous and particulate phases were included.

Table S20. The Spearson's correlation of predicted particle-bound fractions and measured values of OPEs, and median ratio of measured to predicted fraction φ_m/φ_p.

OPEs	Modle	r	r^2	p	B	A	φ_m/φ_p
TCEP	J-P	0,56	0,31	<0.001	-0,01	0,02	543
	koa	0,48	0,23	<0.001	-0,02	0,04	162
TPhP	J-P	0,53	0,28	<0.001	-0,17	0,56	5.0
	koa	0,72	0,51	<0.001	-0,31	0,74	5.0
TEHP	J-P	0,78	0,61	<0.001	0,35	0,54	0.94
	koa	0,77	0,59	<0.001	0,13	0,75	1.04

B: intercept values of the regression. A: slope values of the regression. φ_m/φ_p: The ratio of measured to predicted particle-bound fractions of OPEs.

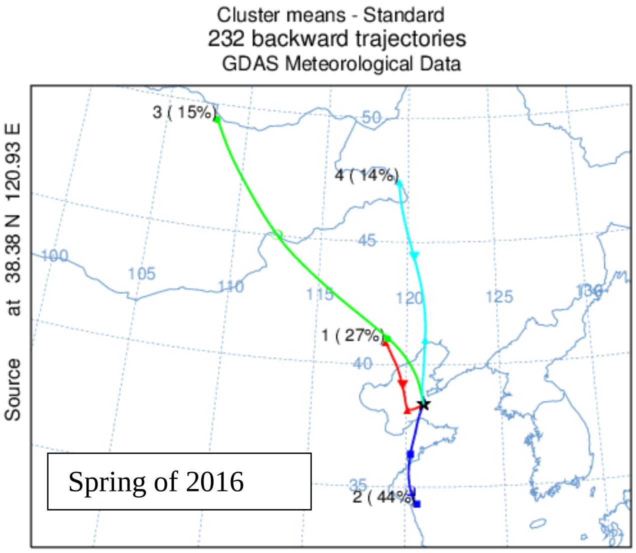

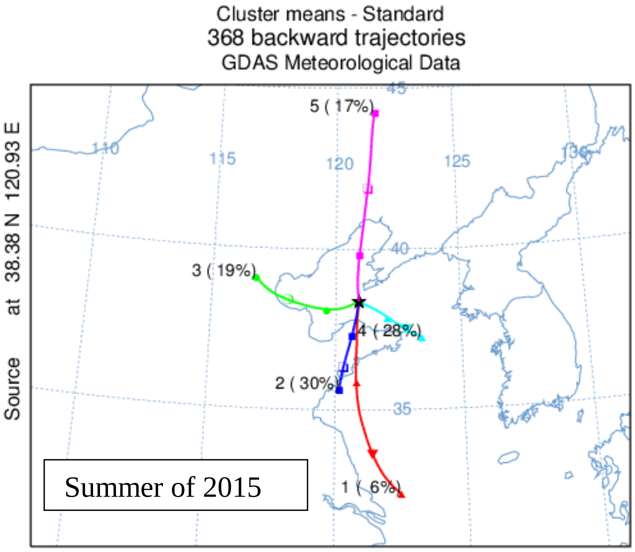

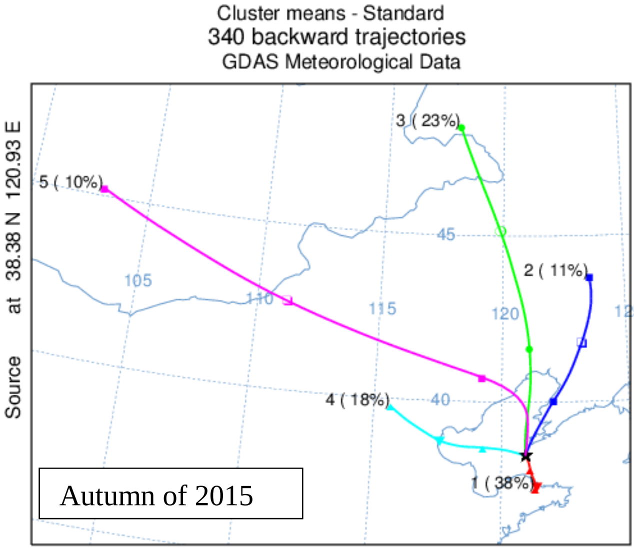

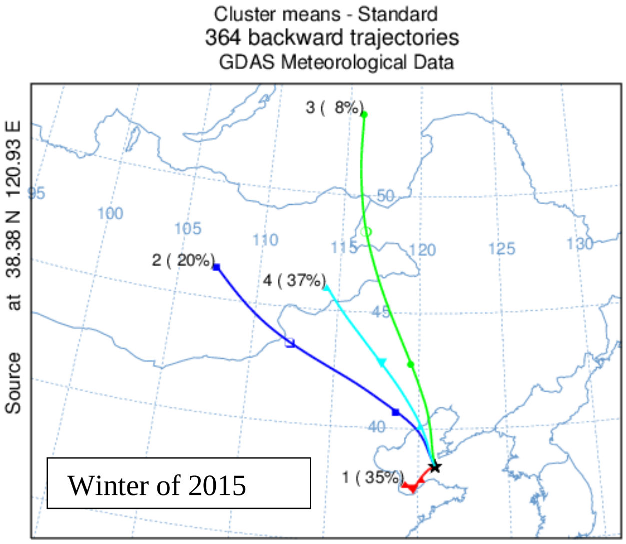

Figure S1. Four seasons' cluster-mean trajectories on North Huangcheng Island

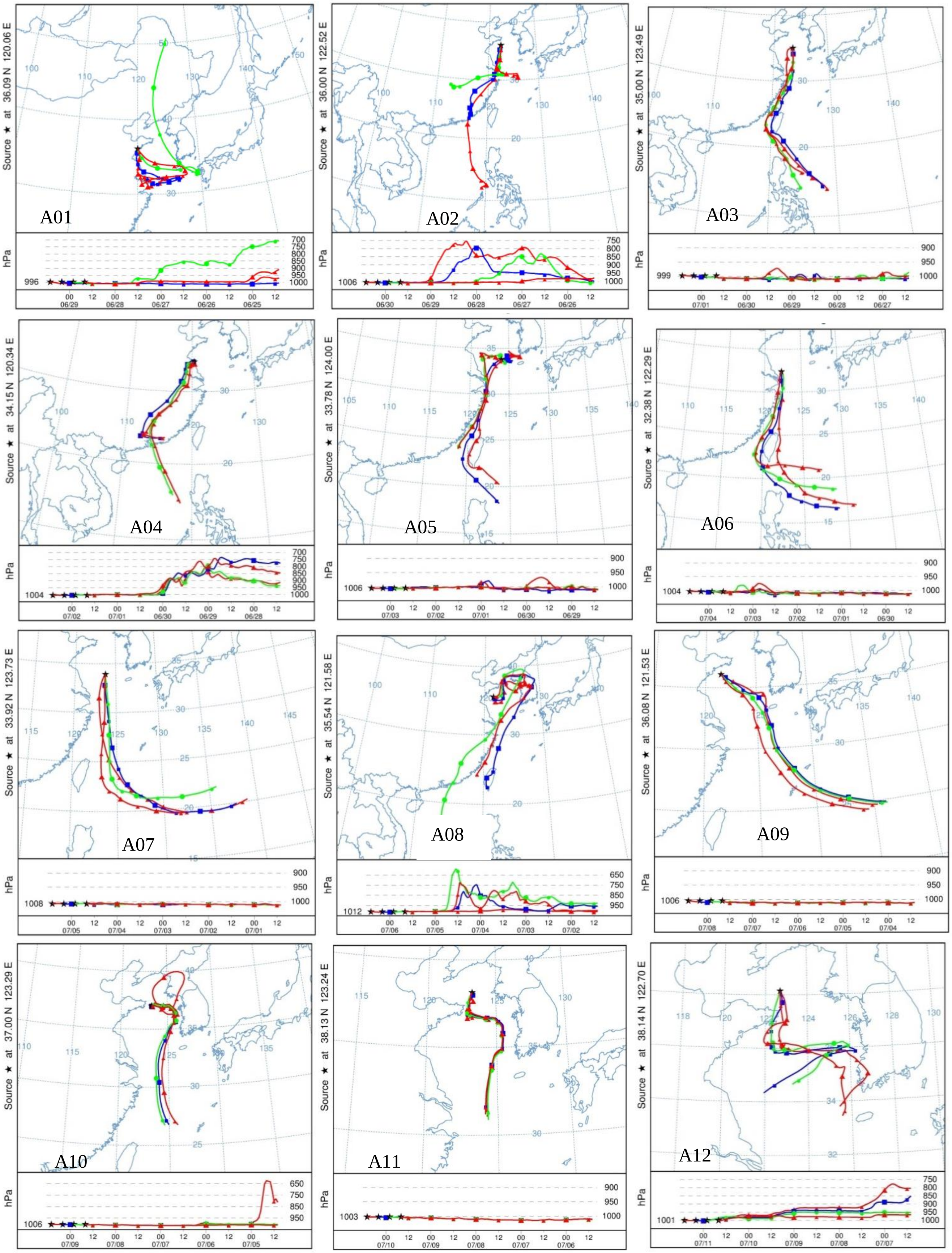

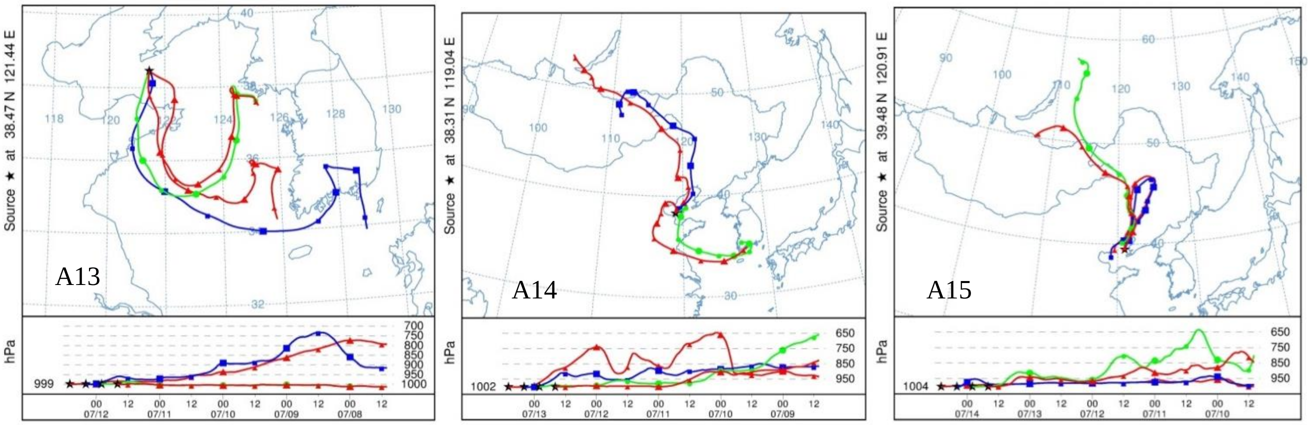

Figure S2. 120 h air mass back trajectories (6 h steps) for cruise sampling.

(The start points of each sampling are used as the sample stations)

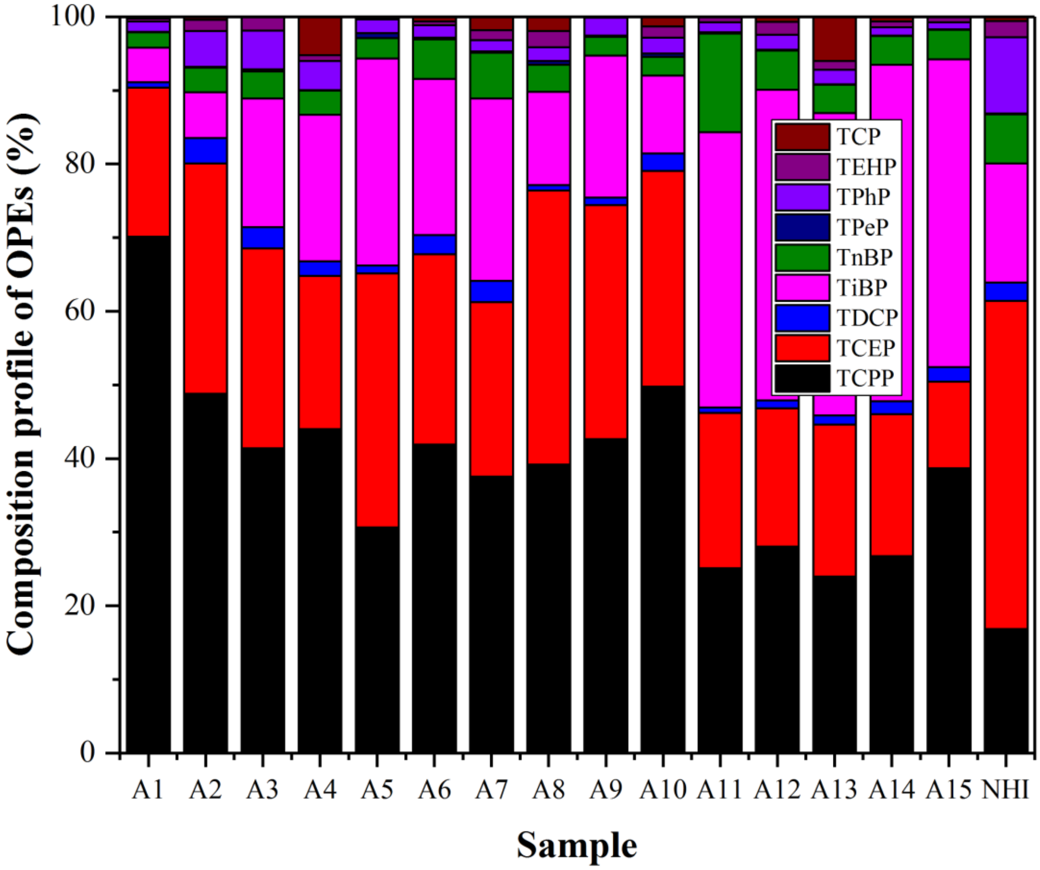

Figure S3. Composition profiles of selected OPEs in air of Bohai and Yellow Seas and North Huangcheng Island (On NHI: using median OPE concentrations)

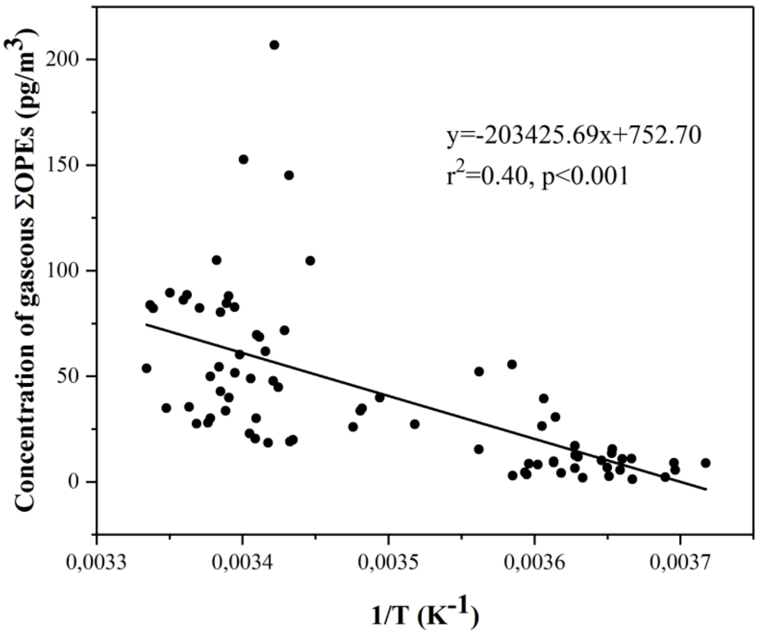

Figure S4. Linear correlations between gaseous OPE concentrations and 1/T for ∑OPEs

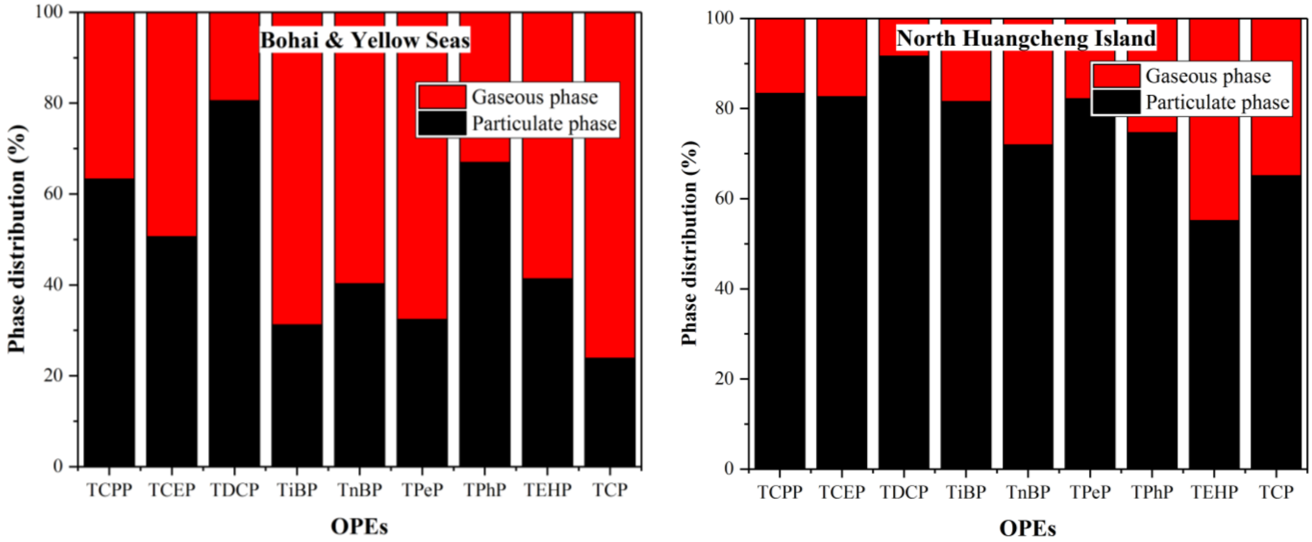

Figure S5. Phase distribution of OPEs in air of Bohai and Yellow Seas and North Huangcheng Island

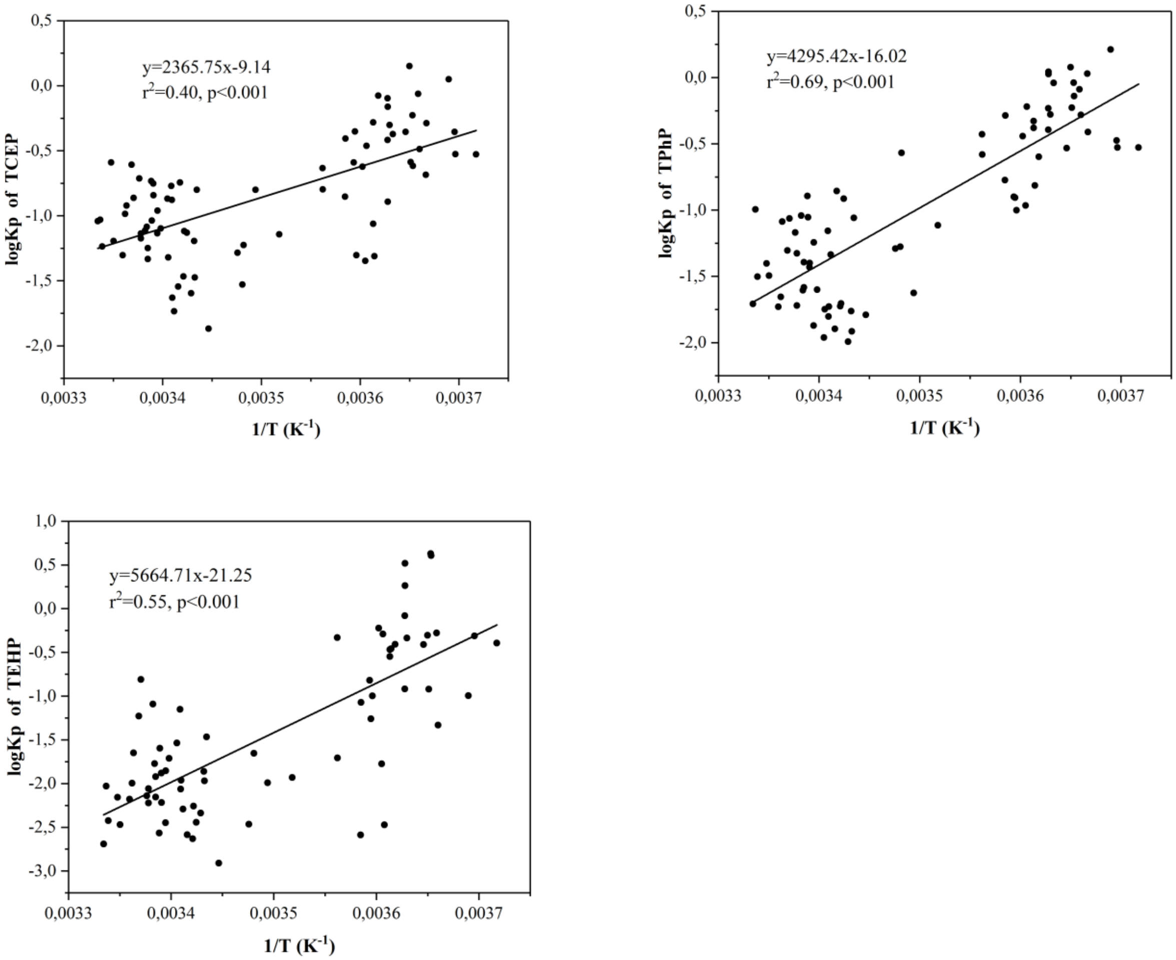

Figure S6. Linear correlations between $logK_p$ and 1/T for TCEP, TPhP and TEHP

Text S1. Instrumental analysis method

An Agilent 7890A gas chromatograph coupled to an Agilent 7010A Triple Quadrupole mass spectrometer (GC-MS/MS) and equipped with a programmed temperature vaporizer (PTV) injector (Agilent, USA) was used for analysis. The MS transfer line and the high sensitivity electron impact ionization source (HSEI) were held at 280 °C and 230 °C, respectively. The MS/MS was operated in Multiple Reaction Monitoring (MRM) mode. The collision cell gases were nitrogen (1.5 mL/min) and helium (2.25 mL/min). Analyses were separated on a HP-5MS Ultra Inert capillary column (30 m × 0.25 mm i.d. × 0.25 μm film thicknesses, J&W Scientific and Agilent Technologies, CA). One microliter of the sample was injected in the pulsed splitless mode with an inlet temperature program held at 50 °C for 0.2 min, increased to 300 °C at 300°C/min and then held for 20 min. High purity helium (99.999%) was used as the carrier gas. The GC oven temperature was held at 50 °C for 2 min, increased to 80 °C at 20 °C /min, then increased to 250 °C at 5 °C/min, finally increased to 300 °C at 15 °C/min, and held for 10 min. Selected ions for quantification and quantitation are listed in Table S7. MassHunter quantitative analysis software (version B06.00, Agilent Technologies, USA) was used for data processing.

Text S2. The calculation methods of the gas/particle partitioning of OPEs

Koa-based absorption model

K_{OA} is used for describing K_P with the assumption that absorption is the dominant distribution process.[23] The relationship between K_P and K_{OA} is:

$$K_P = f_{OM}\frac{\xi_{OCT}}{\xi_{OM}}\frac{MW_{OCT}}{\rho_{oct}MW_{OM}10^{12}}K_{OA}$$

where f_{OM} is the fraction of organic matter (OM) phase in the aerosol, MW_{OCT} and MW_{OM} are the mean molecular weight of octanol and OM, ξ_{OCT} and ξ_{OM} are activity coefficients of the absorbing compound in octanol and OM, ρ_{OCT} is the density of octanol (0.82 kg/ L at 20 °C) and the 10^{12} factor converts the units of the right side of the equation from L/kg to m^3/mg. With the assumptions of $MW_{OCT}/MW_{OM} = 1$ and $\xi_{OCT}/\xi_{OM} = 1$, then the equation can be simplified as:

$$\log K_P = \log K_{OA} + \log f_{OM} - 11.9$$

References

1. Wang, Q.; Zhao, H.; Wang, Y.; Xie, Q.; Chen, J.; Quan, X., Determination and prediction of octanol-air partition coefficients for organophosphate flame retardants. *Ecotoxicol. Environ. Saf.* **2017,** *145*, 283-288.
2. Brommer, S.; Jantunen, L. M.; Bidleman, T. F.; Harrad, S.; Diamond, M. L., Determination of Vapor Pressures for Organophosphate Esters. *J. Chem. Eng. Data* **2014,** *59*, (5), 1441-1447.
3. van den Eede, N.; Dirtu, A. C.; Neels, H.; Covaci, A., Analytical developments and preliminary assessment of human exposure to organophosphate flame retardants from indoor dust. *Environ. Int.* **2011,** *37*, (2), 454-461.
4. Ali, N.; Dirtu, A. C.; Van den Eede, N.; Goosey, E.; Harrad, S.; Neels, H.; t Mannetje, A.; Coakley, J.; Douwes, J.; Covaci, A., Occurrence of alternative flame retardants in indoor dust from New Zealand: indoor sources and human exposure assessment. *Chemosphere* **2012,** *88*, (11), 1276-82.
5. Van den Eede, N.; Dirtu, A. C.; Ali, N.; Neels, H.; Covaci, A., Multi-residue method for the determination of brominated and organophosphate flame retardants in indoor dust. *Talanta* **2012,** *89*, (Supplement C), 292-300.
6. Bergh, C.; Luongo, G.; Wise, S.; Ostman, C., Organophosphate and phthalate esters in standard reference material 2585 organic contaminants in house dust. *Anal. Bioanal. Chem.* **2012,** *402*, (1), 51-59.
7. Brandsma, S. H.; de Boer, J.; Cofino, W. P.; Covaci, A.; Leonards, P. E. G., Organophosphorus flame-retardant and plasticizer analysis, including recommendations from the first worldwide interlaboratory study. *Trac-Trends in Anal. Chem.* **2013,** *43*, 217-228.
8. Ionas, A. C.; Covaci, A., Simplifying multi-residue analysis of flame retardants in indoor dust. *Int. J. Environ. Anal. Chem.* **2013,** *93*, (10), 1074-1083.
9. Cristale, J.; Lacorte, S., Development and validation of a multiresidue method for the analysis of polybrominated diphenyl ethers, new brominated and organophosphorus flame retardants in sediment, sludge and dust. *J. Chromatogr. A* **2013,** *1305*, 267-75.
10. Fan, X.; Kubwabo, C.; Rasmussen, P. E.; Wu, F., Simultaneous determination of thirteen organophosphate esters in settled indoor house dust and a comparison between two sampling techniques. *Sci. Total Environ.* **2014,** *491-492*, 80-6.
11. Castro-Jimenez, J.; Gonzalez-Gaya, B.; Pizarro, M.; Casal, P.; Pizarro-Alvarez, C.; Dachs, J., Organophosphate Ester Flame Retardants and Plasticizers in the Global Oceanic Atmosphere. *Environ. Sci. Technol.* **2016,** *50*, (23), 12831-12839.
12. Möller, A.; Xie, Z. Y.; Caba, A.; Sturm, R.; Ebinghaus, R., Organophosphorus flame retardants and plasticizers in the atmosphere of the North Sea. *Environ. Pollut.* **2011,** *159*, (12), 3660-3665.

13. Möller, A.; Sturm, R.; Xie, Z. Y.; Cai, M. H.; He, J. F.; Ebinghaus, R., Organophosphorus Flame Retardants and Plasticizers in Airborne Particles over the Northern Pacific and Indian Ocean toward the Polar Regions: Evidence for Global Occurrence. *Environ. Sci. Technol.* **2012,** *46*, (6), 3127-3134.

14. Cheng, W. H.; Xie, Z. Q.; Blais, J. M.; Zhang, P. F.; Li, M.; Yang, C. Y.; Huang, W.; Ding, R.; Sun, L. G., Organophosphorus esters in the oceans and possible relation with ocean gyres. *Environ. Pollut.* **2013,** *180*, 159-164.

15. Castro-Jimenez, J.; Berrojalbiz, N.; Pizarro, M.; Dachs, J., Organophosphate Ester (OPE) Flame Retardants and Plasticizers in the Open Mediterranean and Black Seas Atmosphere. *Environ. Sci. Technol.* **2014,** *48*, (6), 3203-3209.

16. Salamova, A.; Ma, Y. N.; Venier, M.; Hites, R. A., High Levels of Organophosphate Flame Retardants in the Great Lakes Atmosphere. *Environ. Sci. Technol. Lett.* **2014,** *1*, (1), 8-14.

17. Salamova, A.; Peverly, A. A.; Venier, M.; Hites, R. A., Spatial and Temporal Trends of Particle Phase Organophosphate Ester Concentrations in the Atmosphere of the Great Lakes. *Environ. Sci. Technol.* **2016,** *50*, (24), 13249-13255.

18. Salamova, A.; Hermanson, M. H.; Hites, R. A., Organophosphate and Halogenated Flame Retardants in Atmospheric Particles from a European Arctic Site. *Environ. Sci. Technol.* **2014,** *48*, (11), 6133-6140.

19. Green, N.; Schlabach, M.; Bakke, T.; Brevik, E.; Dye, C.; Herzke, D.; Huber, S.; Plosz, B.; Remberger, M.; Schøyen, M., Screening of selected metals and new organic contaminants 2007. Norwegian Pollution Control Agency. **2008**.

20. Lai, S.; Xie, Z.; Song, T.; Tang, J.; Zhang, Y.; Mi, W.; Peng, J.; Zhao, Y.; Zou, S.; Ebinghaus, R., Occurrence and dry deposition of organophosphate esters in atmospheric particles over the northern South China Sea. *Chemosphere* **2015,** *127*, 195-200.

21. Sühring, R.; Diamond, M. L.; Scheringer, M.; Wong, F.; Pucko, M.; Stern, G.; Burt, A.; Hung, H.; Fellin, P.; Li, H.; Jantunen, L. M., Organophosphate Esters in Canadian Arctic Air: Occurrence, Levels and Trends. *Environ. Sci. Technol.* **2016,** *50*, (14), 7409-7415.

22. Li, J.; Xie, Z.; Mi, W.; Lai, S.; Tian, C.; Emeis, K.-C.; Ebinghaus, R., Organophosphate Esters in Air, Snow and Seawater in the North Atlantic and the Arctic. *Environ. Sci. Technol.* **2017,** *51*, 6887−6896.

23. Harner, T.; Bidleman, T. F., Octanol-air partition coefficient for describing particle/gas partitioning of aromatic compounds in urban air. *Environ. Sci. Technol.* **1998,** *32*, (10), 1494-1502.

Paper III

Global gridded emissions and atmospheric transport of tris-(1-chloro-2-propyl) phosphate (TCPP)

Global gridded emissions and atmospheric transport of tris-(1-chloro-2-propyl) phosphate (TCPP)

Jing Li[†,⊥], Fangyuan Zhao[‡], Zhiyong Xie[†*], Ralf Ebinghaus[†], Kay-Christian Emeis[†], Chongguo Tian[§], Matthew MacLeod[‡*]

[†]Helmholtz-Zentrum Geesthacht, Centre for Materials and Coastal Research, Institute of Coastal Research, Geesthacht, 21502, Germany

[‡]Department of Environmental Science and Analytical Chemistry, ACES, Stockholm University, Svante Arrhenius väg 8, Stockholm, SE-114 18, Sweden

[§]Key Laboratory of Coastal Environmental Processes and Ecological Remediation, Yantai Institute of Coastal Zone Research, CAS, Yantai, 264003, China

[⊥]Universität Hamburg, Department of Geosciences, Hamburg, 20144, Germany

ABSTRACT

Tris-(1-chloro-2-propyl) phosphate (TCPP) is a high-production volume chemical that is widely used as a flame retardant. It has been frequently detected in air and water globally, including in remote areas. In this study we seek to characterize and constrain uncertainties in global source-to-concentration relationships for TCPP using global transport modeling. We present gridded global emission estimates to air and water that are initially based on the assumption that emissions are directly proportional to the intensity of nighttime artificial light emitted to space from Earth. Then, we update the initial emission rate by comparing measured concentrations of TCPP with predictions from the Berkeley-Trent Global Contaminant Fate Model (BETR-Global). Our updated global gridded emission rate thus combines information from measurements in air and water with modeling of global transport. Thirty-six scenarios that represent combinations of different degradation half-lives of TCPP in air ($t_{1/2,\mathrm{Air}}$: 12, 60, 300 h) and in water ($t_{1/2,\mathrm{Water}}$: 1,440, 3,600, 7,200, 36,000 h), as well as a range of direct-to-water emission factors (E_{W}: 0, 0.5 and 1 times emission to air (E_{A})) were tested in this study. Modeled concentrations of TCPP in the global environment are compared to a database of 129 measurements in air and 22 measurements in ocean water that we assembled from the literature. A separate and independent model, the Canadian Model for Environmental Transport of Organochlorine Pesticides (CanMETOP) is used for cross-validating selected scenarios for TCPP properties and emissions. Correlation coefficients between modeled and measured concentrations (r^2) range between 0.45 and 0.50 in different scenarios, indicating that the model scenarios account for up to 50% of the variability in measured concentrations of TCPP. Our updated global emission scenarios for TCPP have total emissions to air and water between 12.0 and 157 kt/y (1 kt/y=1Gg/y). Among the emission source regions, Europe (38%), North America (24%) and East Asia (13%) release

most TCPP into the global environment in the updated emission scenarios. The model scenario with TCPP degradation half-lives in air and water of 12 h and 3,600 h, respectively, and updated global emissions to air and water of 78.6 kt/y and 39.3 kt/y, respectively, provides good agreement with measurements (r^2=0.48 and 0.46, RMSE=0.95 and 0.81 for model-measurement comparisons of atmospheric and oceanic data respectively), and is suggested as a useful base case reference scenario.

INTRODUCTION

Tris-(1-chloro-2-propyl) phosphate (TCPP) belongs to a family of organophosphate flame retardants (OPEs) that are widely used to reduce the flammability of products and to delay the spread of fire after ignition.[1] TCPP is applied as an additive flame retardant to many industrial products, and is released to the environment through leaching, volatilization and abrasion.[1] As a consequence, TCPP is present in the environment in both air and water.[2-8] TCPP has been measured in remote areas, which is strong evidence that it has potential to undergo long-range transport in the atmosphere.[7-10] However, the atmospheric lifetime of TCPP is highly uncertain, with estimates ranging from 0.5~20 days.[11]

The use of TCPP throughout the world has drastically increased, along with the use of other OPE flame retardants, in response to restrictions on the use of polybrominated diphenyl ethers (PBDEs).[12, 13] In 2013, the consumption of OPEs accounted for approximately 19% of global flame retardant usage, which is comparable to the global usage of all brominated flame retardants (21%).[14] In Europe, the consumption of TCPP accounted for ~50% of total OPE usage around the year 2000, and is thought to have been stable or increased since then.[15] The high use rate and stable or increasing trend reflects the replacement of tris(2-chloroethyl) phosphate (TCEP) by TCPP in Europe due to human health concerns associated with TCEP.[16] Concentrations of TCPP in the atmosphere that are 1-2 orders of magnitude higher than those of PBDEs that they replaced have been reported,[10, 13] highlighting the importance of understanding TCPP as an environmental contaminant.

Emission estimates for TCPP are essential for risk assessment and to provide a baseline to measure future trends, either increases due to further expansion of usage or declines due to possible future regulation.[17, 18] However, at present emission estimates for TCPP are sparse: the European Union (EU) risk assessment reports estimated TCPP emission from the EU area to be 89.56 kg/d (32.69 t/y) in 2000.[15] TCPP emission from the city of Toronto calculated from inverse modeling of concentrations in the atmosphere ranged between 0.17~4.3 t/y (mean: 0.69 t/y).[19] To our knowledge, there are no other scientific studies reporting TCPP emissions.

There are two methods that are commonly used to estimate emissions of industrial chemicals like TCPP that have wide uses in materials and products. The first is a bottom-up method, in which emissions are estimated from data on chemical production and consumption and estimated emission factors. This method requires knowledge of the production and consumption volumes of the target compounds, which are often not easily accessible. TCPP is a relatively new flame-retardant that is globally and widely used. The lack of information on consumption particularly limits the utility of this method for emission estimates of TCPP. The second method combines field measurements of concentrations and inverse chemical fate modeling to calculate emissions, which we call a top-down approach.[19, 20] Gasic et al. demonstrated the top-down approach at the urban scale to estimate emissions of polychlorinated biphenyls (PCBs) in Zurich, Switzerland, using a multimedia mass balance model.[21, 22] That method has also been employed for many other semi-volatile industrial chemicals in urban areas worldwide.[19, 20, 23, 24] Schenker et al. applied a refined version of the top-down approach at the global scale for dichlorodiphenyltrichloroethane (DDT) by using Bayesian updating to update an initial estimate of emissions, along with other model parameters.[25]

In this study, we report on top-down emission rate estimate for TCPP using model updating at the global scale, constrained by measured concentrations of TCPP in the atmosphere and surface ocean. The model-data comparison is also used to examine different scenarios for TCPP degradation rates and ratios of emissions to air and seawater. Compared to Schenker et al.'s work on DDT, we use a simpler emission rate updating method, but a more detailed coupled atmospheric and oceanic transport model than the CliMoChem model employed in that study.

MATERIALS AND METHODS

The Berkeley-Trent Global Contaminant Fate Model (BETR-Global) is used as the long-range transport (LRT) model for emission rate updating.[26, 27] A separate and independent model, the Canadian Model for Environmental Transport of Organochlorine Pesticides (CanMETOP) is adopted for cross-validating selected scenarios for TCPP degradation rates and emission factors.[28, 29]

BETR-Global is a contaminant fate and transport model at the global scale.[26, 27] It divides the globe into grid cells, and chemical fate in each grid cell is described using a multimedia model, with adjacent cells linked by flows of air and water. The multimedia model cells consist of seven compartments: upper atmosphere, lower atmosphere, vegetation, freshwater, soil, ocean and freshwater sediments. In this study, we applied the BETR-Research implementation of BETR-Global in the Python programming language (http://betrs.sourceforge.net). It has three different spatial resolutions: low (15° × 15° grid cells), intermediate (7.5° × 7.5° grid cells) and high (3.75° × 3.75° grid cells). In this work, the high spatial resolution is used to describe the fate and transport of TCPP.

Initial emission rate estimate and updating

Our updating approach to estimate emissions requires an initial global emission field gridded at 3.75° × 3.75° to drive the BETR Global model. Then, this initial emission rate field is updated to optimize agreement between measured and modeled concentrations. The global consumption of OPEs was 370 kt according to a report from Zhang et al. in 2013.[14] The EU risk report pointed out that in Europe, approximately fifty percent of OPEs consumed in the year 2000 was TCPP.[15] We extrapolated this percentage to the global area to arrive at an initial estimate that 185 kt of TCPP was used in 2013 globally. Then, we further assumed total emissions to the atmosphere of 20 kt/y (emission rate into air: E_A) as the initial emission estimate for the LRT model, based on an assumed emission factor of 10% for TCPP.

In order to distribute the initial total global emission estimate into a gridded global model, we assumed that emissions are proportional to nighttime artificial light intensities, as has been applied in earlier sudies.[26, 30-33] We updated the nighttime light intensity map adopted in earlier work with BETR Global using the dimensionless nighttime light index from the Defense Meteorological Satellite Program/Operational Linescan System (DMSP/OLS) for the year 2010.[34] Then we allocated the initial global estimate of TCPP emissions proportional to the nighttime light index data, which were upscaled from 1km resolution in the original dataset to the 3.75° × 3.75° resolution of the BETR Global model. The gridded emission estimates were then used as input into the lower air layer of the BETR model.

For the water phase, a range of direct-to-water emission factors were assumed in this study for low, medium and high emission scenarios with emission rate into water (E_W) set as 0, $0.5E_A$ and E_A.

Physical-chemical properties of TCPP

The air/water partition ratio of TCPP (K_{AW}) was calculated from measured solubility and vapor pressure (VP). Cuthbert et al. reported that the solubility of TCPP in pure water is 1,080 mg/L at 20 °C, which was also adopted by the EU risk report.[15, 35] The solubility at 25 °C (1,160 mg/L) was calculated based on the European Union System for the Evaluation of Substances (EUSES v2.1.2) adjustments of the temperature dependence of solubility.[36] The VP of TCPP is 0.035 Pa at 25 °C.[37] Then the derived Henry's Law Constant (HLC) and log K_{AW} are 0.0099 (Pa·m^3/mol) and -5.4, respectively. The n-octanol/water partition ratio (K_{OW})

also originated from Cuthbert et al. (log K_{OW} =2.7).[35] The n-octanol/air partition ratio (K_{OA}) was calculated from K_{AW} and K_{OW} to be log K_{OA} = 8.1.

The estimated degradation half-life in air ($t_{1/2,Air}$) is 5.73 h using EPI suite 4.0, however Li et al. estimated that the lifetime of TCPP can vary from 0.5 to 20.2 days (namely 12 to 485 h) using quantum chemical calculations that consider the presence of atmospheric water.[11] In order to explore the effect of assuming different $t_{1/2,Air}$, three values (12, 60 and 300 h) were tested in this study. Similarly, different degradation half-lives in water ($t_{1/2,Water}$) were also selected with values of 1,440 , 7,200 and 36,000 h, where the 1,440 h $t_{1/2,Water}$ is sourced from EPI-suite 4.0. Three half-lives in each of soil ($t_{1/2,Soil}$), sediment ($t_{1/2,Sediment}$) and vegetation ($t_{1/2,Vegetation}$) were similarly defined based on EPI-suite estimates (see Table S1), and were co-varied in our model scenarios with $t_{1/2,Water}$. All physical/chemical properties of TCPP used as inputs to BETR Global are listed in Tables S1.

Model spin-up

The pollution of TCPP in environmental media is a long-term process. To simulate the accumulation of TCPP in different media, model spin-up was necessary.[38] We spun-up the model to pseudo steady-state conditions in which the TCPP levels become stable in consecutive years of the model simulation, before the concentrations of TCPP in air and water under the different scenarios were compared to observations.

Updating of emission estimates

The agreement between modeled and measured concentrations was analyzed using linear regression of paired logarithmic values. We calculated the bias between the model and measurements from the intercept of the regression and scaled all emissions by that factor, which exploits the property of the model that emission rate and concentrations are directly proportional to each other for a fixed geographical distribution of emissions.

Database of measured concentrations of TCPP

Measurements of TCPP in air and seawater from remote and rural areas were collected from the literature (Table S2-S3). Comparing measurements to remoteness index calculated using BETR Global assuming emissions proportional to night light emissions,[33] led to measurement data from two studies being excluded from further consideration in this study because they were clearly too high to be explained by global transport modeling (Table S2 and Figure S3; for more details see Text S1). The remaining measurements were averaged as geometric means within grid cells for the two models (BETR: 3.75°×3.75°; CanMETOP: 1°×1°). Thus, empirical measurement data in 129 atmospheric grid cells and 22 aqueous grid cells were used for comparison with output of the BETR model (Figure S1-S2), and data from 166 atmospheric grid cells were compared with the CanMETOP model. The sampling period ranges from 2006 to 2016 for atmospheric data and from 2010 to 2017 for aqueous data. The data were pooled without considering the season and year, since global observations collected all at the same time are not available.

RESULTS AND DISCUSSION

Emission into air

Based on initial exploratory model runs, we selected a set of 27 scenarios that cover all possible combinations of low, medium and high assumptions about $t_{1/2,\mathrm{Air}}$, $t_{1/2,\mathrm{Water}}$ and the rate of emissions to water (Table S4).

Significant correlations were found for all scenarios for both atmospheric (p<1.0E-19, r^2>0.48) and oceanic (p<1.5E-3, r^2>0.40) measured concentrations (Table S5-S8 and Figure S4-S9). Variability in TCPP levels in air in the different scenarios is dominated by variations in E_A and $t_{1/2,\mathrm{Air}}$, while variations of E_W and $t_{1/2,\mathrm{Water}}$ have negligible influence (Table S5-S8). This result indicates that atmospheric TCPP in remote regions is mainly present due to long-range atmospheric transport rather than transport in ocean water and subsequent volatilization. Our earlier study of OPE levels in the Atlantic and Arctic oceans hypothesized that there was volatilization of TCPP from seawater into the atmosphere.[8] The discrepancy results from the log K_{AW} value used in our previous study, which was taken from the SPARC On-Line Calculator estimate of a *HLC* value of 72.8 pa·m^3/mol, with the corresponding log K_{AW} being -1.5.[39] However, the experimental data from Cuthbert et al. for log K_{AW} is -5.4 [35] and in this study we prefer to use the experimentally determined data for log K_{AW}.

The updated estimates of E_A range from 12.5 to 79.4 kt/y and E_W in our scenarios ranges from 0.0 to 79.4 kt/y. According to the comparison between observed and modeled data and earlier quantum chemical modeling[11] , we suggest that $t_{1/2,Air}$ of 12 h is the most reasonable value. When $t_{1/2,Air}$ is prescribed at 12 h, the slope of the logarithm of modeled versus measured concentrations in scenario with E_W =0 and $t_{1/2,Water}$=1,440 h is most close to one (slope=0.990, Table S5). However, it is not realistic that no TCPP is directly released into the water phase with effluents. Therefore, the scenarios with E_W =0.5E_A or E_W=E_A are may be closer to reality. In these scenarios, the slope values are >1 for $t_{1/2,Water}$=1,440 h and <1 for $t_{1/2,Water}$=7,200 h scenarios (Table S5). According to this analysis, a value between 1,440 h and 7,200 h is a reasonable assumption for $t_{1/2,Water}$, since it provides a slope close to one, and has a positive influence on removing bias between measured and modeled concentrations in ocean water (Table S6-S7). Based on these considerations, new scenarios were designed with $t_{1/2,Water}$ set as 3,600 h, which is 2.5 times as long as the 1,440 h assumed initially (Table S9), and corresponding soil and sediment half-lifetime values adjusted accordingly (Table S9). The output of this new scenario assuming that E_W=0.5E_A and $t_{1/2,Air}$=12 h is in very good agreement with the measured concentrations both in air and ocean water phases, and is illustrated in Figure 1 (for other scenarios result see Figures S10-S11). For the water phase, the slope of the regression of the scenario is 0.972 and the intercept is 0.168, with r^2=0.458 and p=5.4E-4. The corresponding E_A is 78.6 kt/y and E_W is 39.3 kt/y, which in total yields global emissions of TCPP of 118 kt/y.

In summary, the proposed range of global TCPP emissions from land into the atmosphere is 12.5 to 79.4 kt/y and global emission to the ocean by rivers and diffuse runoff ranges between 0 to 79.4 kt/y. The total emission of TCPP into air and water in our updated scenarios thus ranges from 12.5 to 160 kt/y. Our "best estimate" of the global emission rate of TCPP from our model updated with the available observed concentrations is 118 kt/y (assuming that E_W=0.5E_A) and the $t_{1/2,\mathrm{Air}}$ and $t_{1/2,\mathrm{Water}}$ values in best agreement with observed concentrations are 12 h and 3,600 h, respectively. Our best estimate global emission rate of 118 kt/y is comparable to our initial estimate of total global production of TCPP, which was 185 kt/y. Our initial estimate of the production or consumption amounts of TCPP thus likely was an underestimate, and high uncertainty will persist until updated and more accurate TCPP usage information becomes available.

Cross validation with the CanMETOP model

In order to validate the suggested scenarios for TCPP emissions, the CanMETOP model was also applied in this study. The CanMETOP model is a three-dimensional dispersion model coupled with two-film models for air-water and air-snow/ice exchange and a fugacity-based mass balance model for soil-air exchange.[28] This model has been previously used to study the regional and global atmospheric transport of POPs.[28, 29] The model version used in this study is the same as that applied in the paper of Ma et al.[29] The model setup in this study covers the entire globe with a horizontal grid resolution of 1×1 latitude/longitude, 14 vertical levels in the atmosphere with the heights ranging from 0 m to 11,000 m. Because the process of ocean circulation is not included in CanMETOP model, the scenarios with E_W=0 are used for this model. The emission into air was input into layers 1 to 8 (0 to 1,200 m) in order to unify the emission input conditions with the BETR model (release into lower layer with an average height of 1,200 m). Three scenarios have been run using CanMETOP model with $t_{1/2,\mathrm{Water}}$=3,600 h and $t_{1/2,\mathrm{Air}}$ set as 12, 60 and 300 h, respectively. The measurements are merged into 1° × 1° grid cells and in total 166 concentration observations in air are adopted for validation. Results from the CanMETOP model also suggest that the best value of $t_{1/2,\mathrm{Air}}$ is 12 h based on consistency between the modeled and observed data (r^2=0.392, p=1.9E-19, slope=0.912 and intercept=-0.074). Compared to BETR model, the CanMETOP model is more sensitive to the $t_{1/2,\mathrm{Air}}$. Higher $t_{1/2,\mathrm{Air}}$ contribute to higher concentrations in remote regions, which flattens the slope of the regression lines (Figure S12).

Comparison of modeled and measured concentrations

Figures 3 and 4 show the spatial comparison of modeled and measured concentrations of TCPP in air and in water with our "best estimate" scenario, namely $t_{1/2,\mathrm{Air}}$=12 h, $t_{1/2,\mathrm{Water}}$=3,600 h, E_W=0.5E_A and total TCPP emissions to air and water of 118 kt/y. The modeled atmospheric data in the European Arctic are all in a range of 0.3 to 7.2 times the measured data except at a location in Ny-Ålesund, Norway, where the model is two orders of magnitude lower than measurements determined by passive sampling. In the Canadian Arctic, the modeled concentrations are all lower than observations except at one site and the median ratio is 0.2 (modeled/measured data). Over the Southern Ocean, the measured levels range from 0.1 to 3.9 pg/m^3 with the corresponding modeled range being 0.01 to 25.3 pg/m^3, and all the modeled data are lower than measurements with a median ratio of 0.2 (modeled/measured data) except at one location that is close to South America (Figure 3). The modeled concentrations over the seas surrounding China are one order of magnitude higher than measured data. Over the Great Lakes (three sites) and European continent (one site in the Czech Republic), as well as three sites from Philippine Sea to Australia (blue dots in Figure 3), the modeled data are one to two orders of magnitude higher than measurements.

In seawater, the modeled concentrations in the European Arctic are hundreds of pg/L, which are 1-10 times lower than the measurements by Li et al. and one order of magnitude higher than those from McDonough et al.[8, 40] This discrepancy may result from the water depth at which Li et al. took surface seawater samples (10 m), while McDonough et al. sampled deep seawater (>300m) and this study modeled the depth (in BETR Global) variance in different seasons. In the Canadian Arctic, the modeled data are 1-5 times lower than the observations. In the seawater of German Bight (North Sea), the modeled data are one order of magnitude higher than the measurements. In coastal seawater of the United States, data for only one site is available, with the detected values being five times higher than the modeled concentration. In Bohai and Yellow Seas (China), most of the modeled concentrations are higher than the observations (range: 2-30 times) except one site which is four times lower than the measurement.

In general, the root mean squared error (RMSE) values for paired observation/model atmospheric and oceanic data are 0.95 and 0.81, which means that 50% of modeled concentrations are within a factor of 8.9 and 6.5 of measurements, respectively. The simulated global seawater TCPP concentrations are validated on the available measurements in only five regions (Figure 4), which documents higher uncertainty in simulated ocean concentrations than in the atmosphere. More observations in seawater in other global regions would be particularly valuable to narrow down uncertainties in the future, such as those of the Aquatic Global Passive Sampling (AQUA-GAPS) network.[41] Nevertheless, the modeled spatial distribution of TCPP concentrations in seawater and atmosphere are meaningful and support better understanding the transport and fate of organic persistent pollutants.

Global distribution of TCPP emissions

The global distribution map of TCPP emissions is shown in Figure 2, and raw data are in the supporting information (SI). Major source regions of TCPP are in Europe (38%), North America (24%) and to a lesser extent in East Asia (13%). The TCPP emission rate into air in Europe ranges from 4.7 to 30 kt/y in our scenarios, with a rate of 30 kt/y in our "best estimate" scenario (Table 1). North America emits 3.0 to 19 kt/y of TCPP (Table 1) with a "best estimate" of 19 kt/y.

Rodgers et al. estimated the release of TCPP into air in the city of Toronto using similar top-down methodology to that employed here, but at a local scale.[19] They estimated emissions of 0.17 to 4.3 t/y, with a mean of 0.69 t/y. For a comparison, the data for Ontario Province (Toronto belongs to) has been extracted from the TCPP emission map (Figure 2) based on its administrative and political boundaries.[42] The emission of Toronto was calculated proportional to its population (20%) relative to that of Ontario (2.6 million in Toronto and 12.9 million in Ontario in 2011).[43] The result shows that 15~95 t/y TCPP are released into air over Toronto (Table S11), which is one to two orders of magnitude higher than the estimate by Rodgers et al (0.17 to 4.3 t/y).[19]

Comparison with bottom-up estimate

The EU risk assessment report estimated emissions of TCPP in the EU using a bottom-up approach to be 32.69 t/y for year 2000.[15]The total emission into the atmosphere over Europe in our scenarios ranges from 1,500 to 9,800 t/y (Table S11, using EU 12 members in 2000), which is 45 to 300 times higher than that estimated in the EU risk report.[15] With the rising consumption of TCPP in Europe since 2000, somewhat higher emissions would be expected, but it is unlikely that this is the only cause of the discrepancy in estimated TCPP emissions.

To provide more data for evaluation of the model results, we evaluated TCPP discharges in European Nordic countries and China using available production and usage information. The method used for this regional bottom-up approach is described in Text S1.

The online database of Substance in preparations in Nordic countries (SPIN) provides data on the usage of TCPP in Scandinavian countries from 2000 to 2015.[44] The reported TCPP usage in these countries ranged from 730 to 3,200 t/y with a mean of 1,500 ± 650 t/y. The estimated emissions using the bottom-up method ranged from 0.84 to 7.0 t/y (mean: 2.3 ± 1.8 t/y (Table S11). This result is two orders of magnitude lower than that calculated by the top-down approach in this study (480 to 3,000 t/y; Table S11).

In China, there are very few TCPP consumption data available. To overcome this problem, a market report on TCPP in China was acquired for this study from Shanghai Shuoxun Chemical Technology Company (SSCTC).[45] This report provides the production volume of TCPP from 2010 to 2015, with a range of 12,000 to 16,000 t/y (mean: 14,000 ± 1300 t/y) and the average domestic consumed TCPP is 8,100 ± 600 t/y. The calculated release rates using the bottom-up approach are 15 to 19 t/y (mean: 17 ± 1.2 t/y), which is one to two orders of magnitude lower than that calculated by the top-down method (range: 950 ~ 6,100 t/y; Table S11).

The emission estimates using the bottom-up method are limited by knowledge on TCPP production and consumption. On the other hand, the quality of measurements that are used for model tuning will affect the result of the top-down approach to a large degree. These limitations are main reasons for the discrepancy in TCPP emission estimates by the two methods.

Comparison with other POPs

Breivik et al. reported the atmospheric emission rates of 22 PCB congeners using the bottom-up method for different consumption scenarios.[17] TCPP is mainly used as additive flame retardant and plasticizer, which is similar with the open usage scenario of PCBs in Breivik et al's research.[17] Since the emissions of the open usage scenario are principally related to K_{OA} values, PCB-28, PCB-31 and PCB-52 (log K_{OA} are 7.9, 7.9 and 8.1, respectively) are adopted for a comparison with TCPP (log K_{OA}=8.1). The average annual emissions of PCB-28, -31, -52 from 1930 to 2000 were 0.65 to167, 0.60 to150 and 0.35 to 84 t/y, respectively, with the maximum values considered closer to reality than the minimum data.[17, 18] The estimated emission rate of PCBs thus is approximately two to three orders of magnitude lower than that of TCPP (12 to 79 kt/y). The higher TCPP consumption volume (estimated as 185 kt/y) than that of PCBs (0.54 ~ 0.87 kt/y) contributes to this emission difference. The total emission factors (=total emission/total production volume) for PCBs (0.1~20%) and TCPP are comparable (6.7 ~43%; Table S12).

In summary, a higher emission rate of TCPP than of other POPs having similar physical-chemical properties is indicated.

Uncertainty analysis

Uncertainties in our estimates originate from both model assumptions and validation data. For the top-down method, the simulated results highly rely on the quality, quantity and spatial coverage of measurements that are used to update the model output. In this study, the interannual variability of TCPP levels was not included in the modeling, although increasing trends of atmospheric TCPP concentrations have been found in the Canadian Arctic (annual increase: 27%) and the Great Lake areas (doubling time: 3.20 ±1.77 years).[4, 7] Neglecting the seasonal and inter-annual variability will introduce uncertainties. Our analysis depends quite strongly on concentrations measured using passive sampling in the GAPS network, and uncertainties and/or bias in these measurements will propagate to our emission estimates. Apart from the measurements, the uncertainty of LRT models is also an important factor. For example, the simulation of some TCPP turnover processes in the environment, such as the gas-particle partitioning, are not well constrained. Both BETR and CanMETOP models use K_{OA}-based parameterizations for gas-particle partitioning, whereas the literature suggests that this may not be ideal.[5] Another uncertainty factor is the properties of TCPP adopted. In this study we selected experimental data based on screening the literature, but uncertainties in properties will affect our results. Furthermore, the assumption that the emission rate is proportional to the nighttime light intensities will also induce uncertainties. Different administrative regions have different regulations and industrial layout, both of which will affect the emission pattern of TCPP. In Europe, TCPP is used as a substitute of TCEP, which has been banned under the REACH legislation.[46] There are no similar restrictions on TCEP in other regions, which may result in higher TCPP emissions in Europe than simulated.

As for the bottom-up method, a general lack of relevant activity information and measured emission factors of TCPP makes the application of this approach very difficult and results in high uncertainties.

Implications

For the first time a gridded global emission estimate for TCPP is presented. The finding on negligible effect of volatilization from seawater to the atmospheric levels confirms that TCPP in remote regions mainly originates from atmospheric transport from source regions, and that seawater appears to be a sink for TCPP. The TCPP levels in remote seawater originate from atmospheric deposition, but also the oceanic transport from source regions may contribute. The suggested half-lifetimes in air (12 h) and seawater (3,600 h) contribute to more accurately characterizing TCPP fate in the global environment. Owing to the uncertainties inherent in our method, the paucity of measurement data in the global atmosphere and oceans, and the poor agreement between our emission estimates and those for the city of Toronto and the EU, the global emission range (12 ~ 157 kt/y) should at best be treated as a preliminary estimate with high uncertainties. On the other hand, the established spatial patterns of TCPP release in this study is an important step for a better clarification of its environmental fate for further research on risk management and policymaking.

ASSOCIATED CONTENT

Supporting information

Additional tables and figures are given in the Supporting Information.

AUTHOR INFORMATION

Corresponding author

*Phone: +49-4152-872330; E-mail address: zhiyong.xie@hzg.de

*Phone: +46 8 674 7168; E-mail address: Matthew.MacLeod@aces.su.se

Author contributions

Z.X. and M.M. designed the research; M.M., J.L. and F.Z. conducted data analysis and method optimization; J.L. and F.Z. carried out modeling; C.T. guided the CanMETOP model; K.E., and R.E. provided important comments and polished the manuscript.

ORCID

Jing Li: 0000-0003-0187-9179

Fangyuan Zhao: 0000-0002-6041-4518

Zhiyong Xie: 0000-0001-8997-3930

Chongguo Tian: 0000-0001-6058-9353

Notes

The authors declare no competing financial interests.

ACKNOWLEDGMENTS

J.L. gratefully acknowledges the China Scholarship Council. F.Z., M.M. and Z.X. received funding from the European Union’s Horizon 2020 research and innovation programme under grant agreement No 689443 via project iCUPE (Integrative and Comprehensive Understanding on Polar Environments).

REFERENCES

1. Van der Veen, I.; de Boer, J., Phosphorus flame retardants: Properties, production, environmental occurrence, toxicity and analysis. *Chemosphere* **2012,** *88*, (10), 1119-1153.
2. Möller, A.; Xie, Z. Y.; Caba, A.; Sturm, R.; Ebinghaus, R., Organophosphorus flame retardants and plasticizers in the atmosphere of the North Sea. *Environ. Pollut.* **2011,** *159*, (12), 3660-3665.
3. Castro-Jimenez, J.; Berrojalbiz, N.; Pizarro, M.; Dachs, J., Organophosphate Ester (OPE) Flame Retardants and Plasticizers in the Open Mediterranean and Black Seas Atmosphere. *Environ. Sci. Technol.* **2014,** *48*, (6), 3203-3209.
4. Salamova, A.; Peverly, A. A.; Venier, M.; Hites, R. A., Spatial and Temporal Trends of Particle Phase Organophosphate Ester Concentrations in the Atmosphere of the Great Lakes. *Environ. Sci. Technol.* **2016,** *50*, (24), 13249-13255.
5. Li, J.; Tang, J. H.; Mi, W. Y.; Tian, C. G.; Emeis, K. C.; Ebinghaus, R.; Xie, Z. Y., Spatial Distribution and Seasonal Variation of Organophosphate Esters in Air above the Bohai and Yellow Seas, China. *Environ. Sci. Technol.* **2018,** *52*, (1), 89-97.
6. Lai, S.; Xie, Z.; Song, T.; Tang, J.; Zhang, Y.; Mi, W.; Peng, J.; Zhao, Y.; Zou, S.; Ebinghaus, R., Occurrence and dry deposition of organophosphate esters in atmospheric particles over the northern South China Sea. *Chemosphere* **2015,** *127*, 195-200.
7. Sühring, R.; Diamond, M. L.; Scheringer, M.; Wong, F.; Pucko, M.; Stern, G.; Burt, A.; Hung, H.; Fellin, P.; Li, H.; Jantunen, L. M., Organophosphate Esters in Canadian Arctic Air: Occurrence, Levels and Trends. *Environ. Sci. Technol.* **2016,** *50*, (14), 7409-7415.
8. Li, J.; Xie, Z.; Mi, W.; Lai, S.; Tian, C.; Emeis, K.-C.; Ebinghaus, R., Organophosphate Esters in Air, Snow and Seawater in the North Atlantic and the Arctic. *Environ. Sci. Technol.* **2017,** *51*, 6887−6896.
9. Castro-Jimenez, J.; Gonzalez-Gaya, B.; Pizarro, M.; Casal, P.; Pizarro-Alvarez, C.; Dachs, J., Organophosphate Ester Flame Retardants and Plasticizers in the Global Oceanic Atmosphere. *Environ. Sci. Technol.* **2016,** *50*, (23), 12831-12839.
10. Salamova, A.; Hermanson, M. H.; Hites, R. A., Organophosphate and Halogenated Flame Retardants in Atmospheric Particles from a European Arctic Site. *Environ. Sci. Technol.* **2014,** *48*, (11), 6133-6140.
11. Li, C.; Chen, J. W.; Xie, H. B.; Zhao, Y. H.; Xia, D. M.; Xu, T.; Li, X. H.; Qiao, X. L., Effects of Atmospheric Water on ·OH-initiated Oxidation of Organophosphate Flame Retardants: A DFT Investigation on TCPP. *Environ. Sci. Technol.* **2017,** *51*, (9), 5043-5051.
12. Marklund, A.; Andersson, B.; Haglund, P., Organophosphorus flame retardants and plasticizers in air from various indoor environments. *J. Environ. Monit.* **2005,** *7*, (8), 814-819.
13. Möller, A.; Sturm, R.; Xie, Z. Y.; Cai, M. H.; He, J. F.; Ebinghaus, R., Organophosphorus Flame Retardants and Plasticizers in Airborne Particles over the Northern Pacific and Indian Ocean toward the Polar Regions: Evidence for Global Occurrence. *Environ. Sci. Technol.* **2012,** *46*, (6), 3127-3134.
14. Zhang, Y., Global market analysis of flame retardant (in Chinese with English abstract). *Fine Specialty Chem.* **2014,** *22*, (8), 20-24.
15. EU Risk Assessment Report, Tris(2-chloro-1-methylethyl) phosphate (TCPP). CAS No.: 13674-84-5. EINECS No.: 237-158-7. **2008**.
16. Green, N.; Schlabach, M.; Bakke, T.; Brevik, E.; Dye, C.; Herzke, D.; Huber, S.; Plosz, B.; Remberger, M.; Schøyen, M., Screening of selected metals and new organic

contaminants 2007. Phosphorous Flame Retardents, Polyfluorinated Organic Compounds, Nitro-PAHs, Silver, Platinum and Sucralose in Air, Wastewater, Treatment Facilities, and Freshwater and Marine Recipients, Report TA2367;. *Norwegian Pollution Control Agency* **2008**.

17. Breivik, K.; Sweetman, A.; Pacyna, J. M.; Jones, K. C., Towards a global historical emission inventory for selected PCB congeners - a mass balance approach 2. Emissions. *Sci. Total Environ.* **2002,** *290*, (1-3), 199-224.

18. Breivik, K.; Sweetman, A.; Pacyna, J. M.; Jones, K. C., Towards a global historical emission inventory for selected PCB congeners - A mass balance approach-3. An update. *Sci. Total Environ.* **2007,** *377*, (2-3), 296-307.

19. Rodgers, T. F. M.; Truong, J. W.; Jantunen, L. M.; Helm, P. A.; Diamond, M. L., Organophosphate Ester Transport, Fate, and Emissions in Toronto, Canada, Estimated Using an Updated Multimedia Urban Model. *Environ. Sci. Technol.* **2018,** *52*, (21), 12465-12474.

20. Bogdal, C.; Wang, Z. Y.; Buser, A. M.; Scheringer, M.; Gerecke, A. C.; Schmid, P.; Muller, C. E.; MacLeod, M.; Hungerbuhler, K., Emissions of polybrominated diphenyl ethers (PBDEs) in Zurich, Switzerland, determined by a combination of measurements and modeling. *Chemosphere* **2014,** *116*, 15-23.

21. Gasic, B.; Moeckel, C.; MacLeod, M.; Brunner, J.; Scheringer, M.; Jones, K. C.; Hungerbuhler, K., Measuring and Modeling Short-Term Variability of PCBs in Air and Characterization of Urban Source Strength in Zurich, Switzerland. *Environ. Sci. Technol.* **2009,** *43*, (3), 769-776.

22. MacLeod, M.; Scheringer, M.; Podey, H.; Jones, K. C.; Hungerbuhler, K., The origin and significance of short-term variability of semivolatile contaminants in air. *Environ. Sci. Technol.* **2007,** *41*, (9), 3249-3253.

23. Bogdal, C.; Muller, C. E.; Buser, A. M.; Wang, Z. Y.; Scheringer, M.; Gerecke, A. C.; Schmid, P.; Zennegg, M.; MacLeod, M.; Hungerbuhler, K., Emissions of Polychlorinated Biphenyls, Polychlorinated Dibenzo-p-dioxins, and Polychlorinated Dibenzofurans during 2010 and 2011 in Zurich, Switzerland. *Environ. Sci. Technol.* **2014,** *48*, (1), 482-490.

24. Buser, A. M.; Kierkegaard, A.; Bogdal, C.; MacLeod, M.; Scheringer, M.; Hungerbuhler, K., Concentrations in Ambient Air and Emissions of Cyclic Volatile Methylsiloxanes in Zurich, Switzerland. *Environ. Sci. Technol.* **2013,** *47*, (13), 7045-7051.

25. Schenker, U.; Scheringer, M.; Sohn, M. D.; Maddalena, R. L.; McKone, T. E.; Hungerbuhler, K., Using Information on Uncertainty to Improve Environmental Fate Modeling: A Case Study on DDT. *Environ. Sci. Technol.* **2009,** *43*, (1), 128-134.

26. MacLeod, M.; von Waldow, H.; Tay, P.; Armitage, J. M.; Wöhrnschimmel, H.; Riley, W. J.; McKone, T. E.; Hungerbuhler, K., BETR global–A geographically-explicit global-scale multimedia contaminant fate model. *Environ. Pollut.* **2011,** *159*, (5), 1442-1445.

27. McLachlan, M. S.; Undeman, E.; Zhao, F. Y.; MacLeod, M., Predicting global scale exposure of humans to PCB 153 from historical emissions. *Environ. Sci.: Proc. Imp.* **2018,** *20*, (5), 747-756.

28. Zhang, L. S.; Ma, J. M.; Venkatesh, S.; Li, Y. F.; Cheung, P., Modeling Evidence of Episodic Intercontinental Long-Range Transport of Lindane. *Environ. Sci. Technol.* **2008,** *42*, (23), 8791-8797.

29. Ma, J. M.; Hung, H. L.; Tian, C.; Kallenborn, R., Revolatilization of persistent organic pollutants in the Arctic induced by climate change. *Nat. Clim. Change* **2011,** *1*, (5), 255-260.

30. von Waldow, H.; MacLeod, M.; Scheringer, M.; Hungerbuhler, K., Quantifying Remoteness from Emission Sources of Persistent Organic Pollutants on a Global Scale. *Environ. Sci. Technol.* **2010,** *44*, (8), 2791-2796.

31. Huang, T.; Tian, C. G.; Zhang, K.; Gao, H.; Li, Y. F.; Ma, J. M., Gridded atmospheric emission inventory of 2,3,7,8-TCDD in China. *Atmos. Environ.* **2015,** *108*, 41-48.

32. Jiang, W. Y. H.; Huang, T.; Mao, X. X.; Wang, L.; Zhao, Y.; Jia, C. H.; Wang, Y. N.; Gao, H.; Ma, J. M., Gridded emission inventory of short-chain chlorinated paraffins and its validation in China. *Environ. Pollut.* **2017,** *220*, 132-141.

33. Goktas, R. K.; MacLeod, M., Remoteness from sources of persistent organic pollutants in the multi-media global environment. *Environ. Pollut.* **2016,** *217*, 33-41.

34. National Geophysical Data Center, Available at: https://ngdc.noaa.gov/eog/dmsp/downloadV4composites.html.

35. Cuthbert, J. M., DM., TCPP: Determination of general physicochemical properties, Report 1613/002. *SafePharm Laboratories, PO Box 45, Derby, UK.* **2002**.

36. Lijzen, J.; Rikken, M., *European Union System for the Evaluation of Substances 2.0 (EUSES 2.0); background report*. 2004.

37. Brommer, S.; Jantunen, L. M.; Bidleman, T. F.; Harrad, S.; Diamond, M. L., Determination of Vapor Pressures for Organophosphate Esters. *J. Chem. Eng. Data* **2014,** *59*, (5), 1441-1447.

38. Malanichev, A.; Mantseva, E.; Shatalov, V.; Strukov, B.; Vulykh, N., Numerical evaluation of the PCBs transport over the Northern Hemisphere. *Environ. Pollut.* **2004,** *128*, (1-2), 279-289.

39. Hilal, S. H.; Karickhoff, S. W.; Carreira, L. A., Prediction of the solubility, activity coefficient and liquid/liquid partition coefficient of organic compounds. *Qsar Comb. Sci.* **2004,** *23*, (9), 709-720.

40. McDonough, C. A.; De Silva, A. O.; Sun, C. X.; Cabrerizo, A.; Adelman, D.; Soltwedel, T.; Bauerfeind, E.; Muir, D. C. G.; Lohmann, R., Dissolved Organophosphate Esters and Polybrominated Diphenyl Ethers in Remote Marine Environments: Arctic Surface Water Distributions and Net Transport through Fram Strait. *Environ. Sci. Technol.* **2018,** *52*, (11), 6208-6216.

41. Lohmann, R.; Muir, D.; Zeng, E. Y.; Bao, L. J.; Allan, I. J.; Arinaitwe, K.; Booij, K.; Helrn, P.; Kaserzon, S.; Mueller, J. F.; Shibata, Y.; Smedes, F.; Tsapakis, M.; Wong, C. S.; You, J., Aquatic Global Passive Sampling (AQUA-GAPS) Revisited: First Steps toward a Network of Networks for Monitoring Organic Contaminants in the Aquatic Environment. *Environ. Sci. Technol.* **2017,** *51*, (3), 1060-1067.

42. Statistics Canada. https://www12.statcan.gc.ca/census-recensement/2011/geo/bound-limit/bound-limit-2011-eng.cfm.

43. Statistics Canada. Statistics Canada 2011 Census Toronto Population; 2011.

44. Substance in preparations in Nordic countries (SPIN) online database. http://www.spin2000.net/spinmyphp/.

45. Shanghai Shuoxun Chemical Technology Company (SSCTC). The Market Research Report of PFRs. http://www.shuoxun-report.com/. **2017**.

46. Annex XIV of REACH. Authorisation List. https://echa.europa.eu/authorisation-list.

Figure legends

Figure 1. The linear regression plots between modeled and observed concentrations in air and seawater of TCPP for scenarios with $t_{1/2,\text{Water}}$=3,600 h and E_W=0.5E_A.

Figure 2. Gridded global emissions of TCPP and contributions of source regions as well as corresponding emission rate (globe: 78.6 kt/y).

Figure 3. Spatial distribution of modeled and observed TCPP concentrations in air (scenario: E_A=78.6 kt/y, $t_{1/2,\text{Air}}$=12 h, $t_{1/2,\text{Water}}$=3,600 h).

Figure 4. Spatial distribution of modeled and observed TCPP concentrations in seawater (scenario: E_A=78.6 kt/y, $t_{1/2,\text{Air}}$=12 h, $t_{1/2,\text{Water}}$=3,600 h).

Table legends

Table 1. Estimated annual emissions of different source regions.

Figure 1.

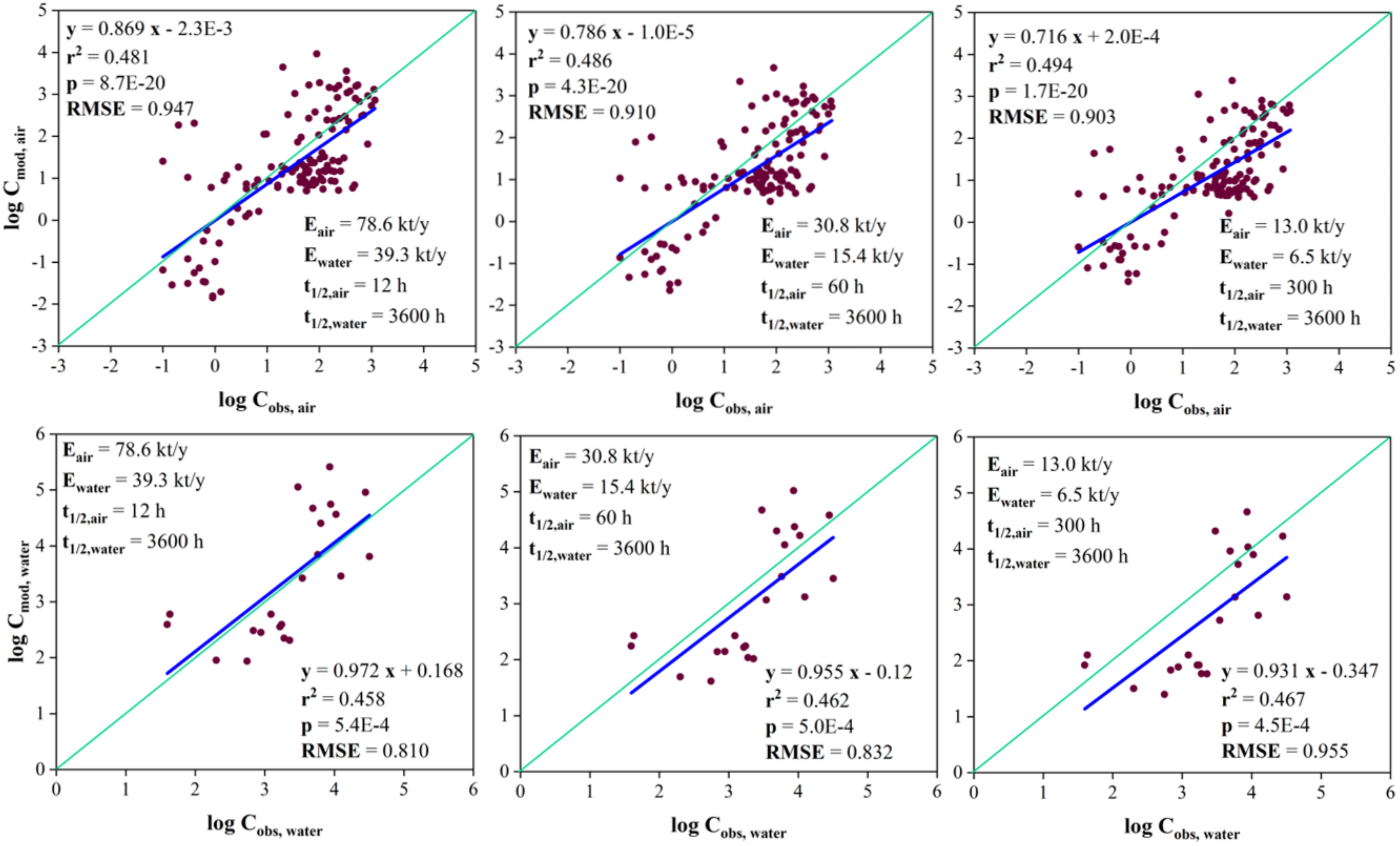
y = 0.869 x - 2.3E-3
r^2 = 0.481
p = 8.7E-20
RMSE = 0.947
E_{air} = 78.6 kt/y
E_{water} = 39.3 kt/y
$t_{1/2,air}$ = 12 h
$t_{1/2,water}$ = 3600 h
y = 0.786 x - 1.0E-5
r^2 = 0.486
p = 4.3E-20
RMSE = 0.910
E_{air} = 30.8 kt/y
E_{water} = 15.4 kt/y
$t_{1/2,air}$ = 60 h
$t_{1/2,water}$ = 3600 h
y = 0.716 x + 2.0E-4
r^2 = 0.494
p = 1.7E-20
RMSE = 0.903
E_{air} = 13.0 kt/y
E_{water} = 6.5 kt/y
$t_{1/2,air}$ = 300 h
$t_{1/2,water}$ = 3600 h
log $C_{mod, air}$
log $C_{obs, air}$
-3 -2 -1 0 1 2 3 4 5
E_{air} = 78.6 kt/y
E_{water} = 39.3 kt/y
$t_{1/2,air}$ = 12 h
$t_{1/2,water}$ = 3600 h
y = 0.972 x + 0.168
r^2 = 0.458
p = 5.4E-4
RMSE = 0.810
E_{air} = 30.8 kt/y
E_{water} = 15.4 kt/y
$t_{1/2,air}$ = 60 h
$t_{1/2,water}$ = 3600 h
y = 0.955 x - 0.12
r^2 = 0.462
p = 5.0E-4
RMSE = 0.832
E_{air} = 13.0 kt/y
E_{water} = 6.5 kt/y
$t_{1/2,air}$ = 300 h
$t_{1/2,water}$ = 3600 h
y = 0.931 x - 0.347
r^2 = 0.467
p = 4.5E-4
RMSE = 0.955
log $C_{mod, water}$
log $C_{obs, water}$
0 1 2 3 4 5 6

Figure 2.

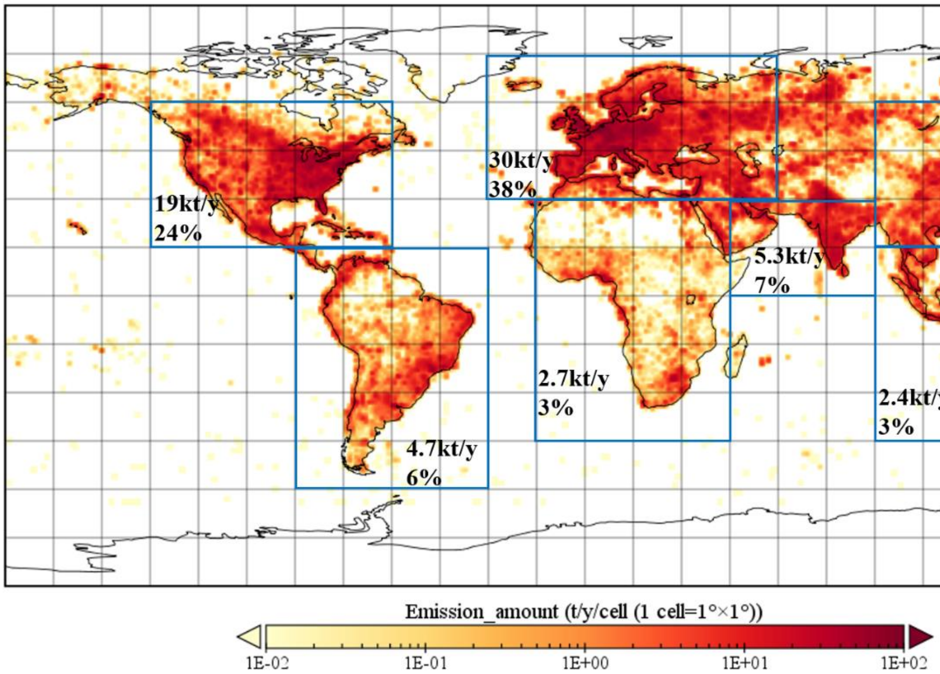
30kt/y
38%
19kt/y
24%
10kt/y
13%
5.3kt/y
7%
2.7kt/y
3%
2.4kt/y
3%
4.7kt/y
6%
Emission_amount (t/y/cell (1 cell=1°×1°))
1E-02
1E-01
1E+00
1E+01
1E+02

Figure 3.

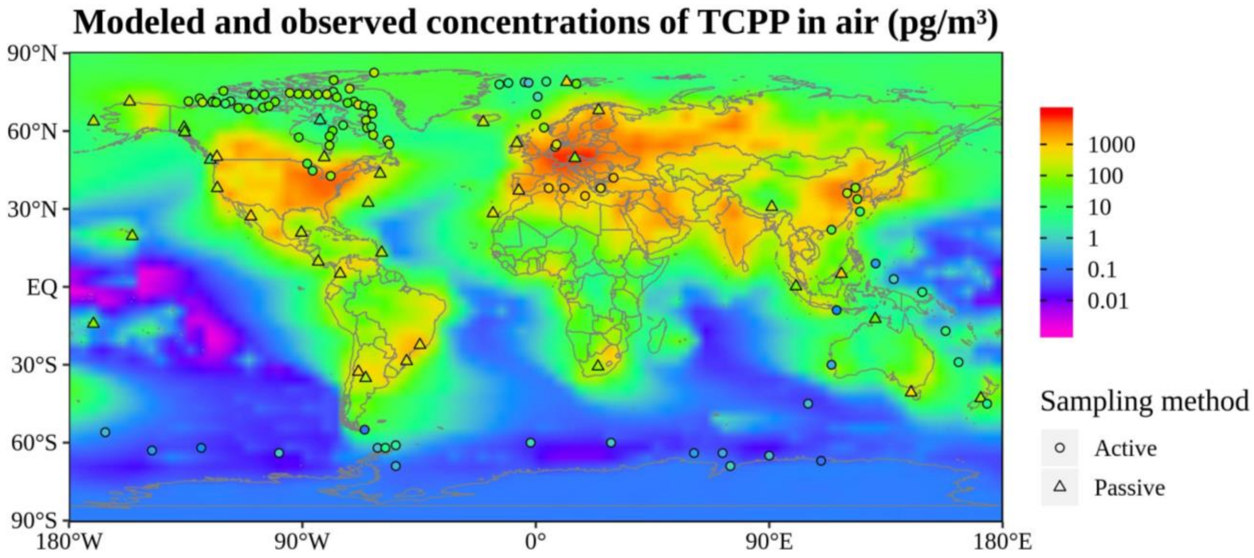

Figure 4.

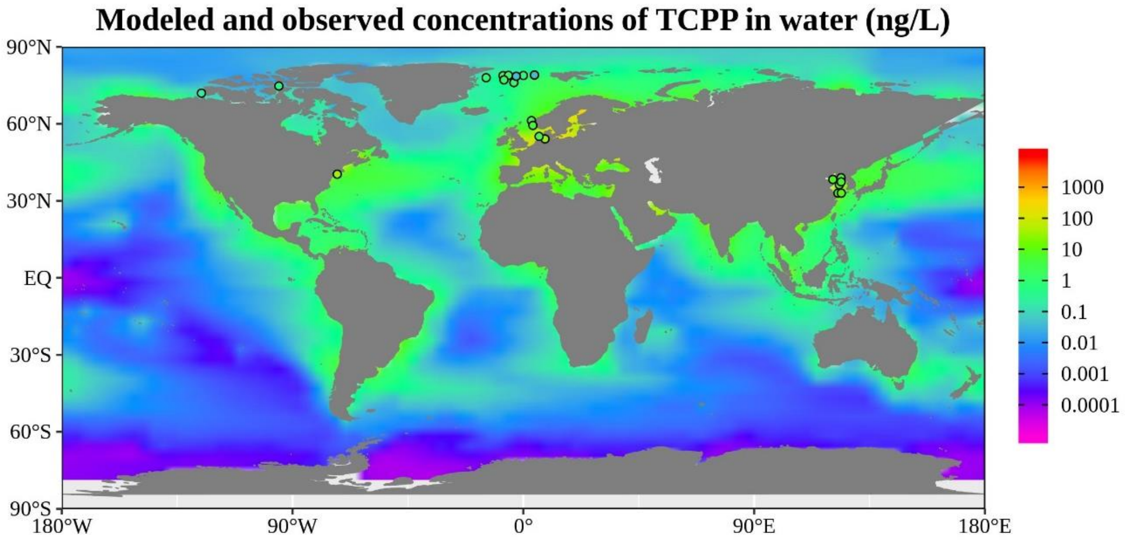

Table 1.

		TCPP emission to air (kt/y)			**TCPP emission to water (kt/y)**		
No.	**Region**	**Min (300_36000)[a]**	**Max (12_1440)**	**“Best Estimate” (12_3600)**	**Min (E_W=0)**	**Max (E_W=E_A, 12_1440)**	**“Best Estimate” (E_W=0.5E_A, 12_3600)**
1	**North America**	3.0	19	19	0	19	9.3
2	**South America**	0.74	4.7	4.7	0	4.7	2.3
3	**Europe**	4.7	30	30	0	30	15
4	**Africa**	0.44	2.8	2.8	0	2.7	1.3
5	**East Asia**	1.6	10	10	0	10	5.0
6	**South Asia**	0.82	5.3	5.2	0	5.0	2.5
7	**Indonesia to Australia**	0.38	2.4	2.4	0	2.4	1.2
8	**Global**	12.5	79.4	78.6	0	79.4	39.3

[a]: The number in the bracket represent the half-lives of TCPP in air and water ($t_{1/2,\mathrm{Air}}$_$t_{1/2,\mathrm{Water}}$).

Table of Content (TOC):

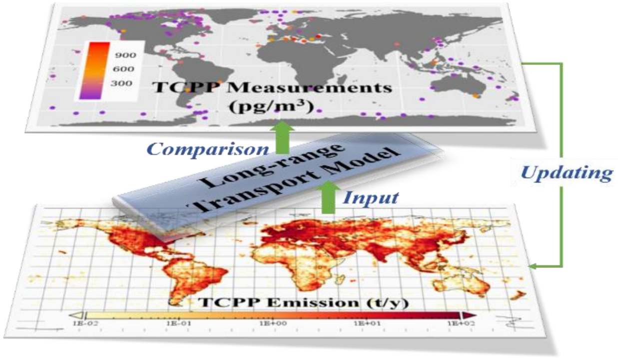

Supporting information of

Global gridded emissions and atmospheric transport of tris-(1-chloro-2-propyl) phosphate (TCPP)

Jing Li[†,⊥], Fangyuan Zhao[‡], Zhiyong Xie[†*], Ralf Ebinghaus[†], Kay-Christian Emeis[†], Chongguo Tian[§], Matthew MacLeod[‡*]

[†]Helmholtz-Zentrum Geesthacht, Centre for Materials and Coastal Research, Institute of Coastal Research, Geesthacht, 21502, Germany

[‡]Department of Environmental Science and Analytical Chemistry, ACES, Stockholm University, Svante Arrhenius väg 8, Stockholm, SE-114 18, Sweden

[§]Key Laboratory of Coastal Environmental Processes and Ecological Remediation, Yantai Institute of Coastal Zone Research, CAS, Yantai, 264003, China

[⊥]Universität Hamburg, Department of Geosciences, Hamburg, 20144, Germany

Corresponding Author

*Phone: +49-4152-872330; E-mail address: zhiyong.xie@hzg.de

*Phone: +46 8 674 7168; E-mail address: Matthew.MacLeod@aces.su.se

Pages: 32

Source file: 1

Tables: 17

Figures: 15

Table of Contents

Source file of global gridded emissions to air:

Grid_emission_into_air.txt txt2raster_Arcgis.txt

The files above are gridded emissions of TCPP to air with latitude range from 90N to 90S and longitude range from 180W to 180E (1×1 degree). Readers can use the python code in file txt2raster_Arcgis.txt to convert the data from .txt to .tif format in Arcgis software, which can be easily shown.

Table S1. The physical/chemical properties of TCPP (at 25°C)

Parameter	Descript	Unit	Value	Source
MW	Molecular weight	g/mol	327	EPI suite 4.0
VP	Vapor pressure	Pa	0.035	Brommer et al.[1]
SL	Solubility	mg/l	1160	Cuthbert et al.[2]
HLC	Herry's law constant	$Pa \cdot m^3/mol$	0.0099	Derived from VP and SL
$\log K_{OW}$	Partitioing ratio:n-octanol/water		2.68	Cuthbert et al.[2]
$\log K_{AW}$	Partitioing ratio:air/water		-5.40	Derived from VP and SL
$\log K_{OA}$	Partitioing ratio:n-octanol/air		8.08	Derived by $\log K_{OW}$-$\log K_{AW}$
$t_{1/2,Air}$	Half-life time in air	h	12, 60, 300	Designed in this study according to Li et al.[3]
$t_{1/2,Freshwater}^{a}$	Half-life time in freshwater	h	1440, 7200, 36000	Referred EPI suite 4.0 and designed in this study
$t_{1/2,Ocean}^{a}$	Half-life time in ocean	h	1440, 7200, 36000	
$t_{1/2,Soil}$	Half-life time in soil	h	2880,14400,72000	
$t_{1/2,Sediment}$	Half-life time in sediment	h	13000,65000,325000	
$t_{1/2,Vegetation}$	Half-life time in vegetation	h	1440, 7200, 36000	Set as same as $t_{1/2,Freshwater}$
DU_{OW}	Internal energy of phase change: n-octanol/water	J/mol	-20000	MacLeod et al.[4]
DU_{OA}	Internal energy of phase change:n-octanol/air	J/mol	-80306	
AE_{Air}	Activation energies in air	J/mol	10000	Wöhrnschimmel et al.[5]
$AE_{Freshwater}$	Activation energies in freshwater	J/mol	30000	
AE_{Ocean}	Activation energies in ocean	J/mol	30000	
AE_{Soil}	Activation energies in soil	J/mol	30000	
$AE_{Sediment}$	Activation energies in sediment	J/mol	30000	
$AE_{Vegetation}$	Activation energies in vegetation	J/mol	30000	

[a]: Same value for $\boldsymbol{t}_{\mathbf{1/2,Freshwater}}$ and $\boldsymbol{t}_{\mathbf{1/2,Ocean}}$ were used and in the rest of the paper use $\boldsymbol{t}_{\mathbf{1/2,Water}}$ to represent for these two parameters.

Table S2. The atmospheric TCPP measurements referred in this study

References	Region	Sampling Date	Samples number	Source files in the references	Adopted in this study or not?
Rauert et al.[6]	South America	2014-2015	5	Table 3; only background samples were used.	Yes
Castro-Jiménez et al.[7]	Mediterranean and Black Seas	2006-2007	5	Table S4; mean values were used for each place.	Yes
Möller et al.[8]	North Sea	2010	20	Table S5; sum of concentrations in particle and gaseous phases were used.	Yes
Salamova et al.[9]	Longyearbyen	2012-2013	1	Table 1; mean value was used	Yes
Salamova et al.[10]	Great Lakes	2012	3	Table 1; mean values were used; only rural and remote sites were chosen.	Yes
Salamova et al.[11]	Great Lakes	2012-2014	3	Table 1; mean values were used; only rural and remote sites were chosen.	Yes
Lai et al.[12]	South China Sea	2013	10	Table A2 and Figure 1	Yes
Li et al.[13]	North Atlantic to Arctic	2014	9	Figure 1	Yes
Li et al.[14]	Bohai and Yellow Seas	2016	16	Figure 2	Yes
Cheng et al.[15]	West Pacific, Indian Ocean and Southern Ocean	2009-2010	29	Figure 2	Yes
Sühring et al.[16]	Canada Arctic	2007-2013	82	Table S5 and S6	Yes
Rauert et al.[17]	GAPS network[a]	2014	36	Table S16-19; use mean values of four quarters; only rural and remote sites were used.	Yes
Castro-Jimenez et al.[18]	Global oceans	2011-2012	115	Table S7	No
Möller et al.[19]	Pacific, Indian, Arctic, and Southern Ocean	2010-2011	30	Table S4	No

[a]: Global Atmospheric Passive Sampling (GAPS) Network

Table S3. The measurements of TCPP in seawater referred in this study

References	Region	Sampling Date	Samples number	Source file in the references
Li et al.[13]	North Atlantic to Arctic	2014	25	Figure 3
McDonough et al.[20]	Canada Arctic	2014-2016	5	Figure 2 and 3
Kim et al.[21]	Long Land (USA)	2016-2017	1	Table 1, use mean value of three seawater samples
Bollmann et al.[22]	North Sea	2010	31	Figure 1 and personal communication
Zhong et al.[23]	Bohai and Yellow Seas	2012	49	Table S4; mean values were used for each site.

Table S4. The designed scenarios for TCPP emission estimate

$t_{1/2,\mathrm{Air}}$ **(h)**	$t_{1/2,\mathrm{Water}}$ **(h)**^{a}	E_W**=0**	E_W**=0.5** E_A	E_W**=**E_A
12	**1440**	Scenario 1	Scenario 10	Scenario 19
12	**7200**	Scenario 2	Scenario 11	Scenario 20
12	**36000**	Scenario 3	Scenario 12	Scenario 21
60	**1440**	Scenario 4	Scenario 13	Scenario 22
60	**7200**	Scenario 5	Scenario 14	Scenario 23
60	**36000**	Scenario 6	Scenario 15	Scenario 24
300	**1440**	Scenario 7	Scenario 16	Scenario 25
300	**7200**	Scenario 8	Scenario 17	Scenario 26
300	**36000**	Scenario 9	Scenario 18	Scenario 27

^{a}:When $t_{1/2,\mathrm{Water}}$=1440h, the corresponding $t_{1/2,\mathrm{Soil}}$ and $t_{1/2,\mathrm{Sediment}}$ are 2880 h and 13000 h, respectively.
When $t_{1/2,\mathrm{Water}}$=7200h, the corresponding $t_{1/2,\mathrm{Soil}}$ and $t_{1/2,\mathrm{Sediment}}$ are 14400 h and 65000 h, respectively.
When $t_{1/2,\mathrm{Water}}$=36000h, the corresponding $t_{1/2,\mathrm{Soil}}$ and $t_{1/2,\mathrm{Sediment}}$ are 72000 h and 325000 h, respectively.

Table S5. The slope values of regression between modeled and measured logarithm concentrations of 27 scenarios

$t_{1/2,\mathrm{Air}}$**_**$t_{1/2,\mathrm{Water}}$	E_A	**Slope of air sites**			**Slope of water sites**		
		E_W**=0**	E_W**=0.5** E_A	E_W**=**E_A	E_W**=0**	E_W**=0.5**E_A	E_W**=**E_A
12_1440	**79.4**	0.866	0.866	0.867	0.990	1.089	1.113
12_7200	**78.0**	0.869	0.870	0.870	0.833	0.930	0.947
12_36000	**77.3**	0.871	0.871	0.871	0.788	0.903	0.921
60_1440	**31.5**	0.783	0.783	0.783	0.962	1.062	1.092
60_7200	**30.4**	0.787	0.787	0.787	0.821	0.915	0.936
60_36000	**30.0**	0.789	0.789	0.789	0.779	0.888	0.910
300_1440	**13.5**	0.712	0.713	0.713	0.919	1.024	1.060
300_7200	**12.8**	0.717	0.717	0.718	0.801	0.894	0.920
300_36000	**12.5**	0.719	0.719	0.720	0.765	0.867	0.894

Table S6. The intercept values of regression between modeled and measured logarithm concentrations of 27 scenarios

$t_{1/2,\mathrm{Air}}$**_**$t_{1/2,\mathrm{Water}}$	E_A	**Intercept of air sites**			**Intercept of water sites**		
		E_W**=0**	E_W**=0.5** E_A	E_W**=**E_A	E_W**=0**	E_W**=0.5**E_A	E_W**=**E_A
12 _1440	**79.4**	-4.2E-04	-2.1E-04	2.1E-05	-0.696	-0.644	-0.536
12_7200	**78.0**	-1.1E-03	8.8E-05	1.3E-03	0.395	0.540	0.696
12_36000	**77.3**	-2.0E-03	1.5E-04	2.3E-03	0.777	0.904	1.063
60_1440	**31.5**	-4.9E-04	-1.6E-05	4.7E-04	-0.844	-0.871	-0.807
60_7200	**30.4**	-1.3E-03	-5.8E-06	1.3E-03	0.158	0.233	0.357
60_36000	**30.0**	-2.0E-03	1.6E-04	2.3E-03	0.523	0.590	0.718
300_1440	**13.5**	-7.4E-04	2.2E-05	7.9E-04	-0.927	-1.023	-1.003
300_7200	**12.8**	-1.9E-03	-2.1E-04	1.5E-03	-0.037	-0.016	0.074
300_36000	**12.5**	-2.6E-03	1.8E-04	2.9E-03	0.304	0.330	0.428

Table S7. The r^2 values of regression between modeled and measured logarithm concentrations of 27 scenarios

$t_{1/2,\mathrm{Air}}$ $t_{1/2,\mathrm{Water}}$	E_A	r^2 **of air sites**	r^2 **of water sites**

		E_W=0	E_W=0.5 E_A	E_W=E_A	E_W=0	E_W=0.5E_A	E_W=E_A
12 _1440	**79.4**	0.479	0.480	0.480	0.517	0.498	0.493
12_7200	**78.0**	0.481	0.481	0.481	0.449	0.432	0.430
12_36000	**77.3**	0.481	0.481	0.481	0.420	0.402	0.401
60_1440	**31.5**	0.484	0.484	0.484	0.529	0.508	0.501
60_7200	**30.4**	0.487	0.487	0.487	0.456	0.434	0.431
60_36000	**30.0**	0.488	0.488	0.488	0.425	0.404	0.402
300_1440	**13.5**	0.490	0.490	0.490	0.542	0.517	0.509
300_7200	**12.8**	0.495	0.495	0.495	0.466	0.438	0.434
300_36000	**12.5**	0.496	0.496	0.497	0.433	0.407	0.404

Table S8. The RMSE values between modeled and measured logarithm concentrations of 27 scenarios

$t_{1/2,Air}$_ $t_{1/2,Water}$	E_A	**RMSE of air sites**			**RMSE of water sites**		
		E_W=0	E_W=0.5 E_A	E_W=E_A	E_W=0	E_W=0.5E_A	E_W=E_A
12 _1440	**79.4**	0.948	0.948	0.947	1.032	0.905	0.879
12_7200	**78.0**	0.947	0.947	0.947	0.733	0.872	0.982
12_36000	**77.3**	0.948	0.947	0.946	0.729	1.023	1.175
60_1440	**31.5**	0.911	0.911	0.910	1.194	1.039	0.972
60_7200	**30.4**	0.908	0.907	0.907	0.825	0.801	0.834
60_36000	**30.0**	0.907	0.906	0.905	0.742	0.855	0.947
300_1440	**13.5**	0.906	0.906	0.905	1.361	1.209	1.129
300_7200	**12.8**	0.900	0.899	0.898	0.971	0.860	0.827
300_36000	**12.5**	0.898	0.896	0.895	0.842	0.813	0.836

Table S9. New designed scenarios with $t_{1/2,Water}$ set as 3600 h

$t_{1/2,Air}$ (h)	$t_{1/2,Water}$ (h)	E_W=0	E_W=0.5 E_A	E_W=E_A
12	**3600**	Scenario 28	Scenario 31	Scenario 34
60	**3600**	Scenario 29	Scenario 32	Scenario 35
300	**3600**	Scenario 30	Scenario 33	Scenario 36

[a]:When $t_{1/2,Water}$=3600h, the corresponding $t_{1/2,Soil}$ and $t_{1/2,Sediment}$ are 7200 h and 32500 h, respectively.

Table S10. The regression result of modeled data by CanMETOP and measurements

Total Emission (kt/y)		**Half-lifetime**		**Regression result (for measurements in air)**				
E_A	E_W	$t_{1/2,Air}$	$t_{1/2,Water}$	**Slope**	**Intercept**	r^2	p	**RMSE**
78.6	**0**	**12 h**	**3600 h**	0.912	-0.074	0.392	1.9E-19	1.118
30.8	**0**	**60 h**	**3600 h**	0.579	0.907	0.409	1.8E-20	0.817
13.0	**0**	**300 h**	**3600 h**	0.270	1.433	0.226	9.6E-11	0.892

Table S11. Comparison of estimated emissions in this study with literatures

Region	**Atmospheric emission of TCPP (t/y)**			**Method**	**Reference**
	“Best Estimate” (12_3600)	**Min (300_36000)**	**Max (12_1440)**		
Canada	2801	444	2830	Top-down	this study
Ontario	463	73	467	Top-down	this study
Toronto[a]	94	15	95	Top-down	this study
Toronto	0.69 (mean)	0.17	4.3	Top-down	Rodgers et al.[24]

EU[b]	9756	1546	9854	Top-down	this study
EU	33	NA	NA	Bottom-up	EU risk report[25]
Nordic Countries	3002	476	3032	Top-down	this study
Nordic Countries	2.3 ± 1.8 (mean)	0.84	7.0	Bottom-up	this study
China	5995	950	6056	Top-down	this study
China	17 ± 1.2(mean)	15	19	Bottom-up	this study

Table S12. The comparison of emissions for different compounds

Region	Name[a]	log K_{AW}	log K_{OW}	log K_{OA}	Emission phase	Consumption (kt/y)	Emission (t/y)	Total emission factor	Estimated duration	Method	Reference
Global	PCB-28	-2.0	5.7	7.9	Atmosphere	0.87	0.65~167	0.1~20%	1930~2000	Bottom-up	Breivik et al. [26]
	PCB-31	-2.0	5.7	7.9	Atmosphere	0.75	0.60~150	0.1~20%			
	PCB-52	-1.8	6.1	8.3	Atmosphere	0.54	0.35~84	0.1~15%			
	TCPP	-5.4	2.7	8.1	Atmosphere	185	12000~79000 (78600)	6.7 ~43% (42%)		Top-down	this study

[a]: The CAS numbers for the compounds: PCB-28: 7012-37-5; PCB-31: 16606-02-3; PCB-52: 35693-99-3.

Table S13. Emission factor for different processes during TCPP formulation and usage

Classification	Subdivided		Emission factor	Emission factor code#	Reference
Formulation	Medium, small system house, house using pre-formulated polyol, no data on large house		0.00025	1.0	25
Conversion	For calendering	High volatility group	0.00125	2.1	27
	For extrusion	High volatility group	0.00025	2.2	
	For blown film	High volatility group	0.00125	2.3	
	For injection moulding	High volatility group	0.00025	2.4	
	For spread coating	High volatility group	0.00025	2.5	
	Default for other specific process (indoor)	High volatility group	0.00025	2.6	
	Default for other specific process (outdoor)	High volatility group	0.00125	2.7	
	For spread coating		0	2.8	
Manufacture	Rigid foam	**In total**	**0.00125**	**3.1**	
		Foam production (Board manufacture): 0.025%	0.00025	3.1.1	25
		Adhesive pressing: 0.1%	0.001	3.1.2	
	Flexible foam	**In total**	**0.0005112**	**3.2**	
		Foam production: 0.05012% (handling, curing, storage)	0.0005012	3.2.1	25
		Foam cutting and manufacture of furniture	0.000002	3.2.2	
		Rebonding : 0.0004%	0.000004	3.2.3	
		Loose crumb: 0.0004%	0.000004	3.2.4	
	Spray foam	0.096% for risk assessment (based on the rate of release in service)	0.00096	3.3	
	One-component foam	0.096% for risk assessment	0.00096	3.4	
Products in-Service	Rigid foam	**In total**	**0.0025**	**4.1**	
		Rigid foam (in-structural use in buidling)	0.0000	4.1.1	25
		Rigid foam (adhesive pressed foam) (1,5% of total rigid foam)	0.0025	4.1.2	
	Flexible foam (indoor=outdoor; default)	0.25%	0.0025	4.2	
	Spray foam	Negligible	0	4.3	
	One-component foam	Negligible	0	4.4	
	ESD* outdoor service-volatility to air	High volatility group	0.0025	4.5	27
	ESD indoor service-volatility to air	High volatility group	0.0025	4.6	

#: This code is used for identify the factor for each emission scenario. *ESD: Emission Scenario Document.

Table S14. The NACE usage of TCPP in Nordic countries from SPIN

Usage classification	NACE Code				Emission factor	Emission factor code[#]
Manufacture of chemicals and chemical products	24	C20			0.00025	1.0
Manufacture of rubber and plastic products	25	C22			0.0005112	3.2
Manufacture of machinery and equipment	29	C28			0.0025	4.5
Construction	45	F41	F42	F43	0.00375	3.2 and 4.1[*]
Wholesale trade and commission trade, except of motor vehicles and motorcycles	51	G46			0.0025	4.2
Retail trade, except of motor vehicles and motorcycles; repair of personal and household goods	52	G47			0.0025	4.2
Private households with employed persons	95				0.0025	4.2
Manufacture of fabricated metal products, except machinery and equipment	C25				0.0025	4.5
Manufacture of computer, electronic and optical products	C26				0.0025	4.5
Undifferentiated goods- and services-producting activities of private households for own use	T98				0.0025	4.2
Unknown	NA[a]				0.00025[a]	

[#]: Refer the code in Table S13.

[a]: “Unknown” represent the amount of total TCPP usage ($V_{national}$) subtract sum of NACE usage (V_{NACE}). The emission factor of this part was estimated as 0.00025.

[*] OPEs used in contraction could emission from the manufacture and service stages, so the emission factor is the sum of these two stages.

Table S15. Annual usage of TCPP of Nordic countries (unit: t)

Year	Denmark	Finland	Sweden	Norway	Total
2000	553	616	195	43	1407
2001	704	812	145	50	1711
2002	584	1008	99	148	1839
2003	381	1474	129	52	2036
2004	47	1771	81	48	1947
2005	41	1571	110	46	1768
2006	222	2852	114	36	3224
2007	217	1477	121	40	1855
2008	177	1641	132	42	1992
2009	105	913	100	39	1157
2010	199	1111	84	43	1437
2011	193	720	93	43	1049
2012	92	723	91	59	965
2013	136	394	129	75	734
2014	166.5	370.9	148	63	749
2015	185	189	130	307	811
Mean	250 ± 200	1100 ± 670	120 ± 30	70 ± 68	1500 ± 650
Total	4000	17600	1900	1100	24700

Table S16. TCPP annual emission of Nordic countries (unit: t)

Year	Denmark	Finland	Sweden	Norway	Total
2000	0.66	1.3	0.23	0.06	2.2
2001	0.54	0.20	0.12	0.06	0.92
2002	0.39	2.1	0.12	0.54	3.2
2003	0.16	3.0	0.09	0.07	3.4
2004	0.07	4.0	0.07	0.08	4.2
2005	0.02	4.7	0.08	0.09	4.9
2006	0.33	6.5	0.08	0.09	7.0
2007	0.28	1.2	0.09	0.10	1.7
2008	0.15	1.1	0.10	0.10	1.5
2009	0.17	0.79	0.11	0.09	1.2
2010	0.12	1.2	0.09	0.10	1.5
2011	0.16	0.89	0.14	0.08	1.3
2012	0.14	0.63	0.05	0.12	0.94
2013	0.16	0.46	0.07	0.15	0.84
2014	0.18	0.49	0.08	0.11	0.86
2015	0.18	0.51	0.08	0.26	1.0
Mean	0.23 ± 0.17	0.18 ± 1.8	0.1 ± 0.04	0.13 ± 0.12	2.3 ± 1.8
Total	3.7	29	1.6	2.1	36

Table S17. The TCPP emission of China in each year (unit: t)

Year	Emission sectors						
	Production	Formulation	Plastic	Textile	Paint	Others	Total
2010	0.12	1.8	8.5	2.1	0.88	1.6	15

2011	0.14	2.1	9.6	2.4	1.0	1.8	17
2012	0.13	2.0	9.0	2.3	0.94	1.7	16
2013	0.14	2.0	9.3	2.3	1.0	1.8	16
2014	0.14	2.0	9.5	2.4	1.0	1.8	17
2015	0.16	2.3	11	2.7	1.1	2.0	19
Mean	0.14 ± 0.01	2.0 ± 0.15	9.4 ± 0.69	2.4 ± 0.17	0.98 ± 0.07	1.8 ± 0.13	17 ± 1.2
Total	0.84	12	56	14	5.9	11	100

Table S18. Estimated total emission factor of consumed TCPP for Bottom-up method

Region	Consumption volume input (kt)	Emission volume (t)	Total emission factor
Nordic countries	1.5 ± 0.65	2.3 ± 1.8	0.10%
China	8.1 ± 0.6	17 ± 1.2	0.21%

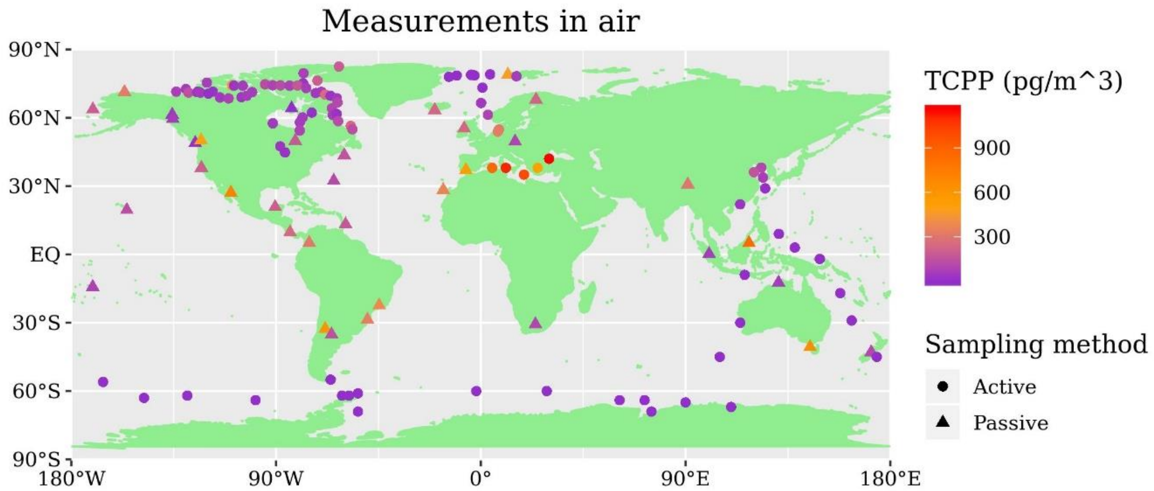

Figure S1: The global measurements in air of rural and remote areas (in 3.75° degree)

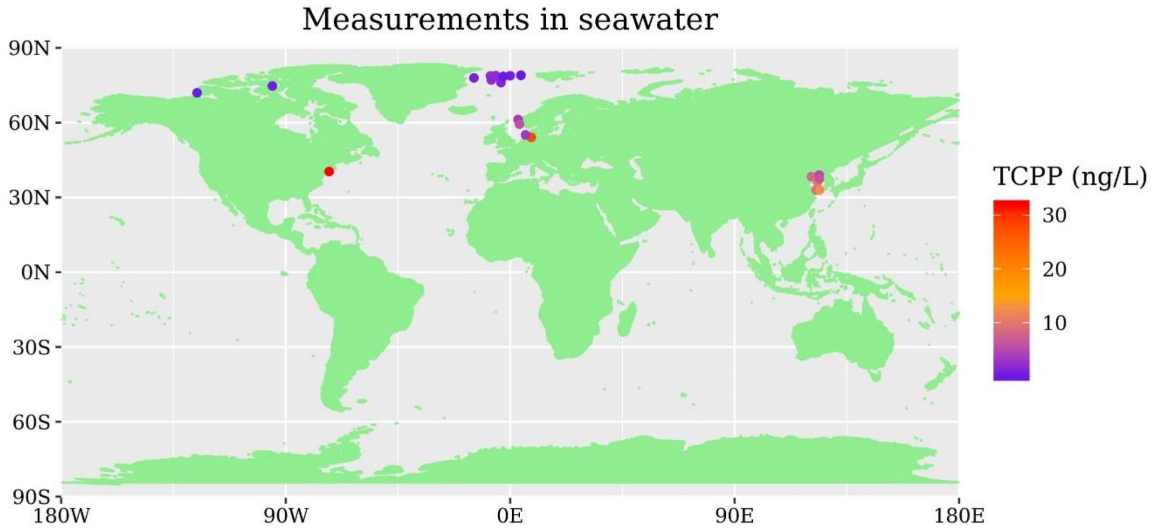

Figure S2: The global measurements in water of remote areas (in 3.75° degree)

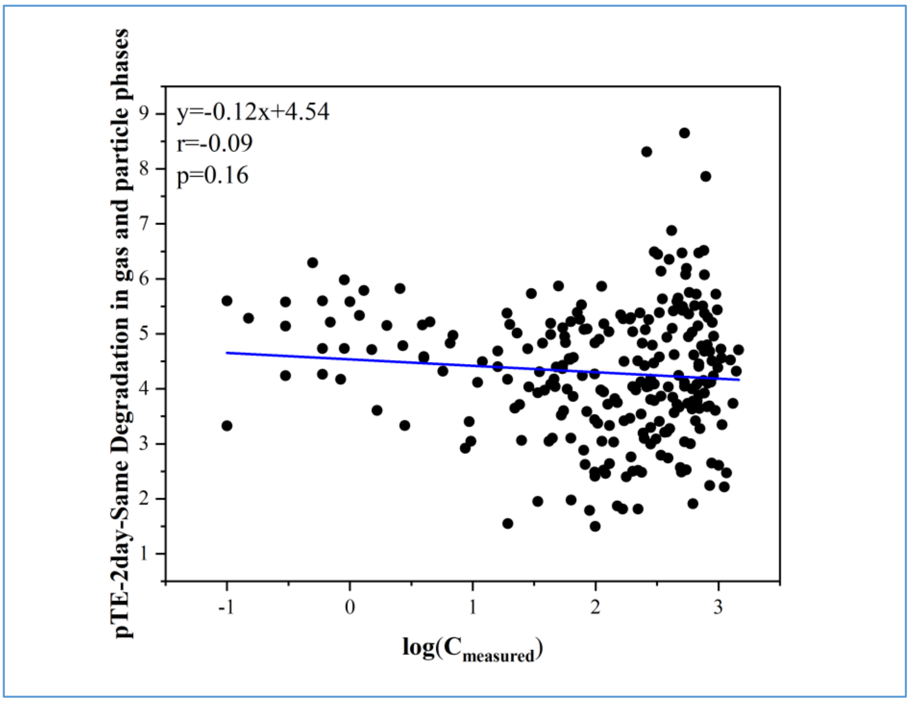

(a)

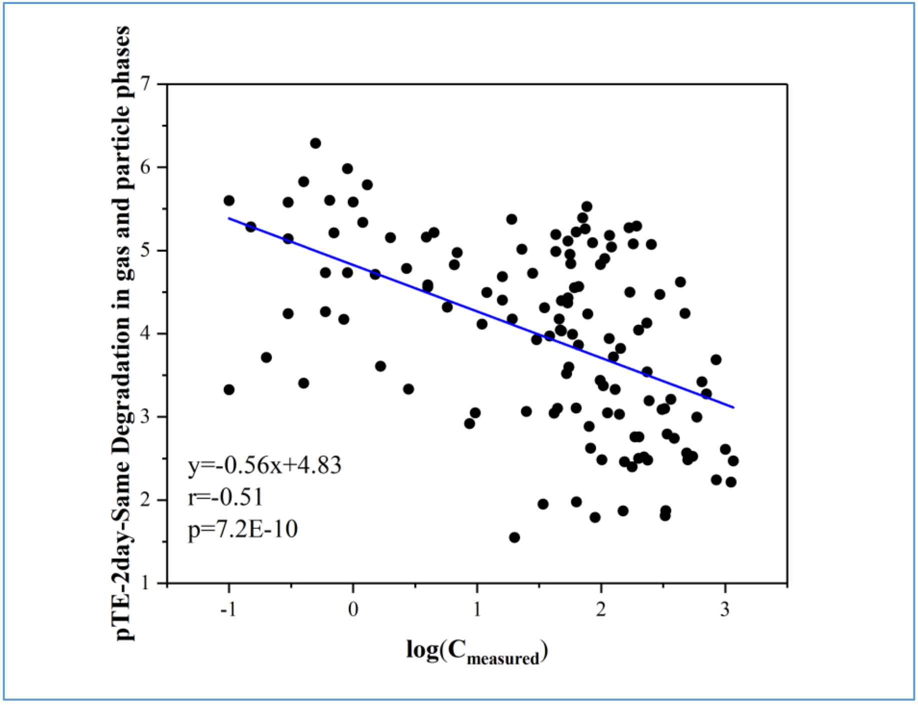

(b)

Figure S3: The linear regression between measured concentrations of TCPP and remoteness (pTE) (a: all the observed data that collected; b: selected observed data in this study)

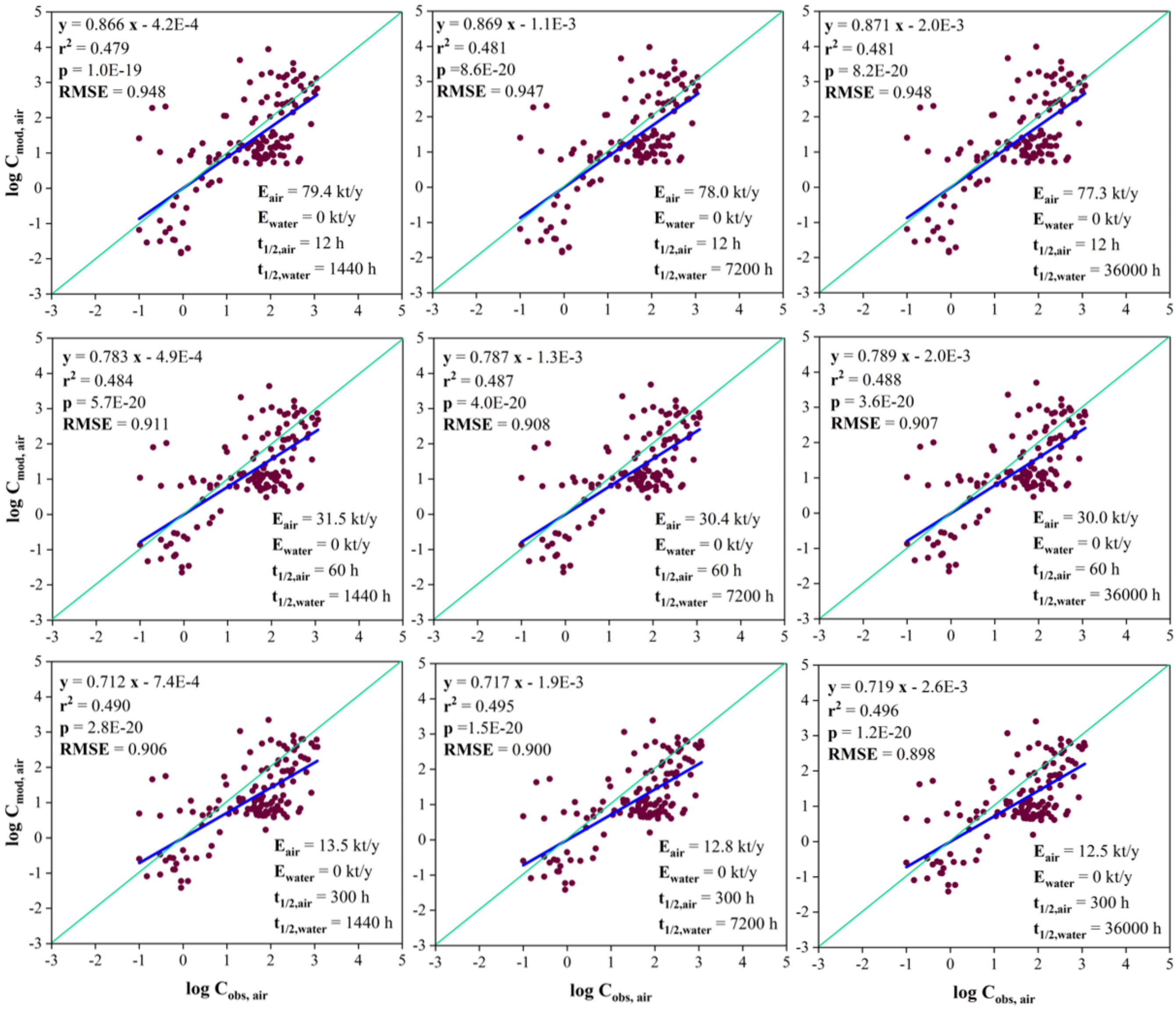

Figure S4:The linear regression plot between modeled and measured concentrations in air of TCPP for scenarios on E_W=0

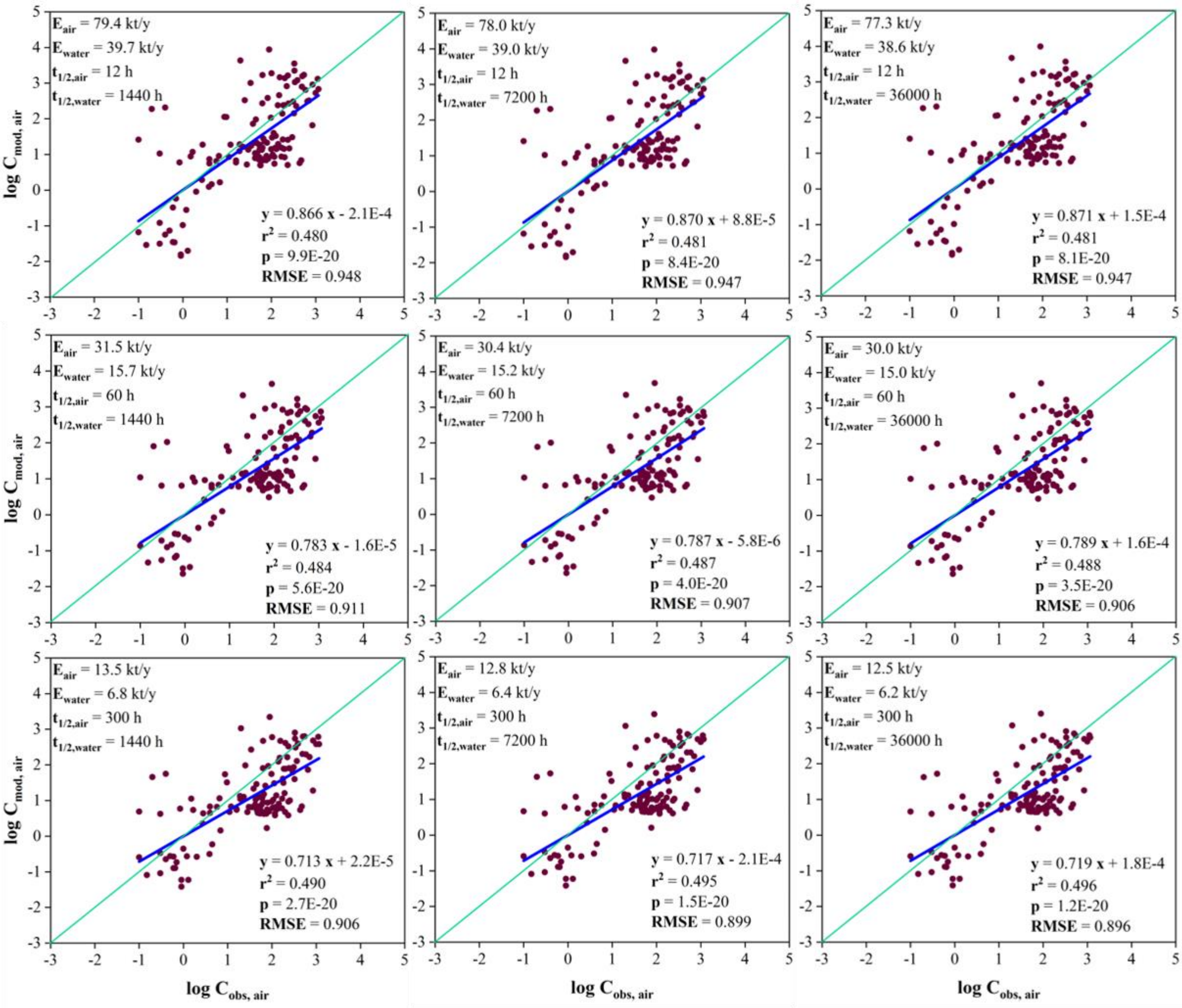

Figure S5: The linear regression plot between modeled and measured concentrations in air of TCPP for scenarios on E_W=0.5E_A

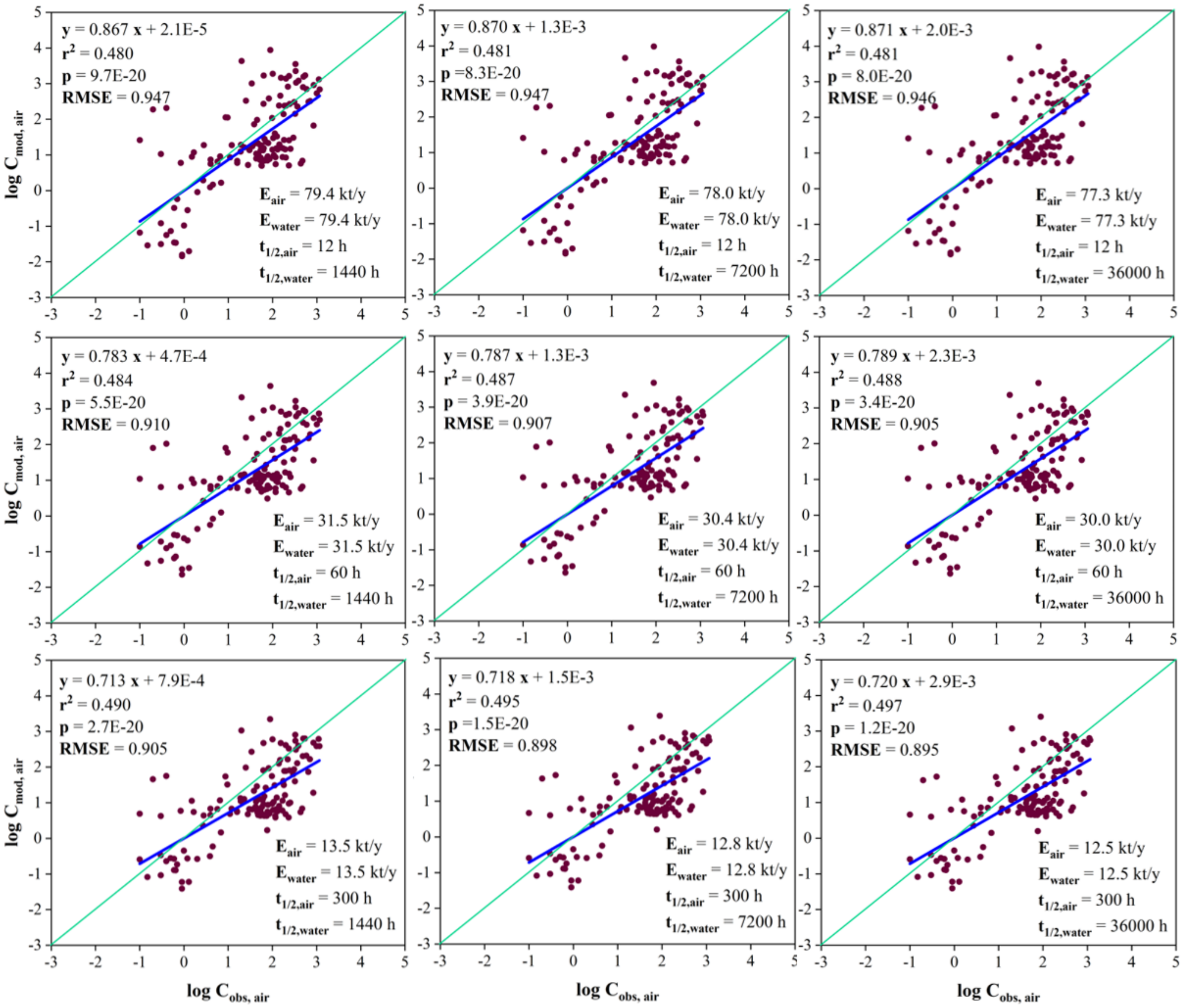

Figure S6:The linear regression plot between modeled and measured concentrations in air of TCPP for scenarios on E_W=E_A

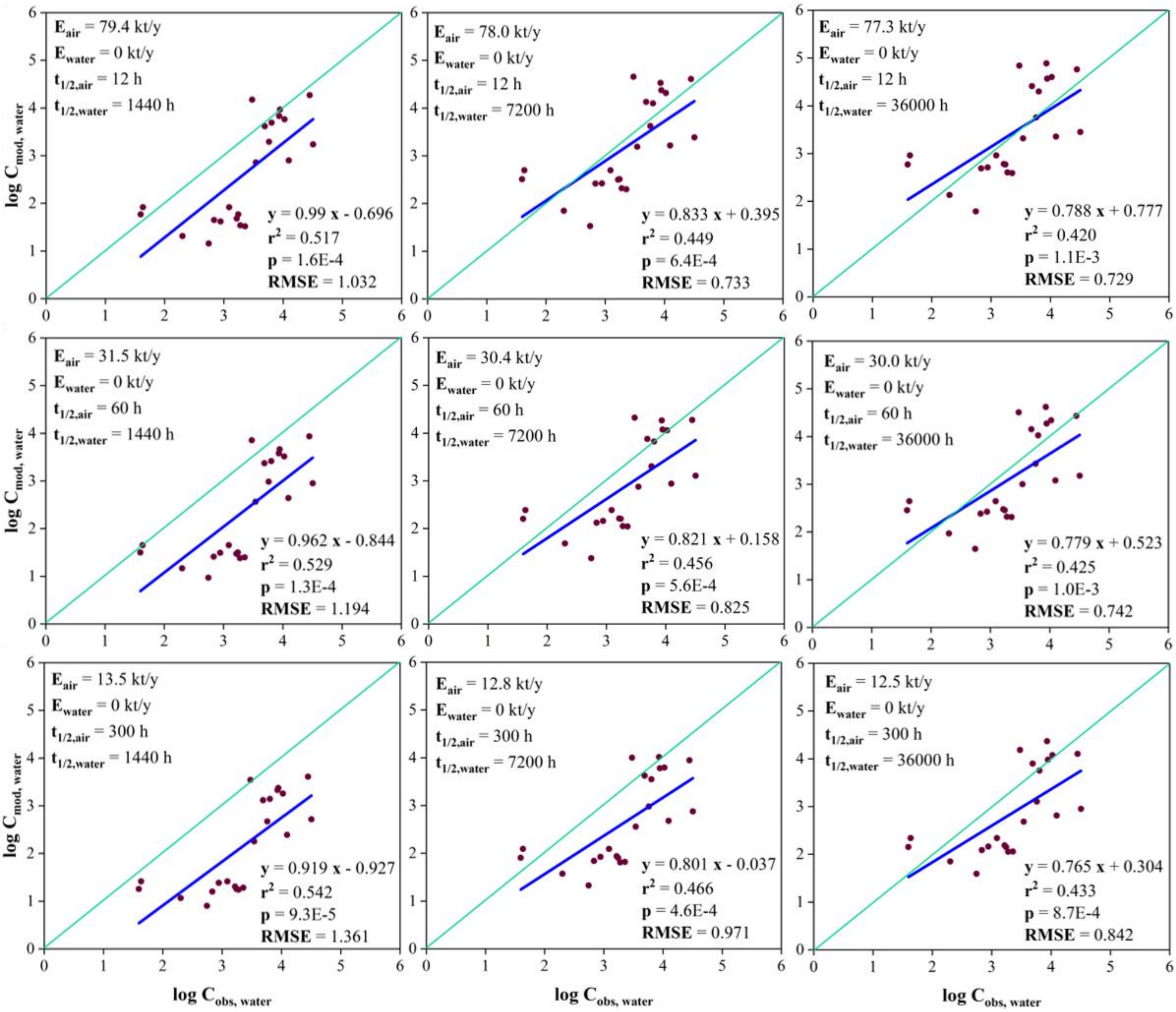

Figure S7: The linear regression plot between modeled and measured concentrations in water of TCPP for scenarios on *E*W=0

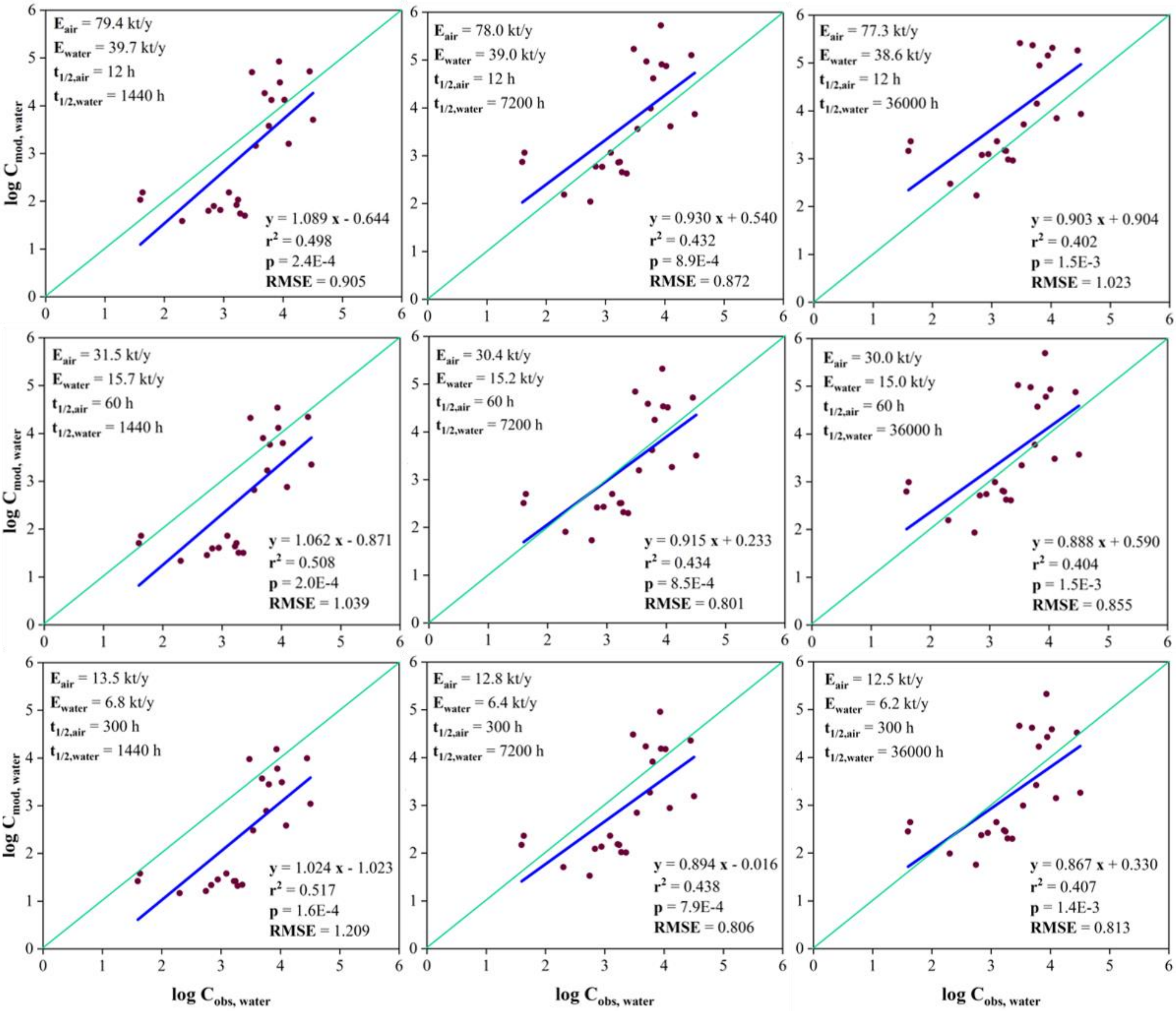

Figure S8: The linear regression plot between modeled and measured concentrations in water of TCPP for scenarios on E_W=0.5E_A

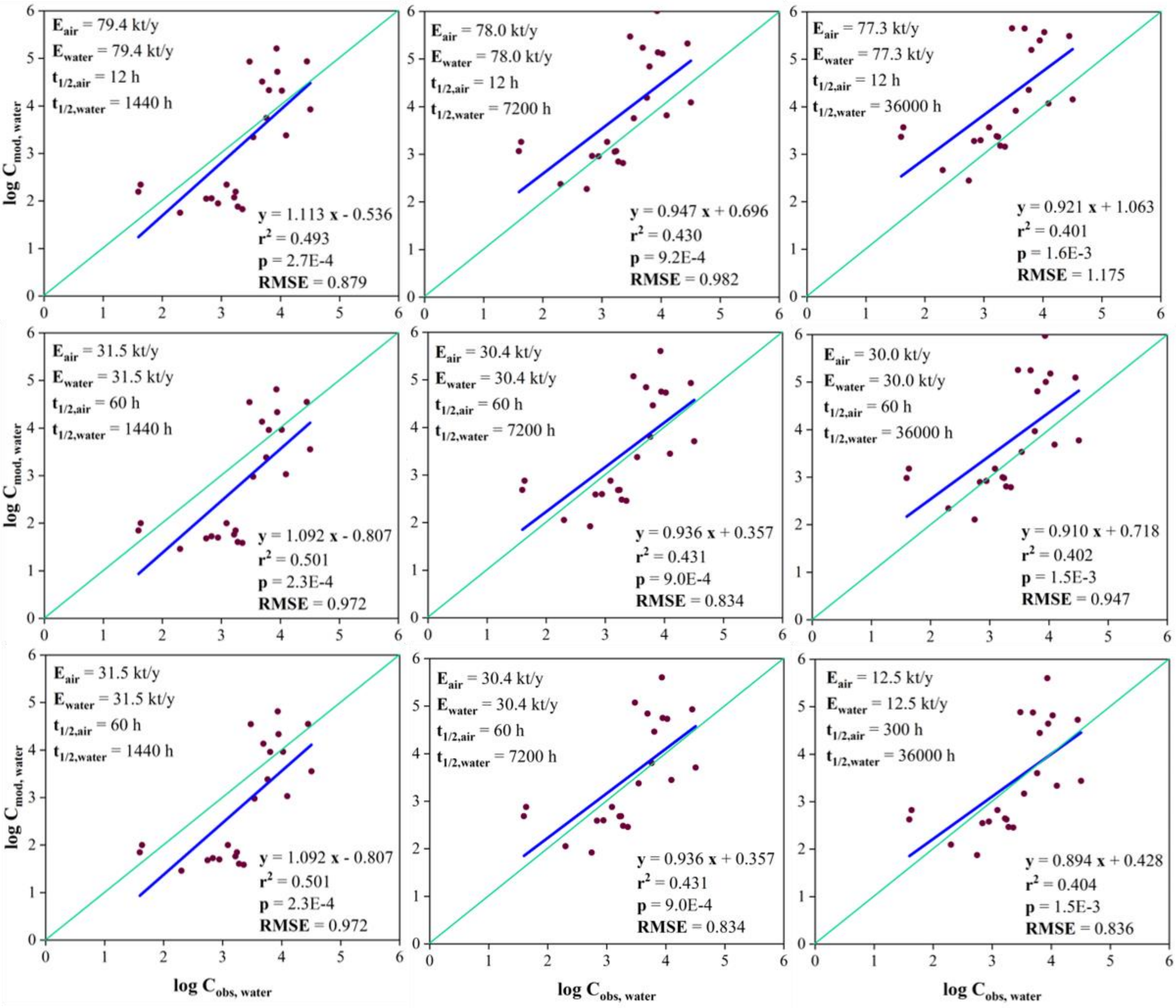

Figure S9: The linear regression plot between modeled and measured concentrations in water of TCPP for scenarios on *E*W=*E*A

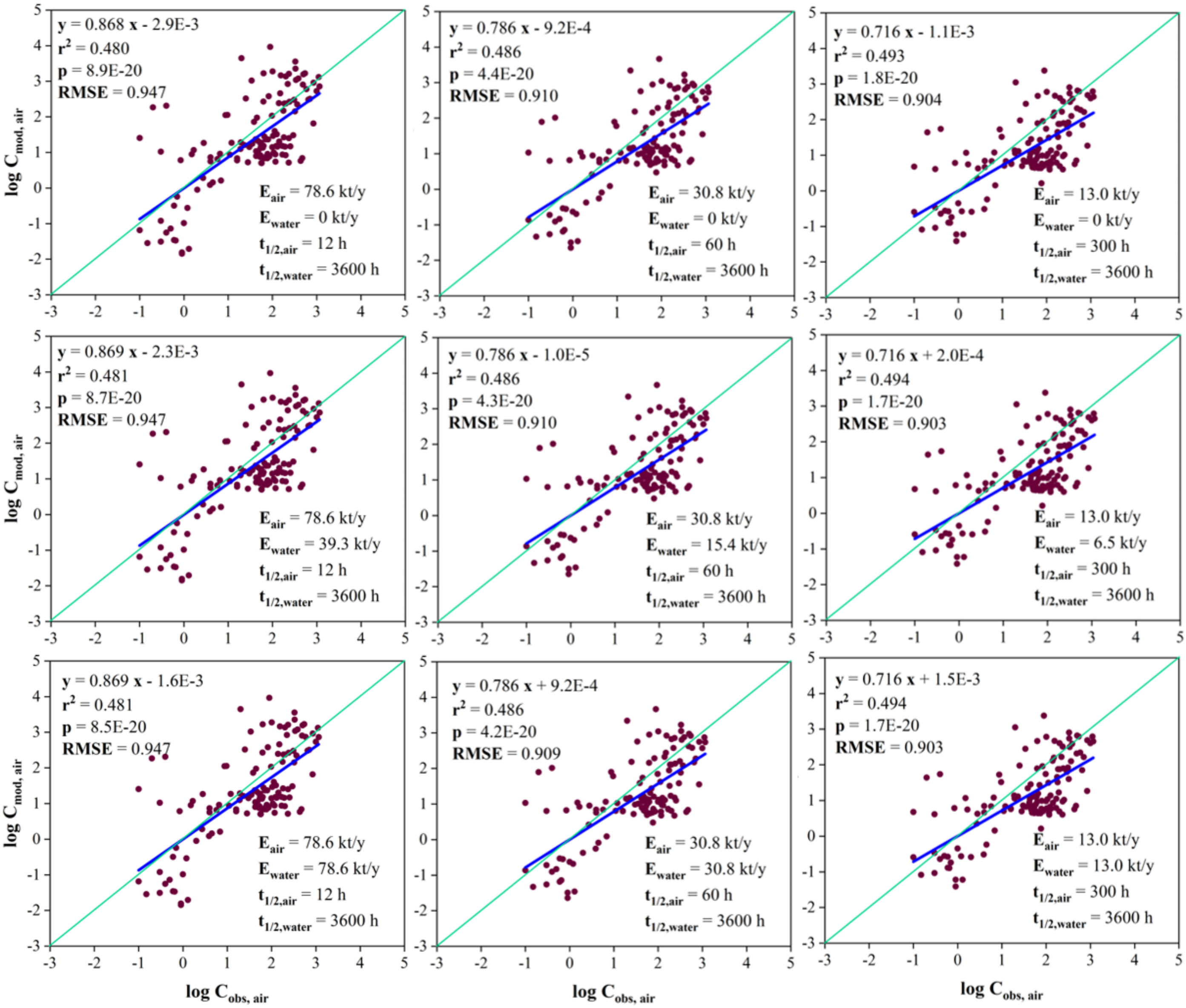

Figure S10: The linear regression plot between modeled and measured concentrations in air of TCPP for scenarios on $t_{1/2,Water}$=3600 h

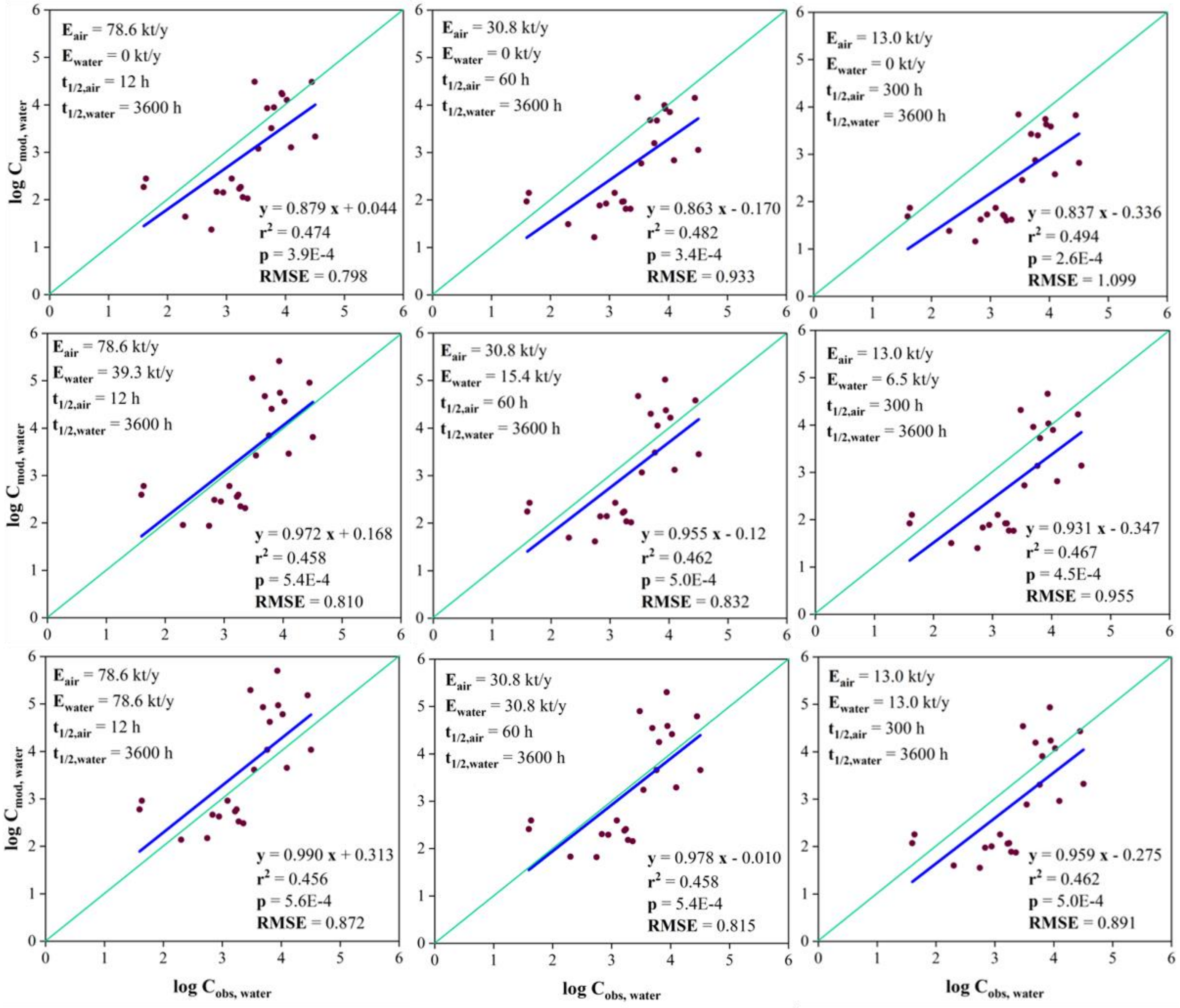

Figure S11: The linear regression plot between modeled and measured concentrations in water of TCPP for scenarios on $t_{1/2,\mathrm{Water}}$=3600 h

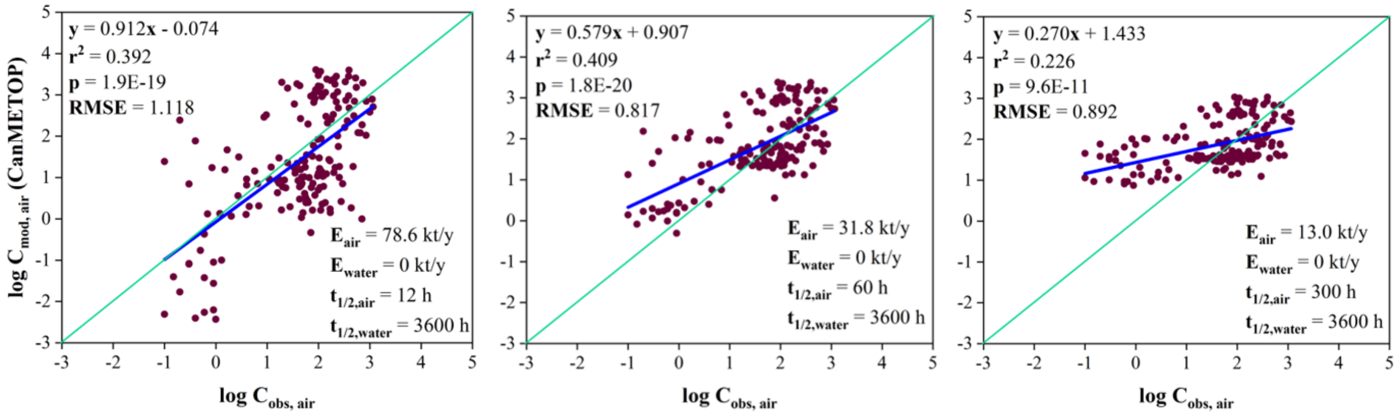

Figure S12: The linear regression plot between modeled by CanMETOP and measured concentrations in air of TCPP for scenarios on $t_{1/2,\mathrm{Water}}$=3600 h and E_W=0

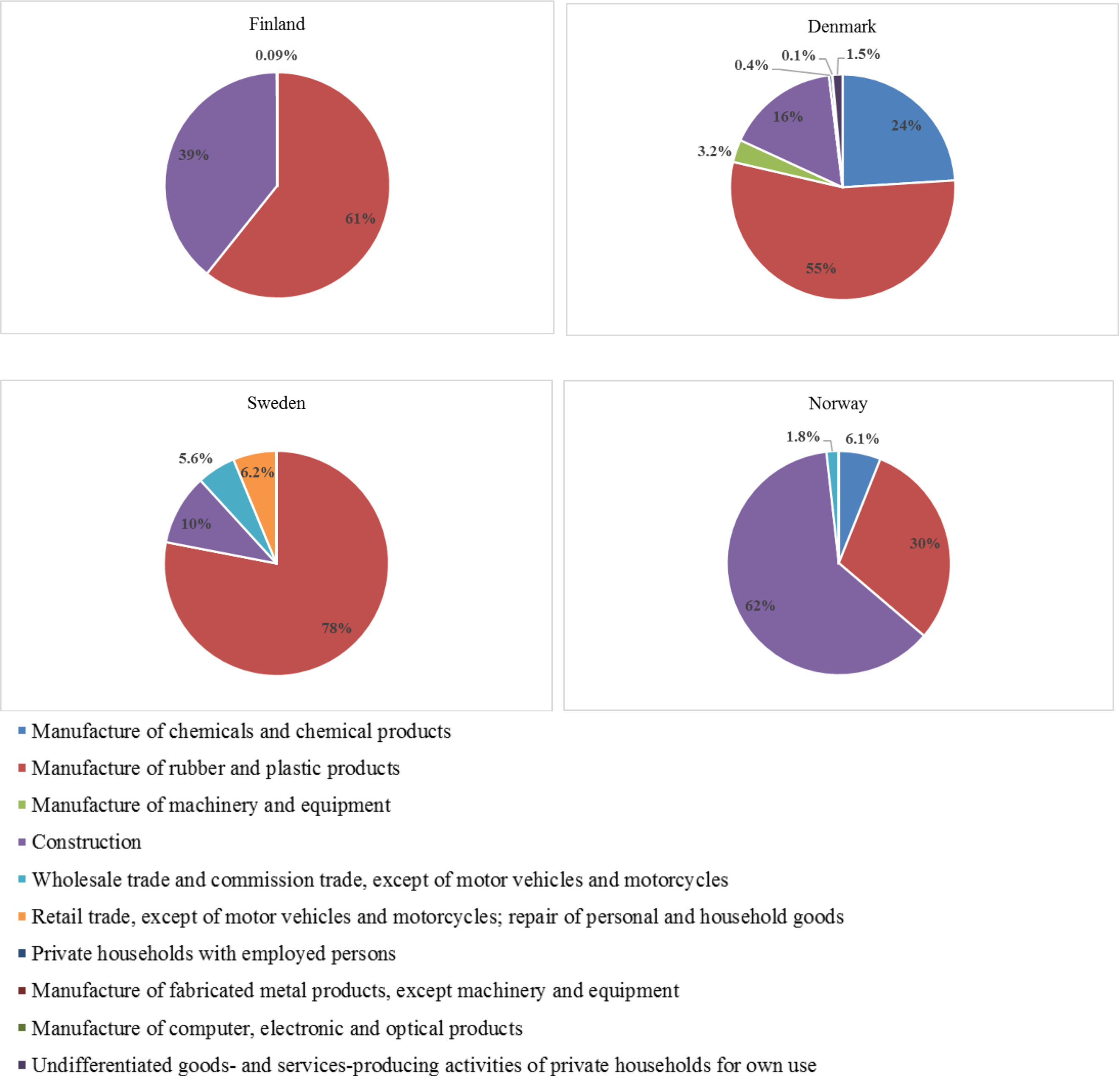

Figure S13. The usage pattern of TCPP in Nordic countries

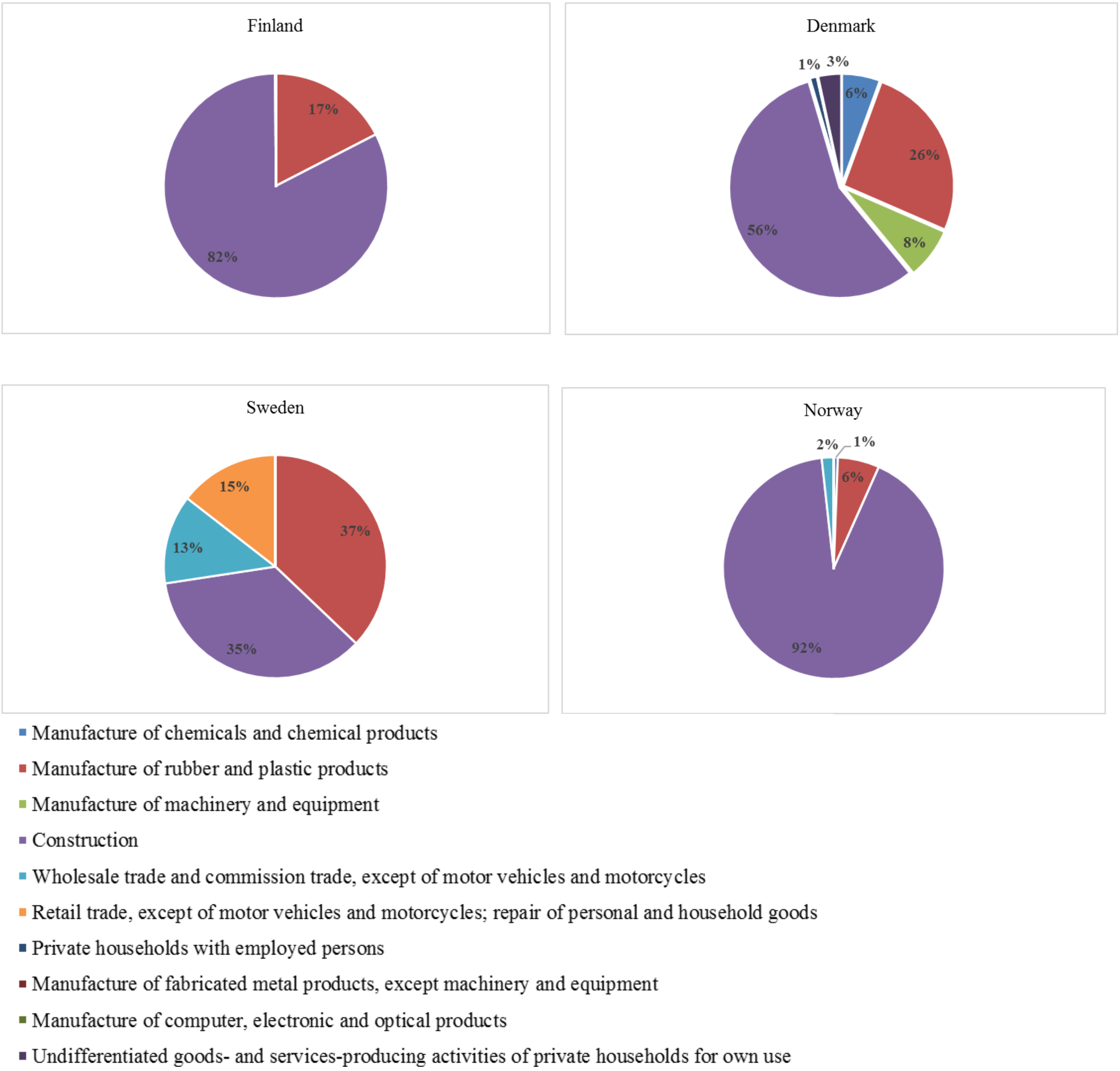

Figure S14: The emission pattern of Nordic countries during the period of 2000 to 2015

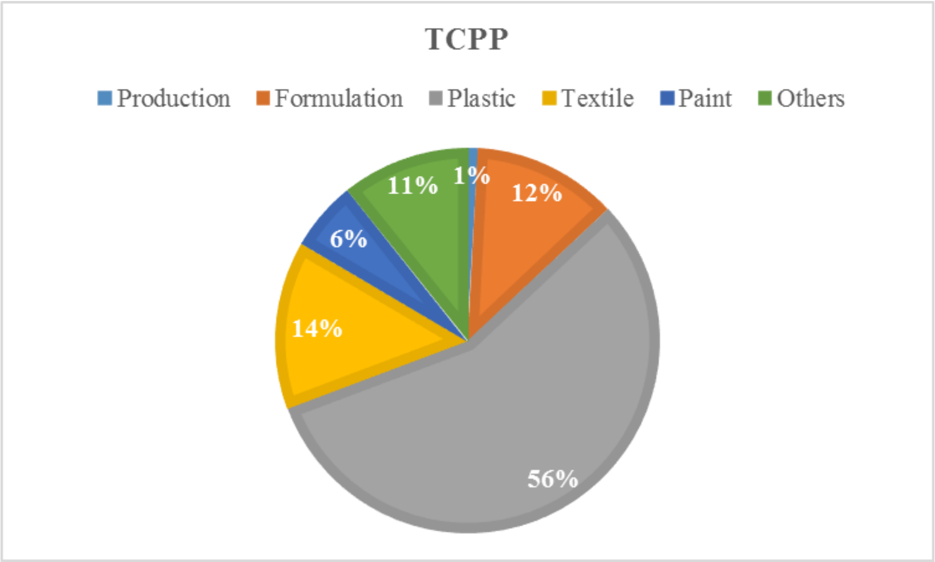

Figure S15. Emission pattern of TCPP in China

Text S1 Selection of measuremnets

In order to know the quality of the measurements, this study adopted quantified remoteness of entire globe from pollutants' emission sources calculated by Göktas et al.[28] The remoteness is generally used as an evidence of chemicals' long-range transport potential.[29] Göktas et al. investigated four hypothetical chemicals classes with different partitioning properties (volatile, semi-volatile, hydrophilic, low-volatility) and having two different half-lives in air (60-day and 2-day).[28] According to the properties of TCPP, this study choose the quantified remoteness of hydrophilic chemicals with scenario that has 2-day half-life both in gaseous and particulate phases for comparison. There is no significant correlations were found between remoteness and the collected measurements (Figure S3a). Considering this result, the measurement data from two studies were excluded because they were too high to be explained by global transport modeling (Table S2). For the rest of the data, significant negative correlation (p=2.3E-13, r=-0.51; Figure S3b) was found between remoteness and measurements in air, substantiating the decreasing trend in atmospheric concentrations from sources to remote regions.

Text S2 Estimate TCPP emission in Nordic countries and China using bottom-up method

1.1. Bottom-up Emission Estimate Frame Work

TCPP can be released into the atmosphere during their production, formulation as well as during the manufacture and usage of the products that contain TCPP.[25] Firstly, the emission sectors are defined for the target region according to the industry and consumption information. Then the emission factors for corresponding sectors are acquired from literatures. Finally, the emissions were estimated through multiplying the volumes in release sectors by the corresponding emission factors. With the production and consumption information that could be achieved, the TCPP emissions in Scandinavian countries and China are calculated in this research.

1.1.1. Data Source

The online database of Substance in preparations in Nordic countries (SPIN) provides data on the usage of TCPP in Scandinavian countries from 2000 to 2015.[30] In China, there is very few TCPP consumption data available. To overcome this problem, a market report on TCPP in China was acquired for this study from Shanghai Shuoxun Chemical Technology Company (SSCTC). Reports that released by SSCTC was ever referred by Jiang et al. to investigate the emissions of short-chain chlorinated paraffins in China.[31] The TCPP report from SSCTC provides the annual production and usage data, import/export of TCPP products, as well as consumption patterns.[32]

1.1.2. Emission Estimate of TCPP in Nordic Countries

The SPIN database provides not only the national total use of TCPP in Nordic countries, but also the industrial use registered with NACE codes (the statistical classification of economic activities in the European Community, abbreviated as NACE).[30] According to the industrial usage, the TCPP emission can be estimated as follows:

$$E_{t,k} = \sum_{m=1}^{n} C_{t,k,m} \times f_m \tag{5}$$

$E_{t,k}$ is the emission of TCPP in year t, country k. $C_{t,k,m}$ is the consumption of TCPP in year t, country k and NACE categories m. f_m is the emission factor of NACE categories m. The emission factors are collected from the literature and used in the estimate of TCPP emissions (Table S13 and S14). The total usage and consumption patterns of TCPP in Nordic countries are showed in Table S15 and Figure S13, respectively. According to the EU risk report, there is no TCPP producer in Nordic countries, so it is unnecessary to consider the emission from production.[25] The EU risk report found that only 40% of TCPP in the matrix is available for release during the manufacture and service life of materials, so this loss percentage is also considered.[25]

1.1.3. Emission Estimate of TCPP in China

According to the market report furnished by SSCTC, in China, TCPP are mainly used in the industries of plastic (55%), textile (11%), paint (12%) and others (22%). Six emission sectors are defined in this study, including (1) production, (2) formulation, (3) plastic sector, (4) textile sector, (5) paint sector, (6) others sector.

The annual national emissions were acquired as follows:

$$E_{j,t}^{T} = C_{j,t} \times f_j \tag{1}$$

$E_{j,t}^{T}$ is the total national emission of sector *j* in year *t*. $C_{j,t}$ is the national consumption in sector *j*, year *t*. f_j is the TCPP emission factor in sector *j*. $C_{j,t}$ is estimated by total national consumption in year *t* multiply the consumed TCPP fraction in sector *j*. The total national consumption is calculated by using the sum of total national production and the import volume minus the export volume in year *t*. The total production of TCPP has increased from 12 kt in 2010 to 16 kt in 2015 and is expected to increase to 24 kt in 2021.[32] Among the produced TCPP, approximately 45% are used for export. Considering imported TCPP, the domestic consumption ranged from 7.3 to 9.1 kt in 2010 to 2015.[32]

1.1.3.1. Emission factors for consumption sectors in China

The emission factors in this study are originated from A-tables of the Technical Guidance Document (TGD),[33] the Emission Scenario Document (ESD) for Additives Used in the Plastics Industry,[27] the European Union (EU) risk assessment reports[25, 34, 35] and reference Document on Best Available Techniques for the Textiles Industry.[36]

1.1.3.2. Emission factor from production of PFRs

For the production of TCPP, the default value for the production of basic chemicals from TGD is adopted in this study.[33] Based on the vapor pressure of TCPP (*VP*<1 Pa), a default factor of 0.00001 is used, which from Table A1.1 of TGD.

1.1.3.3. Emission factor from formulation

According to Table A2.1 of TGD, the default factor of the process of formulation for chemicals (*VP*<10 Pa) used in synthesis is estimated as 0.0025.[33] EU risk report evaluated that the emission factor for the system formulation of TCPP is 0.00025.[25] Compared with the generic calculations from TGD, the EU risk report considered more realistic scenarios. Therefore, In this study, the factor of 0.00025 from EU risk report is adopt for TCPP in formulation sector.[25]

1.1.3.4. Emission factor from plastic sector

For plastic applications, the ESD defaults override those presented in the A-tables from TGD.[27, 33] According to ESD, the flame retardants in plastic additives could be released during the manufacture including raw material handling, compounding, conversion, and during the service life of products.[27] During the handling, the emission loss into the air is evaluated as zero.[27] For the compounding, the emission factor is estimated as 0.00025, with the vapor pressure of TCPP falls within the bracket identified as 'high' within the ESD (>6.5E-4 Pa at 20°C).[25, 27] For the conversion and the plastic products in service-life, the emission factors are both suggested as 0.0025.[27] In total, the emission from plastic sector is 0.00525.

1.1.3.5. Emission factor from textile sector

For textile industry, TCPP can be released from finishing according to the Document on Best Available Techniques for the Textiles Industry.[36] A factor of 0.0041 is used in this study, which used for reactant cross-linking agent in the document. No document provides the emission factor for textile in service life. In this study, a factor of 0.0025 is adopted referred to the emission during service life in plastic sector.[27] In total, the emission factor for the PFRs in the textile sector is 0.0066.

1.1.3.6. Emission factor from paint sector

A more elaborate ESD on coating industry (Paints, Laquers and Varnishes) is currently being developed.[37] However, this document estimated the emission based on the consumption of coating products,[37] which arise the difficulties to evaluate. Because limited usage information is available regarding the paint products that contained TCPP. In TGD, the default emission factors for the paint in application is zero, because the TCPP belongs to the non-volatile class as classified in TGD.[33] Nevertheless, most TCPP are additive flame retardants, which can be migrate to the surface and released into the atmosphere during the service life of the paint.[35, 38] Therefore, in this study, an emission factor of 0.0025 is adopted for the service loss of paint, referred to the plastic sector. In total, the emission factor for the TCPP in the paint sector is 0.0025.

1.1.3.7. Emission factor from other sector

There is no detailed information in SSCTC that explained that how this part of TCPP are used.[32] A factor of 0.0025 is assumed for the entire emission in this sector in this study referred to the paint sector. There is no doubt that this “guess” of emission factor would cause uncertainties to the final evaluation.

1.1.3.8. Loss percentage

During the manufacture and service life of materials, only 40% of TCPP in the matrix is available for release according to EU risk report.[25] For the sector of plastic, textile, paint and others, the final emission factors are calculated by original factor in each sector multiply the loss percentage.

1.2. Results of bottom-up estimate

1.2.1. Emission of TCPP in Nordic countries and China

In Nordic countries, TCPP are mainly released from construction industry and manufacture of rubber and plastic products. The average emission of TCPP in these countries was 2.3 ± 1.8 t/y, with a total discharge of 36 t from year 2000 to 2015 (Table S16). Among the Nordic countries, Finland emitted most TCPP into the air (mean 0.69 ± 0.28 t/y). The emission patterns of TCPP in each Nordic countries were shown in Figure S14.

The annual emission of TCPP in China was 17 ± 1.2 t (Table S17) from 2010 to 2015, with a total release amount of 100 t. The plastic sector emits the most among all emission source categories (Figure S15) with an average discharge of 9.4 ± 0.7 t/y, followed by the textile sector (mean: 2.4 ± 0.2 t/y), others (1.8 ± 0.1 t/y), formulation (2.0 ± 0.2 t/y) and paint sectors (1.0 ± 0.1 t/y) (Table S17).

The total emission factor of TCPP in Nordic countries and China are 0.14 ± 0.06 % and 0.21 ± 0.00 %, respectively.

1.2.2. Uncertainty Analysis

For the bottom-up method, the limited information of TCPP production and consumption pattern contributes to the uncertainty of TCPP emission. For example, In Nordic countries, the recorded data on SPIN may deviate from the actual data in some extent,[30] which may also happen in SSCTC report for China. Furthermore, there is lack of measured emission factors for specific emission scenarios, which also could induce the uncertainties in a large degree.

REFERENCES

1. Brommer, S.; Jantunen, L. M.; Bidleman, T. F.; Harrad, S.; Diamond, M. L., Determination of Vapor Pressures for Organophosphate Esters. *J. Chem. Eng. Data* **2014,** *59*, (5), 1441-1447.
2. Cuthbert, J. M., DM., TCPP: Determination of general physicochemical properties, Report 1613/002. *SafePharm Laboratories, PO Box 45, Derby, UK.* **2002**.
3. Li, C.; Wei, G. L.; Chen, J. W.; Zhao, Y. H.; Zhang, Y. N.; Su, L. M.; Qin, W. C., Aqueous OH Radical Reaction Rate Constants for Organophosphorus Flame Retardants and Plasticizers: Experimental and Modeling Studies. *Environ. Sci. Technol.* **2018,** *52*, (5), 2790-2799.
4. MacLeod, M.; Scheringer, M.; Hungerbuhler, K., Estimating enthalpy of vaporization from vapor pressure using Trouton's rule. *Environ. Sci. Technol.* **2007,** *41*, (8), 2827-2832.
5. Wohrnschimmel, H.; MacLeod, M.; Hungerbuhler, K., Emissions, Fate and Transport of Persistent Organic Pollutants to the Arctic in a Changing Global Climate. *Environ. Sci. Technol.* **2013,** *47*, (5), 2323-2330.
6. Rauert, C.; Harner, T.; Schuster, J. K.; Quinto, K.; Fillmann, G.; Castillo, L. E.; Fentanes, O.; Ibarra, M. V.; Miglioranza, K. S. B.; Rivadeneira, I. M.; Pozo, K.; Puerta, A. P.; Zuluagaj, B. H. A., Towards a regional passive air sampling network and strategy for new POPs in the GRULAC region: Perspectives from the GAPS Network and first results for organophosphorus flame retardants. *Sci. Total Environ.* **2016,** *573*, 1294-1302.
7. Castro-Jimenez, J.; Berrojalbiz, N.; Pizarro, M.; Dachs, J., Organophosphate Ester (OPE) Flame Retardants and Plasticizers in the Open Mediterranean and Black Seas Atmosphere. *Environ. Sci. Technol.* **2014,** *48*, (6), 3203-3209.
8. Möller, A.; Xie, Z. Y.; Caba, A.; Sturm, R.; Ebinghaus, R., Organophosphorus flame retardants and plasticizers in the atmosphere of the North Sea. *Environ. Pollut.* **2011,** *159*, (12), 3660-3665.
9. Salamova, A.; Hermanson, M. H.; Hites, R. A., Organophosphate and Halogenated Flame Retardants in Atmospheric Particles from a European Arctic Site. *Environ. Sci. Technol.* **2014,** *48*, (11), 6133-6140.
10. Salamova, A.; Ma, Y. N.; Venier, M.; Hites, R. A., High Levels of Organophosphate Flame Retardants in the Great Lakes Atmosphere. *Environ. Sci. Technol. Lett.* **2014,** *1*, (1), 8-14.
11. Salamova, A.; Peverly, A. A.; Venier, M.; Hites, R. A., Spatial and Temporal Trends of Particle Phase Organophosphate Ester Concentrations in the Atmosphere of the Great Lakes. *Environ. Sci. Technol.* **2016,** *50*, (24), 13249-13255.
12. Lai, S.; Xie, Z.; Song, T.; Tang, J.; Zhang, Y.; Mi, W.; Peng, J.; Zhao, Y.; Zou, S.; Ebinghaus, R., Occurrence and dry deposition of organophosphate esters in atmospheric particles over the northern South China Sea. *Chemosphere* **2015,** *127*, 195-200.
13. Li, J.; Xie, Z.; Mi, W.; Lai, S.; Tian, C.; Emeis, K.-C.; Ebinghaus, R., Organophosphate Esters in Air, Snow and Seawater in the North Atlantic and the Arctic. *Environ. Sci. Technol.* **2017,** *51*, 6887−6896.

14. Li, J.; Tang, J. H.; Mi, W. Y.; Tian, C. G.; Emeis, K. C.; Ebinghaus, R.; Xie, Z. Y., Spatial Distribution and Seasonal Variation of Organophosphate Esters in Air above the Bohai and Yellow Seas, China. *Environ. Sci. Technol.* **2018,** *52*, (1), 89-97.

15. Cheng, W. H.; Xie, Z. Q.; Blais, J. M.; Zhang, P. F.; Li, M.; Yang, C. Y.; Huang, W.; Ding, R.; Sun, L. G., Organophosphorus esters in the oceans and possible relation with ocean gyres. *Environ. Pollut.* **2013,** *180*, 159-164.

16. Sühring, R.; Diamond, M. L.; Scheringer, M.; Wong, F.; Pucko, M.; Stern, G.; Burt, A.; Hung, H.; Fellin, P.; Li, H.; Jantunen, L. M., Organophosphate Esters in Canadian Arctic Air: Occurrence, Levels and Trends. *Environ. Sci. Technol.* **2016,** *50*, (14), 7409-7415.

17. Rauert, C.; Schuster, J. K.; Eng, A.; Harner, T., Global Atmospheric Concentrations of Brominated and Chlorinated Flame Retardants and Organophosphate Esters. *Environ. Sci. Technol.* **2018,** *52*, (5), 2777-2789.

18. Castro-Jimenez, J.; Gonzalez-Gaya, B.; Pizarro, M.; Casal, P.; Pizarro-Alvarez, C.; Dachs, J., Organophosphate Ester Flame Retardants and Plasticizers in the Global Oceanic Atmosphere. *Environ. Sci. Technol.* **2016,** *50*, (23), 12831-12839.

19. Möller, A.; Sturm, R.; Xie, Z. Y.; Cai, M. H.; He, J. F.; Ebinghaus, R., Organophosphorus Flame Retardants and Plasticizers in Airborne Particles over the Northern Pacific and Indian Ocean toward the Polar Regions: Evidence for Global Occurrence. *Environ. Sci. Technol.* **2012,** *46*, (6), 3127-3134.

20. McDonough, C. A.; De Silva, A. O.; Sun, C. X.; Cabrerizo, A.; Adelman, D.; Soltwedel, T.; Bauerfeind, E.; Muir, D. C. G.; Lohmann, R., Dissolved Organophosphate Esters and Polybrominated Diphenyl Ethers in Remote Marine Environments: Arctic Surface Water Distributions and Net Transport through Fram Strait. *Environ. Sci. Technol.* **2018,** *52*, (11), 6208-6216.

21. Kim, U. J.; Kannan, K., Occurrence and Distribution of Organophosphate Flame Retardants/Plasticizers in Surface Waters, Tap Water, and Rainwater: Implications for Human Exposure. *Environ. Sci. Technol.* **2018,** *52*, (10), 5625-5633.

22. Bollmann, U. E.; Möller, A.; Xie, Z. Y.; Ebinghaus, R.; Einax, J. W., Occurrence and fate of organophosphorus flame retardants and plasticizers in coastal and marine surface waters. *Water Res.* **2012,** *46*, (2), 531-538.

23. Zhong, M. Y.; Tang, J. H.; Mi, L. J.; Li, F.; Wang, R. M.; Huang, G. P.; Wu, H. F., Occurrence and spatial distribution of organophosphorus flame retardants and plasticizers in the Bohai and Yellow Seas, China. *Mar. Pollut. Bull.* **2017,** *121*, (1-2), 331-338.

24. Rodgers, T. F. M.; Truong, J. W.; Jantunen, L. M.; Helm, P. A.; Diamond, M. L., Organophosphate Ester Transport, Fate, and Emissions in Toronto, Canada, Estimated Using an Updated Multimedia Urban Model. *Environ. Sci. Technol.* **2018,** *52*, (21), 12465-12474.

25. EU Risk Assessment Report, Tris(2-chloro-1-methylethyl) phosphate (TCPP). CAS No.: 13674-84-5. EINECS No.: 237-158-7. **2008**.

26. Breivik, K.; Sweetman, A.; Pacyna, J. M.; Jones, K. C., Towards a global historical emission inventory for selected PCB congeners - A mass balance approach-3. An update. *Sci. Total Environ.* **2007,** *377*, (2-3), 296-307.

27. Series on Emission Scenario Documents Number 3, Emission Scenario Document on Plastics Additives. ENV/JM/MONO(2004)8/REV1.

28. Goktas, R. K.; MacLeod, M., Remoteness from sources of persistent organic pollutants in the multi-media global environment. *Environ. Pollut.* **2016,** *217*, 33-41.

29. von Waldow, H.; MacLeod, M.; Scheringer, M.; Hungerbuhler, K., Quantifying Remoteness from Emission Sources of Persistent Organic Pollutants on a Global Scale. *Environ. Sci. Technol.* **2010,** *44*, (8), 2791-2796.

30. Substance in preparations in Nordic countries (SPIN) online database. http://www.spin2000.net/spinmyphp/. Accessed in 01.2018.

31. Jiang, W. Y. H.; Huang, T.; Mao, X. X.; Wang, L.; Zhao, Y.; Jia, C. H.; Wang, Y. N.; Gao, H.; Ma, J. M., Gridded emission inventory of short-chain chlorinated paraffins and its validation in China. *Environ. Pollut.* **2017,** *220*, 132-141.

32. Shanghai Shuoxun Chemical Technology Company (SSCTC). The Market Research Report of PFRs. http://www.shuoxun-report.com/. **2017**.

33. Technical Guidance Document on Risk Assessment in support of Commission Directive 93/67/EEC on Risk Assessment for New Notified Substances, Commission regulation (EC) No 1488/94 on Risk Assessment for Existing Substances and Directive 98/8/EC of the European Parliament and of the Council concerning the placing of biocidal products on the market. European Commission Joint Research Centre, European Communities. **2003**.

34. EU Risk Assessment Report, Tris(2-chloro-1-(chloromethyl)ethyl) phosphate (TDCP). CAS No.: 13674-87-8. EINECS No.: 237-159-2. **2008**.

35. EU Risk Assessment Report, Tris(2-chloroethyl) phosphate (TCEP) CAS-No.: 115-96-8. EINECS-No.: 204-118-5. **2009**.

36. Reference Document on Best Available Techniques for the Textiles Industry. Integrated Pollution Prevention and Control (IPPC). **2003**.

37. Series on Emission Scenario Documents Number 22, Emission Scenario Document on coating industry (Paints, Laquers and Varnishes). ENV/JM/MONO(2009)24.

38. Van der Veen, I.; de Boer, J., Phosphorus flame retardants: Properties, production, environmental occurrence, toxicity and analysis. *Chemosphere* **2012,** *88*, (10), 1119-1153.

Paper IV

Global multimedia source-receptor relationships for tris-(1-chloro-2-propyl) phosphate (TCPP)

Global multimedia source-receptor relationships for tris-(1-chloro-2-propyl) phosphate (TCPP)

Jing Li[†,⊥], Fangyuan Zhao[‡], Zhiyong Xie[†*], Ralf Ebinghaus[†], Kay-Christian Emeis[†,⊥], Chongguo Tian[§], Matthew MacLeod[‡*]

[†]Helmholtz-Zentrum Geesthacht, Centre for Materials and Coastal Research, Institute of Coastal Research, Geesthacht, 21502, Germany

[‡]Department of Environmental Science and Analytical Chemistry, ACES, Stockholm University, Svante Arrhenius väg 8, Stockholm, SE-114 18, Sweden

[§]Key Laboratory of Coastal Environmental Processes and Ecological Remediation, Yantai Institute of Coastal Zone Research, CAS, Yantai, 264003, China

[⊥]Universität Hamburg, Department of Geosciences, Hamburg, 20144, Germany

ABSTRACT

Tris-(1-chloro-2-propyl) phosphate (TCPP) is an organophosphate ester (OPE) that is widely used as a flame retardant. It has been detected in the environment globally even in pristine areas. This study investigated the global source-receptor relationships of TCPP using a multimedia long-range transport (LRT) model, namely, the Berkeley-Trent Global Contaminant Fate Model (BETR-Global). In a scenario with global emission rates to air and water of 78.6 kt/y and 39.8 kt/y, respectively, 114 t of TCPP are found in the Arctic (after spin up for eight years) which is two orders of magnitude higher than the amount found in the Antarctic (0.36 t). More than 95.0% of TCPP in polar regions is present in seawater, and oceanic transport is the major pathway that conveys TCPP to Arctic seawater (89.1%).In contrast, oceanic and atmospheric transport are both important for the Antarctic. Europe, Asia and North America are identified as the major source areas for Arctic TCPP contamination, due to not only the high emission rates in these regions, but also their relative proximity to the Arctic. For the Antarctic, TCPP mainly originates from South America and the Indonesia to Australia region, which reflects that the chemical is not efficiently transported across the equator from regions of higher emission in the northern hemisphere. A seasonal trend is shown for TCPP transport in air with higher concentrations in winter than in summer in polar regions, mainly due to the variations in hydroxyl radical concentrations and temperatures.

INTRODUCTION

Tris-(1-chloro-2-propyl) phosphate (TCPP) is a chlorinated organophosphate ester (OPE) that has been used extensively throughout the world.[1] It is mainly used as an additive flame retardant, which means it can easily leach into the environment during its application lifetime.[1] TCPP accounted for more than fifty percent of OPEs consumed in Europe in 2000, and this number is expected to have remained stable or even increased since that time.[2] Because of its high production and usage as well as global occurrence even in polar regions, TCPP has attracted increasing scientific attention.[3-6]

Pollutants that can be transported over long distances via air and water are an international concern.[7] The Task Force on Hemispheric Transport of Air Pollution (TF-HTAP) was established in 2005 to improve the understanding of intercontinental transport of air pollution in the northern hemisphere.[8] Wöhrnschimmel et al. reported that air pollution with α-hexachlorocyclohexane (α-HCH) showed periods of high self-pollution in source regions due to its emission peak occurring at different times.[7] Malanichev et al. highlighted that the contamination of polychlorinated biphenyls (PCBs) in the Arctic in 1996 were mainly derived from emissions in Europe and Russia followed by the Americas.[9] Moreover, North America has been recognized as the major contributor to Arctic ozone pollution.[10]

In an earlier study, we developed gridded global TCPP emissions estimates by comparing modeled concentrations generated with a multimedia long-range transport (LRT) model under different emission scenarios with measured concentrations.[11] In addition to emission estimates, these model scenarios can provide useful information for assessing the global distribution of TCPP and source-receptor relationships and transport pathways, which is the aim of this paper.

In this study, we present model results for our preferred global TCPP emission scenario with a focus on 1) the TCPP contamination levels in remote environments, 2) the relative contribution of anthropogenic emissions in different global regions to the pollution of polar regions, and 3) major pathways that contribute to TCPP pollution in polar regions in our model scenario. Long-range transport in both the oceans and the atmosphere through the coupled atmosphere-ocean system is modeled in the Berkeley-Trent Global Contaminant Fate Model (BETR-Global).

METHODS

Emissions estimate

Gridded global emissions of TCPP were modeled in several scenarios using BETR-Global in our previous work.[11] The modeled and measured concentrations were compared for remote receptor stations.[11] The results showed that 50% of modeled TCPP levels were within a factor of 8.9 and 6.5 of the measurements in air and seawater, respectively, with our preferred "best estimate" scenario.[11] The "best estimate" scenario set the half-lives of TCPP in air and water as 12 and 3,600 h, respectively, and the release of TCPP directly to water (Ew) was considered to occur at half the rate of the release to air (Ea). This study uses this "best estimate" scenario to explore source-receptor relationships for TCPP. In this scenario, the total global emission rates of TCPP to air (Ea) and water (Ew) are 78.6 kt/y (Gg/y) and 39.3 kt/y, respectively, and are directly proportional to the intensity of artificial light emitted to space from Earth at nighttime.

The BETR-Global model

BETR-Global is a multimedia chemical fate and LRT model at the global scale.[12, 13] It represents the global environment as grid cells, and each cell contains up to seven compartments: upper atmosphere, lower atmosphere, vegetation, freshwater, ocean, soil and freshwater sediment. BETR-Research is the implementation of BETR-Global in the Python programming language (http://betrs.sourceforge.net). In this study, we adopted BETR-Research with a spatial resolution of 3.75° × 3.75° grid cells. The physical/chemical properties of TCPP applied as inputs to BETR Global are listed in Table S1.

Global source-receptor relationships

Seven continental areas are studied as TCPP source regions in this study, including four northern hemisphere areas defined by the TF-HTAP (North America, Europe, East Asia, South Asia, Figure 1) and three southern hemisphere areas (South America, Africa and the Indonesia to Australia region, Figure 1). The polar regions (Arctic and Antarctic) are defined as the principal receptor regions of interest (Figure 1).

The source-receptor relationships are simulated by running the model with global emissions first and then with emissions only occurring in one source region at a time (eight scenarios). The rest of the world, excluding the target source regions, is also set as an emission region in a ninth scenario to validate the results. To clarify the contributions of releases of TCPP to air and water, these scenarios are run with emissions only to air (only Ea), only to water (only Ew) and to both air and water (Ea+Ew). In total of 24 scenarios are designed (Table S2). In each scenario, the model is run for eight years (spin-up) to achieve stable environmental TCPP levels, considering the accumulations from the various media. The statistics in this study for source-receptor relationships are conducted using the results of 8th year.

RESULTS AND DISCUSSION

Global TCPP pollution

The modeled global annual mean concentrations of TCPP are 186 pg/m^3 in lower air, 20.5 pg/m^3 in upper air and 2,280 pg/L in seawater. The spatial distribution of TCPP levels in air and seawater are shown in Figure 2 and 3. High modeled concentrations are found in the northern hemisphere (annual mean: 352 pg/m^3 in lower air and 4,430 pg/L in seawater) at levels one order of magnitude higher than those of the south hemisphere (annual mean: 20.7 pg/m^3 in lower air, 134 pg/L in seawater), reflecting the stronger anthropogenic sources in the northern hemisphere. Over the northern Pacific and northern Atlantic Oceans, high concentrations in air (up to hundreds of pg/m^3) are found. There is a marked annual outflow of TCPP from East Asia towards North America associated with the prevailing westerly wind over the northern Pacific (Figure 2).[14] TCPP-laden air is delivered by a westerly wind flow from North America to the northern Atlantic Ocean towards Western Europe (Figure 2).[15]

TCPP pollution in source regions

In source regions, local emissions account for over 80.0% of TCPP contamination (Table S3 and S4). Atmospheric releases (Ea) are the major source of local TCPP air pollution (>98.2%), and it contribute from 5.9% (South Asia) to 31.6% (Indonesia to Australia) (mean: 19.4%) of the TCPP in regional seawater through atmospheric deposition (Table S5). For North America, Europe and South America, the contributions of extraregional sources to the total environmental burden of TCPP are all less than 3.0% (Table S3 and S4). The Indonesia and Australia area contributes more than 8.0% of the TCPP pollution in East Asia. Europe is the dominant extraregional pollution source for both South Asia (>2.5%) and Africa (6.2% in scenario with only Ea). The global distribution of TCPP levels in air with each source region is shown in Figure 4.

TCPP pollution in the polar regions

The annual average TCPP concentrations are 16.2 pg/m^3, 38.1 pg/m^3 and 136 pg/L in the Arctic lower air, upper air and seawater compartments, respectively (scenario: Ew+Ea; Table S6). In total, 114 t of TCPP is found in the Arctic, with 98.4% distributed in seawater (113 t) and 1.6%

in air (1.9 t) (Table S7, S8). Ea contributes more than 99.8% of TCPP in the Arctic atmosphere (Table S9). However, in Arctic seawater, 51.4% of TCPP originated from Ea and 48.6% from Ew (Table S9). The major contributor of TCPP in the Arctic is Europe (23.0%, 26.4 t), followed by East Asia (7.8%, 8.9 t) and North America (0.9%, 1.0 t) (Table 1 and S7). The other major contributors are northern Europe and northern Asia (north of Russia), which are not included in target source regions in this study (Table S10). For TCPP in the Arctic that originated from Europe, Ea and Ew account for 48.0% and 51.6% (Table S9), respectively. Ew is the major source (76.2%) from East Asia that affects the Arctic rather than Ea (23.8%), which is in contrast to the results for North America (Table S9).

For the Antarctic, the annual mean concentrations of TCPP are 0.10 pg/m^3, 0.13 pg/m^3 and 0.10 pg/L in lower air, upper air and seawater, respectively (scenario: (Ew+Ea); Table S6), which are 2-3 orders of magnitude lower than those of the Arctic. An amount of 0.36 t TCPP is found in the Antarctic, with 95.7% in seawater and 4.3% in air, which are similar proportions as those in the Arctic (Table S11 and S12). The difference with the Arctic is that Ea plays a more important role (83.0%) than Ew (17.0%) in the Antarctic (Table S13). South America (57.0%), the Indonesia to Australia region (18.4%) and Africa (2.3%) are the main sources of TCPP in the Antarctic (Table 1 and S12). Moreover, all three regions polluted the Antarctic with TCPP from Ea (>80.0%, Table S13).

Loading pathways to polar regions

As discussed above, most of the inventory of TCPP in polar regions is present in seawater (Arctic: 98.4%, Antarctic: 95.7%). TCPP can be transported to polar seawater through ocean current transport, atmospheric transport and deposition, as well as a combination of the two. In order to identify the pathways that convey TCPP to polar seawater, four more scenarios were designed by disabling the water inflow, wet deposition, dry deposition and air-seawater exchange processes in polar regions, respectively. In these scenarios, TCPP emission that occurs both in air and water (Ea+Ew) globally was used. Results show that, oceanic transport accounts for 89.1% of TCPP in Arctic seawater, followed by wet deposition (9.7%, Table S14). Dry deposition and air-seawater exchange processes have little impact. For the Antarctic, the dominant input pathway is also oceanic transport (46.3%), although its role is less important than in the Arctic. Atmospheric deposition contributes more than 40.0% of TCPP in Antarctic seawater (wet deposition: 24.9%, dry deposition: 9.7%, air-seawater exchange: 8.1%, Table S14). In both Arctic or Antarctic, wet deposition is the major pathway that conveys TCPP from air to seawater. The total contributions of oceanic and atmospheric transport are less than 100% (Arctic: ~98.9%, Antarctic: ~89.0%) in Arctic and Antarctic seawater, which is due to the change of dynamic equilibrium when disabling processes in the designed scenarios.

Seasonal variation in TCPP LRT

A seasonal trend is observed for modeled TCPP levels in the air in the polar receptor regions, with higher concentrations in winter than in summer. In February, a total of 5,070 kg TCPP is found in Arctic air, which is two orders of magnitude higher than in August (35.4 kg) (scenario: Ew+Ea). For the Antarctic, there is 45.6 kg of TCPP in August (winter in the southern hemisphere), which is two orders of magnitude higher than that of February (0.47 kg).

Several factors could contribute to this phenomenon, such as seasonally variable hydroxyl radical (·OH) concentrations, wind patterns, temperatures and precipitation conditions. To clarify the impact of these factors, four scenarios were designed using constant values (annual mean) instead of seasonal data for these four factors. The results show that the ·OH concentration is the major contributor to this phenomenon, followed by temperature (Table S15), whereas wind patterns and precipitation have little effect on the seasonal variance of TCPP levels in polar regions (Table S15). The ·OH radical is the major oxidant that destroys chemicals in the atmosphere. It is produced by a photochemical reaction, so it occurs at higher levels in the summer (when there is more direct sunlight) than in the winter. In the polar regions, when it is dark for up to 24 hours in the winter, the atmospheric ·OH radical concentrations are basically zero in the winter. When the ·OH concentrations and temperatures in the model were set as the annual means for each cell, the concentrations in February were only two times higher than those in summer (Table S15), which validated the assumption that the ·OH level and temperature variability are the dominant factors for the seasonal trend of TCPP inventories in the polar regions.

Comparison with CanMETOP model

The Canadian Model for Environmental Transport of Organochlorine Pesticides (CanMETOP) was run to compare results with those of BETR-Global. The CanMETOP model is a global multimedia long-range atmospheric transport model with a resolution of 1°×1°. It includes 14 vertical levels in the atmosphere with heights ranging from 0 m to 11,000 m, three soil layers, and water and ice/snow layers. Since the water transport process is not considered in the CanMETOP model, the scenarios with emission only occurring in air were run with this model. TCPP was input into the 1st to 8th air layers (0 to 1,200 m) to correspond to the atmospheric levels of the lower air compartment in BETR-Global (lower air: average height is 1,200 m). For BETR-Global, scenarios were run with the water transport process disabled in order to correspond with the CanMETOP model. In the Arctic, the modeled annual mean TCPP concentration is comparable in air (CanMETOP: 10.4 pg/m^3, BETR: 16.1 pg/m^3, Table S16). However, the modeled annual mean concentrations in seawater and total amounts in air and seawater are all one order of magnitude lower in CanMETOP (Table S16) than in BETR-Global experiments. For the Antarctic, the amount and concentrations simulated by CanMETOP model are one to two orders of magnitude lower than those of BETR-Global. This discrepancy mainly results from the degradation rate simulation in these two models. As described above, the BETR model uses monthly variable ·OH concentrations in air, with very low values in winter in polar regions, and even zero during polar night. However, in CanMETOP, a constant degradation rate is used globally. This setup leads to a lower mass of TCPP in polar regions compared with BETR Global.

Uncertainty analysis

Ocean current transport is a pathway that is relatively slow to spread pollutants from continents to remote areas. In this study, each scenario was run for eight years, since preliminary model runs indicated that TCPP levels in air and seawater became stable after that many years of model time. However, the transport by ocean water may require a longer time, which may affect the results. To quantity this uncertainty, we ran the scenario with global emissions and emissions only occurring in water for 50 years. The results show that the increase rates are small; 0.26% and 0.56% for the amount of TCPP found in the Arctic and Antarctic, respectively.

The "best estimate" emission scenario adopted in this study has been suggested as a preliminary estimate with high uncertainties.[11] The uncertainties inherent in the underlying emission estimate method introduce errors in the model boundary conditions of the present study. Apart from this emission input, the uncertainties of LRT models should also be considered. For example, gas-particle partitioning is not well constrained, as discussed in our former study.[11] Another factor of uncertainty are the properties of the TCPP used in the model, which may influence the results. Despite these uncertainties, this study partially fills a gap in our knowledge of the environmental fate of TCPP that has important implications for policy makers and regulations.

ASSOCIATED CONTENT

Supporting Information

Additional tables and figures are given in the Supporting Information.

AUTHOR INFORMATION

Corresponding author

*Phone: +49-4152-872330; E-mail address: zhiyong.xie@hzg.de

*Phone: +46 8 674 7168; E-mail address: Matthew.MacLeod@aces.su.se

ORCID

Jing Li: 0000-0003-0187-9179

Fangyuan Zhao: 0000-0002-6041-4518

Zhiyong Xie: 0000-0001-8997-3930

Chongguo Tian: 0000-0001-6058-9353

Notes

The authors declare no competing financial interests.

ACKNOWLEDGMENTS

J.L. gratefully acknowledges the China Scholarship Council. F.Z., M.M. and Z.X. received funding from the European Union’s Horizon 2020 research and innovation programme under grant agreement No 689443 via project iCUPE (Integrative and Comprehensive Understanding on Polar Environments).

REFERENCES

1. Van der Veen, I.; de Boer, J., Phosphorus flame retardants: Properties, production, environmental occurrence, toxicity and analysis. *Chemosphere* **2012,** *88*, (10), 1119-1153.
2. EU Risk Assessment Report, Tris(2-chloro-1-methylethyl) phosphate (TCPP). CAS No.: 13674-84-5. EINECS No.: 237-158-7. **2008**.
3. Li, J.; Xie, Z.; Mi, W.; Lai, S.; Tian, C.; Emeis, K.-C.; Ebinghaus, R., Organophosphate Esters in Air, Snow and Seawater in the North Atlantic and the Arctic. *Environ. Sci. Technol.* **2017,** *51*, 6887−6896.
4. Castro-Jimenez, J.; Gonzalez-Gaya, B.; Pizarro, M.; Casal, P.; Pizarro-Alvarez, C.; Dachs, J., Organophosphate Ester Flame Retardants and Plasticizers in the Global Oceanic Atmosphere. *Environ. Sci. Technol.* **2016,** *50*, (23), 12831-12839.
5. Salamova, A.; Hermanson, M. H.; Hites, R. A., Organophosphate and Halogenated Flame Retardants in Atmospheric Particles from a European Arctic Site. *Environ. Sci. Technol.* **2014,** *48*, (11), 6133-6140.
6. Sühring, R.; Diamond, M. L.; Scheringer, M.; Wong, F.; Pucko, M.; Stern, G.; Burt, A.; Hung, H.; Fellin, P.; Li, H.; Jantunen, L. M., Organophosphate Esters in Canadian Arctic Air: Occurrence, Levels and Trends. *Environ. Sci. Technol.* **2016,** *50*, (14), 7409-7415.
7. Wohrnschimmel, H.; MacLeod, M.; Hungerbuhler, K., Global multimedia source-receptor relationships for persistent organic pollutants during use and after phase-out. *Atmos. Pollut. Res.* **2012,** *3*, (4), 392-398.
8. HTAP, The Task Force on Hemispheric Transport of Air Pollution (TF HTAP). http://www.htap.org/.
9. Malanichev, A.; Mantseva, E.; Shatalov, V.; Strukov, B.; Vulykh, N., Numerical evaluation of the PCBs transport over the Northern Hemisphere. *Environ. Pollut.* **2004,** *128*, (1-2), 279-289.
10. Shindell, D. T.; Chin, M.; Dentener, F.; Doherty, R. M.; Faluvegi, G.; Fiore, A. M.; Hess, P.; Koch, D. M.; MacKenzie, I. A.; Sanderson, M. G.; Schultz, M. G.; Schulz, M.; Stevenson, D. S.; Teich, H.; Textor, C.; Wild, O.; Bergmann, D. J.; Bey, I.; Bian, H.; Cuvelier, C.; Duncan, B. N.; Folberth, G.; Horowitz, L. W.; Jonson, J.; Kaminski, J. W.; Marmer, E.; Park, R.; Pringle, K. J.; Schroeder, S.; Szopa, S.; Takemura, T.; Zeng, G.; Keating, T. J.; Zuber, A., A multi-model assessment of pollution transport to the Arctic. *Atmos. Chem. Phys.* **2008,** *8*, (17), 5353-5372.
11. Li, J.; Zhao, F. Y.; Xie, Z. Y.; Ebinghaus, R.; Emeis, K. C.; Tian, C. G.; MacLeod, M., Global gridded emissions and atmospheric transport of Tris-(1-chloro-2-propyl) phosphate (TCPP) (submitted to Environ. Sci. Technol.). **2019**.
12. MacLeod, M.; von Waldow, H.; Tay, P.; Armitage, J. M.; Wöhrnschimmel, H.; Riley, W. J.; McKone, T. E.; Hungerbuhler, K., BETR global–A geographically-explicit global-scale multimedia contaminant fate model. *Environ. Pollut.* **2011,** *159*, (5), 1442-1445.
13. McLachlan, M. S.; Undeman, E.; Zhao, F. Y.; MacLeod, M., Predicting global scale exposure of humans to PCB 153 from historical emissions. *Environ. Sci.: Proc. Imp.* **2018,** *20*, (5), 747-756.
14. Liu, H. Y.; Jacob, D. J.; Bey, I.; Yantosca, R. M.; Duncan, B. N.; Sachse, G. W., Transport pathways for Asian pollution outflow over the Pacific: Interannual and seasonal variations. *J. Geophys. Res.-Atmos.* **2003,** *108*, (D20).

15. Li, Q. B.; Jacob, D. J.; Bey, I.; Palmer, P. I.; Duncan, B. N.; Field, B. D.; Martin, R. V.; Fiore, A. M.; Yantosca, R. M.; Parrish, D. D.; Simmonds, P. G.; Oltmans, S. J., Transatlantic transport of pollution and its effects on surface ozone in Europe and North America. *J. Geophys. Res.-Atmos.* **2002,** *107*, (D13).

Figure legends

Figure 1. Source and receptor regions adopted in this study.

Figure 2. Global distribution of TCPP concentrations in lower air (3.75°×3.75°)

Figure 3. Global distribution of TCPP concentrations in seawater (3.75°×3.75°)

Figure 4. Global concentration levels of TCPP in air with different source regions (with emission only occurring into air).

Figure 5. The global distribution of TCPP concentrations in February and August.

Table legends

Table 1. Relative contribution of source regions to the pollution of TCPP in polar regions

Figure 1.

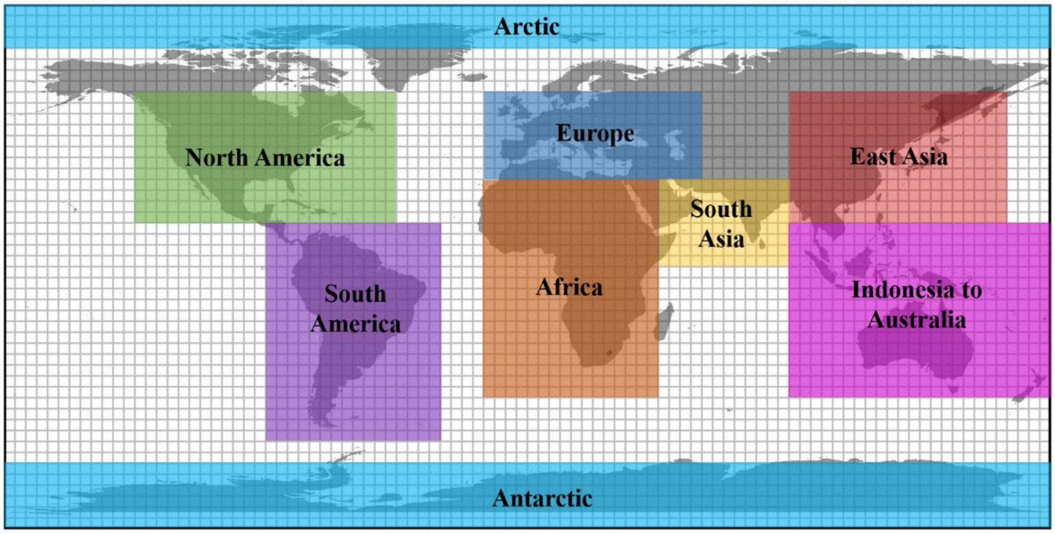

Figure 2.

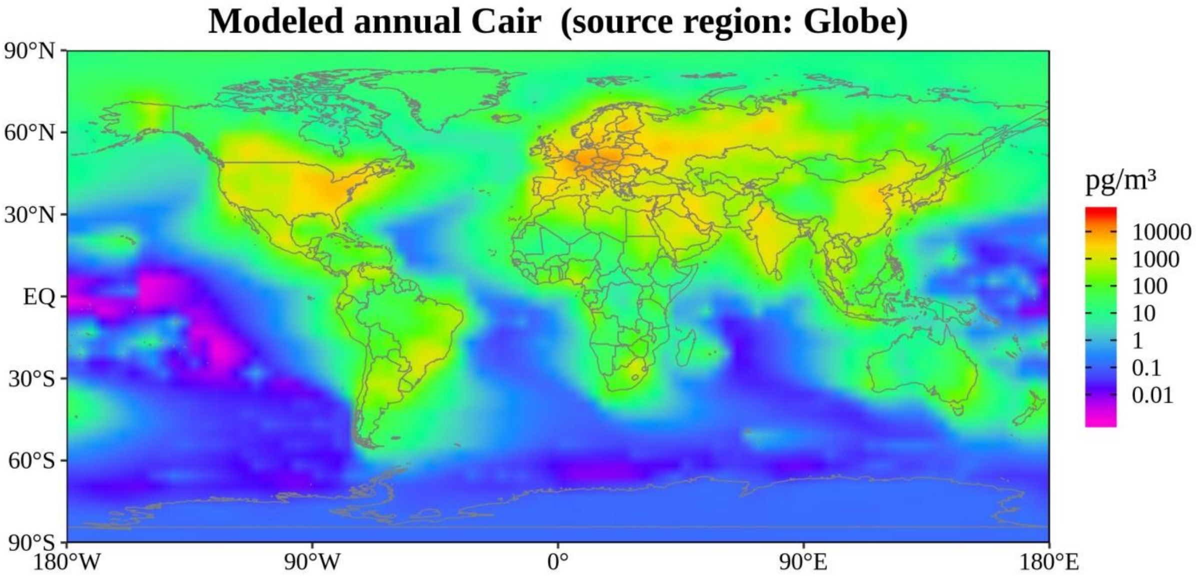

Figure 3.

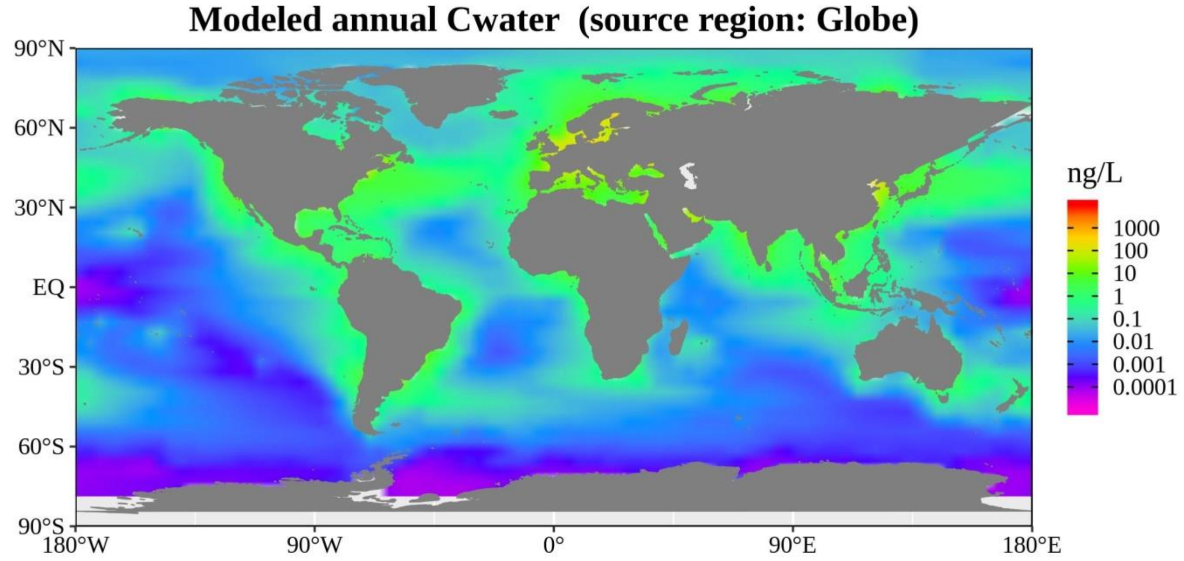
Modeled annual Cwater (source region: Globe)

Figure 4.

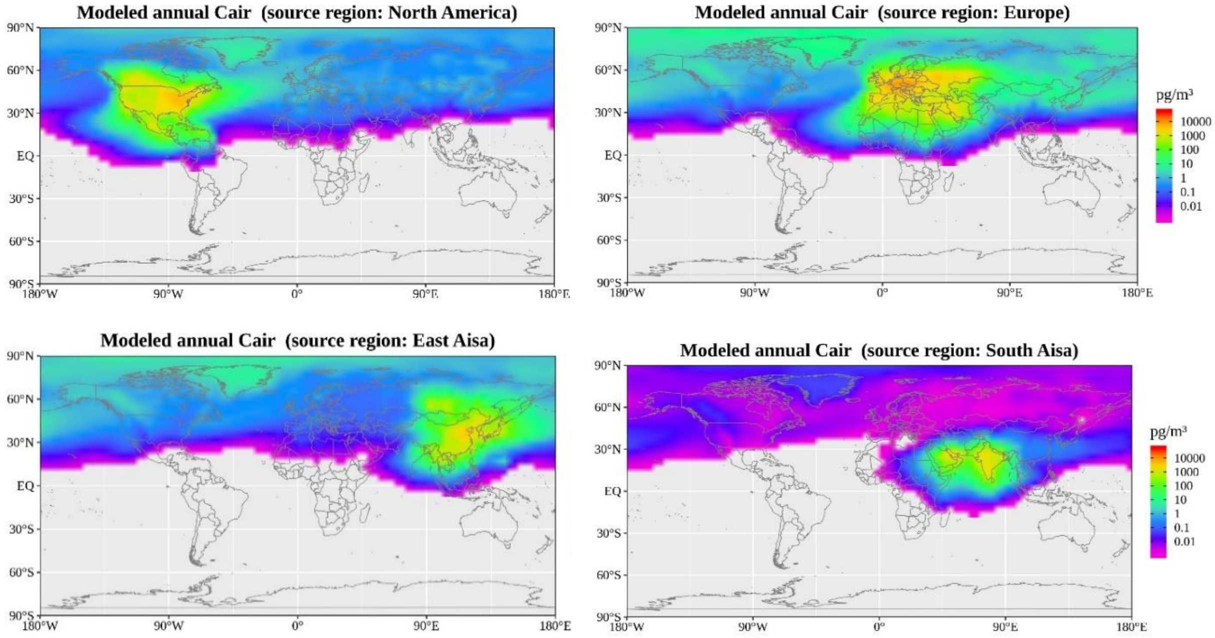
Modeled annual Cair (source region: North America)

Modeled annual Cair (source region: Europe)

Modeled annual Cair (source region: East Aisa)

Modeled annual Cair (source region: South Aisa)

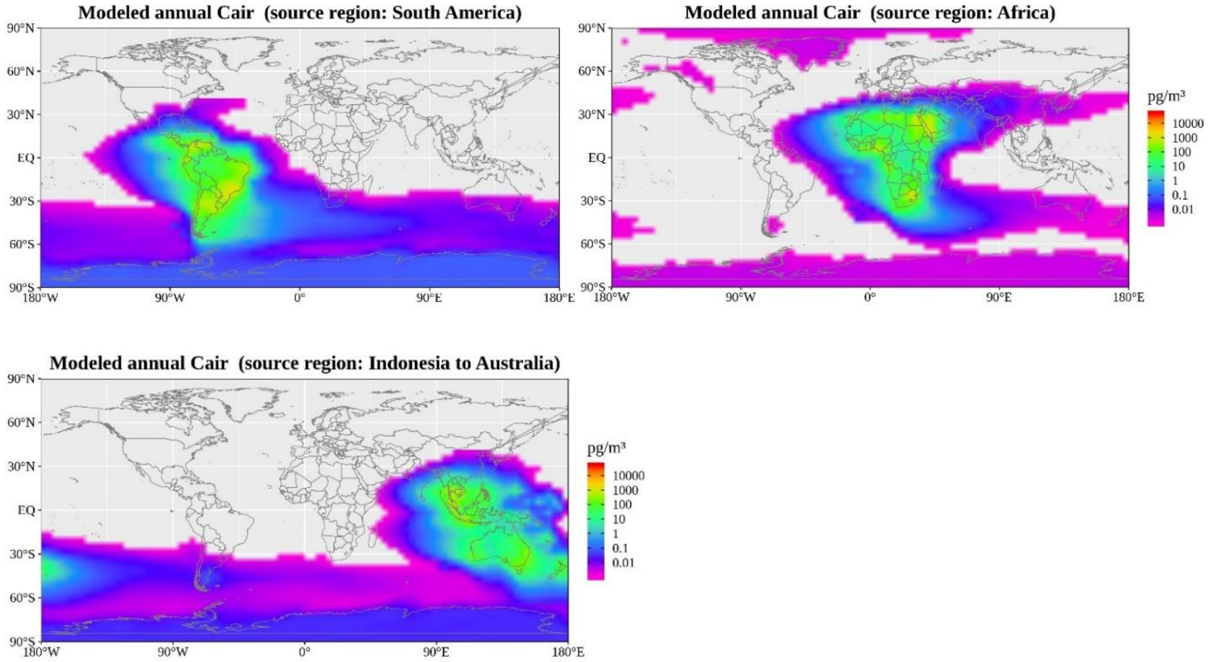
Modeled annual Cair (source region: South America)
Modeled annual Cair (source region: Africa)
Modeled annual Cair (source region: Indonesia to Australia)
90°N
60°N
30°N
EQ
30°S
60°S
90°S
180°W
90°W
0°
90°E
180°E
pg/m³
10000
1000
100
10
1
0.1
0.01

Figure 5.

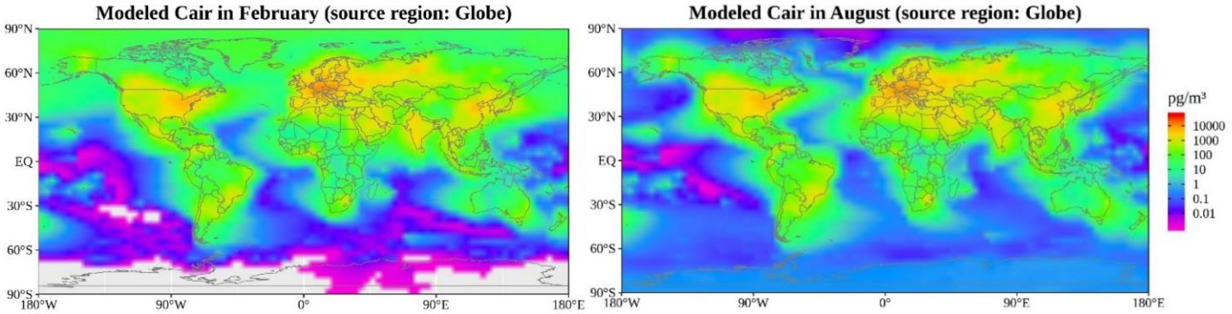
Modeled Cair in February (source region: Globe)
Modeled Cair in August (source region: Globe)
90°N
60°N
30°N
EQ
30°S
60°S
90°S
180°W
90°W
0°
90°E
180°E
pg/m³
10000
1000
100
10
1
0.1
0.01

Table 1:

Source regions	Contribution to Arctic (air + seawater)			Contribution to Antarctic (air + seawater)		
	Ea=78.6 kt/y Ew=0	Ea=0 Ew=39.3 kt/y	Ea=78.6 kt/y Ew=39.3 kt/y	Ea=78.6 kt/y Ew=0	Ea=0 Ew=39.3 kt/y	Ea=78.6 kt/y Ew=39.3 kt/y
North America	1.62%	0.009%	0.855%	0.000%	0.000%	0.000%
Europe	21.2%	24.8%	23.0%	0.000%	0.000%	0.000%
East Asia	3.55%	12.4%	7.79%	0.000%	0.000%	0.000%
South Asia	0.019%	0.000%	0.010%	0.000%	0.000%	0.000%
South America	0.000%	0.000%	0.000%	58.0%	51.8%	57.0%
Africa	0.001%	0.000%	0.001%	2.29%	2.25%	2.28%
Indonesia to Australia	0.000%	0.000%	0.000%	19.9%	11.1%	18.4%
Rest of the world	73.6%	62.7%	68.4%	19.8%	34.8%	22.3%
Sum	100%	100%	100%	100%	100%	100%

TOC: Table of Content

Supporting information of

Global multimedia source-receptor relationships for tris-(1-chloro-2-propyl) phosphate (TCPP)

Jing Li[†,⊥], Fangyuan Zhao[‡], Zhiyong Xie[†*], Ralf Ebinghaus[†], Kay-Christian Emeis[†], Chongguo Tian[§], Matthew MacLeod[‡*]

[†]Helmholtz-Zentrum Geesthacht, Centre for Materials and Coastal Research, Institute of Coastal Research, Geesthacht, 21502, Germany

[‡]Department of Environmental Science and Analytical Chemistry, ACES, Stockholm University, Svante Arrhenius väg 8, Stockholm, SE-114 18, Sweden

[§]Key Laboratory of Coastal Environmental Processes and Ecological Remediation, Yantai Institute of Coastal Zone Research, CAS, Yantai, 264003, China

[⊥]Universität Hamburg, Department of Geosciences, Hamburg, 20144, Germany

Corresponding Author

*Phone: +49-4152-872330; E-mail address: zhiyong.xie@hzg.de

*Phone: +46 8 674 7168; E-mail address: Matthew.MacLeod@aces.su.se

Pages: 8

Tables: 16

Contents

Table S1. The physical/chemical properties of TCPP (at 25°C)

Parameter	Descript	Unit	Value	Source
MW	Molecular weight	g/mol	327	EPI suite 4.0
VP	Vapor pressure	Pa	0.035	Brommer et al.[1]
SL	Solubility	mg/l	1160	Cuthbert et al.[2]
HLC	Herry's law constant	$Pa\cdot m^3/mol$	0.0099	Derived from VP and SL
log K_{OW}	Partitioing ratio:n-octanol/water		2.68	Cuthbert et al.[2]
log K_{AW}	Partitioing ratio:air/water		-5.40	Derived from VP and SL
log K_{OA}	Partitioing ratio:n-octanol/air		8.08	Derived by log K_{OW}-logK_{AW}
$t_{1/2,Air}$	Half-life time in air	h	12	Li et al.[3]
$t_{1/2,Freshwater}$	Half-life time in freshwater	h	3600	
$t_{1/2,Ocean}$	Half-life time in ocean	h	3600	
$t_{1/2,Soil}$	Half-life time in soil	h	7200	
$t_{1/2,Sediment}$	Half-life time in sediment	h	32500	
$t_{1/2,Vegetation}$	Half-life time in vegetation	h	3600	
DU_{OW}	Internal energy of phase change: n-octanol/water	J/mol	-20000	MacLeod et al.[4]
DU_{OA}	Internal energy of phase change:n-octanol/air	J/mol	-80306	
AE_{Air}	Activation energies in air	J/mol	10000	Wöhrnschimmel et al.[5]
$AE_{Freshwater}$	Activation energies in freshwater	J/mol	30000	
AE_{Ocean}	Activation energies in ocean	J/mol	30000	
AE_{Soil}	Activation energies in soil	J/mol	30000	
$AE_{Sediment}$	Activation energies in sediment	J/mol	30000	
$AE_{Vegetation}$	Activation energies in vegetation	J/mol	30000	

Table S2. Designed scenarios in this study

Source regions	Ea=78.6 kt Ew=0	Ea=0 Ew=39.3 kt	Ea=78.6 kt Ew=39.3 kt
North America	1	10	19
Europe	2	11	20
East Asia	3	12	21
South Asia	4	13	22
South America	5	14	23
Africa	6	15	24
Indonesia to Australia	7	16	25
Rest of the world	8	17	26
Global	9	18	27

Table S3. Source-receptor relationships for continental regions with emission only occur in air

Source regions	**Receptors (Scenario: Ea=78.6 kt/y; Ew=0)**						
	North America	**Europe**	**East Asia**	**South Asia**	**South America**	**Africa**	**Indonesia to Australia**
North America	98.1%	0.087%	0.073%	0.005%	0.489%	0.032%	0.000%
Europe	0.229%	97.8%	0.720%	2.51%	0.004%	6.16%	0.000%
East Asia	0.165%	0.010%	83.0%	1.14%	0.000%	0.002%	5.17%
South Asia	0.003%	0.001%	0.718%	92.0%	0.000%	1.20%	1.99%
South America	1.04%	0.000%	0.000%	0.000%	99.3%	3.44%	0.035%
Africa	0.00%	0.033%	0.001%	0.255%	0.024%	88.4%	0.024%
Indonesia to Australia	0.00%	0.000%	14.85%	2.03%	0.027%	0.043%	92.1%
Rest of the world	0.460%	2.12%	0.629%	2.10%	0.140%	0.717%	0.681%
Sum	100%	100%	100%	100%	100%	100%	100%

Table S4. Source-receptor relationships for continental regions with emission only occur in water

Source regions	**Receptor (Scenario: Ea=0; Ew=39.3 kt/y)**						
	North America	**Europe**	**East Asia**	**South Asia**	**South America**	**Africa**	**Indonesia to Australia**
North America	98.9%	0.008%	0.000%	0.000%	0.145%	0.001%	0.000%
Europe	0.000%	99.5%	0.000%	3.432%	0.000%	0.359%	0.000%
East Asia	0.001%	0.000%	91.0%	0.107%	0.000%	0.000%	3.50%
South Asia	0.000%	0.000%	0.352%	90.9%	0.000%	0.008%	1.33%
South America	1.01%	0.000%	0.000%	0.000%	99.8%	0.449%	0.011%
Africa	0.000%	0.006%	0.000%	0.011%	0.012%	99.1%	0.011%
Indonesia to Australia	0.000%	0.000%	8.68%	0.076%	0.003%	0.004%	94.8%
Rest of the world	0.088%	0.467%	0.011%	5.43%	0.067%	0.114%	0.384%
Sum	100%	100%	100%	100%	100%	100%	100%

Table S5. Relative contributions of emission in air (Ea) and water (Ew) for source regions

Local source	**TCPP in local air**		**TCPP in local seawater**	
	From Ea	From Ew	From Ea	From Ew
North America	99.8%	0.145%	18.0%	81.8%
Europe	99.2%	0.423%	26.1%	73.9%
East Asia	99.5%	0.461%	22.5%	77.5%
South Asia	99.8%	0.165%	5.86%	94.1%
South America	99.6%	0.415%	22.8%	77.2%
Africa	99.9%	0.144%	8.73%	91.3%
Indonesia to Australia	98.2%	1.77%	31.6%	68.4%
Mean	99.4%	0.503%	19.4%	80.6%

Table S6. Annual mean concentrations of TCPP in polar regions with different source regions (in air: pg/m^3, in seawater: pg/L)

Source regions (emission: Ea=78.6 kt/y, Ew=39.3 kt/y)	**Receptor: Arctic**			**Receptor: Antarctic**		
	Lower air	Upper air	Seawater	Lower air	Upper air	Seawater
North America	1.09E+00	2.73E+00	1.32E+00	9.60E-11	1.26E-10	1.01E-10
Europe	4.22E+00	1.17E+01	2.78E+01	9.15E-12	1.19E-11	1.63E-11
East Asia	2.15E+00	5.85E+00	1.54E+01	2.51E-11	3.25E-11	7.74E-11
South Asia	1.42E-02	3.49E-02	1.52E-02	4.02E-10	5.06E-10	5.53E-09
South America	5.52E-07	1.42E-06	2.92E-05	6.76E-02	8.68E-02	5.61E-02
Africa	1.13E-03	2.87E-03	1.19E-03	2.62E-03	3.49E-03	2.06E-03
Indonesia to Australia	4.55E-05	1.08E-04	4.32E-05	2.36E-02	2.97E-02	1.96E-02
Global	1.62E+01	3.81E+01	1.36E+02	1.05E-01	1.33E-01	9.78E-02

Table S7. Amount of TCPP that found in Arctic with different source regions (kg)

Source regions	**Amount in Arctic air**			**Amount in Arctic seawater**		
	Ea=78.6 kt/y Ew=0	Ea=0 Ew=39.3 kt/y	Ea=78.6 kt/y Ew=39.3 kt/y	Ea=78.6 kt/y Ew=0	Ea=0 Ew=39.3 kt/y	Ea=78.6 kt/y Ew=39.3 kt/y
North America	1.34E+02	7.86E-02	1.34E+02	8.36E+02	4.98E+00	8.44E+02
Europe	5.37E+02	9.94E-01	5.56E+02	1.21E+04	1.36E+04	2.58E+04
East Asia	2.80E+02	9.13E-02	2.80E+02	1.84E+03	6.80E+03	8.64E+03
South Asia	1.66E+00	1.62E-03	1.66E+00	9.46E+00	9.26E-03	9.47E+00
South America	6.19E-05	7.66E-06	6.96E-05	5.85E-03	2.22E-02	2.80E-02
Africa	1.36E-01	8.12E-05	1.36E-01	7.49E-01	7.35E-04	7.50E-01
Indonesia to Australia	4.79E-03	4.29E-04	5.22E-03	2.48E-02	2.26E-03	2.71E-02
Rest of the world	8.94E+02	3.30E+00	8.98E+02	4.31E+04	3.43E+04	7.74E+04
Global	1.85E+03	4.46E+00	1.85E+03	5.79E+04	5.47E+04	1.13E+05

Table S8. Relative contribution of source regions to TCPP that found in Arctic

Source regions	**Contribution to Arctic air (lower + upper)**			**Contribution to Arctic seawater**		
	Ea=78.6 kt/y Ew=0	Ea=0 Ew=39.3 kt/y	Ea=78.6 kt/y Ew=39.3 kt/y	Ea=78.6 kt/y Ew=0	Ea=0 Ew=39.3 kt/y	Ea=78.6 kt/y Ew=39.3 kt/y
North America	7.24%	1.76%	7.25%	1.45%	0.009%	0.750%
Europe	29.1%	22.3%	30.0%	20.9%	24.8%	22.9%
East Asia	15.2%	2.05%	15.1%	3.18%	12.4%	7.67%
South Asia	0.090%	0.036%	0.090%	0.016%	0.000%	0.008%
South America	0.000%	0.000%	0.000%	0.000%	0.000%	0.000%
Africa	0.007%	0.002%	0.007%	0.001%	0.000%	0.001%
Indonesia to Australia	0.000%	0.010%	0.000%	0.000%	0.000%	0.000%
Rest of the world	48.4%	73.9%	48.5%	74.4%	62.7%	68.7%
Sum	100%	100%	101%	100%	100%	100%

Table S9. Relative contribution of Ea and Ew to TCPP that found in Arctic

Source regions	**TCPP in Arctic air**		**TCPP in Arctic seawater**		**TCPP in Arctic air+seawater**	
	From Ea	From Ew	From Ea	From Ew	From Ea	From Ew
North America	99.6%	0.059%	99.0%	0.590%	99.1%	0.517%
Europe	96.7%	0.179%	47.0%	52.7%	48.0%	51.6%

East Asia	100%	0.033%	21.3%	78.7%	23.8%	76.2%
Global	99.8%	0.241%	51.4%	48.6%	52.2%	47.8%

Table S10. Other contributors of Arctic TCPP

Source regions	Arctic air			Arctic seawater			Arctic (air+seawater)		
	Ea=78.6 kt/y Ew=0	Ea=0 Ew=39.3 kt/y	Ea=78.6 kt/y Ew=39.3 kt/y	Ea=78.6 kt/y Ew=0	Ea=0 Ew=39.3 kt/y	Ea=78.6 kt/y Ew=39.3 kt/y	Ea=78.6 kt/y Ew=0	Ea=0 Ew=39.3 kt/y	Ea=78.6 kt/y Ew=39.3 kt/y
North Europe	12.0%	65.0%	12.1%	52.9%	47.5%	50.3%	51.6%	47.5%	49.7%
North Aisa	20.2%	3.56%	20.2%	11.0%	7.17%	9.12%	11.2%	7.17%	9.30%
Middle Aisa	7.37%	0.921%	7.36%	1.28%	0.002%	0.658%	1.47%	0.002%	0.767%
Sum	39.6%	69.5%	39.6%	65.2%	54.7%	60.1%	64.4%	54.7%	59.7%

Table S11. Amount of TCPP that found in Antarctic with different source regions (kg)

Source regions	Mass of TCPP in Antarctic air (lower + upper)			Mass of TCPP in Antarctic seawater		
	Ea=78.6 kt/y Ew=0	Ea=0 Ew=39.3 kt/y	Ea=78.6 kt/y Ew=39.3 kt/y	Ea=78.6 kt/y Ew=0	Ea=0 Ew=39.3 kt/y	Ea=78.6 kt/y Ew=39.3 kt/y
North America	1.67E-09	6.31E-10	1.44E-08	5.93E-08	5.98E-08	3.41E-07
Europe	7.68E-10	2.80E-12	1.36E-09	3.31E-08	1.81E-10	9.14E-08
East Asia	1.50E-09	2.20E-09	3.70E-09	1.73E-07	2.54E-07	4.28E-07
South Asia	4.21E-08	1.55E-08	5.76E-08	1.29E-05	2.49E-05	3.77E-05
South America	9.93E+00	2.57E-02	9.96E+00	1.63E+02	3.17E+01	1.95E+02
Africa	4.00E-01	3.29E-04	4.00E-01	6.44E+00	1.37E+00	7.82E+00
Indonesia to Australia	3.38E+00	9.52E-04	3.39E+00	5.61E+01	6.82E+00	6.29E+01
Rest of the world	1.56E+00	1.55E-04	1.56E+00	5.75E+01	2.13E+01	7.88E+01
Global	1.53E+01	2.71E-02	1.53E+01	2.83E+02	6.12E+01	3.45E+02

Table S12. Relative contribution of source regions to TCPP that found in Antarctic

Source regions	Contribution to Antarctic air			Contribution to Antarctic seawater		
	Ea=78.6 kt/y Ew=0	Ea=0 Ew=39.3 kt/y	Ea=78.6 kt/y Ew=39.3 kt/y	Ea=78.6 kt/y Ew=0	Ea=0 Ew=39.3 kt/y	Ea=78.6 kt/y Ew=39.3 kt/y
North America	0.00%	0.00%	0.00%	0.00%	0.00%	0.00%
Europe	0.00%	0.00%	0.00%	0.00%	0.00%	0.00%
East Asia	0.00%	0.00%	0.00%	0.00%	0.00%	0.00%
South Asia	0.00%	0.00%	0.00%	0.00%	0.00%	0.00%
South America	65.0%	94.7%	65.1%	57.7%	51.8%	56.6%
Africa	2.62%	1.21%	2.62%	2.27%	2.25%	2.27%
Indonesia to Australia	22.1%	3.5%	22.1%	19.8%	11.1%	18.2%
Rest of the world	10.2%	0.57%	10.2%	20.3%	34.8%	22.9%
Sum	100%	100%	100%	100%	100%	100%

Table S13. Relative contribution of Ea and Ew to TCPP in Antarctic

Source regions	TCPP in Antarctic air		TCPP in Antarctic seawater		TCPP in Antarctic air+seawater	
	From Ea	From Ew	From Ea	From Ew	From Ea	From Ew
South America	99.7%	0.258%	83.7%	16.3%	84.5%	15.5%
Africa	99.9%	0.082%	82.4%	17.6%	83.3%	16.7%
Indonesia to Australia	100%	0.028%	89.2%	10.8%	89.7%	10.3%

Global	99.8%	0.177%	82.2%	17.8%	83.0%	17.0%

Table S14 Relatively contribution of transport pathways that convey TCPP to polar regions

Pathway	Arctic	Antarctic
water inflow	89.1%	46.3%
Wet deposition	9.71%	24.9%
Dry depossition	0.019%	9.70%
Air-seawater exchange	0.08%	8.06%

Table S15. The effect of ·OH concentration, temperature (T), air flow and precipitation (prep.) on the seasonal TCPP levels in air of Arctic

Scenario	**Arctic air**		
	Feb (kg)	**Aug (kg)**	**Ratio (Feb/Aug)**
Original	5.07E+03	3.54E+01	143
·OH=annual mean	1.00E+03	8.38E+01	12.0
T=annual mean	4.08E+03	6.51E+01	62.6
Air flow= annual mean	4.62E+03	2.61E+01	177
Prep.=annual mean	4.89E+03	4.21E+01	116
OH,T=annual mean	4.00E+02	1.87E+02	2.14
OH,T,air flow=annual mean	3.65E+02	1.89E+02	1.93
OH,T,air flow,prep.=annual mean	2.44E+02	1.63E+02	1.50

Table S16. Comparison the result of BETR and CanMETOP model

Scenario: Ea=78.6 kt/y, Ew=0 No water transport	**Receptor: Arctic**		**Receptor: Antarctic**	
	BETR	**CanMETOP**	**BETR**	**CanMETOP**
Cair (lower air, pg/m^3)	16.1	10.4	0.105	0.016
Cwater (pg/L)	47.0	1.41	0.470	0.002
Total mass in air (t)	1.84	0.277	0.015	0.004
Total mass in seawater (t)	32.0	1.39	1.00	0.004

References

1. Brommer, S.; Jantunen, L. M.; Bidleman, T. F.; Harrad, S.; Diamond, M. L., Determination of Vapor Pressures for Organophosphate Esters. *J. Chem. Eng. Data* **2014,** *59*, (5), 1441-1447.
2. Cuthbert, J. M., DM., TCPP: Determination of general physicochemical properties, Report 1613/002. *SafePharm Laboratories, PO Box 45, Derby, UK.* **2002**.
3. Li, J.; Zhao, F. Y.; Xie, Z. Y.; Ebinghaus, R.; Emeis, K. C.; Tian, C. G.; MacLeod, M., Global gridded emissions and atmospheric transport of Tris-(1-chloro-2-propyl) phosphate (TCPP) (submitted to Environ. Sci. Technol.). **2019**.
4. MacLeod, M.; Scheringer, M.; Hungerbuhler, K., Estimating enthalpy of vaporization from vapor pressure using Trouton's rule. *Environ. Sci. Technol.* **2007,** *41*, (8), 2827-2832.
5. Wohrnschimmel, H.; MacLeod, M.; Hungerbuhler, K., Emissions, Fate and Transport of Persistent Organic Pollutants to the Arctic in a Changing Global Climate. *Environ. Sci. Technol.* **2013,** *47*, (5), 2323-2330.

Declaration

(Eidesstattliche Erklärung)

I hereby declare, on oath, that I have written the present dissertation by my own and have not used other than the acknowledged resources and aids.

Hiermit erkläre ich an Eides statt, dass ich die vorliegende Dissertationsschrift selbst verfasst und keine anderen als die angegebenen Quellen und Hilfsmittel benutzt habe.

Hamburg, den Jing Li